Developmental Functions of Drosophila ASPP and RASSF8

Yanxiang Zhou

University College London

September 2014

A thesis submitted for the degree of Doctor of Philosophy

Supervisor: Nicolas Tapon
Cancer Research UK
London Research Insititute

Declaration

I, Yanxiang Zhou, confirm that the work presented in this thesis is my own. Where information has been derived from other sources, I confirm that this has been indicated in the thesis.

Yanxiang Zhou

Abstract

Epithelial cells are connected to each other via intercellular junctions, which are established, remodelled and maintained by a complex molecular machinery. Aberrant regulation of cell-cell junctions leads to loss of tissue organisation and is a hallmark of cancer formation. Although many kinases that regulate the phosphorylation of junctional proteins have been described, much less is known about the reversal of phosphorylation by phosphatases.

This thesis investigates the role of Drosophila ASPP, a scaffold protein that is localised at adherens junctions, as a regulatory subunit for PP1s. In vitro, ASPP can bind to PP1 using its RVXF motif and SH3 domain. In vivo, ASPP co-localises with the PP1α96A and PP1β9C isoforms at cell-cell junctions in the pupal retina and ASPP function is at least partially dependent on its ability to bind to PP1. Furthermore, ASPP can recruit two additional coiled coil containing scaffold proteins, RASSF8 and Ccdc85, to form trimeric complexes with PP1α96A. *ccdc85* mutants that were generated in this work have a rough eye, similar to *ASPP* mutants, suggesting a similar function in vivo.

Two potential substrates for the ASPP/PP1 complex were tested: (1) Yki a transcriptional co-activator that is part of the Hippo pathway and (2) Baz, a scaffold protein that is required for cell polarity. Although no evidence for dephosphorylation of Yki was found, Baz can be dephosphorylated in vitro. The well-described aPKC phosphorylation site (S980) and five additional serine/threonine residues are strongly dephosphorylated by ASPP/PP1.

My work also identified three potential regulators/scaffolds of ASPP/PP1. The Hippo pathway kinase Wts can phosphorylate RASSF8, the E3 ubiquitin ligase Sina can ubiquitylate and degrade ASPP and the junctional protein Magi can associate with RASSF8 at adherens junctions. Finally, novel potential regulators, scaffolds or substrates of the ASPP/PP1 complex were identified through AP-MS experiments and tested for their ability to modulate the *ASPP* depletion phenotype in vivo.

Acknowledgement

Nothing important in life is done without the help and encouragement of others. For the shared joy of this PhD journey I would like to thank:

First and foremost Nic, for being a dedicated, outstanding supervisor and scientist. But even more, thank you for your kind, generous and patient nature.
Without everyone else, who worked in the lab, this would have been nowhere near as fun! Thanks for creating such a special atmosphere in the lab: Birgit, Alice, Tobi, Micha, Eunice, Rachael, Yanlan, Paulo, Gaspar, Maxine, Ieva, Ohad, Poppy, Lennart, Tessa, Jen, Nicola, Billel and Annabel.
Of course, there are our neighbours, who contributed at least as much to the special atmosphere of the fifth floor: Barry, Ruth, George, Clara, Neil, Eliana, Mariana, Graham, Ichha, Ahmed, Mario and Rob.
For collaboration, support and reagents: Karin Barnouin, Andrew Chalmers, Alexandre Djiane, Terence Gilbank, Matthias Gstaiger, Simon Hauri, Svend Kjaer, Shaun Maloney, Stephane Mouilleron, Cathie Pfleger, Franck Pichaud, Bram Snijders, Sharon Tooze and Rhian Walther.
For moral support and acknowledging each other in the acknowledgement section of a thesis, my wife Judy.
Funding was provided by Cancer Research UK and Boehringer Ingelheim Fonds.

I dedicate this work to my grandmother, who never stopped pursuing knowledge.

Contents

List of Figures

List of Genotypes

Fig. 3.4A: yw eyFlp; FRT 42D, ubi-GFP-ASPP, $ASPP^{d}$ / FRT 42D, ubi-mCherry
Fig. 3.4A: yw eyFlp; FRT 42D, ubi-GFP-ASPP-FA, $ASPP^{d}$ / FRT 42D, ubi-mCherry
Fig. 3.4B–B": yw hsFlp; FRT 42D, ubi-GFP-ASPP, $ASPP^{d}$ / FRT 42D, arm-LacZ
Fig. 3.4C-C": yw hsFlp; FRT 42D, ubi-GFP-ASPP-FA, $ASPP^{d}$ / FRT 42D, arm-LacZ
Fig. 3.5A: $ASPP^{2.93}$ / $ASPP^{1}$
Fig. 3.5B: $ASPP^{d}$ / $ASPP^{8}$
Fig. 3.5C: FRT 42D, ubi-GFP-ASPP, $ASPP^{d}$ / $ASPP^{8}$
Fig. 3.5D: FRT 42D, ubi-GFP-ASPP-FA, $ASPP^{d}$ / $ASPP^{8}$
Fig. 3.6A: $ASPP^{d}$ / $ASPP^{8}$
Fig. 3.6B: FRT 42D, ubi-GFP-ASPP, $ASPP^{d}$ / $ASPP^{8}$
Fig. 3.6C: FRT 42D, ubi-GFP-ASPP-FA, $ASPP^{d}$ / $ASPP^{8}$
Fig. 3.6E: (additional to 6A–C): $ASPP^{2.93}$ / $ASPP^{1}$
Fig. 3.6F: male MS1096-GAL4; UAS-ASPP-HA / +
Fig. 3.6G: male MS1096-GAL4; UAS-ASPP-FA-HA / +
Fig. 3.6H: male MS1096-GAL4
Fig. 3.7A: $ASPP^{d}$ / $ASPP^{8}$; FRT 82B, Csk^{1jd8} / +
Fig. 3.7B: FRT 42D, ubi-GFP-ASPP-FA, $ASPP^{d}$ /$ASPP^{8}$; FRT 82B, Csk^{1jd8} / +
Fig. 3.7C: (additional to 7A and B) $ASPP^{d}$ / +; FRT 82B, Csk^{1jd8} / +
FRT 42D, ubi-GFP-ASPP, $ASPP^{d}$ /$ASPP^{8}$; FRT 82B, Csk^{1jd8} / +
Fig. 3.8B: control: $ASPP^{2.93}$ / $ASPP^{1}$
$ASPP^{-/-}$: $ASPP^{d}$ / $ASPP^{8}$
wt: FRT 42D, ubi-GFP-ASPP, $ASPP^{d}$ / $ASPP^{8}$
FA: FRT 42D, ubi-GFP-ASPP-FA, $ASPP^{d}$ / $ASPP^{8}$
Fig. 3.9A, A': ubi-GFP-PP1α87B (III)
Fig. 3.9B, B': ubi-GFP-PP1α96A (III)
Fig. 3.9C, C': PBac{681.P.FSVS}$flw^{CPTI001360}$
Fig. 3.10A: FRT 82B, ry^{506}, e^{1}, PP1α96A^{2}
Fig. 3.10B: flw^{1}
Fig. 3.10C,D: flw^{1}; FRT 82B, ry^{506}, e^{1}, PP1α96A^{2}
Fig. 3.11A: w^{iso}
Fig. 3.11B: flw^{1}; FRT 82B, ry^{506}, e^{1}, PP1α96A^{2}
Fig. 3.12: 96A2: FRT 82B, ry^{506}, e^{1}, PP1α96A^{2}
9C1: flw^{1}
double: flw^{1}; FRT 82B, ry^{506}, e^{1}, PP1α96A^{2}

Fig. 3.18A, A': ccdc85$^{C1.1}$ / Df(2L)Exel7014
Fig. 3.18B: P(GMR-GAL4)#12 / +; UAS-cd8-GFP / +
Fig. 3.18C: P(GMR-GAL4)#12/ UAS-ccdc85

Fig. 4.1A: yw eyFlp; FRT 82B, RASSF8^{6} / FRT 82B, ubi-GFP
Fig. 4.1B: yw eyFlp; FRT 82B, kib$^{\Delta 32}$ / FRT 82B, ubi-GFP
Fig. 4.1C: yw eyFlp; FRT 82B, kib$^{\Delta 32}$, RASSF8^{6} / FRT 82B, ubi-GFP
Fig. 4.1D: yw eyFlp; FRT 82B, crb$^{82\text{-}04}$ / FRT 82B ubi-GFP
Fig. 4.1E: yw eyFlp; FRT 82B, crb$^{82\text{-}04}$, RASSF8^{6} / FRT 82B, ubi-GFP
Fig. 4.1F: yw eyFlp; FRT 82B, crb^{8F105}, RASSF8^{6} / FRT 82B, ubi-GFP

Fig. 4.2A, A': yw eyFlp; ex^{697} ,FRT 40A / +; FRT 82B, RASSF8^{6} / FRT 82B, ubi-GFP
Fig. 4.2B, B': yw eyFlp; ex^{697} ,FRT 40A / +; FRT 82B, wts$^{M5.41}$ / FRT 82B, ubi-GFP
Fig. 4.2C, C': yw eyFlp; ex^{697} ,FRT 40A / +; FRT 82B, kib$^{\Delta 32}$ / FRT 82B, ubi-GFP
Fig. 4.2D, D': yw eyFlp; ex^{697} ,FRT 40A / +; FRT 82B, kib$^{\Delta 32}$, RASSF8^{6} / FRT 82B, ubi-GFP
Fig. 4.2E, E': yw eyFlp; ex^{697} ,FRT 40A / +; FRT 82B, crb^{11A22} / FRT 82B, ubi-GFP
Fig. 4.2F, F': yw eyFlp; ex^{697} ,FRT 40A / +; FRT 82B, crb^{11A22}, RASSF8^{6} / FRT 82B, ubi-GFP

Fig. 4.3A, A', D, D': yw hsFlp; FRT 82B, RASSF8^{6} / FRT 82B, ubi-GFP
Fig. 4.3B, B', E, E': yw hsFlp; FRT 82B, kib$^{\Delta 32}$ / FRT 82B, ubi-GFP
Fig. 4.3C, C', F, F': yw hsFlp; FRT 82B, kib$^{\Delta 32}$, RASSF8^{6} / FRT 82B, ubi-GFP

Fig. 4.7A, A': baz^{CC01941}; FRT 42D, ASPP^{d} / FRT 42D, ubi-mCherry

Fig. 4.8A, A': yw eyFlp; G454, Act>y+>GAL4, src-GFP / +; FRT 82B, crb$^{82\text{-}04}$ / FRT 82B, tub-Gal80
Fig. 4.8B, B': yw eyFlp; G454, Act>y+>GAL4, src-GFP / ASPP^{GD9567}; FRT 82B / FRT 82B, tub-Gal80
Fig. 4.8C, C': yw eyFlp; G454, Act>y+>GAL4, src-GFP / ASPP^{GD9567}; FRT 82B, crb$^{82\text{-}04}$ / FRT 82B, tub-Gal80

Fig. 5.4A, A', A": ubi-RASSF8, RASSF8^{6} / Df(3R)BSC321
Fig. 5.4A, A', A": ubi-RASSF8-SA, RASSF8^{6} / Df(3R)BSC321

Fig. 5.5A: en-GAL4/+; UAS-Wts (89e11)/+

Fig. 5.6A: w^{iso}
Fig. 5.6B: RASSF8^{6}/ Df(3R)BSC321
Fig. 5.6C: ubi-RASSF8, RASSF8^{6} / Df(3R)BSC321
Fig. 5.6D: ubi-RASSF8-SA, RASSF8^{6} / Df(3R)BSC321

Fig. 5.8A, A', A", C, C', C": ptc-GAL4/UAS-sina-Myc
Fig. 5.8B, B', B", D, D', D": ptc-GAL4/UAS-sina.ΔRING-Myc

Fig. 5.11A, A': w^{iso} **Fig. 5.11B, B':** P(GMR-GAL4)#12, ASPP^{GD9567}/+
Fig. 5.11C, C': P(GMR-GAL4)#12, ASPP^{GD9567}/+; Df(3L)BSC394/+
Fig. 5.11D, D': P(GMR-GAL4)#12, ASPP^{GD9567}/+; Df(3R)Exel6167/+
Fig. 5.11E, E': P(GMR-GAL4)#12, ASPP^{GD9567}/Df(2L)Exel6001
Fig. 5.11F, F': P(GMR-GAL4)#12, ASPP^{GD9567}/Df(2L)Exel6022

List of Tables

List of Abbreviations

AP-MS	Affinity Purification - Mass-Spectrometry
APF	After puparium formation
aPKC	atypical Protein Kinase C
Arm	Armadillo
aSC	anterior scutellar bristle
ASPP	Apoptosis stimulating protein of p53
ATP	Adenosine triphosphate
Baz	Bazooka
Ccdc	Coiled coil domain containing
Crb	Crumbs
Csk	C-terminal Src kinase
DAPI	4',6-diamidino-2-phenylindole
DGRC	Drosophila Genomics Resource Center
Dlg	Discs large
DNA	Deoxyribonucleic acid
Dpp	Decapentaplegic
Ds	Dachsous
dsRNA	double stranded RNA
Ecad	E-cadherin
Ed	Echinoid
EDTA	Ethylenediaminetetraacetic acid
EGFR	Epidermal growth factor receptor
En	Engrailed
Ex	Expanded
eyFlp	eyeless driven Flippase
FERM	4.1 protein, Ezrin, RadixinÊand Moesin
Fj	Four-jointed
Flp	Flippase
FRT	flippase recognition target
Ft	Fat
GDP	Guanosine diphosphate
GFP	Green fluorescent protein
GMR	Glass multiple reporter
GPCR	G protein-coupled receptor
HA	Human influenza hemagglutinin
Hh	Hedgehog
Hid	Head involution defective
Hpo	Hippo

HRP	Horseradish peroxidase
hsFlp	heat-shock promoter driven Flippase
I-2	Inhibitor 2
IOC	Interommatidial cell
IP	immunoprecipitation
JAM	Junctional adhesion molecule
Kib	Kidney and brain
LATS	Large tumour suppressor
LFQ	Label-free quantification
Lgl	Lethal giant larvae
MAGUK	Membrane-associated guanylate kinase
MARCM	Mosaic analysis with a repressible cell marker
Mats	Mob as a tumour suppressor
Mer	Merlin
MF	Morphogenetic Furrow
mRNA	messenger RNA
MST	Mammalian sterileÊ20-like kinase
MYPT	The myosin phosphatase targeting
Par	Partitioning defective
PBM	PDZ binding motif
PBS	Phosphate-buffered saline
PCP	Planar cell polarity
PCR	Polymerase chain reaction
PDZ	PSD95, Dlg1, ZO1
PP1	Protein phosphatase 1
PP2A	Protein phosphatase 2
PPP	Phosphoprotein phosphatase
PTP	Protein tyrosine phosphatases
RA	Ras association
RASSF	Ras association domain family
RIPA	Radioimmunoprecipitation assay
RNA	Ribonucleic acid
RNAi	RNA interference
S2	Schneider 2
Sav	Salvador
SCF	Skp, Cullin, F-box
Scrib	Scirbble
Sd	Scalloped
SEM	Scanning electron microscopy
SH3	Src homology 3
Sina	Seven-in-absentia
Sqh	Spaghetti Squash
Src	Sarcoma
TAZ	Tafazzin
TBS	Tris-buffered saline
TEAD	TEA domain

UAS	Upstream activating sequence
Ubi	Ubiquitin
UTR	Untranslated region
w	white
WAVE	WASP-family verprolin-homologous
Wts	Warts
YAP	Yes-associated protein
YFP	Yellow fluorescent protein
Yki	Yorkie

Chapter 1.

Introduction

In this PhD thesis I used the model organism *Drosophila melanogaster* to study the cellular function of a phosphatase complex. This introduction covers three main topics to provide the background of the thesis and introduce the challenges that I tried to address. Firstly, I will briefly outline the benefits of the model organism and describe the development of the *Drosophila* eye, the tissue I most frequently used. Secondly, I will cover the protein families that make up the phosphatase complex: the PP1 family that consists of catalytic phosphatase subunits, and the ASPP (Apoptosis stimulating protein of p53) and N-terminal RASSF (Ras Association Domain Family) families that are potential regulatory subunits. Lastly, I will portray the molecular context of two potential substrates of the complex: Hippo signalling for Yki/YAP/TAZ and apical-basal cell polarity for Baz/PAR3.

1.1. *Drosophila* as a model organism

Drosophila melanogaster, also known as the common fruit fly, has many advantages that make it a suitable model organism to study biological principles. Especially for genetic experiments, it has become a model of choice due to its short generation time and ease of maintenance. In this subchapter I will briefly describe the history and benefits of using *Drosophila* and provide more details on the development of the fly

eye. The aim of this subchapter is to motivate my choice of *Drosophila* as a model in general and the developing eye in particular.

1.1.1. *Drosophila* can be used to study principles of biology and human disease

A century ago, Thomas H. Morgan was studying spontaneous mutations in his *Drosophila* colonies and traced the inheritance of these mutations. Through this work, he discovered general principles of heredity, such as genetic linkage and sex-linked inheritance. His laboratory became known as the Fly Room (From Nobel Lectures 1965). Starting with his lab's early experiments, *Drosophila* was used to investigate basic principles of biology. Numerous mutants have been isolated that were first obtained from random events and later deliberately induced. These studies did not only provide insights into biology, but also supplied practical techniques for experimental handling and genetic manipulation of fruit flies. A notable example is the discovery that chromosomal inversions can suppress crossing over during meiosis (Dobzhansky 1931). Thus, it became possible to stably keep lethal mutations as heterozygotes through the use of "balancer chromosomes" with multiple inversions. Today, *Drosophila* geneticists can draw on an ever-expanding collection of tools to generate targeted mutant and transgenic flies (see Materials and Methods).

Additional to understanding fundamental principles of biology, the vast array of tools of *Drosophila* research can also be used to study human disease more directly. This can be done in two ways. Firstly, the function of genes that are conserved between humans and flies can be studied in *Drosophila*. With the complete sequencing of the *Drosophila* genome (Adams et al. 2000, Myers et al. 2000) it became apparent that about 60 % of all human genes that are disease associated are conserved in *Drosophila* (Chien et al. 2002). Function and genetic interactions with other genes can be uncovered in flies that are likely to be transferable to the human orthologues. However, the use of flies in medical research goes even beyond the study of orthologous genes. Although not immediately relevant for this thesis, *Drosophila* can be used to

directly test compounds in phenotype-based screening (Gasque et al. 2013) and for drug profiling (Dar et al. 2012).

Another benefit of *Drosophila* is its simpler genome. As an invertebrate, it often has fewer copies per gene, while vertebrates usually possess multiple copies due to two rounds of genome duplication events in early vertebrate evolution (Dehal and Boore 2005). For instance, in the case of *ASPP* and *ccdc85*, two genes I investigated in this thesis, I could study null mutant phenotypes in single mutants, instead of having to generate double or triple mutants in mice.

1.1.2. The *Drosophila* eye develops from an epithelial layer

To study the effect of mutants and transgenes, I have mostly used the developing pupal retina as a model tissue. The compound eye of *Drosophila* consists of about 750 hexagonally shaped individual subunits called ommatidia. The highly stereotypical arrangement of the adult eye is generated during larval and pupal development in waves of proliferation, differentiation and apoptosis (Wolff and Ready 1993). The adult eye is especially suited to the investigation of defects in proliferation, apoptosis and cell-cell contacts, as even minor defects can be easily detected as eye roughness when multiplied through the repeated ommatidial units. Thus, the adult eye has been extensively used to conduct large-scale genetic screens for perturbation in these processes.

Each of the light-sensing ommatidia consists of eight photoreceptor cells and supporting cells (Fig. 1.1 and 1.2C). Four lens-secreting cone cells sit immediately atop of the photoreceptor cells, which are surrounded by two primary pigment cells, six secondary pigment cells and three tertiary pigment cells. The pigment cells optically insulate neighbouring clusters of photoreceptor cells from stray light. In addition to the above-mentioned cells, three mechanosensitive bristle complexes can be found around each ommatidium. The secondary pigment cells are shared with one neighbouring ommatidium, while tertiary pigment cells and bristles are shared with two neighbouring ommatidia. The secondary and tertiary pigment cells are collectively referred to as interommatidial cells (IOCs).

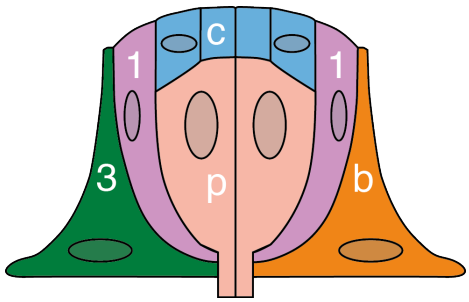

Figure 1.1.: Cross-section of an ommatidium during pupal development
Lens-secreting cone cells (c) sit atop of photoreceptor cells (p). Primary pigment cells (1) surround them. Further distal are secondary pigment cells (not visible in this view), tertiary pigment cells (3) and the bristle complex (b). Compare to Fig. 1.2C for X-Y section at the same developmental stage. Adapted with permission from Carthew 2007, copyright of original held by Elsevier.

During embryonic development, a cluster of around 20 cells are specified as an eye primordium under the control of the eye specification cascade (Kumar 2010), a complex gene regulatory network involving *eyeless* and *twin-of-eyeless*, which encode two paired domain/homeodomain transcription factors similar to vertebrate PAX6. This embryonic primordium invaginates to give rise to the larval eye-antennal imaginal disc, a bi-layered epithelial tissue composed of closely apposed layers: the pseudostratified disc proper and the squamous peripodial membrane. The eye-antennal disc produces the retina itself, as well as the antenna and head capsule. Cells within the eye disc proper (hereafter referred to as "eye disc") epithelium proliferate asynchronously during the first and second larval stages (or instars). During the third larval instar, cells begin to commit to specific fates. Differentiation starts from the posterior part of the imaginal disc in a physical indentation known as the morphogenetic furrow (MF), which sweeps anteriorly across the disc during the third instar (Treisman 2012). The MF is driven by the secreted morphogen Hedgehog, which promotes the localised expression of the Bone Morphogenetic Protein family member Decapentaplegic (Dpp). Hh and Dpp combine to initiate the expression of the pro-neural factor Atonal, which resolves to regularly spaced individual cells under the influence of Notch signalling, giving rise to the first photoreceptor R8 at regular intervals in the MF. Posterior

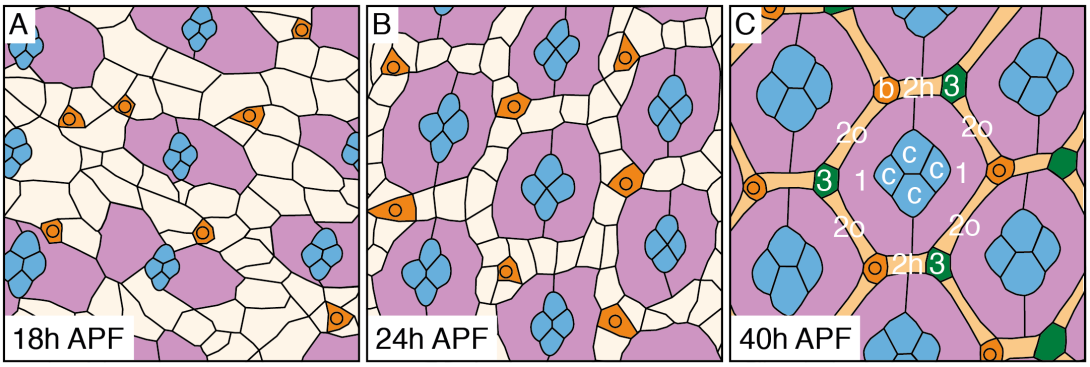

Figure 1.2.: During the pupal stage, supernumerary cells are eliminated by apoptosis

The illustrations depict the development of the pupal retina and are based on confocal images.

(A) At 18 h APF, the clusters that were already formed in the third instar larval stage have each recruited two primary pigment cells (purple). Bristle cells (orange) have been specified at this stage. In apical X-Y confocal sections, only the cone cells (blue) are visible, while all photoreceptor cells are basal of the cone cells and thus invisible.

(B) At 24 h APF, the undifferentiated cells (pale) that will become secondary and tertiary pigment cells have arranged into single layers between the pairs of primary pigment cells. Supernumerary IOCs are eliminated from the tissue by apoptosis in the following eight hours.

(C) At 40 h APF, the final pattern has formed. The different cell types are indicated: cone cells (c), bristles (b), primary pigment cells (1), secondary pigment cells (2o and 2h) and tertiary pigment cells (3). Secondary pigment cells can have a horizontal position (2h, contacting four primary pigment cells) or an oblique position (2o, contacting two primary pigment cells).

to the MF, pre-clusters of cells form by sequential recruitment of undifferentiated cells that will give rise to the other photoreceptors. A subset of cells not initially recruited to the pre-clusters undergo one last round of divisions (second mitotic wave) in the wake of the MF. At the end of the third larval instar, the cell clusters contain all photoreceptor cells and the four cone cells. By this time the photoreceptor cell bodies have descended basally, thus in confocal sections of the apical IOCs, the photoreceptors cannot be seen.

By 18 h after puparium formation (APF), the clusters have recruited two cells that will become primary pigment cells (Monserrate and Brachmann 2007). At the same time, bristles are specified (Fig. 1.2A). The bristles, like other invertebrate sensory organs, are comprised of a group of four cells (Cagan and Ready 1989). The four cells arise in three consecutive rounds of cell divisions. Out of those four cells, only the neuron and its glial cell survive in the adult animal (Perry 1968). Between 18 and 24 h APF, the remaining undifferentiated cells arrange themselves into a single layer between the pairs of primary pigment cells (Fig. 1.2B and Larson et al. 2008, Monserrate and Brachmann 2007). As the number of the undifferentiated cells still exceeds the number of cells required in the adult eye, cells begin to be eliminated by apoptosis. By 32 h APF, the final number of cells has been reached and secondary/tertiary pigment cells have attained their final positions (Monserrate and Brachmann 2007). Most often, the final arrangement is visualised at 40 h APF using cell membrane markers (Fig. 1.2C). 40 h is chosen, as the rearrangement has finished, but IOCs are still easily visualised. From this time point onwards, IOCs constrict their apical surface so that it becomes impossible to count them properly.

1.1.3. The compound eye can be used as a read-out for defects in cell-cell adhesion and apoptosis

The first type of defects that can affect the patterning of IOCs is the disruption of cell-cell contacts. This is due to the requirement for cell-adhesion molecules during remodelling of the tissue to form a single IOC layer. Between 18–24 h APF, Notch signalling (Bao 2014) and the immunoglobulin superfamily adhesion molecules Roughest

(Rst or Irregular Chiasm), Kirre (Kin of Irre), Hibris and Sns (Sticks'n'stone) (Bao and Cagan 2005, Bao et al. 2010) are important. Delta (Dl), the Notch ligand, is expressed in cone cells at 18 h APF, leading to higher Notch levels in primary pigment cells (Bao 2014). In these cells, Notch enhances the expression of Hibris and Sns, while decreasing the expression of Rst and Kirre. Thus, primary pigment cells express Hibris/Sns, while IOCs express Rst/Kirre (Bao and Cagan 2005, Bao et al. 2010) due to an unknown mechanism. Rst and Kirre preferentially bind in trans to Hibris and Sns, forming trans-heterodimers (Bao and Cagan 2005, Bao et al. 2010). This leads to the preferred formation of cell-cell contacts between primary pigment cells and IOCs. Furthermore, while the contact surface between primary pigment cells and IOCs are maximised, the inter-IOC contacts are minimised. As a result, a single layer of IOCs forms between primary pigment cells (Bao and Cagan 2005).

Particularly striking is the minimisation of inter-IOC contacts when the single layer is initially formed. For a brief period of time, IOCs have elliptically shaped apical profiles. Inter-IOC contacts shrink to points (Bao and Cagan 2005). This is also the stage where cell contacts and junctions are very dynamic, as small perturbations can cause gaps in adherens junctions (Langton et al. 2009). At the same time, adherens junctions and particularly E-Cadherin (Grzeschik and Knust 2005) are required for the correct localisation of Rst/Kirre/Hibris/Sns. Any disruption to the adherens junctions (Grzeschik and Knust 2005), or to any of the four adhesion molecules leads to the failure of forming a single layer of IOCs (Bao and Cagan 2005, Bao et al. 2010). In the case of disrupting Rst, Kirre, Hibris or Sns, superfluous IOCs do not undergo apoptosis (Bao et al. 2010). However, it is not entirely clear why apoptosis fails. One possibility is that intact junctions are required for the transmission of a death signal.

The second type of defect that can interrupt the patterning of the fly eye is by directly modifying the propensity of IOCs to undergo apoptosis. Based on cell-ablation experiments, it has been proposed that primary pigment cells secrete Spitz, an EGFR (Epidermal Growth Factor Receptor) ligand that promotes the survival of IOCs through the inhibition of the pro-apototic Hid protein (Miller and Cagan 1998, Monserrate and Brachmann 2007). Direct mutation of *hid* (Bao et al. 2010) as well as

genes of the Hippo pathway (see 1.4) that promote apoptosis such as *kibra* (Genevet et al. 2010, Yu et al. 2010) also lead to the survival of IOCs, resulting in supernumerary cells at 40 h APF. The molecular nature of the signal that determines which IOCs undergo apoptosis is unclear. However, being adjacent to bristle cells and in a horizontal position (for definition see Fig 1.2C) increases the chance of an IOC undergoing apoptosis (Monserrate and Brachmann 2007).

1.2. Protein dephosphorylation

Proteins can undergo various post-translational modifications (e.g., phosphorylation, ubiquitylation and acetylation) which can modulate their function, stability or subcellular localisation. Phosphorylation, or the transfer of γ-phosphate from ATP, is one of the best studied and is involved in regulatory steps of all key cellular functions, Protein phosphorylation is highly dynamic due to its reversibility, leading to a balance between phosphorylation, which is catalysed by protein kinases and dephosphorylation, which is catalysed by phosphoprotein phosphatases. In this subchapter, I will give a broad overview of different families of protein phosphatases and a more detailed description of the PP1 family with an emphasis on the importance of regulatory subunits in PP1 complexes.

1.2.1. Protein phosphorylation regulates many cellular processes

Most commonly, serine, threonine and tyrosine residues are phosphorylated to form phosphomonoesters. Among these three residues, in humans, 86 % are phosphoserines, followed by 12 % phosphothreonines and 3 % phosphotyrosines (Olsen et al. 2006). Although this thesis is only concerned with serine and threonine phosphorylation, further residues can phosphorylated. In bacteria, histidine and aspartate are phosphorylated, as part of two-component signal transduction (Stock et al. 2000) and at least theoretically, phosphorylation of cysteine, arginine, lysine and glutamate are possible.

Phosphorylation as a reversible modification to adjust enzyme activity was first studied by Fischer and Krebs (Fischer and Krebs 1955). They discovered that a kinase, the enzyme that catalyzes the transfer of the γ-phosphate, is required to activate phosphorylase. To reverse the activation, the phosphate on phosphorylase can be hydrolyzed (dephosphorylation) with the help of a phosphatase (Cori and Cori 1945).

Today, many more functions of protein phosphorylation are known. The following three examples that involve proteins mentioned in this thesis only scrape at the surface of the diverse spectrum of functionality. (i) In addition to activating enzymes as in the case of phosphorylase, phosphorylation can also inhibit enzymatic activity, for example when the kinase Src is phosphorylated (Okada et al. 1991) by C-terminal Src kinase (Csk). (ii) Furthermore, phosphorylation can generate new protein binding surfaces, as it adds negative charges and bulk. For instance, 14-3-3 adaptor proteins specifically bind to phosphorylated proteins (Muslin et al. 1996). (iii) Phosphorylation can also influence the cellular localisation of proteins. For example Bazooka (Baz), a polarity determinant, can be excluded from the baso-lateral membrane of epithelial cells, when it is phosphorylated by Par1 (Benton and St Johnston 2003). From this incomplete list of functions it already becomes clear that both proteins phosphorylation and dephosphorylation must be carefully calibrated.

1.2.2. Serine/threonine phosphatases form protein complexes with regulatory subunits

The number of kinases and phosphatases within the human genome provides an interesting view on the balance between phosphorylation and dephosphorylation. For tyrosine phosphorylation, the scoreboard is even. There are 90 kinases (Manning et al. 2002) and 107 phosphatases (Alonso et al. 2004) in humans. Assuming a roughly commensurate specificity and number of substrates, this would equalise the action of kinases and phosphatases. However for serine/threonine phosphorylation, the numbers are not comparable. While there are 428 kinases (Manning et al. 2002), only about 40 phosphatases exist (Bollen et al. 2010). This apparent conundrum

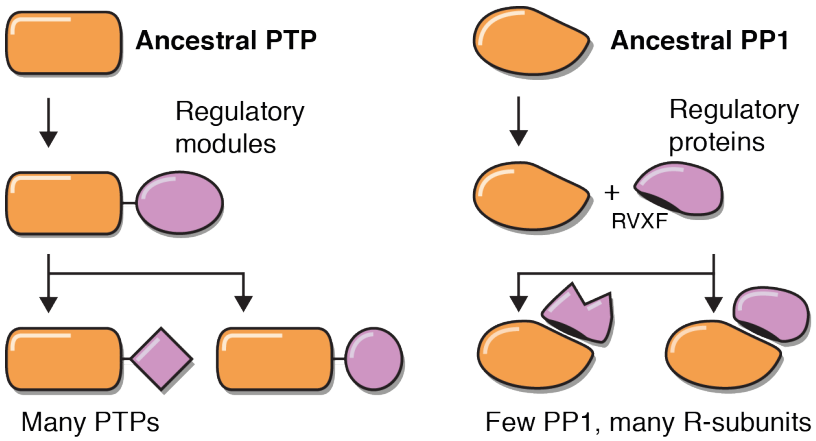

Figure 1.3.: PP1s non-covalently associate with regulatory subunits
During evolution, protein tyrosine phosphatases (PTPs) acquired regulatory modules that are fused to the catalytic domain. Thus, with novel substrates and regulatory requirements, more copies of PTPs were kept in the genome. The family of PP1 serine/threonine phosphatases in contrast binds to regulatory subunits non-covalently. Thus, only few PP1s, but many more PP1 regulatory proteins can be found in genomes. Adapted with permission from Moorhead et al. 2009, copyright of original held by Portland Press.

in numbers is solved when taking into account the different domain architectures. While tyrosine phosphatases have evolved as fusion proteins of regulatory domains attached to catalytic domains, many serine/threonine phosphatases just consist of the catalytic domain (Moorhead et al. 2009). The specificity of serine/threonine phosphatases is maintained by separate regulatory subunits that bind to the catalytic subunit non-covalently (Fig. 1.3). Thus, taking the regulatory subunits into account, there are probably several hundred serine/threonine phosphatase complexes (Heroes et al. 2013) to counterbalance the 428 kinases.

1.2.3. The PPP family shares the same catalytic core residues, but differs in holoenyzme composition

The group of serine/threonine phosphatases can be divided into three families that have arisen separately during evolution: phosphoprotein phosphatases (PPPs), metal-dependent protein phosphatases (PPMs) and FCP/SCP (TFIIF-associating compo-

nent of RNA polymerase II C-terminal domain CTD phosphatase/small CTD phosphatase) family phosphatases (Shi 2009). While PPPs and PPMs use divalent metal cations to activate a water nucleophile for hydrolysis of the phosphate, FCP/SCP family phosphatases rely on a conserved aspartate as the initial nucleophile.

The main interest of this thesis is PP1, a highly conserved group of phosphatases belonging to the PPP family. PP1 is only one out of the seven groups that comprise the PPP family. Other groups are: PP2A, PP2B/Calcineurin, PP4, PP5, PP6 and PP7 (Shi 2009). All groups share the same catalytic core residues. Within each group, conservation between species is very high, so that for example human PP1 can replace its yeast orthologue (Gibbons et al. 2007). This suggests that evolution is acting on the regulatory subunits to change or extend the range of substrates, rather than on the catalytic subunits (Moorhead et al. 2009).

The best-studied groups among the seven are PP1, PP2A and PP2B/Calcineurin. The main difference between these groups is that while PP1 has nearly 200 potential regulatory subunits that share little similarity with each other (Heroes et al. 2013), PP2A and PP2B/Calcineurin holoenzymes (referring to the ensemble of catalytic subunit, regulatory subunit and other scaffolds) have a very stereotypical complex composition.

The PP2A complex is a heterotrimer that consists of the catalytic or C subunit, a scaffold (A subunit) and a regulatory or B subunit (Shi 2009). There are four families of B subunits; each is comprised of several isoforms. PP2B/Calcineurin is also a heterotrimer (Shi 2009). The core enzyme consists of a catalytic subunit (Calcineurin A) and a regulatory subunit (Calcineurin B). Several different isoforms of the catalytic and regulatory subunits exist. Additionally, for full activity, binding to a Ca^{2+}-bound Calmodulin scaffold is required.

1.2.4. The PP1 catalytic subunit associates with different regulatory proteins to increase substrate specificity

From the disproportionately low number of serine/threonine phosphatases in comparison to kinases, it is clear that the catalytic subunit alone cannot provide sufficient

specificity. This is indeed the case for PP1 (Bollen et al. 2010, Peti et al. 2013). Unlike kinases with defined substrate consensus sites, PP1 does not recognize any sequence specific pattern. Moreover, small peptides derived from bona fide substrates are not efficiently dephosphorylated by PP1, suggesting that other features of the full-length substrates must be important (Bollen et al. 2010).

Specificity for PP1 is provided by regulatory subunits that directly bind to the catalytic subunit. They promote activity either by localising PP1 in proximity to its substrate and/or by directly modifying the substrate binding surface of PP1 (Bollen et al. 2010). There are two known mechanism of how substrate specifying subunits work. (i) Neurabin/Spinophilin (Dancheck et al. 2011, Ragusa et al. 2010) and PNUTS (Choy et al. 2014) achieve selectivity by sterically hindering non-specific substrates from accessing the active site of PP1. (ii) In contrast, MYPT1 (Terrak et al. 2004) and NIPP1 (O'Connell et al. 2012) extend the substrate binding site of PP1 and modify its electrostatic properties. None of these interactors have any influence on the conformation of PP1. They only change substrate specificity by increasing or decreasing PP1/substrate binding surfaces.

While the above mentioned regulators do not block the active site, like most other PP1 regulators (Hendrickx et al. 2009), they are able to reduce the activity of PP1 towards non-specific substrates, such as phosphorylase, without any detrimental effect on their bona fide substrates. However, there is a small group of regulators that are also termed inhibitors, which can block the activity of PP1 completely. At least some of them, namely I-2 (Hurley et al. 2007) and CPI-17 (Eto et al. 2007) achieve this by blocking the active site of PP1, thus barring substrates from accessing the catalytic core.

1.2.5. Binding to PP1 is facilitated by different binding motifs

With the discovery of the first few PP1 interactors, it became apparent that they shared little sequence similarity. However, small regions that confer binding to PP1 could be identified (Johnson et al. 1996). One of those regions corresponds to the RVXF motif, a binding motif that can be found in most of the known PP1 interactors.

The definition of the RVXF motif has undergone several rounds of refinements (Hendrickx et al. 2009, Meiselbach et al. 2006, Wakula et al. 2003). Based on biochemical binding assays for PP1 interactors, a good compromise between specificity and sensitivity is the five residue [KR][KR][VI]{FIMYDP}[FW] definition (Hendrickx et al. 2009)—in curly brackets are the residues that are disallowed. Basic residues are often found N-terminally and acidic residues C-terminally of the motif (Egloff 1997, Hendrickx et al. 2009).

Other motifs that have been described are far less common. Only few PP1 interactors share the SILK motif (Hendrickx et al. 2009, Huang et al. 1999), the MyPhoNE motif (Hendrickx et al. 2009, Terrak et al. 2004) or the ΦΦ/ΦΦ-R motif (Choy et al. 2014). The SILK motif, defined as [GS]IL[KR], is found in I-2 (Huang et al. 1999) and six other PP1 interactors, N-terminally of the RVXF motif (Hendrickx et al. 2009). MyPhoNE, or myosin phosphatase N-terminal element, is found in MYPT1 (Terrak et al. 2004) and six additional PP1 interactors (Hendrickx et al. 2009). As with the SILK motif, the MyPhoNE motif is only found N-terminally of the RVXF motif (Terrak et al. 2004). The ΦΦ motif (O'Connell et al. 2012) or its extended version, ΦΦ-R (Choy et al. 2014), which includes an additional arginine residue, is found C-terminally of the RVXF motif in four PP1 interactors.

1.2.6. Multiple motifs can increase binding affinity to PP1

All motifs described are binding to distinct surfaces of PP1 that are remote of the catalytic site (Choy et al. 2014, Hurley et al. 2007, Terrak et al. 2004). Thus, they serve as anchors for binding without changing the conformation of PP1, or inhibiting its catalytic activity (Peti et al. 2013). The stability of the PP1 conformation seems to be a more general feature, as binding to small molecule inhibitors that attach to the catalytic core also does not change the PP1 conformation (Kelker et al. 2009, Kita et al. 2002, Maynes et al. 2001 2006, Ragusa et al. 2010).

Due to the distinct binding sites of the motifs, a combination of different motifs can be used to engage a single PP1 subunit. This fact can also aid in identifying novel PP1 interactors. As each motif is too short to be specific enough for genome wide

searches for PP1 interactors, several motifs combined could increase the sensitivity and specificity of the search (Heroes et al. 2013). Discovering further PP1-binding motifs will make database searches more specific. Having more than one binding motif can also increase the affinity between PP1 and its interactors (Hendrickx et al. 2009).

1.2.7. Substrate targeting subunit and inhibitor can bind to PP1 simultaneously

An added layer of complexity is that substrate targeting subunit and inhibitor can bind to PP1 at the same time. The formation of this type of trimeric complex has been shown for GADD34/I-1/PP1 (Connor et al. 2001), Neurabin/I-2/PP1(Terry-Lorenzo et al. 2002) and Sds22/I-3/PP1 (Lesage et al. 2007). Initially, these complexes were not thought to be possible, as most regulatory subunits rely on their RVXF motif to bind to PP1 that can only engage with one RVXF motif at a time. However, it has been structurally shown that at least in the case of Neurabin/I-2/PP1, I-2 uses it SILK motif instead of its RVXF motif for binding to PP1 when Neurabin is present (Dancheck et al. 2011). The trimeric Neurabin/I-2/PP1 complex is normally inactive, as I-2 inhibits PP1. Only upon phosphorylation of I-2 (Hemmings et al. 1982), it is released from the catalytic core of PP1 and PP1 activity is restored. Thus, the complex can be switched on and off quickly depending on other signalling events.

The flexibility of I-2 to switch between its canonical binding mode via its RVXF motif and the SILK-only binding mode within the trimeric Neurabin/I-2/PP1 complex is facilitated by the intrinsically disordered nature of I-2 (Dancheck et al. 2011). I-2 belongs to the group of intrinsically disordered proteins (IDPs) that do not have a defined tertiary structure and only become folded when bound to interacting proteins (Tompa 2005). As some estimates assign 70 % of all PP1 interactors as partially disordered (Bollen et al. 2010), it is possible that this sort of trimeric complex between substrate specifying subunit, inhibitor and PP1 is widespread.

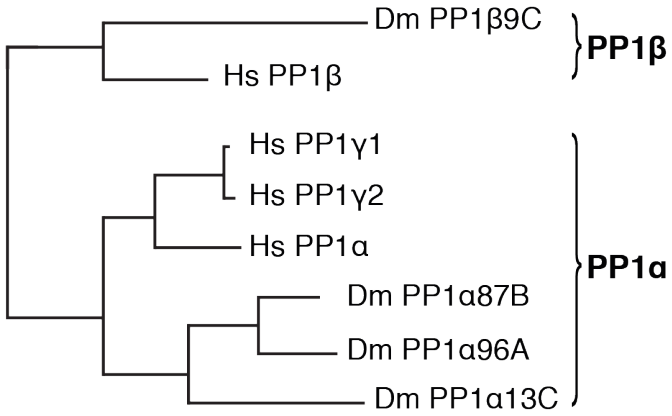

Figure 1.4.: PP1s can be grouped into PP1αs and PP1βs

Distance tree based on alignment between human and Drosophila PP1s. There are two large groups of PP1s, PP1αs and PP1βs. The distance tree was generated using BioNJ (Gascuel 1997) and was based on an alignment created by ClustalW (Larkin et al. 2007). The length of the branches corresponds to the distance between the sequences.

1.2.8. Humans and *Drosophila* have several PP1 isoforms that are highly conserved

In humans, there are four PP1 isoforms, PP1α, PP1β, PP1γ1 and PP1γ2 (Bollen et al. 2010). The difference between the isoforms is very small. Only few residues are different, mostly at the N- and C-termini. Most regulatory subunits do not distinguish between the isoforms and bind to all with similar affinities. A notable exception is MYPT1, the myosin phosphatase targeting subunit, which preferentially binds to PP1β (Hurley et al. 2007, Scotto-Lavino et al. 2010, Terrak et al. 2004).

In *Drosophila*, there are four PP1 isoforms, PP1α13C, PP1α87B, PP1α96A and PP1β9C (Dombrádi et al. 1990 1993). The three *Drosophila* PP1αs are orthologous to the human PP1α and PP1γ1/2 isoforms, while PP1β9C is more similar to human PP1β (Fig. 1.4). Unusually, *Drosophila* PP1α13C and PP1α87B have short C-termini not found in other organisms (Fig. 3.1D). In *Drosophila*, two regulatory subunits are known to bind to a subset of catalytic isoforms. MYPT-75D, the ortholog of human MYPT1, preferentially binds to PP1β9C (Vereshchagina et al. 2004) and Uri,

a chaperone, binds to all three PP1α isoforms, but not to PP1β9C (Kirchner et al. 2008).

1.2.9. Current challenges and outlook

The biggest challenge in the field of PPPs is the identification of bona fide substrate/phosphatase pairs (Brautigan 2013). Especially for PP1 substrates, the identification of the regulatory subunit is the crucial step, as the catalytic subunit displays no specificity. A complete description of substrate/phosphatase pairs additionally requires to include scaffolds that localise the PP1 holoenzyme, inhibitors and further regulatory mechanisms that modify phosphatase activity.

Two obstacles complicate the identification of novel PP1 holoenzymes and their biological substrates. (1) Firstly, in contrast to protein tyrosine phosphatases (PTPs), no substrate trapping mutants (Blanchetot et al. 2005) can be generated for PP1s. In PTP substrate trapping mutants, the enzymatic activity is lost, but substrate-binding capability is preserved. Thus, affinity purification of these mutants readily co-purify substrates. The reason why PTP trapping mutants can be generated is that the first nucleophile is a cysteine residue. When mutated to serine, catalytic function is eliminated, while the overall tertiary structure is preserved. However, PPPs in contrast rely on divalent metal cations as first nucleophiles. Thus, mutations that affect the binding of the metals will always have consequences for the structural integrity of the protein. (2) Secondly, as with other enzymes that remove post-translational modifications, such as deubiquitinating enzymes, it is helpful if a reliable source of a modified (phosphorylated) substrate is established first. Optimally, a kinase for specific phosphorylation sites should be known. In most cases, neither condition is fulfilled.

Ultimately, identifying novel PP1 regulatory subunits means that small molecule drugs could be developed that target specific PP1 holoenzymes. This could prove to be superior to inhibiting or activating (Reither et al. 2013) the PP1 catalytic subunit, which obviously can lead to unspecific side-effects. As a proof-of-principle, PP1 regulatory subunits have been successfully targeted by small molecules in phenotype-

based screens (Boyce et al. 2005, Tsaytler et al. 2011). With increased knowledge of PP1 holoenzymes, target-based approaches with specific PP1 substrates in mind might be used in the development of novel PP1 inhibitors and activators.

1.3. ASPP and N-terminal RASSF family proteins

ASPP (Apoptosis-stimulating protein of p53) family proteins are primarily known for their regulation of p53-dependent transcription, while N-terminal RASSF family proteins have been described as potential tumour suppressors or oncoproteins, but are not well studied. Previous work from our lab showed a connection between these two protein families. *Drosophila* ASPP and RASSF8 form a complex at cell-cell junctions to maintain junctional integrity. In this subchapter, I will describe what is known about these two protein families, as they are potential regulatory subunits of a PP1 complex.

1.3.1. The ASPP family of proteins is characterised by ankyrin repeats and an SH3 domain

ASPP family proteins are characterised by two conserved regions (Fig. 1.5). The N-terminal region contains coiled coils and the C-terminal region contains four ankyrin repeats and an SH3 domain. There are three members of this family in humans, ASPP1/2 (Samuels-Lev et al. 2001) and iASPP (inhibitor of ASPP) (Bergamaschi et al. 2003), while *Drosophila* has only one orthologue, ASPP (Langton et al. 2007).

ASPP1 and ASPP2 have an additional globular domain at their N-terminus that structurally resembles the Ras-association (RA) domain of human RASSF8 (Tidow et al. 2007). RA domains belong to the ubiquitin-fold family and some RA domains bind to the small GTPases of the Ras family (Wohlgemuth et al. 2005). To predict if RA domains are able to bind to Ras family proteins, modelling based on structures containing RA domain/Ras complexes can be used (Chan et al. 2013, Kiel et al. 2007). However, although modelling suggested that the RA-like domain of ASPP1/2 could

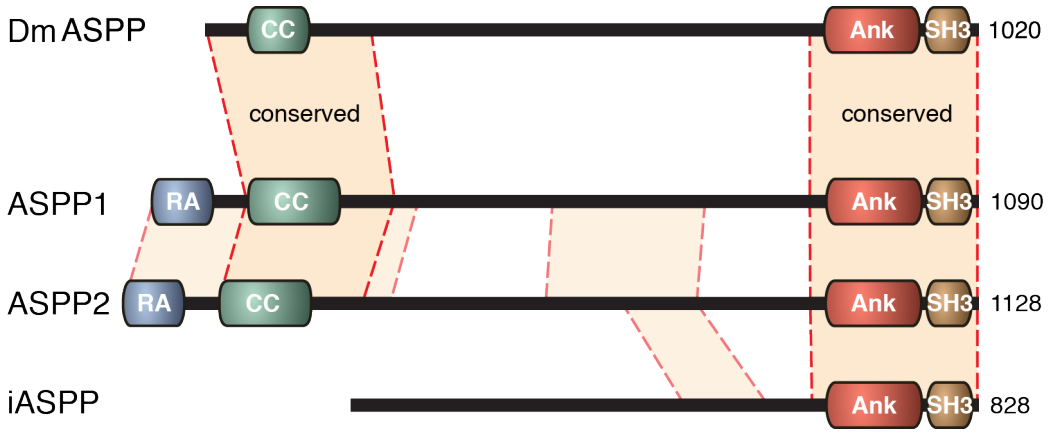

Figure 1.5.: The N- and C-termini are conserved between human ASPP1/2 and *Drosophila* ASPP

Domain structure of ASPP family proteins in Drosophila and humans. The *Drosophila* ASPP N-terminus is conserved in ASPP1/2, while its C-terminus is conserved in all three human ASPP family members. Coiled coil regions were predicted by jpred3 (Cole et al. 2008). Although the predicted coiled coil regions are of different length, they share high sequence similarity, suggesting a similar tertiary structure. The RA-like domain of ASPP1/2 annotation is based on the ASPP2 N-terminus structure (Tidow et al. 2007). Four ankyrin repeats and SH3 domain annotation based on ASPP2 structure (Gorina and Pavletich 1996).

not bind to Ras (Tidow et al. 2007), two recent studies have shown the opposite (Wang et al. 2013a, Wang et al. 2013b).

1.3.2. ASPP family proteins regulate p53 dependent transcription

The ASPP family is primarily known for their regulation of p53 dependent transcription of pro-apoptotic genes (Bergamaschi et al. 2003, Samuels-Lev et al. 2001). The binding between ASPP family proteins and p53 was first described for p53BP2, a truncated form of ASPP2 (Iwabuchi et al. 1994). This binding requires the ankyrin repeats and the SH3 domain of p53BP2. This was confirmed by a co-crystal structure of p53BP2 and p53 (Gorina and Pavletich 1996).

Later, ASPP1 (Samuels-Lev et al. 2001) and iASPP (Bergamaschi et al. 2003) were described as additional p53 interacting partners. While ASPP1/2 promote the

transcription of p53 targets that are pro-apoptotic, such as *BAX* and *PIG3*, they do not alter the transcription level of cell cycle arrest genes such as $p21^{WAF1}$ (Samuels-Lev et al. 2001). iASPP, as its name suggests, works antagonistically to ASPP1/2, by competing with ASPP1/2 for binding to p53 (Bergamaschi et al. 2003, Slee et al. 2004). Once bound to p53, iASPP inhibits the transcription of pro-apoptotic p53 target genes (Bergamaschi et al. 2003). The ASPP family proteins not only bind and regulate p53, but also other p53 family proteins, namely p63 and p73 (Bergamaschi et al. 2003, Canning et al. 2012).

It is interesting to note that ASPP1 and ASPP2 have different functions in vivo (see below). However, in most experiments in vitro, they are treated as equal and show perfect interchangeability in many cell culture experiments (e.g., Samuels-Lev et al. 2001, Wang et al. 2013b).

1.3.3. iASPP and p63 are important for the homeostasis of the epidermis

In contrast to the other ASPP family members, iASPP does not share a conserved N-terminal region (Fig. 1.5). Thus, *Drosophila* ASPP is more likely to be a functional equivalent of ASPP1/2. However, iASPP is more ancient than the split between vertebrates and invertebrates, as *Caenorhabditis elegans* has an iASPP orthologue (Ce-iASPP), but no obvious ASPP1/2 orthologue (Bergamaschi et al. 2003). Since ASPP1/2 are more closely related to *Drosophila* ASPP, I will primarily describe ASPP1/2 in this introduction and only briefly mention what is known about iASPP in this subsection.

Originally, iASPP was described to bind to the transcription factor RelA/p65 (Yang et al. 1999). Although, this was confirmed independently (Herron et al. 2005), it is not clear whether this interaction is important in vivo (Notari et al. 2011). Instead, an important function of iASPP seems to be the regulation of p63 in stratified epithelia (Chikh et al. 2011, Notari et al. 2011). iASPP is co-expressed with p63 in the proliferating basal layer of the epidermis and loss of iASPP leads to the premature differentiation of keratinocytes (Chikh et al. 2011, Notari et al. 2011). Spontaneous

mutations in *iASPP* that were found in mice and cattle lead to defects of the skin, heart and hair, supporting the idea that iASPP is important for the homeostasis of the epidermis (Herron et al. 2005, Simpson et al. 2009, Toonen et al. 2012). It is interesting to note that ASPP2 in contrast is required in differentiated keratinocytes of the apical layers of the epidermis. ASPP2 prevent the formation of squamous cell carcinomas by blocking the expression of p63 in differentiated keratinocytes (Tordella et al. 2013). Thus, in the epidermis at least, although ASPP2 and iASPP have antagonistic functions, they do not act within the same cell to regulate p53 family dependent transcription.

1.3.4. ASPP1/2 have p53 independent functions in vivo

ASPP family proteins have p53 family independent functions as well. This is most apparent in *ASPP1* mutant mice (Hirashima et al. 2008). If ASPP1/2 were key activators of p53, loss of *ASPP1/2* would be expected to cause some phenotypic similarity compared to *p53* mutant mice. *p53* deficient mice are highly tumour prone (Donehower et al. 1992) and show various developmental defects (Armstrong et al. 1995, Rotter et al. 1993, Sah et al. 1995). In contrast, *ASPP1* mutant mice do not develop tumours and only show defects during the establishment of the lymphatic system (Hirashima et al. 2008), a phenotype that is not observed in *p53* deficient mice. Furthermore, *p53* deficiency in *ASPP1* null mutant mice does not worsen the lymphatic phenotype (Hirashima et al. 2008), suggesting that in vivo, ASPP1 has p53 independent functions.

ASPP2 heterozygous mutant mice are more tumour prone (Kampa et al. 2009, Vives et al. 2006), suggesting that this might be due to misregulation of p53. However, the two different mutants that were generated differ in their propensity to genetically interact with *p53*. While in the case of the deletion of exon 3, *p53* heterozygosity increased tumour susceptibility (Vives et al. 2006), in the other case (deletion of exon 10–17), it did not (Kampa et al. 2009). Additionally, targeting of exon 3 was only semi-lethal and a small number of homozygous mutants were born (Vives et al. 2006), while the bigger deletion proved to be lethal in early embryogenesis (Kampa et al.

2009). Although these results support a tumour-suppressing role of ASPP2, they also suggest that ASPP2 has p53-independent functions.

1.3.5. ASPP1/2 have many binding partners other than p53

The array of different binding partners that have been found for ASPP1/2 suggest what these p53-independent functions might be (Kampa et al. 2009). In this subsection, I will focus on four aspects: (i) Regulation of oncogenic Ras-induced senescence, (ii) regulation of the Hippo pathway, (iii) regulation of cell-cell junctions and (iv) the association with PP1.

Oncogenic Ras-induced senescence depends on ASPP2

Oncogenic Ras can induce senescence, a state of irreversible growth arrest, in non-transformed cells (Campisi and d'Adda di Fagagna 2007). This is dependent on ASPP2, but independent of p53 (Wang et al. 2011d). The N-terminus of ASPP2 plays an important role as it contains the RA-like domain that can directly bind to oncogenic Ras (Wang et al. 2013a, Wang et al. 2013b). The requirement of the RA-like domain is also observed in a mouse tumour model, where *ASPP2* mutant fibroblasts that expressed oncogenic Ras were injected into the flanks of nude mice. The RA-like domain of ASPP2 alone inhibits Ras-induced tumour growth as effectively as full length ASPP2 (Wang et al. 2012).

Although ASPP2 activates the Ras/Raf/ERK pathway (Wang et al. 2013a, Wang et al. 2013b) the main effector for oncogenic Ras, several observations suggest a more complicated model than a linear ERK activation by ASPP2 leading to senescence. Firstly, there is feedback regulation: ASPP1/2 and p53-dependent transcription is enhanced by oncogenic Ras (Wang et al. 2013a), which might be partially due to the activating phosphorylation of ASPP2 by ERK (Godin-Heymann et al. 2013). Secondly, the N-terminus of ASPP2 can also bind to ATG5/ATG12 (Autophagy5/Autophagy12), thereby preventing Ras-induced autophagy and promoting Ras-induced senescence (Wang et al. 2012). However, the relationship between autophagy and senescence are not entirely clear (Gewirtz 2013).

Although the mechanistic details require further work, there is at least a consensus that ASPP2 is required for oncogene-induced senescence and thus acts as a tumour suppressor in this context. In the next subsection, I will introduce the interaction of ASPP1/2 with members of the Hippo pathway. In this case, it is not yet clear whether ASPP1/2 act as tumour suppressors or oncoproteins.

ASPP1 interacts with core components of the Hippo pathway

YAP (Yes-activated protein), a transcriptional co-activator and core member of the Hippo pathway (see 1.4.2) has been described to directly bind to p53BP2, the ASPP2 fragment (Espanel and Sudol 2001). An interaction between YAP and ASPP2 was also found in several recent proteomics experiments (Couzens et al. 2013, Hauri et al. 2013, Kohli et al. 2014, Wang et al. 2014). The YAP paralogue TAZ (transcriptional co-activator with PDZ-binding motif) (see 1.4.2) can also bind to ASPP2 (Liu et al. 2011). Additionally, it was shown that the Hippo pathway downstream kinases LATS1 and LATS2 could bind to and phosphorylate ASPP1 (Aylon et al. 2010, Vigneron et al. 2010).

Despite this mounting evidence of binding between ASPP family proteins and members of the Hippo pathway, there is no overarching model for the biological function of these interactions. On the one hand it was proposed that ASPP1 might have a pro-apoptotic role (Aylon et al. 2010). ASPP1 is phosphorylated by LATS2, in the presence of oncogenic Ras and translocates to the nucleus to drive the expression of p53 dependent pro-apoptotic genes.

On the other hand ASPP family proteins might also have an anti-apoptotic role (Liu et al. 2011, Vigneron et al. 2010). ASPP1 can decrease the S127 phosphorylation of YAP, leading to nuclear YAP accumulation (see 1.4.2) and an increase in YAP-dependent (anti-apoptotic) transcription (Vigneron et al. 2010). Although Vigneron et al. suggest that ASPP1 acts through competing with LATS2 to decrease YAP S127 phosphorylation (Vigneron et al. 2010), an alternative model could also explain this observation: ASPP1 could dephosphorylate YAP S127 directly as part of a phosphatase complex. This alternative model was proposed for the ASPP2/PP1

complex, which can dephosphorylate TAZ on S89, the equivalent site to YAP S127 (Liu et al. 2011 and see 1.4.3). However, this pro-growth function in antagonising the LATS1/2 tumour suppressor is not consistent with the idea that ASPP2 acts as a tumour suppressor in vivo (Kampa et al. 2009, Vives et al. 2006).

ASPP2 interacts with the polarity determinant PAR3 and is required for the de novo formation of tight junctions

Another layer of complexity in ASPP function was added when ASPP2 and *Drosophila* ASPP were found at tight junctions (Cong et al. 2010, Sottocornola et al. 2010) and adherens junctions (Langton et al. 2009) respectively. In *Drosophila*, ASPP is required for proper adherens junction formation during retinal morphogenesis (see 1.3.9). Similarly, mammalian tight junction formation requires ASPP2, which binds to and recruits PAR3 to nascent cell-cell contacts (Cong et al. 2010, Sottocornola et al. 2010). Upon ASPP2 depletion, cells in culture cannot form a proper impermeable epithelial monolayer, similar to loss of PAR3 (Cong et al. 2010). Loss of ASPP2 in vivo, also causes defects in apical-basal polarity in the retina and neuroepithelium (Sottocornola et al. 2010).

ASPP family proteins directly bind to PP1 via their RVXF motifs

All members of the human ASPP family can also bind to PP1 (Helps et al. 1995, Liu et al. 2011, Llanos et al. 2011, Skene-Arnold et al. 2013). ASPP1 and ASPP2 bind to PP1 via a canonical RVXF motif (Egloff 1997, Llanos et al. 2011, Skene-Arnold et al. 2013). In contrast, iASPP does not have an RVXF motif. Whether the degenerate motif in iASPP that aligns to the RVXF motif of ASPP1/2 could bind to PP1 in a similar manner as the canonical motif is unclear (Llanos et al. 2011, Skene-Arnold et al. 2013).

As interactors of PP1s, ASPP family proteins could act as regulatory subunits for the catalytic PP1 subunit. In this case, any protein that binds to ASPP family proteins might form a trimeric complex with ASPP and PP1 and undergo dephosphorylation. This has been proposed for p53 (Helps et al. 1995). However, PP1 and

p53 both bind to the C-terminal anykrin repeats and SH3 domain of p53BP2 (the ASPP2 fragment). A trimeric complex could not be observed (Helps et al. 1995). For TAZ, the Hippo pathway transcriptional co-activator, it has been shown that ASPP2 might indeed act as regulatory scaffold for PP1 (Liu et al. 2011 and see 1.4.3). For other ASPP binding partners, this hypothesis has not been tested.

1.3.6. ASPP family proteins can shuttle between the nucleus and the cytoplasm

A model that could explain the multitude of functions of ASPPs is based on the idea that the cellular localisation of ASPP would define its function (Vigneron et al. 2010). This model is very attractive, as the reported localisation of ASPP family proteins is highly context-dependent. Initially, ASPP family proteins were thought to be predominantly cytoplasmic (Samuels-Lev et al. 2001). However, to directly influence p53-dependent transcription, ASPP family proteins would have to be able to translocate to the nucleus. This is possible, as the C-terminal ankyrin repeats of ASPP family proteins are sufficient for nuclear accumulation (Sachdev et al. 1998, Slee et al. 2004). More recently, *Drosophila* ASPP (Langton et al. 2009) and ASPP2 (Cong et al. 2010, Sottocornola et al. 2010) have also been found at cell-cell junctions and at the plasma membrane (Wang et al. 2013a, Wang et al. 2013b).

In a simple model, one could assume that in the cytoplasm, ASPP1/2 would inhibit LATS1/2 function, thus be anti-apoptotic (Vigneron et al. 2010), while nuclear ASPP1/2 would enhance p53 activity and be pro-apoptotic (Aylon et al. 2010) and junctional ASPP2 would only be required in certain cells such as epithelial cells. However, the reality is possibly more complicated. Nuclear accumulation is only a snapshot of what is likely to be a dynamic process, where nuclear import only needs to be slightly more efficient than nuclear export. Furthermore, the cellular distribution of ASPP is not static. For example, phosphorylation can tilt the balance. ASPP1 can be phosphorylated by LATS2, which leads to nuclear translocation in the presence of oncogenic Ras (Aylon et al. 2010). ASPP2 can also be phosphorylated by ERK, detaching it from the plasma membrane and inducing cytoplasmic and

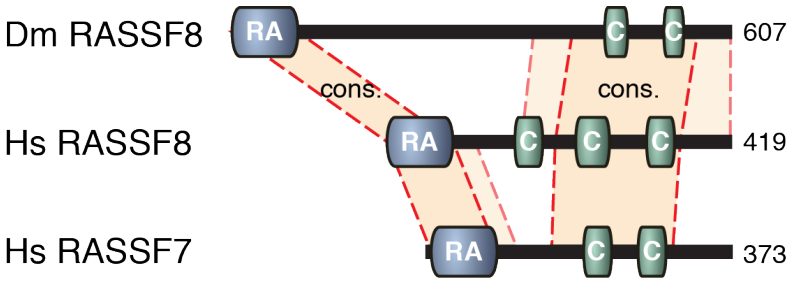

Figure 1.6.: *Drosophila* RASSF8 has conserved N- and C-termini
Domain structure of RASSF8 in *Drosophila* and RASSF7/8 in humans. The *Drosophila* RASSF8 has a conserved RA domain and a conserved C-terminus that contains coiled coil regions. The C-terminus of Drosophila RASSF8 is more similar to human RASSF8 than RASSF7. Coiled coil regions were predicted by jpred3 (Cole et al. 2008). The RA domain annotation is based on the human RASSF8 RA domain structure (PDB: 2CS4).

nuclear localisation (Godin-Heymann et al. 2013). Lastly, iASPP can be phosphorylated during the G2/M transition, which prevents its dimerisation and causes nuclear accumulation (Lu et al. 2013).

The recent description of a Ran-GDP-dependent nuclear import for specific ankyrin repeats (Lu et al. 2014) is another step towards understanding the control of ASPP localisation. If specific residues in two consecutive ankyrin repeats are hydrophobic, this enables binding to the GDP-bound form of the nuclear transport factor Ran. Binding allows the ankyrin repeat-containing protein to piggyback with Ran-GDP into the nucleus, when it is imported with NTF2, a nuclear transport factor (Lu et al. 2014). Identifying the signals and contexts that affect ASPP localisation will be necessary to understand how the different interaction partners contribute to the overall function of ASPP family proteins.

1.3.7. N-terminal RASSF family proteins are putative tumour suppressors and oncoproteins

N-terminal RASSF family proteins are characterised by an RA domain at their N-termini and coiled coil regions at their C-termini (Fig. 1.6). In *Drosophila*, there are three members of this family: RASSF8, CG13875 and CG32150 (Sherwood et al.

2009). Humans have four orthologues: RASSF7, 8, 9 and 10. *Drosophila* RASSF8 is the only orthologue of human RASSF7 and RASSF8, while CG13875 and CG32150 resemble human RASSF9 and RASSF10 more closely.

Although their name might suggest a close relationship with the classical RASSF family proteins (RASSF1–6 in humans and RASSF in *Drosophila*), there is no evidence that these two families are more closely related than other proteins containing RA domains (Sherwood et al. 2009). The RA domain of human RASSF7 (Chan et al. 2013, Takahashi et al. 2011) and RASSF9 (Rodriguez-Viciana et al. 2004) can bind to oncogenic Ras, but human RASSF8 and 10 cannot (Chan et al. 2013). Furthermore, *Drosophila* RASSF8 could not bind Rab11, another small GTPase (Eunice Chan—unpublished observations) and human RASSF8 could not bind to RalA, CDC42 and RAB11 (Gail Doughton—unpublished observation). So far, the functional significance of binding of the N-terminal RASSFs to small GTPases remains little explored.

1.3.8. Human N-terminal RASSF family members are putative tumour suppressors and oncoproteins

In contrast to ASPP family proteins, N-terminal RASSF family members are less well studied. There are no obvious unifying themes, except the for notion that N-terminal RASSF family can either be tumour suppressors or oncoproteins. In this subsection, I will present what is known about the human orthologues before introducing *Drosophila* RASSF8 in the next subsection. CG13875 and CG32150 are currently being studied in our lab and will be the subject of another PhD thesis.

RASSF7 is the only member of the N-terminal RASSF family that was suggested to function as an oncoprotein. In many types of cancer, RASSF7 levels are increased (Underhill-Day et al. 2011). RASSF7 expression is upregulated under hypoxic conditions (Recino et al. 2010), which are found in the centre of large solid tumours. Two potential mechanisms explaining how RASSF7 might be required for tissue growth have been proposed. Firstly, in *Xenopus* embryos (Sherwood et al. 2008) and human cell lines (Recino et al. 2010), RASSF7 is required for mitosis. RASSF7 is localised at centrosomes and is required to activate Aurora B, a mitotic

kinase, perhaps due to a role controlling in microtubule dynamics (Recino et al. 2010). Another mechanism for the pro-growth function of RASSF7, is its ability to inhibit pro-apoptotic JNK signalling (Takahashi et al. 2011). RASSF7 can bind to N-Ras via its RA-domain and also to MKK7, a MAP kinase kinase. These interactions allow RASSF7 to inhibit the activation of JNK by MKK7 (Takahashi et al. 2011).

RASSF8 is a putative tumour suppressor. Expressing RASSF8 in a lung cancer cell line can decrease its propensity to grow in soft agar (Falvella et al. 2006). Conversely, stable transfection with shRNAs targeting RASSF8 in carcinoma cells, increases their ability to form tumours, when injected into immune-deficient mice (Lock et al. 2010). Similarly to *Drosophila* RASSF8 (see below), human RASSF8 is found to stabilise cell-cell junctions (Lock et al. 2010).

The function of RASSF9 and RASSF10 are less well studied. It has been suggested that RASSF9, which is also known as P-CIP1 (PAM C-terminal interactor protein-1), could aid vesicular trafficking of the enzyme Peptidyl-glycine alpha-amidating monooxygenase or PAM (Chen et al. 1998). More recently, *RASSF9* gene function was described to be necessary for mouse skin development. *RASSF9* mutants showed excess proliferation of cells within the epidermis and the dermis and aberrant differentiation (Lee et al. 2011). Whether this is connected to its reported function on PAM is unknown.

Similar to RASSF8, RASSF10 expression inhibits colony formation in soft agar (Hill et al. 2011). RASSF10 localises to the perinuclear region, but seems to be restricted to the nucleus when the cell undergoes mitosis (Hill et al. 2011). It is not known how RASSF10 functions molecularly to inhibit proliferation. However, the *RASSF10* gene is epigenetically silenced by promoter methylation in some types of cancer (Volodko et al. 2014).

1.3.9. *Drosophila* RASSF8 and ASPP form a complex to regulate junctional integrity, at least in part through Csk

Our lab has studied *Drosophila* ASPP and RASSF8 for several years (Langton et al. 2007 2009). Initially, we became interested in RASSF8 as it was identified in a

yeast two-hybrid screen as a putative interaction partner of the kinase Warts (Giot et al. 2003), a core component of the Hippo pathway (see 1.4.1). The same screen also suggested that ASPP was a binding partner of RASSF8. *Drosophila* ASPP is the only orthologue of the human ASPP family and *Drosophila* RASSF8 is the only orthologue of human RASSF7 and RASSF8 (Fig. 1.5 and 1.6).

In contrast to human ASPP family proteins, *Drosophila* ASPP does not seem to bind to *Drosophila* p53 (Langton et al. 2007), as many of the key residues that are found at the interaction surface between ASPP2 and p53 (Gorina and Pavletich 1996) are not conserved (Langton et al. 2007). Furthermore, ASPP has never been observed in the nucleus, but was rather found at adherens junctions (Langton et al. 2009). This does not exclude a context-dependent nuclear function for ASPP, as the residues that are part of the Ran-GDP dependent nuclear import signal (see 1.3.5) are conserved. Despite the difference in p53 binding, ASPP appears to limit growth in *Drosophila* as well, since *ASPP* null mutant flies are bigger overall and have overgrown wings and eyes (Langton et al. 2007).

Similar to ASPP and mammalian RASSF8, *Drosophila* RASSF8 is localised at cell-cell junctions in epithelial cells; it co-localises with E-cadherin at adherens junctions (Langton et al. 2009). RASSF8 and ASPP form a complex and are mutually dependent for their junctional localisation. Together they regulate junctional integrity. In particular during the remodelling phase of retinal development at around 26 h APF (see 1.1.3), when supernumerary cells are eliminated by apoptosis and cell-cell junctions are dynamically rearranged, lack of RASSF8 or ASPP leads to gaps in adherens junctions in IOCs. This is at least in part due to the activation of Csk, an inhibitor of the tyrosine kinase Src, by ASPP (Langton et al. 2009). ASPP and RASSF8 are thought to form a complex that causes the local activation of Csk at adherens junctions. This is proposed to inhibit Src by phosphorylation of a C-terminal residue that promotes Src auto-inhibition, thereby preventing it from dissolving adherens junctions (Langton et al. 2009).

The phenotypes of *RASSF8* null mutant flies resemble those of *ASPP* null mutant flies (Langton et al. 2007 2009). Both mutants are slightly overgrown, have larger

wings and rough eyes. However, there are also subtle differences. *RASSF8* null mutant flies have rounder wings than *ASPP* null mutant flies and the eye roughness appears to be more severe. Thus, although the function of RASSF8 and ASPP are coupled, they might have independent functions as well.

1.4. The Hippo signalling pathway

How to stop growing when the appropriate size has been reached is a key question for any developing multicellular organism. The Hippo pathway is a conserved signalling network that regulates developmental and homeostatic growth, as well as a number of cell fate choices. It was initially discovered using genetic screens for growth suppressors in *Drosophila*. Over the last few years many inputs have been described that feed into the Hippo pathway. In this subchapter I will describe the core components of the Hippo pathway with a particular focus on the transcriptional co-activator Yorkie (Yki), a potential substrate of the ASPP/PP1 complex.

1.4.1. The conserved Hippo pathway consists of a core kinase cascade that inhibits proliferation and promotes apoptosis

Five proteins can be considered as the core of the Hippo pathway: two kinases and their two scaffolding partners, as well as a transcriptional co-activator (Fig. 1.7A and Yu et al. 2013). The kinase Warts (Wts) was the first member of the Hippo pathway described to cause overgrowth when mutated in mitotic clones (Justice et al. 1995, Xu et al. 1995). Wts acts together with its binding partner Mats (Mob1 as tumour suppressor) (Lai et al. 2005) to phosphorylate and inactivate the transcriptional co-activator Yki (Huang et al. 2005). Wts is itself activated by the upstream Ste20-like kinase Hippo (Hpo) (Harvey et al. 2003, Jia et al. 2003, Pantalacci et al. 2003, Udan et al. 2003, Wu et al. 2003), which functions in concert with its scaffold binding partner Salvador (Sav) (Kango-Singh et al. 2002, Tapon et al. 2002).

All five proteins are conserved in humans. Hpo has two orthologues, MST1/2 (Mammalian Sterile 20-like) that can both phosphorylate and activate LATS1/2

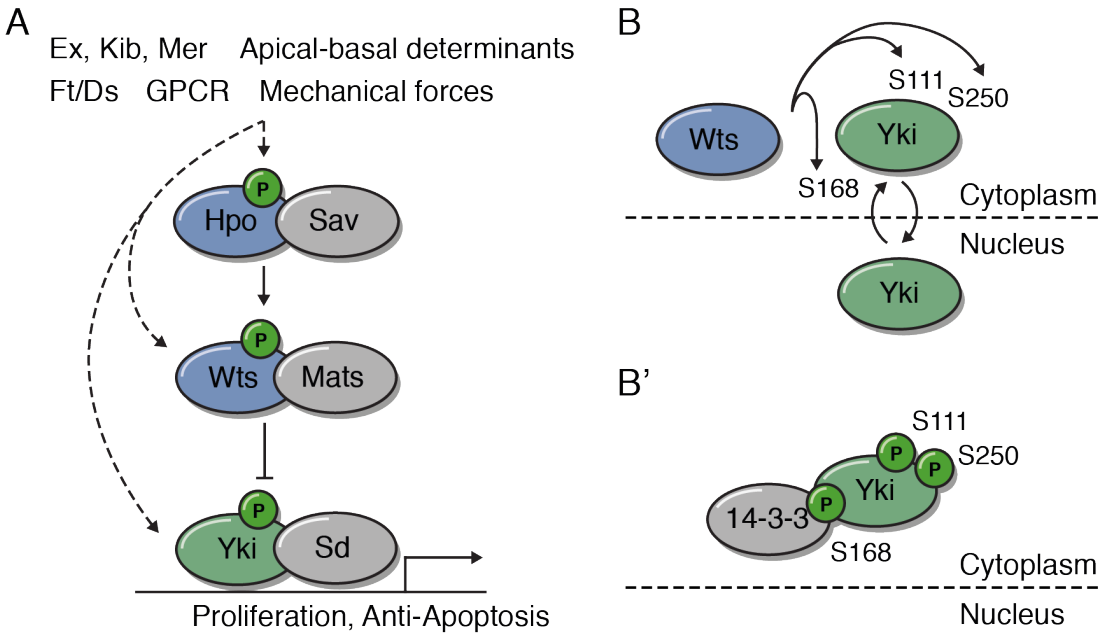

Figure 1.7.: The conserved Hippo pathway regulates proliferation and apoptosis
(A) Different stimuli can regulate the Hippo pathway. The regulation can act on different core members. When the core kinase Hpo is activated, it can phosphorylate and activate Wts, the downstream kinase, which in turn phosphorylates and inactivates the transcriptional co-activator Yki.
(B) Wts can phosphorylate three serines on Yki. Unphosphorylated Yki can shuttle between the cytoplasm and the nucleus, where it acts together with the transcription factor Sd.
(B') Phosphorylation of S168 creates a 14-3-3 binding site. 14-3-3 is able to retain Yki in the cytoplasm.

(Large tumour suppressor), the orthologues of Wts (Chan et al. 2005). Mats and Sav have orthologues in humans as well, MOB1A/B and SAV1 respectively. Importantly, the signalling cascade is conserved, and activation of MST1/2 leads to the subsequent phosphorylation and inactivation of YAP (Dong et al. 2007, Zhao et al. 2007) and TAZ (Lei et al. 2008), the Yki orthologues.

Together with the transcription factor Scalloped (Sd) (Goulev et al. 2008, Wu et al. 2008, Zhang et al. 2008), or TEAD1–4 in humans (Zhao et al. 2008), Yki drives the transcription of proliferation and anti-apoptotic genes such as *diap1* (*Drosophila* Inhibitor of Apoptosis Protein 1), *cyclinE* (Huang et al. 2005) and *bantam* (Nolo

et al. 2006, Thompson and Cohen 2006). Some of the Yki transcriptional targets, such as *expanded* (*ex*), *merlin* (*mer*) or *four-jointed* (*fj*), are upstream activators of the pathway (Cho et al. 2006, Hamaratoglu et al. 2006 and see below). Thus a negative feedback loop is thought to limit signalling activity.

1.4.2. Yki and its orthologues YAP/TAZ are transcriptional co-activators that are retained in the cytoplasm upon phosphorylation

Yki is phosphorylated by Wts on three serine residues, S111, S168 and S250 (Dong et al. 2007, Oh and Irvine 2008 2009) that fit the H-x-[HKR]-x-x-[ST] Wts consensus sequence derived from peptide phosphorylation experiments using LATS1 (Hao et al. 2008). Phosphorylation of S168 generates a binding site for the adaptor protein 14-3-3 (Dong et al. 2007, Oh and Irvine 2008). Upon binding to 14-3-3, Yki is preferentially retained in the cytoplasm and thus inactivated (Fig. 1.7B). Phosphorylation of S111 and S250 also inhibit Yki function (Oh and Irvine 2009). However, the exact mechanism how these two phosphorylated sites regulate Yki is unclear. Similarly, YAP (Hao et al. 2008, Zhao et al. 2007) and TAZ (Lei et al. 2008) can be phosphorylated by LATS1/2 on four and five serines, respectively. All three serines that are phosphorylated in Yki are also found in YAP and TAZ. As in Yki, phosphorylation of S127 in YAP and S89 in TAZ, the corresponding residues to S168 in Yki, inhibits transcription by promoting 14-3-3 binding and retention in the cytoplasm (Lei et al. 2008, Zhao et al. 2007).

Additionally, the levels of YAP and TAZ can be regulated by proteasomal degradation. A similar mechanism has not been found for Yki. S397 of YAP (Zhao et al. 2010) and S311 of TAZ (Liu et al. 2010), two residues that have no obvious equivalents in Yki, are initially phosphorylated by LATS1/2. In a secondary step, casein kinase 1 phosphorylates nearby residues, promoting binding of the E3 ubiquitin ligase complex $SCF^{\beta TRcP}$, which ubiquitylates and degrades YAP/TAZ (Liu et al. 2010, Zhao et al. 2010). TAZ can also be phosphorylated by GSK3, a kinase that is inhibited by the

PI3K pathway. Phosphorylation on two N-terminally located serines, S58 and S62 by GSK3 also promotes degradation via $SCF^{\beta TRcP}$ (Huang et al. 2012).

In many studies, YAP and TAZ are treated as functionally interchangeable or they are not differentially analysed. However, YAP is slightly larger than TAZ and contains an N-terminal proline-rich region, one more WW domain and an SH3-binding domain (Varelas 2014). Thus, it is likely that some of the binding partners and therefore functionality differ between YAP and TAZ. In vivo, *Yap* knock-out mice die at embryonic day 8.5 (Morin-Kensicki et al. 2006), while *Taz* knock-out mice mostly reach adulthood (Hossain et al. 2007). This suggests that YAP and TAZ have different roles during development. Yet a certain degree of redundancy must exist, as Yap and Taz are both required during early embryonic development and *Yap; Taz* double mutant mice do not even reach the 16-cell stage (Nishioka et al. 2009).

1.4.3. TAZ can be dephosphorylated by an ASPP2/PP1 complex

As phosphorylation is central to the activation of Hippo signalling, reversing the phosphorylation is equally important. The scaffold protein RASSF, the only member of the classical RASSF family in *Drosophila*, (Polesello and Tapon 2007) is part of a PP2A complex that inhibits Hippo signalling by dephosphorylating Hpo (Ribeiro et al. 2010). Whether this is conserved is unclear, as in humans, there are six classical RASSF family proteins, some of which are activating while others are inhibitory with respect to Hippo signalling (Ikeda et al. 2009, Praskova et al. 2004).

YAP and TAZ can also be dephosphorylated. S127 of YAP (Wang et al. 2011b) and S89 of TAZ (Byun et al. 2014, Liu et al. 2010) can be dephosphorylated by PP1. Additionally, YAP appears also to be dephosphorylated by PP2A (Schlegelmilch et al. 2011). The difficulty in interpreting three of these studies (Byun et al. 2014, Schlegelmilch et al. 2011, Wang et al. 2011b) is that all experiments that investigate YAP/TAZ regulation only involve the catalytic phosphatase subunit. Regulatory subunits are not mentioned or considered. As noted (see 1.2.3 and 1.2.4), the catalytic subunits of PP1 and PP2A have little specificity by themselves. Thus, it is uncer-

tain if the observed dephosphorylation reactions would also occur under physiological conditions in vivo.

In contrast, Liu et al. identified ASPP2 as the regulatory subunit of a PP1 complex that dephosphorylates TAZ, but not YAP (Liu et al. 2010). They provide several crucial pieces of evidence that ASPP2/PP1 can dephosphorylate TAZ. They demonstrate binding between TAZ and ASPP2, as well as an increase in TAZ S89 phosphorylation upon ASPP2 knockdown. However, most importantly, Liu et al. show that, in contrast to wild type ASPP2, a PP1-binding deficient ASPP2 (RVXF mutant) neither promotes TAZ S89 dephosphorylation in 293T cells, nor inhibits 14-3-3 binding to TAZ. These two experiments show that an ASPP2/PP1 complex can promote TAZ dephosphorylation.

1.4.4. Different cues modulate Hippo signalling

The known upstream regulation of the Hippo pathway can be roughly subdivided into five groups: (i) The Expanded (Ex), Kibra (Kib), Merlin (Mer) complex, (ii) apical-basal polarity determinants (iii) Fat (Ft) and Dachsous (Ds) dependent planar cell polarity (PCP), (iv) G-protein coupled receptors (GPCRs) and (v) mechanical forces sensed through the actin cytoskeleton.

The Expanded, Kibra, Merlin complex regulates Hippo signalling

A recurring theme in Hippo pathway regulation is the influence of regulators that are membrane bound and localised either at apical junctions, or baso-laterally (Genevet and Tapon 2011). One group of apically localised proteins that affects Hippo signalling is the Ex, Kib and Mer complex (Baumgartner et al. 2010, Genevet et al. 2010, McCartney et al. 2000, Yu et al. 2010). All three proteins are scaffold proteins. Mutations in either *ex* (Boedigheimer and Laughon 1993), *kib* or *mer* (LaJeunesse et al. 1998) causes tissue overgrowth.

Furthermore, *ex*, *kib* and *mer* genetically interact. Double mutants of *ex* and *mer* show enhanced overproliferation when compared to the single mutants (Hamaratoglu et al. 2006, McCartney et al. 2000). Similarly, *kib* loss-of-function also enhances the

overproliferation of *ex* and *mer* mutants (Baumgartner et al. 2010, Genevet et al. 2010, McCartney et al. 2000, Yu et al. 2010). This is especially noticeable in the developing eye. Firstly, double mutant combinations of *ex*, *kib* and *mer* strongly increase the number of extra IOCs. While single mutants have few extra IOCs, any double mutant combination causes massive overproliferation that is reminiscent of *hpo*, *wts* or *sav* mutants (Hamaratoglu et al. 2006, Yu et al. 2010). Secondly, Hippo pathway targets are substantially upregulated in double mutant clones, while single mutant clones show no detectable change (Baumgartner et al. 2010, Yu et al. 2010).

Although early studies suggested that the regulation of Hippo pathway target genes by Ex was through activating the kinase cascade (Hamaratoglu et al. 2006), later it was reported that Ex can directly bind to and inactivate Yki independently of the core kinases (Badouel et al. 2009, Oh et al. 2009). Yki localises to the sub-apical membrane when Ex is overexpressed (Badouel et al. 2009). However, this does not exclude the possibility that Ex, Kib and Mer could also activate the core kinases in parallel of sequestering Yki, especially since Sav can directly bind to Kib and Mer, while Hpo can directly bind to Ex (Yu et al. 2010). Indeed, recent work suggests that Mer directly binds to Wts and recruits it to the apical membrane, where it is activated by the Hpo/Sav complex (Yin et al. 2013).

Kib and Mer have orthologues in humans, KIBRA and NF2. KIBRA and NF2 are also functionally equivalent of Kib and Mer, as they bind to each other and promote YAP phosphorylation by LATS1/2 (Zhang et al. 2010). Ex does not have a direct orthologue in mammals (Bossuyt et al. 2014). AMOT (Angiomotin), a tight junction-associated protein seems to be the functional equivalent of Ex. AMOT can bind to YAP/TAZ directly to recruit them to the tight junctions, leading to reduced nuclear YAP/TAZ activity (Chan et al. 2011, Wang et al. 2011c, Zhao et al. 2011). Furthermore, AMOT interacts with NF2 and is required for NF2 function (Yi et al. 2011).

Additional to the Ex, Kib and Mer complex, core components of the pathway have also been shown to localise sub-apically. A certain fraction of Hpo is found at the apical membrane in larval eye imaginal discs (Grzeschik et al. 2010) and Mats is

mostly found apically (Ho et al. 2010). In cultured S2 cells, Hpo is associated with the membrane fraction (Yu et al. 2010). This has led to the idea that the apical membrane is a key site for the activation of the Hippo core kinase cascade.

Apical-basal determinants influence Yki activity

Apical-basal determinants (see 1.5) can also influence Yki activity. Crumbs (Crb), a sub-apically localised transmembrane protein is required for the localisation of Ex (Chen et al. 2010, Ling et al. 2010, Robinson et al. 2010). Loss of *crb* leads to overgrowth phenotypes and the activation of Yki target genes, similar to loss of *ex*. Although Crb stabilises Ex at the sub-apical membrane, it also targets Ex for degradation via the proteasome (Ribeiro et al. 2014). Thus, not only loss of *crb*, but also overexpression of Crb leads to an upregulation of Yki targets through loss of Ex function (Grzeschik et al. 2010). The role of Crb in regulating Hippo signalling is conserved in humans. Knock-down of CRB3 leads to the upregulation of YAP target genes (Varelas et al. 2010). Similar to Crb, the sub-apically localised kinase aPKC (atypical Protein Kinase C) can induce an upregulation of Yki targets when overexpressed (Grzeschik et al. 2010, Sun and Irvine 2011).

Crb and aPKC overexpression can lead to a spreading of the apical domain at the expense of the basal domain (see 1.5.7). Thus, the loss of baso-lateral determinants, which also causes spreading of the apical domain (see 1.5.7), would be expected to result in a similar upregulation of Yki target genes. Indeed, this is observed when *scribble* (*scrib*) or *lethal giant larvae* (*lgl*) are lost in mitotic clones of larval imaginal discs (Grzeschik et al. 2010). In combination with oncogenic Ras, the loss of *scrib* or *lgl* causes hyperproliferation and invasive growth (Brumby and Richardson 2003, Pagliarini and Xu 2003). In breast cancer cells, human SCRIB has been directly implicated in YAP inhibition by scaffolding the core kinase cassette and promoting YAP phosphorylation (Cordenonsi et al. 2011).

Fat/Ds dependent planar cell polarity, GPCRs and mechanical stress also regulate Yki activity

Another group of upstream regulators include the two atypical cadherins Ft (Fat) and Ds (Dachsous), which can form hetero-dimers through their extracellular domains (Clark et al. 1995). The interaction between Ft and Ds is modulated by the Golgi kinase Four-jointed (Fj) (Ishikawa et al. 2008). Fj can phosphorylate both Ft and Ds while they transit through the Golgi apparatus. While the phosphorylation of Ft increases its affinity towards Ds, the phosphorylation of Ds decreases its affinity towards Ft (Brittle et al. 2010, Simon et al. 2010). Loss of *ft* leads to the upregulation of Yki targets (Bennett et al. 2006, Cho et al. 2006, Feng and Irvine 2007, Silva et al. 2006, Tyler and Baker 2007, Willecke et al. 2006). The exact mechanism through which Ft/Ds influence Hippo signalling is debated. Initially, it was proposed that Ft might act entirely through regulating Ex levels (Bennett et al. 2006, Silva et al. 2006, Willecke et al. 2006). However, subsequently, it was shown that in some tissues *ex; ft* double mutants have a stronger overgrowth phenotype as either single mutant (Feng and Irvine 2007, Tyler and Baker 2007), suggesting that Ft and Ex have separate functions. Ft/Ds might regulate the Hippo pathway, through the inhibition of the atypical myosin Dachs by Ft (Cho et al. 2006). Dachs can in turn promote Wts degradation (Cho et al. 2006, Rauskolb et al. 2011).

Ft and Ds are also known to regulate PCP, a form of polarity that allows cells to orient themselves in the plane of an epithelium. Two distinct systems control PCP: the Ft/Ds and the Frizzled/Flamingo systems (Simons and Mlodzik 2008). Loss of any component leads to loss of planar tissue organisation, for example misoriented hair in the wing blade, as cells lose the ability to align along the correct axis. (Simons and Mlodzik 2008). In many tissues, Fj and Ds are expressed in opposing gradients along the proximo-distal axis, while Ft expression is unpatterned (Yang et al. 2002). The tissue-wide gradient is responsible for the localisation of Ft and Ds to the two opposing sides of a cell (Brittle et al. 2012). In this way each cell know its orientation along the axis of the gradient.

GPCRs have recently been identified as regulators of YAP/TAZ activity (Miller et al. 2012, Mo et al. 2012, Yu et al. 2012). Small extracellular ligands can bind and activate GPCRs (Miller et al. 2012, Yu et al. 2012), or GPCRs can be activated by proteolytic cleavage (Mo et al. 2012). Downstream signalling is mediated by Rho GTPases in the former instance (Miller et al. 2012, Yu et al. 2012), but seems to be Rho-independent in the latter (Mo et al. 2012). As Rho GTPases can regulate actin dynamics (Ridley 2006), F-actin might also be involved in the transduction of the signal to YAP/TAZ.

Perturbation of the F-actin cytoskeleton was initially shown in *Drosophila* to modulate Yki activity (Fernández et al. 2011, Sansores-Garcia et al. 2011). An increase in F-actin, achieved for example by mutating actin filament capping proteins, leads to an increased Yki activity (Fernández et al. 2011, Sansores-Garcia et al. 2011). This actin-sensing function is conserved in mammalian tissue culture cells (Aragona et al. 2013, Dupont et al. 2011, Wada et al. 2011). The actin cytoskeleton is known to mediate many of the cellular effects of physical tension, and Yki/YAP/TAZ have been proposed to connect cell proliferation and cell fate choice to the cell's physical environment by responding to cytoskeletal tension (Halder et al. 2012). Indeed, plating tissue culture cells on a stiff extracellular matrix activated YAP/TAZ, while soft conditions lead to YAP/TAZ inhibition. However, the dependence of this Yki/YAP/TAZ regulatory mechanism on the core kinase cascade remains debated.

1.5. Baz/PAR3 and epithelial cell polarity

Cell polarity is required for any asymmetric cellular function. Some cells are transiently polarised for example when they move in a specific direction. Other cells, such as neurons or epithelial cells, stably maintain their polarised architecture. In this subchapter I will describe the organisation of epithelial cells along their apical-basal axis in *Drosophila* and compare it to mammalian epithelial cells. I will focus on the polarity determinant Bazooka (Baz), as it is a further potential substrate of the ASPP/PP1 complex.

1.5.1. Epithelial cells are subdivided into distinct regions along the apical-basal axis

Epithelial tissues are one of the basic building blocks in animals. In epithelia, one or more layers of cells form a sheet-like structure. The two sides of the epithelial sheet are physically separated and can adopt different properties. Three characteristics define epithelial cells (McCaffrey and Macara 2011): (1) Epithelial cells have intercellular contacts. These contacts maintain cell cohesion, allow the epithelium to withstand mechanical forces and enable neighbouring cells to communicate with each other. (2) During expansion of the epithelium, oriented cell divisions parallel to the axis of the epithelial sheet ensure that both daughter cells remain within the sheet. Thus, the architecture of the epithelium is maintained when it is growing. (3) Each cell has a different molecular composition along the two opposing sides of the epithelial sheet. This apical-basal polarity allows the epithelium to distinguish between the two sides.

Along the apical-basal axis of epithelial cells, several distinct domains of the plasma membrane can be distinguished (Fig. 1.8) that fulfil different functional roles (St Johnston and Ahringer 2010). On the apical side, the membrane that faces the luminal space or the external milieu is often highly extended. Especially in absorbtive tissues, small protrusions known as microvilli decorate this side to maximise the contact surface. On the lateral side, the most apical structures are adherens junctions, which provide a mechanical link between neighbouring cells and hold epithelial tissues together. Basal to the adherens junctions are septate junctions, which serve as physical barriers and limit diffusion through the intercellular space (occluding junctions). The basal side is in contact with the basement membrane, which links the epithelium to the underlying connective tissue.

In each domain, characteristic protein complexes associate with the plasma membrane. These protein complexes are not only found in epithelial cells, but are a feature that is shared between different polarised cells. Many of the proteins described below were first discovered in *C. elegans* embryos (Hoege and Hyman 2013). In *Drosophila* these polarity proteins are also important in the non-epithelial neuroblasts and in oocytes.

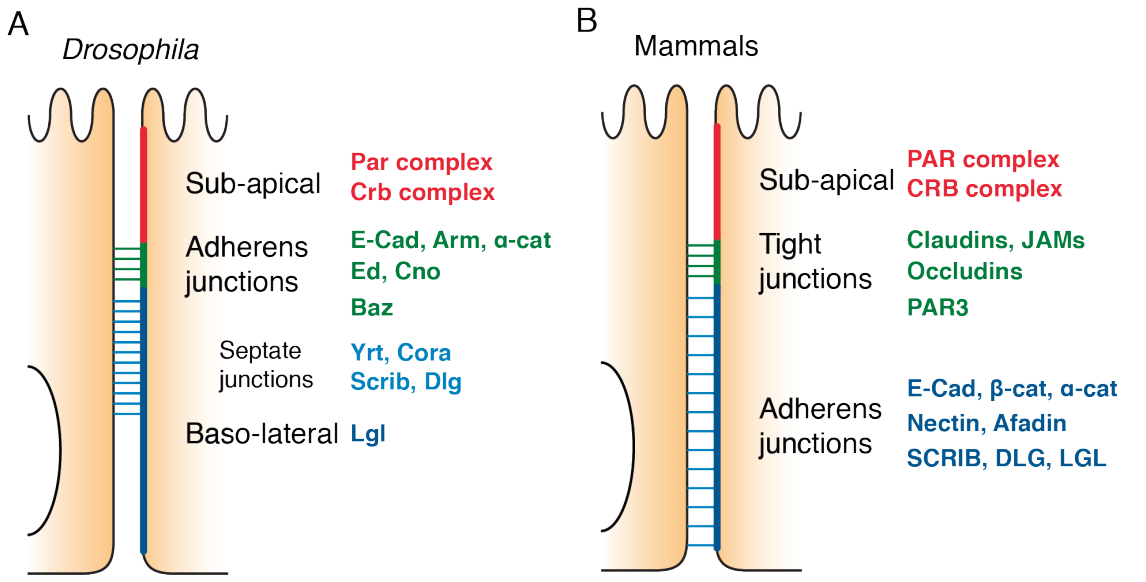

Figure 1.8.: Epithelial cells have distinct membrane domains along the apical-basal axis

The general layout of epithelial cells in *Drosophila* (A) and mammals (B) is similar. Most notably, the occluding junctions that restrict para-cellular diffusion in *Drosophila* (septate junctions) are basal to the adherens junctions, while in mammals the occluding junctions (tight junctions) are apical to the adherens junctions.

1.5.2. The Crb and Par complexes define the sub-apical region

In epithelial cells, the most apical region of the lateral membrane is referred to as the sub-apical region or marginal zone. In this region, the Crb and the Par (Partitioning defective) complexes are localised. The Crb complex consists of the transmembrane protein Crb, the MAGUK (membrane associated guanylate kinase) protein Sdt (Stardust) and the PDZ domain containing protein Patj (Bulgakova and Knust 2009). Sdt serves as scaffold for the other proteins. It binds to Crb (Bachmann et al. 2001, Hong et al. 2001) and to Patj (Bachmann et al. 2004) via different domains. Additionally, the Crb complex can associate with the Four point one, Ezrin, Radixin, Moesin (FERM) domain containing proteins Moesin (Moe), Yurt (Yrt) and Ex (Chen et al. 2010, Laprise et al. 2006, Ling et al. 2010, Médina et al. 2002, Robinson et al. 2010).

The other protein complex in the sub-apical region, the Par complex, consists of the PDZ domain containing Par6 and aPKC. Par6 can directly bind to aPKC (Hutterer

et al. 2004). Additionally, a small GTPase, Cdc42, can bind to Par6 in its GTP-bound form (Hutterer et al. 2004). Cdc42 relieves the inhibition of the catalytic activity of aPKC by Par6 (Atwood et al. 2007). The Par complex and the Crb complex are connected by direct binding between Sdt and Par6 (only shown for mammalian orthologues Wang et al. 2004), Crb and Par6 (Kempkens et al. 2006), as well as by phosphorylation of Crb through aPKC (Sotillos et al. 2004).

1.5.3. Baz can associate with the Par complex, but is localised at adherens junctions in epithelia

In some systems, the PDZ domain containing protein Baz (known as PAR3 in vertebrates) is considered as a core component of the Par complex. This stems from observations in non-epithelial systems such as *C. elegans* embryos, *Drosophila* oocytes and *Drosophila* neuroblasts, where Baz (par-3 in *C. elegans*) is found in the same membrane domain as Par6 and aPKC (St Johnston and Ahringer 2010). Furthermore, Baz can directly bind to aPKC (Wodarz et al. 2000) and Par6 (Petronczki and Knoblich 2001). However, in many epithelial systems such as *Drosophila* embryos (Harris and Peifer 2005) or photoreceptors (Nam and Choi 2003), Baz co-localises with adherens junction markers, basal to the Crb and Par complexes. Similarly, mammalian PAR3 is also often found basal of the Par complex (Afonso and Henrique 2006, Martin-Belmonte et al. 2007, Satohisa et al. 2005).

Two independent mechanisms are required to separate Baz from the Par complex (Fig. 1.9). Firstly, Baz/PAR3 can be phosphorylated by aPKC on a conserved serine (S980 in Baz), which leads to the dissociation of Baz/PAR3 from aPKC (Nagai-Tamai et al. 2002, Morais-de Sá et al. 2010). Secondly, Crb can compete with Baz to bind to Par6 (Morais-de Sá et al. 2010). In several epithelia in *Drosophila*, both mechanisms are required to exclude Baz from the sub-apical region. (Morais-de Sá et al. 2010, Walther and Pichaud 2010). To prevent Baz from spreading into the baso-lateral membrane (Fig. 1.9B), Par1, a baso-laterally localised kinase, phosphorylates Baz on S151 and S1085 (Benton and St Johnston 2003). Phosphorylation allows the adaptor protein 14-3-3 to bind, which is thought to dissociate Baz from the plasma membrane.

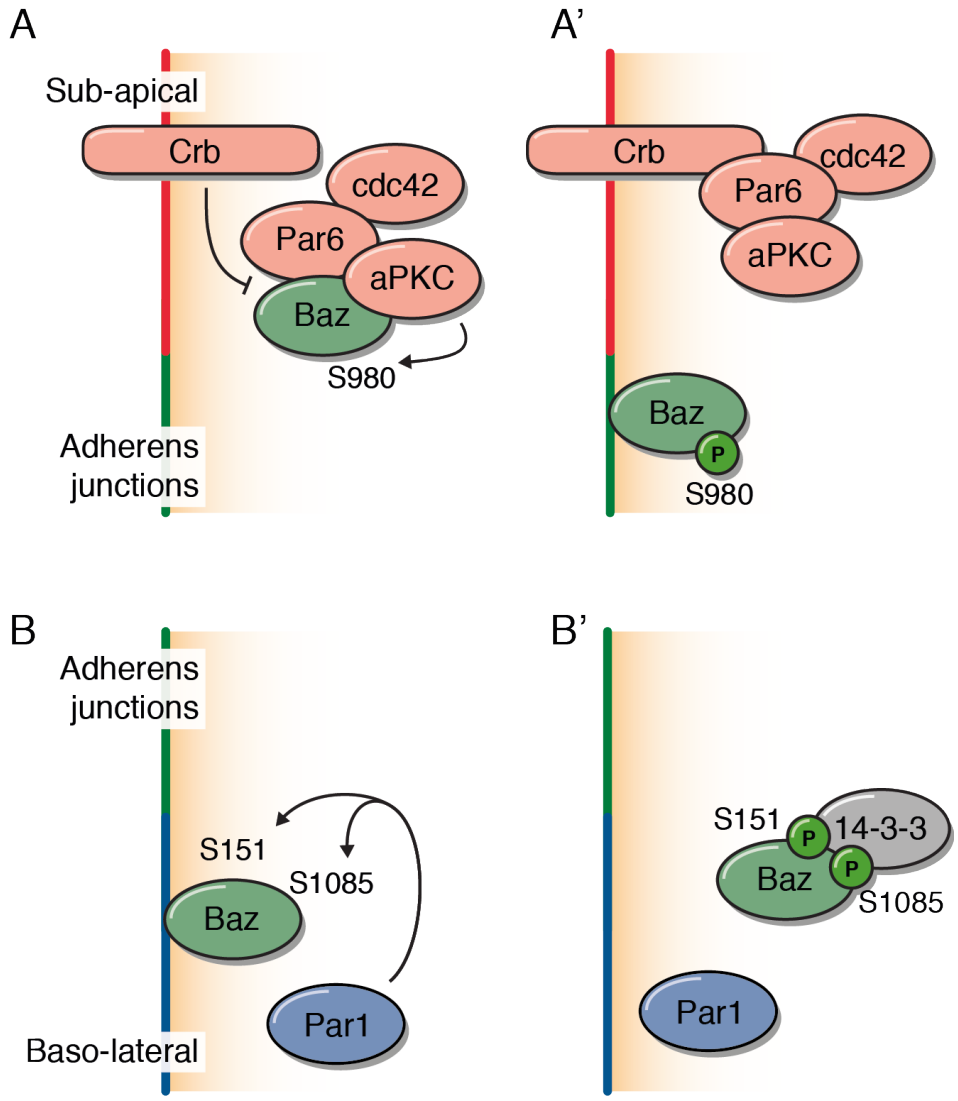

Figure 1.9.: Baz localization to adherens junctions is regulated by phosphorylation

(A) Baz can directly bind to Par6 and aPKC. (A') Phosphorylation of Baz by aPKC on S980 and competition for Par6 binding by Crb leads to the apical exclusion of Baz. (B) Baz is thought to be able to diffuse along the plasma membrane. In the basolateral region, Par1 phosphorylates Baz on S151 and S1085. (B') Both sites are phosphorylation-dependent 14-3-3 binding sites. 14-3-3 binding leads to the dissociation of Baz from the membrane.

Furthermore, phosphorylation of S151 prevents Baz multimerisation, while the phosphorylation of S1085 reduces aPKC binding (Benton and St Johnston 2003). The Par1 phosphorylation sites are conserved in mammals (Hurd et al. 2003, Izaki et al. 2005). However, aPKC binding is not inhibited by 14-3-3 binding to PAR3 (Izaki et al. 2005). The phosphorylation of Baz/PAR3 can be reversed by phosphatases. S1085 is dephosphorylated by a PP2A phosphatase complex in *Drosophila* (Krahn et al. 2009). How the other sites of Baz are dephosphorylated is unknown. In PAR3, the equivalent residues to Baz S151 and S980 can be dephosphorylated by the catalytic PP1 subunit alone (Traweger et al. 2008). However, as PP1 normally acts as a multimeric holoenzyme that requires regulatory subunits (see 1.2.4), it is not clear if PP1 could dephosphorylate PAR3 in vivo.

Baz (Krahn et al. 2010) and PAR3 (Horikoshi et al. 2011) can directly associate with the plasma membrane by binding to phosphoinositide lipids in a conserved region close to the C-terminus. It had been suggested that the second PDZ domain of PAR3 may also bind to phosphoinositides (Wu et al. 2007a), but the binding appears to be much weaker than binding through the conserved C-terminal region (Horikoshi et al. 2011). Rho-kinase can phosphorylate Baz on unidentified residues within the conserved C-terminus and thereby inhibits phosphoinositide binding (Matos Simões et al. 2010). It is not clear if this mechanism is conserved in mammalian PAR3, as Rho-kinase has instead been reported to disrupt the binding between PAR3 and the Par complex (Nakayama et al. 2008).

In addition to being actively excluded form the sub-apical and baso-lateral regions, Baz has also been reported to bind several adherens junction components. Echinoid (Ed), a Nectin-like cell adhesion molecule, as well as Armadillo (Arm, orthologue of β-catenin), have PDZ binding motifs that mediate their binding to Baz (Wei et al. 2005). Mammalian Nectin-1 and Nectin-3 can also bind to PAR3 (Takekuni et al. 2003). By interacting with these proteins, Baz has been proposed to promote adherens junction assembly. Indeed, Baz initiates accumulation of new adherens junction material in cellularising embryos and photoreceptors (McGill et al. 2009, McKinley et al. 2012, Walther and Pichaud 2010).

1.5.4. Adherens junctions are required to connect neighbouring cells

Adherens junctions have two core complexes that are required for their function as mechanical links between neighbouring cells (Harris and Tepass 2010). The first complex consists of the adhesion molecule E-Cadherin, the transcription factor/scaffold protein Arm (β-catenin in mammals) and the actin-binding protein α-catenin. E-Cadherin has extracellular cadherin repeats that mediate homophilic trans-interactions (Harris and Tepass 2010). Intracellularly, E-Cadherin directly binds Arm (Oda et al. 1994, Tepass et al. 1996). Via Arm, E-cadherin is connected to α-catenin, which can directly bind to the actin cytoskeleton (Rimm et al. 1995). However, some biochemical studies suggest that a simple quaternary complex of E-Cadherin, Arm, α-catenin and F-actin may not form (Drees et al. 2005, Yamada et al. 2005), though recent in vivo work disputes this view (Desai et al. 2013).

The second complex consists of the Nectin-like Ed and Canoe (Cno), an Afadin orthologue (Harris and Tepass 2010). Similar to E-Cadherin, Ed can also mediate interactions between neighbouring cells. It binds in-trans to other Ed molecules (Islam et al. 2003) and intracellularly associates with Cno (Wei et al. 2005). Through Cno, Ed is connected to the actin cytoskeleton (Sawyer et al. 2009).

1.5.5. Septate junctions seal the intercellular space

Basal of the adherens junctions are septate junctions, which seal the intercellular space and prohibit free para-cellular diffusion (St Johnston and Ahringer 2010). The septate junctions mark the apical part of the baso-lateral membrane. Several proteins with extracellular domains are necessary for the formation and maintenance of septate junctions. These include three Claudin family members Megatrachea (Behr et al. 2003), Sinuous (Wu et al. 2004) and Kune-Kune (Nelson et al. 2010), the Na^+/K^+-ATPase (Paul et al. 2003), Neurexin (Baumgartner et al. 1996), Gliotactin , Neuroglian (Genova and Fehon 2003, Schulte et al. 2003), Contactin (Faivre-Sarrailh et al. 2004), Lachesin (Llimargas et al. 2004) and Fasciclin III (Snow et al. 1989). Intracel-

lularly, the two FERM domain containing proteins Yrt and Coracle (Cora) (Laprise et al. 2009), as well as the MAGUK protein Varicose (Wu et al. 2007b) are localised at septate junctions and required for their function. Although most proteins listed above affect each other's localisation, it is not entirely clear if they all form a single physical complex.

1.5.6. The Scrib group of proteins defines the baso-lateral domain

Another group of proteins that resides on the baso-lateral membrane is the Scrib group. This group comprises the two PDZ domain-containing proteins Scrib and Discs large (Dlg), as well as the WD-40 repeat protein Lgl. Sometimes, the three proteins are referred to as a complex. However, so far only an indirect interaction between Scrib and Dlg via a third protein, GUK-holder, has been described (Mathew et al. 2002). They are generally grouped together because they partially co-localise and function together to regulate cell polarity, sharing some mutant phenotypes (Bilder et al. 2000). Scrib and Dlg co-localise with septate junction proteins in the apical part of the baso-lateral membrane (Bilder and Perrimon 2000, Woods and Bryant 1991), while Lgl spreads along the full length of the baso-lateral membrane (Bilder et al. 2000). Despite the co-localisation of the Scrib group with septate junction proteins, the two groups seem to be distinct entities. In FRAP experiments, Dlg showed a fast recovery, while septate junction proteins were largely immobile (Oshima and Fehon 2011). Lastly, the kinase Par1, which phosphorylates Baz, is also localised at the baso-lateral membrane (Benton and St Johnston 2003).

1.5.7. Mutual regulation is required to maintain the molecular identity of the distinct domains

The molecular complexes described above establish and maintain the distinct identities of the membrane domains by mutual regulation (Tepass 2012). Although the

required complexes can vary between contexts, the idea of mutual antagonisms is a recurring theme.

The best-characterised mutual antagonism is between the apical Par/Crb complexes and the baso-lateral Scrib group. This interaction is conserved between *Drosophila* and vertebrate systems (Chalmers et al. 2005). The loss of apical determinants such as aPKC (Chalmers et al. 2005, Wodarz et al. 2000) or Crb (Bilder et al. 2003, Tanentzapf and Tepass 2003) leads to the spread of baso-lateral determinants. Conversely, the loss of the Scrib group leads to the spread of apical determinants (Bilder et al. 2000). This mutual antagonism is at least partially due to the phosphorylation of Lgl by aPKC. aPKC can phosphorylate Lgl in order to remove it from the plasma membrane on the apical side (Betschinger et al. 2003, Hutterer et al. 2004, Plant et al. 2003, Yamanaka et al. 2003). Conversely, Lgl binds to the Par complex and inhibits the activity of aPKC (Atwood and Prehoda 2009, Yamanaka et al. 2003)

Another mutually antagonistic interaction is observed between the Yrt/Cora group and the Crb complex (Laprise et al. 2009). The Yrt/Cora group of septate junction proteins comprises Yrt, Cora, Neurexin and the Na^+/K^+-ATPase. During organogenesis of the *Drosophila* embryo (stages 11–13), removing either the Yrt/Cora group or the Crb complex leads to the spreading of the other along the plasma membrane. It is unknown if this mutual antagonistic pair is required in any other context to maintain apical-basal polarity.

It has been proposed on the basis of computational modelling that mutual antagonism alone is not sufficient for efficient membrane polarisation (Fletcher et al. 2012). Additionally, a positive feedback loop driven by Crb cis-homo-multimerisation might be required.

1.5.8. In mammalian epithelial cells, the adherens junctions are basal to the tight junctions

The general structure of epithelial cells is similar in *Drosophila* compared to mammals (Fig. 1.8). The most striking difference is that, in mammalian epithelia, the occluding junctions (tight junctions) are apical of the baso-laterally localised ad-

herens junctions (St Johnston and Ahringer 2010). Tight junctions are functional equivalents of septate junctions, but morphologically and molecularly, they are strikingly different (Furuse and Tsukita 2006). Two groups of adhesion molecules that are found in mammalian tight junctions (JAMs and Occludins) are not found in the *Drosophila* genome.

Despite the shuffling of the occluding junctions and the adherens junctions, the polarity determinants are not affected in their apical-basal order. As in *Drosophila*, the PAR and CRB complexes are found in the apical region in mammalian epithelial cells. PAR3 is associated with the most apical cell-cell junctions (Baz with adherens junctions and PAR3 with tight junctions). Lastly, the SCRIB group is found at the baso-lateral membrane.

In contrast to the polarity determinants that are in the same topological order, the functional components of adherens junctions are not. Thus, E-Cadherin, α- and β-catenin, as well as Nectin and Afadin (the Ed and Cno orthologues) are baso-lateral to the tight junctions in mammalian epithelial cells.

1.6. Aims of this thesis

During epithelial tissue development, the establishment and subsequent maintenance of cell-cell contacts is crucial to the function of the tissue (see 1.5). The aim of this thesis is to elucidate the molecular details how the scaffold proteins ASPP and RASSF8 regulate cell-cell junction dynamics in a developmental context. Previously, our lab had shown that both proteins form a complex and localise at adherens junctions in epithelial tissues, where they are required to maintain junctional integrity during developmental tissue remodelling (Langton et al. 2007 2009).

At the time I started this work, our lab had already gained some insights into the regulation of adherens junctions by ASPP through Csk/Src (see 1.3.9). In parallel, our collaborators in Zurich, led by Matthias Gstaiger, provided an extensive proteomic analysis of the mammalian ASPP network suggesting a new additional function. In AP-MS experiments with human ASPP1/2 and RASSF8 as bait, Ser/Thr protein

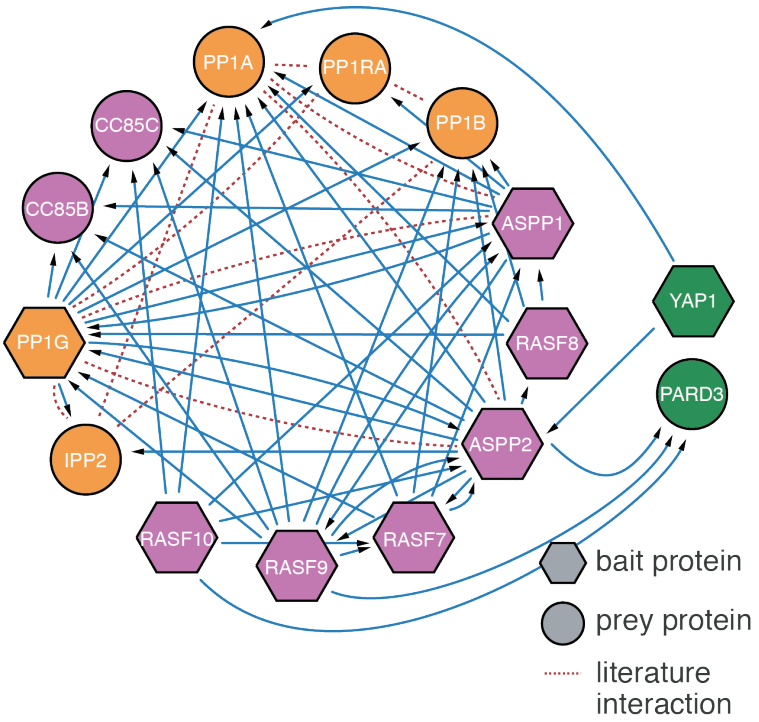

Figure 1.10.: Interaction network of ASPP and N-terminal RASSF family proteins from AP-MS experiments

Bait proteins (hexagons) were affinity purified and associated preys identified using mass spectrometry. Arrows point away from bait proteins towards the retrieved prey proteins. Previously described interactions are shown as dashed lines. Colouring indicates ASPP and N-terminal RASSF family proteins (purple in the lower right corner), PP1 catalytic subunits and canonical regulatory subunits (orange), Ccdc85 family proteins (purple in the upper left corner) and potential substrates of ASPP/PP1 complexes (green). Adapted from (Hauri et al. 2013).

phosphatases of the PP1 family were pulled down (Fig. 1.10). Conversely, ASPP1/2 were also detected in a pull-down of PP1γ. Since ASPP1/2 possesses a conserved, PP1 binding RVXF motif, this suggested that ASPP and N-terminal RASSF family proteins could act as PP1 regulatory subunits at cell-cell junctions. This thesis is primarily focused on testing this hypothesis.

In the following result section (Chapter 3), I will describe the complex that forms between *Drosophila* PP1, ASPP and RASSF8. Chapter 4 explores two potential substrates of this complex: The transcriptional co-activator Yki/YAP and the po-

larity determinant Baz/PAR3. Chapter 5 outlines the potential regulation of the ASPP/RASSF8 complex by Hippo signalling. Chapter 6 concludes the results section and examines further possible substrates and regulators.

Chapter 2.

Materials and Methods

2.1. Molecular biology: DNA

2.1.1. Genomic DNA isolation

Fly genomic DNA was isolated using the DNeasy Blood & Tissue Kit (Qiagen). One male fly was homogenised in 180 µL PBS and processed according to the cultured cell protocol provided by the manufacturer. The final elution volume was 100 µL. For PCR reactions (see 2.1.3), 1 µL of the extracted DNA was used.

2.1.2. cDNA isolation for cloning

cDNA was obtained in a two-step process. Firstly, total RNA was obtained from *Drosophila* S2 cells or tissue using the RNeasy Mini Kit (Qiagen). Secondly, cDNA was produced from 2 µg of total RNA using the First Strand cDNA Synthesis Kit for RT-PCR (Roche). Alternatively, if available, cDNA clones from the DGRC (*Drosophila* Genomics Resource Center) collection were used as template for PCR.

2.1.3. Polymerase Chain reaction

DNA segments of interest were amplified using the appropriate oligonucleotides (see 2.1.15) in a PTC-200 Peltier thermal cycler (MJ Research). For all molecular cloning, Pwo Master (Roche) with 3' to 5' proofreading activity was used. For genotyping,

Taq PCR Master Mix Kit (Qiagen) with lower fidelity was used. Typical reactions were carried out in 50 µL volume with a final concentration of 200 nM of forward and reverse primer.
The standard PCR program used was as follows:

Hot start:	95 °C for 2 min
Denaturation:	95 °C for 15 s
Annealing:	50–65 °C for 30 s (normally 55°C, adjusted to primers)
Extension:	72 °C for 1 min per kb of product
Final extension:	72 °C for 8 min

The denaturation, annealing and extension steps were repeated for 32 cycles.

DNA purification

For cloning, the product was purified after PCR. For restriction enzyme based cloning (see 2.1.7), the PCR product was purified using the QIAquick PCR Purification Kit (Qiagen). For generating entry vectors for the Gateway system (see 2.1.6), the PCR product was separated on 1 % agarose gels stained with ethidium bromide (Sigma-Aldrich). Gel slices containing the product were purified using the QIAquick Gel Extraction Kit (Qiagen). This was done to remove primer dimers that would compete with the PCR product to recombine with the entry vector.

2.1.4. RT-PCR

Total RNA was isolated from ten flies using the RNeasy Mini Kit (Qiagen). Isolated RNA was treated with DNase (Promega) for 37 °C for 30 minutes before adding DNase Stop Solution (Promega) and another incubation at 65 °C for 10 minutes to inactivate DNase. cDNA was synthesised from 1 µ g of isolated RNA with oligo(dT) primers using the First Strand cDNA Synthesis Kit for RT-PCR (Roche) according to the manufacurer's instructions. Lastly, a standard PCR was carried out using the synthesised cDNA as template for 30 cycles.

2.1.5. Agarose gel/DNA visualisation

DNA was separated by size using 1 % agarose gels containing ethidium bromide (Sigma-Aldrich). The agarose was dissolved in 0.5x TAE buffer. Gels were imaged using a BioDocIt (UVP) imaging system.

2.1.6. Gateway cloning

All *Drosophila* S2 cell expression vectors were obtained using Gateway cloning (Invitrogen). The system is based on reversible recombination by two enzymes called LR clonase and BP clonase. The LR clonase recombines DNA flanked by attL1 and attL2 sequences with DNA flanked by attR1 and attR2 sequences. The recombination not only exchanges the DNA fragments, but also generates different flanking sequences. attL1/2 become attB1/2, while attR1/2 become attP1/2. The new attB1/2 and attP1/2 are recognised by the BP clonase. Thus, BP clonase can reverse the recombination carried out by LR clonase.

Entry vectors

In the initial cloning step, entry vectors were generated. Target DNA was amplified by PCR using primers containing attB1 and attB2 sequences, as well as a Kozak sequence (ACC) in front of an ATG start codon for the forward primer. The PCR product was recombined with the Gateway pDONR/Zeo Vector (Invitrogen) using Gateway BP clonase II Enzyme mix (Invitrogen) according to the manufacturer's protocol.

Expression vectors

Expression vectors were obtained in the second step by recombining the entry vector containing the target DNA with an expression vector using Gateway LR clonase II Enzyme mix (Invitrogen) according to manufacturer's protocol. Most *Drosophila* expression vectors come from the *Drosophila* Gateway Vector Collection. The nomenclature of these vectors indicates the promoter as well as the type and placement of

the tag. For example, the pAFW vector is a plasmid (p) that contains the actin (A) promoter and codes for a FLAG-tag (F) upstream of the Gateway cassette (W). The different tags that were used in this thesis are: FLAG-tag (F), GFP-tag (G), HA-tag (H), Myc-tag (M) and V5-tag (V).

2.1.7. Restriction-based cloning

For the generation of some Gateway vectors (see 2.1.16 and 2.1.18), Restriction-based cloning was used. Vectors and the amplified target DNA (insert) were digested using suitable restrictions enzymes (NEB). The vectors were treated with Alkaline Phosphatase (NEB) to avoid self-ligation of the vector. Digested DNA was purified using the QIAquick Gel Extraction Kit (Qiagen). Subsequently, the vector and insert, in a 1:3 molar ratio, were ligated at 16 °C overnight using T4 DNA Ligase (NEB).

2.1.8. Site-directed mutagenesis

Site-directed mutagenesis was performed using a primer pair of 33 nucleotide length with the altered codon in the middle. The PCR was carried out using PfuTurbo DNA Polymerase (Stratagene). 50 ng of plasmid DNA was used as template in a 50 µL reaction. As for standard PCR reactions, primers were added to a final concentration of 200 nM.

The PCR program used was as follows:

Hot start:	95 °C for 2 min
Denaturation:	95 °C for 30 s
Annealing:	55 °C for 60 s (normally 55°C, adjusted to primers)
Extension:	68 °C for 2 min per kb of plasmid

The denaturation, annealing and extension steps were repeated for 30 cycles.

2.1.9. N-/C-terminal truncations

For truncations of either end of a target DNA, a PCR was carried out using primers that only amplify the shorter DNA segment of interest.

2.1.10. Deletions

For deletions, two PCRs were carried out with primers amplifying both ends flanking the deletion. The primers in the middle were chosen to contain a restriction enzyme site that did not occur elsewhere within the amplified DNA. Both products were digested with the appropriate enzyme and ligated. The ligated product served as template for PCR with attB1 and attB2 sites for the generation of entry vectors (see 2.1.6).

2.1.11. Bacterial transformation

One Shot TOP10 Competent cells (Invitrogen) were incubated with plasmid DNA on ice for 10 minutes, then heat-shocked at 42 °C for 25 seconds and then chilled on ice. SOC medium (Invitrogen) was added and the mixture was incubated for 37 °C for 1 h and plated on LB agar plates with appropriate antibiotics. The plates were incubated overnight at 37 °C. In the case of cloning expression vectors for the Gateway system that had no insert, One Shot ccdB Survival Competent cells (Invitrogen) were used instead of TOP10 cells.

2.1.12. Plasmid purification

For Minipreps, single colonies were isolated from LB agar plates and incubated in 5 mL LB at 37 °C over night. For Midipreps, single colonies were isolated and incubated in 5 mL LB for 8 h at 37 °C. The 5 mL culture was added to 100 mL LB and incubated at 37 °C over night. Plasmid DNA was isolated from the over night cultures using QIAprep Spin Miniprep Kit (Qiagen) and HiSpeed Plasmid Midi Kit (Qiagen) according to the manufacturer's protocol.

2.1.13. Sequencing

DNA was sequenced by the Equipment Park using their specified protocols. PCR products were purified using the DyeEx Spin kit (Qiagen) according to the manufacturer's protocol.

2.1.14. dsRNA production

To generate dsRNA for RNAi in S2 cells, appropriate DNA templates were amplified using PCR. The PCR product was gel purified using QIAquick Gel Extraction Kit (Qiagen). The purified DNA was transcribed in vitro using the MEGAscript T7 Transcription Kit (Ambion) according to the manufacturer's protocol. The reaction was run over night at 37 °C. The transcribed RNA was precipitated in 0.1 M sodium acetate containing 70 % Ethanol at -20 °C for 10 min. The RNA was washed twice with 70 % ethanol. Dried RNA was dissolved in water and stored at -80 °C.

2.1.15. List of oligonucleotides

Table 2.1.: List of oligonucleotides

Generating pKC26w	
mini-white 451 f	TACGCCATCAATTAAACACAAAGTG
mini-white r	GCCCTGGCACCCGCACCGCGGACTAGTACTAGTTCCAGTG AAATCCAAGC
pW25 DraIII mut f	CACATCGTCGAATACCACCTGCCCCAGTTCGGG
pW25 DraIII mut r	CCCGAACTGGGGCAGGTGGTATTCGACGATGTG
Generating pKC26w_W/GW	
3' GW casette	TAAGGTTCCTTCACAAAGATCC
5' GW casette	CGGGGTACCACGCGTACAAGTTTGTACAAAAAAGCTGA
5' GFP GW casette	CGGGGTACCCACCATGGTGAGCAAGGGCG
RNAi	
Wts RNAi f	TAATACGACTCACTATAGGGCACAAAGTGGGACTGCC
Wts RNAi r	TAATACGACTCACTATAGGGGCAGGGTTTTCATCGCATAC
lacZ RNAi f	TAATACGACTCACTATAGGTTGCCGGGAAGCTAGAGTAA
lacZ RNAi r	TAATACGACTCACTATAGGGCCTTCCTGTTTTTGCTCAC

List of oligonucleotides (continued)

dsRed f	CTAATACGACTCACTATAGGGAGCGAGGACGTCATCAAGG AGT
dsRed r	CTAATACGACTCACTATAGGGAGGGTGATGTCCAGCTTGG AGT
ASPP RNAi f	CTAATACGACTCACTATAGGGAGCAGTAGCTCTTGCCGTT TCC
ASPP RNAi r	CTAATACGACTCACTATAGGGAGTTTTGCAACTGCAACAG AGG
ASPP RNAi #2 f	TAATACGACTCACTATAGGGTCCTCAAGTCGCAGGAGGT
ASPP RNAi #2 r	TAATACGACTCACTATAGGGCCTTCTCGCTGAACAGTGC
PP1α13C RNAi f	TAATACGACTCACTATAGGGATGGCGGAGGTTCTCAATTT
PP1α13C RNAi r	TAATACGACTCACTATAGGGGATATCGCCGCAGATCTTGA
PP1α87B RNAi f	TAATACGACTCACTATAGGGATGGGCGACGTGATGAATA
PP1α87B RNAi r	TAATACGACTCACTATAGGGCCGCAGATCTTCAACGGT
PP1α96A RNAi f	TAATACGACTCACTATAGGGTCGGATATCATGAACATCGAC
PP1α96A RNAi r	TAATACGACTCACTATAGGGGCCTCCAGCTCCAGGAGTAT
PP1β9C RNAi f	TAATACGACTCACTATAGGGATGGGCGACTTCGATCTG
PP1β9C RNAi r	TAATACGACTCACTATAGGGAGTCGCCGAGGAACAAGTAG
Genotyping	
ccdc85 genotyping f	TGCCTCGAATCTGGTGGGGA
ccdc85 genotyping r	ATGAAGAGGAGCCCGCGGA
PP1α96A genotyping f	GCGGAAATGTTGCTGAAGCA
PP1α96A genotyping r	CAATGATCACTTACCCGCGT
RT-PCR	
CG3558 RT 1060f	TTCCCGTGCTGGGACCTGC
CG3558 RT 1470r	CAGTTCACTCACCACAGGCTCG
Ccdc85 RT 900f	GCGTGCGCTGAAGGAGCA
Ccdc85 RT 1320r	GTTCAGCGTGTGGGCATGAC
RpL32 f	GACGCTTCAAGGGACAGTATCTG
RpL32 r	GCAGTAAACGCGGTTCTGCATGAG
Site directed mutagenesis	
RASSF8 S209A f	GAGAAATCGCTGGCCAATCCGCTGGAC
RASSF8 S209A r	GTCCAGCGGATTGGCCAGCGATTTCTC
RASSF8 Y297A f	CTAGTCCCACCACCAGCTCGTGACCCGCCACCC
RASSF8 Y297A r	GGGTGGCGGGTCACGAGCTGGTGGTGGGACTAG
ASPP V812A,F814A f	AAGCTGGGTCGAAGGGCCAGCGCTGATCCGCTG
ASPP V812A,F814A r	CAGCGGATCAGCGCTGGCCCTTCGACCCAGCTT

List of oligonucleotides (continued)

ASPP W987K f	GATGCCGAGAACGAGAAGTGGTGGGCACGGAAT
ASPP W987K r	ATTCCGTGCCCACCACTTCTCGTTCTCGGCATC
Baz S151A f	ATGGTGCGTCGCAGCGCTGATCCCAATCTGCTG
Baz S151A r	CAGCAGATTGGGATCAGCGCTGCGACGCACCAT
Baz S980A f	GCTTTGGGACGACGCGCCATCTCTGAGAAGCAC
Baz S980A r	GTGCTTCTCAGAGATGGCGCGTCGTCCCAAAGC
Baz S1085A f	ATGAAGAAGTCCTCGGCGTTGGAGTCGCTCCAG
Baz S1085A r	CTGGAGCGACTCCAACGCCGAGGACTTCTTCAT
Baz S169D f	AGTAACAAACGCTGGGACGCGGCGGCTCCCCAC
Baz S169D r	GTGGGGAGCCGCCGCGTCCCAGCGTTTGTTACT
Baz S180D f	TACGCTGGCGGGGATGACCCGGAGCGCCTGTTT
Baz S180D r	AAACAGGCGCTCCGGGTCATCCCCGCCAGCGTA
Baz S235D f	CAGCCGTTTGCCCGAGACGGTCGCCTGTCGATG
Baz S235D r	CATCGACAGGCGACCGTCTCGGGCAAACGGCTG
Baz S239D f	CGATCCGGTCGCCTGGACATGCAATTTCTTGGC
Baz S239D r	GCCAAGAAATTGCATGTCCAGGCGACCGGATCG
Baz T712E f	GCCGAGGCCATGGAGGAGCTACGTCGGGCAATG
Baz T712E r	CATTGCCCGACGTAGCTCCTCCATGGCCTCGGC
Baz S806D f	GGCGGAGGTGGTGGCGACGCTGGCAATGAGATG
Baz S806D r	CATCTCATTGCCAGCGTCGCCACCACCTCCGCC
Baz S815D f	GAGATGAATAGATGGGACAATCCCGTTTTGGAT
Baz S815D r	ATCCAAAACGGGATTGTCCCATCTATTCATCTC
Baz S1126D f	CGGGCGGCGGTGGTCGACGAACCGGATGCGAGC
Baz S1126D r	GCTCGCATCCGGTTCGTCGACCACCGCCGCCCG
Baz S1131D f	GACGAACCGGATGCGGACAAGCCCCGCAAGACC
Baz S1131D r	GGTCTTGCGGGGCTTGTCCGCATCCGGTTCGTC
Baz T1136E f	GACAAGCCCCGCAAGGAGTGGCTTTTGGAGGAT
Baz T1136E r	ATCCTCCAAAAGCCACTCCTTGCGGGGCTTGTC
Baz S1169D,S70D f	AAACACGGCTGCAAGGACGACCGGGCCAAGAAG
Baz S1169D,S70D r	CTTCTTGGCCCGGTCGTCCTTGCAGCCGTGTTT
Baz S1170D f	CACGGCTGCAAGTCGGACCGGGCCAAGAAGCCA
Baz S1170D r	TGGCTTCTTGGCCCGGTCCGACTTGCAGCCGTG
Baz S1176D f	CGGGCCAAGAAGCCAGACATACTGCGCGGTATC
Baz S1176D r	GATACCGCGCAGTATGTCTGGCTTCTTGGCCCG
Baz T1410E f	TTTGTGACGCAGGTGGAGATACGGGAGCAGAGC
Baz T1410E r	GCTCTGCTCCCGTATCTCCACCTGCGTCACAAA
Magi P323A f	TCTCACTGGCTGGATGCGCGGCTCTCCAAGTAC
Magi P323A r	GTACTTGGAGAGCCGCGCATCCAGCCAGTGAGA

List of oligonucleotides (continued)

Magi P370A f	ACGCAGTACGAGAACGCAGTGCTGGAGGCCAAG
Magi P370A r	CTTGGCCTCCAGCACTGCGTTCTCGTACTGCGT
Sina C87A f	CCGCCGATCCTGCAGGCCTCCAGCGGGCACCTG
Sina C87A r	CAGGTGCCCGCTGGAGGCCTGCAGGATCGGCGG
Deletions	
ASPP 1-234 attB1	GGGGACAAGTTTGTACAAAAAAGCAGGCTTCACCATGAA GGAGCCGACGAACACTTTG
ASPP 1-234 attB2	GGGGACCACTTTGTACAAGAAAGCTGGGTGCTGCTGCTG CTGCTGATG
ASPP 231-795 attB1	GGGGACAAGTTTGTACAAAAAAGCAGGCTTCACCATGCA ACAGCAGCAGCACCA
ASPP 231-795 attB2	GGGGACCACTTTGTACAAGAAAGCTGGGTGGCTGGTTGT CACGGTTGT
ASPP 796-1020 attB1	GGGGACAAGTTTGTACAAAAAAGCAGGCTTCACCATGAA CATCAAGGAGCGAACG
ASPP 796-1020 attB2	GGGGACCACTTTGTACAAGAAAGCTGGGTGGCCGCACTT CAGCGAT
Baz 1-1096 attB1	GGGGACAAGTTTGTACAAAAAAGCAGGCTTCACCATGAA GGTCACCGTCTGCTT
Baz 1-1096 attB2 stop	GGGGACCACTTTGTACAAGAAAGCTGGGTTTTACAGCTC CTGCACCATAGTCT
Baz 1097-end attB1	GGGGACAAGTTTGTACAAAAAAGCAGGCTTCACCATGCA GATGTCGGATGAGCCG
Baz 1097-end (stop) attB2 r	GGGGACCACTTTGTACAAGAAAGCTGGGTTTCACACCTT GGAGGCGTG
PP1α96A ΔC attB2 stop	GGGGACCACTTTGTACAAGAAAGCTGGGTGTTATCGTCG CTTGTCGGCGG
PP1β9C ΔC attB2 stop	GGGGACCACTTTGTACAAGAAAGCTGGGTGTTACTTCTT CTCGGATGGTTT
RASSF8 attB1	GGGGACAAGTTTGTACAAAAAAGCAGGCTTCACCATGGA ACTTAAAGTATGGGTGGA
RASSF8 1-134 r	GGGGGGATCCGTTCGACTTTTGCTTTAGCAAAGT
RASSF8 1-181 r	GGGGGGATCCCGGTGCTCCCATGGCCGTTT
RASSF8 attB2 stop	GGGGACCACTTTGTACAAGAAAGCTGGGTTTCATACATAT ATGCCTTCAGGATTAAAA
RASSF8 214-end f	GGGGGGATCCATGACCAGCACGGGTAGCAA
RASSF8 221-end f	GGGGGGATCCCCACCCGCACCTACAAATGG

List of oligonucleotides (continued)

Cloning	
PP1α13C attB1	GGGGACAAGTTTGTACAAAAAAGCAGGCTTCACCATGGC GGAGGTTCTCAAT
PP1α13C attB2 stop	GGGGACCACTTTGTACAAGAAAGCTGGGTTCTACTTCTT GCGCTTCTCGA
PP1α87B attB1	GGGGACAAGTTTGTACAAAAAAGCAGGCTTCACCATGGG CGACGTGATGAATA
PP1α87B attB2 stop	GGGGACCACTTTGTACAAGAAAGCTGGGTGTTACTTTTT ACGCTTGTCGG
PP1α96A attB1	GGGGACAAGTTTGTACAAAAAAGCAGGCTTCACCATGTC GGATATCATGAACATCG
PP1α96A attB2 stop	GGGGACCACTTTGTACAAGAAAGCTGGGTTTTATTTTTT CTTGTTTTTATTGTTAGCT
PP1β9C attB1	GGGGACAAGTTTGTACAAAAAAGCAGGCTTCACCATGGG CGACTTCGATCTG
PP1β9C attB2 stop	GGGGACCACTTTGTACAAGAAAGCTGGGTTTTATTTCTT CTTGTTGGTCG
Ccdc85 attB1	GGGGACAAGTTTGTACAAAAAAGCAGGCTTCACCATGTC CGGCAATCAACAG
Ccdc85 attB2 stop	GGGGACCACTTTGTACAAGAAAGCTGGGTTTTAGAGCGG CTCCAGGGC
MYPT-75D attB1	GGGGACAAGTTTGTACAAAAAAGCAGGCTTCACCATGAT CAAGGGCATTCTGATAC
MYPT-75D attB2	GGGGACCACTTTGTACAAGAAAGCTGGGTGCATCAGGAC GCAACACCT
Sina attB1	GGGGACAAGTTTGTACAAAAAAGCAGGCTTCACCATGTC CAATAAAATCAACCCGAAG
Sina attB2	GGGGACCACTTTGTACAAGAAAGCTGGGTGGACCAGAGA TATGGTCACGT
Sqh attB1	GGGGACAAGTTTGTACAAAAAAGCAGGCTTCACCATGTC ATCCCGTAAGACCGC
Sqh attB2 stop	GGGGACCACTTTGTACAAGAAAGCTGGGTTTTACTGCTC ATCCTTGTCCT

2.1.16. Generation of cell culture plasmids

Generation of pAVW and pAWV

N- and C-terminally V5-tag expressing vectors are not part of the *Drosophila* Gateway Vector Collection. In order to express V5-tagged proteins, pAVW and pAWV vectors were generated from FLAG-tag vectors. The DNA encoding the FLAG-tag was cut out from pAFW and pAWF using ScaI and AgeI restriction enzymes (NEB). Synthesized single stranded oligos (Sigma-Aldrich) containing the V5-tag flanked by ScaI and AgeI restriction sites (see 2.1.15) were annealed by heating to 95 °C in a water bath and slowly cooled to room temperature. The annealed V5-DNA fragment was cut with ScaI and AgeI and ligated with cut pAFW and pAWF using T4 DNA Ligase (NEB).

2.1.17. List of cell culture plasmids

All plasmids that were used for cell culture were generated using Gateway cloning. For the nomenclature of the plasmids that were used see 2.1.6. If the plasmid was readily available or derived from an available entry clone using an LR reaction, the originator is given in the source column. cDNA indicates that cDNA from primary fly tissue served as template, DGRC indicates that the template was obtained from DGRC and mutagenesis indicates that an available entry vector was used as template for mutagenesis.

Table 2.2.: List of plasmids for cell culture

Name	Backbone	Source
14-3-3ε pAWF	pAWF	N. Tapon/M. Wehr
14-3-3ζ pAWF	pAWF	N. Tapon/M. Wehr
aPKC pAHW	pAHW	N. Tapon/P. Ribeiro
ASPP 1-234 pAFW	pAFW	Mutagenesis
ASPP 231-795 pAFW	pAFW	Mutagenesis
ASPP 796-1020 pAFW	pAFW	Mutagenesis
ASPP FA pAFW	pAFW	Mutagenesis

List of plasmids for cell culture (continued)

ASPP FA pAHW	pAFW	Mutagenesis
ASPP FA pAMW	pAMW	Mutagenesis
ASPP FA/WK pAMW	pAMW	Mutagenesis
ASPP pAFW	pAFW	N. Tapon/P. Langton
ASPP pAGW	pAGW	N. Tapon/P. Langton
ASPP pAHW	pAMW	N. Tapon/P. Langton
ASPP pAMW	pAMW	N. Tapon/P. Langton
ASPP WK pAMW	pAMW	Mutagenesis
Baz pAFW	pAFW	A. Wodarz
Baz pAMW	pAMW	A. Wodarz
Baz S1085A pAFW	pAFW	Mutagenesis
Baz S1126,31D T1136E pAFW	pAFW	Mutagenesis
Baz S1126D pAFW	pAFW	Mutagenesis
Baz S1169,70,76D pAFW	pAFW	Mutagenesis
Baz S1169,70D pAFW	pAFW	Mutagenesis
Baz S1176D pAFW	pAFW	Mutagenesis
Baz S151A pAFW	pAFW	Mutagenesis
Baz S169D pAFW	pAFW	Mutagenesis
Baz S180D pAFW	pAFW	Mutagenesis
Baz S235D pAFW	pAFW	Mutagenesis
Baz S239D pAFW	pAFW	Mutagenesis
Baz S806D pAFW	pAFW	Mutagenesis
Baz S815D pAFW	pAFW	Mutagenesis
Baz S980A pAFW	pAFW	Mutagenesis
Baz T1410E pAFW	pAFW	Mutagenesis
Baz T712E pAFW	pAFW	Mutagenesis
BazC pAGW	pAGW	Mutagenesis
BazN pAGW	pAGW	Mutagenesis
Ccdc85 pAFW	pAFW	DGRC (RE60986)
Ccdc85 pAMW	pAMW	DGRC (RE60986)
GFP pAFW	pAFW	N. Tapon
GFP pAMW	pAMW	N. Tapon
Hpo pAWF	pAWF	N.Tapon
Hpo pAWH	pAWF	N. Tapon

List of plasmids for cell culture (continued)

Hpo pAWM	pAWM	N. Tapon
Hs RASSF8 isoformA	pTO-N-HAStrep	A. Chalmers
Magi P323A pAFW	pAFW	Mutagenesis
Magi P370A pAFW	pAFW	Mutagenesis
Magi pAFW	pAFW	N. Tapon/M. Wehr
Magi ΔWW pAFW	pAFW	A. Djiane
MYPT-75D pAWG	pAWG	DGRC (LD4660)
PP1α13C pAFW	pAFW	cDNA
PP1α13C pAHW	pAHW	cDNA
PP1α87B pAFW	pAFW	cDNA
PP1α87B pAHW	pAHW	cDNA
PP1α96A pAFW	pAFW	cDNA
PP1α96A pAHW	pAHW	cDNA
PP1α96A pAVW	pAVW	cDNA
PP1α96A ΔC pAFW	pAFW	cDNA
PP1β9C pAFW	pAFW	cDNA
PP1β9C pAHW	pAHW	cDNA
PP1β9C ΔC pAFW	pAFW	cDNA
RASSF pAFW	pAFW	N. Tapon
RASSF8 pAMW	pAMW	N. Tapon/E. Chan
RASSF8 pAWF	pAWF	N. Tapon/E. Chan
RASSF8 pAWH	pAWH	N. Tapon/E. Chan
RASSF8 Y297A pAWF	pAWF	Mutagenesis
RASSF8-SA pAWF	pAWF	Mutagenesis
RASSF8-SA pAWH	pAWH	Mutagenesis
RASSF8-Δ1 pAWH	pAWH	Mutagenesis
RASSF8-Δ2 pAWH	pAWH	Mutagenesis
Sec15 pAFW	pAFW	N. Tapon/E. Chan
Sina C87A pAFW	pAWF	Mutagenesis
Sina pAFW	pAWF	DGRC (HL08111)
Sqh pAFW	pAFW	DGRC (LD14743)
WAVE pAWF	pAWF	N. Tapon/E. Chan
Yki pAWF	pAWF	N. Tapon

2.1.18. Generation of plasmids for injection into *Drosophila* embryos

Generation of pKC26w, pKC26w_W, pKC26w_GW and pKC26w_WG

The pKC26 vector that was available in the lab from the Vienna RNAi stocks centre was not suitable for PhiC31 mediated insertion at most attP sites (see 2.3.3), as it only contained half of the *mini-white* gene. Half of the *mini-white* gene is not sufficient for the expression of the red eye pigment. When pKC26 is recombined into a restriction-based attP locus with the other half of the *mini-white* gene, red pigment is produced. This is useful to ensure the correct insertion of a transgene. However, only few attP site carrying flies (e.g., VIE217, see 2.3.2) have the other half of the *mini-white* gene. Thus, I decided to restore the whole *mini-white* gene to allow the insertion into any attP locus yielding a visible eye marker.

The original pKC26 vector contained an attB site for PhiC31 mediated recombination, an *ubiquitin* promoter upstream of a multiple cloning site for restriction-based cloning and half of the *mini-white* gene. The missing half of *mini-white*, flanked by DraIII and SpeI restriction sites, was cloned from pW25 into pCR-Blunt II-TOPO (Invitrogen). A DraIII restriction site within the *mini-white* fragment was silently mutagenized to allow restriction-based cloning of the fragment into pKC26. The resulting vector was named pKC26w.

In order to allow Gateway cloning (see 2.1.6), a Gateway cassette was inserted by restriction-based cloning using primers containing NheI and KpnI sites. Three vectors were created, pKC26w_W, pKC26w_GW and pKC26w_WG. The first vector only has a Gateway cassette, while the other two code for N- and C-terminal GFP-tags as well. The pKC26w_WG vector was generated by Pedro Gaspar. To allow easy exchange or removal of the *ubiquitin* promoter, all three vectors have an additional MluI restriction site inserted upstream of the Gateway cassettes. Thus, a single MluI digest, followed by self-ligation will generate promoterless vectors.

Table 2.3.: List of plasmids for injection

Name	Backbone	Source
UAS-ASPP-FA-HA	pUASg-HA	Mutagenesis
UAS-ASPP-HA	pUASg-HA	Mutagenesis
UAS-Ccdc85	pUASg	DGRC (RE60986)
Ubi-GFP-ASPP	pKC26w GW	Mutagenesis
Ubi-GFP-ASPP-FA	pKC26w GW	Mutagenesis
Ubi-GFP-PP1α87B	pKC26	Mutagenesis
Ubi-GFP-PP1α96A	pKC26	Mutagenesis
Ubi-RASSF8-GFP	pKC26	N. Tapon/E. Chan
Ubi-RASSF8-SA-GFP	pKC26	Mutagenesis

2.2. Molecular Biology: Cell culture and protein

2.2.1. *Drosophila* Cell Culture

Drosophila S2 cells were maintained at 25 °C in Schneider's *Drosophila* Medium (Gibco) supplemented with 10 % Fetal Bovine Serum (Sigma-Aldrich) and 100 unit/mL penicillin and 100 µg/mL streptomycin (Gibco) in 75 cm^2 cell culture flasks (Corning).

2.2.2. Transient transfection

For DNA transfections, 30 min prior to transfection, $3x10^6$ S2 cells were seeded per well of a 6-well plate (Corning) in 2 mL of serum-containing Schneider's *Drosophila* Medium (Gibco). 200-400 ng of DNA per plasmid were transfected per well using Effectene Transfection Reagent (Qiagen) according to the manufacturer's protocol. The amount of Enhancer and Effectene Reagent used per well was 3.2 µL and 10 µL respectively. Cells were lysed/prepared for immunofluorescence 48 h after transient transfection.

2.2.3. RNAi in S2 cells

For RNAi, 1.5x10^6 S2 cells were seeded per well of a 6-well plate 1 h before. 25 ng of dsRNA was diluted in 1 mL of serum-free Schneider's *Drosophila* Medium (Gibco) per well. The dsRNA was added for 30 minutes. Subsequently, 2 mL of serum-containing Schneider's *Drosophila* Medium (Gibco) were added. Cells were lysed/prepared for immunofluorescence 72 h after adding dsRNA. For parallel RNAi and transient transfection, 24 h after adding dsRNA, the transfection was carried out as described above.

2.2.4. Proteasome inhibitor treatment

For proteasome inhibition experiments, S2 cells were treated with 50 µM MG132 (Calbiochem) and 50 µM calpain inhibitor I (Ac-LLnL-CHO or LLnL) (Sigma) for 4 h before cell lysis.

2.2.5. Cell lysis

For immunoprecipitations (IPs), S2 cells were washed once with PBS before lysis. The lysis was carried out with 200 µL of HEPES lysis buffer supplemented with protease inhibitor cocktail with EDTA (Roche) for one well of a 6-well plate. The lysis was left on ice for 10 minutes. For detecting phospho-proteins (e.g., mobility shift assays, phospho-specific antibody Western blot), additionally, Phosphatase Inhibitor Cocktail 2 and 3 (Sigma-Aldrich) and 20mM NaF were added to the lysis buffer. The soluble lysis fraction was obtained through centrifugation (16,000 g, 20 minutes).

2.2.6. Tissue lysis

Fly heads

Fly heads were collected from adult flies. For each sample, 250 heads were lysed in 400 µL HEPES lysis buffer supplemented with Phosphatase Inhibitor Cocktail 2 and 3 (Sigma-Aldrich) and 20mM NaF with the help of a Kontes Pellet Pestle Cordless Motor (Kimble Chase). The lysate was bound to 80 µL of Anti-HA-Agarose beads

(Sigma-Aldrich) for 1 h at 4 °C. The IPed material was eluted in Sample Loading buffer.

2.2.7. Co-immunoprecipitation (co-IP)

Half of the soluble S2 cell lysate (100 µL, see above) from the lysis of one well of a 6-well plate was added to 20 µL of ANTI-FLAG M2 Affinity Gel (Sigma-Aldrich) or 15 µL of GFP-Trap agarose (ChromoTek) in 100 µL HEPES lysis buffer. The lysate and the beads were incubated for 1 h at 4 °C. After the binding, the beads were washed four times with 1 mL of HEPES lysis buffer. The IPed material was eluted in Sample Loading buffer.

Indirect IP

For co-IPs of overexpressed ASPP and RASSF8 from S2 cells, the vectors were separately transfected into different cells to avoid aggregation. Cleared lysates from cells overexpressing ASPP and RASSF8 were then mixed before adding to beads. Binding, washing and elution was carried out as for regular co-IPs.

2.2.8. Western Blotting

For protein analysis, either 5 µL of cleared protein lysate from one well of a 6-well plate or half of the IPed material were denatured in Sample Loading buffer for 5 minutes at 95 °C. The denatured samples were loaded into NuPAGE Novex 4-12 % Bis-Tris Mini gels (Invitrogen) and run for 1 h at 195 V in XCell SureLock Mini-Cells (Invitrogen) with NuPAGE MOPS SDS Running Buffer (Invitrogen).

Proteins were transferred from the gels onto methanol activated Amersham Hybond-P PVDF membranes (GE Healthcare) using Mini-PROTEAN Tetra Cells (Biorad). The blotting procedure was done at 100 V for 1.5 h in Tris-Glycine blotting buffer.

After blotting, the membranes were blocked in PBS with 5 % (w/v) skimmed milk powder for 30 minutes at room temperature. Primary antibody in the appropriate

concentrations (see 2.2.10) dissolved in PBS with 5 % (w/v) skimmed milk powder was used to replace the blocking solution. The membrane was incubated with the primary antibody overnight at 4 °C. Subsequently, the membrane was washed for four times with PBST to remove unbound primary antibody. After the wash, the membrane was incubated for 30 minutes at room temperature with horseradish peroxidase conjugated secondary antibody in the appropriate concentration (see 2.2.10) diluted in PBS with 5 % (w/v) skimmed milk powder. Afterwards, unbound secondary antibody was washed off for five times with PBST. Lastly, proteins on the membrane were visualised by chemiluminescence using ECL Plus Western Blotting Substrate (Pierce). Amersham Hyperfilm ECL (GE Healthcare) was used to capture the chemiluminescence signal.

2.2.9. Generation of antibodies

The pS209 antibody was generated by Eurogentec. In vitro synthesised peptides of the sequence CHEKSLpSNPLD were injected into rabbits. Purification of the antibody was also carried out by Eurogentec.

2.2.10. Antibodies used for Western blotting

Table 2.4.: List of antibodies for Western blotting

Primary Antibody	Species	Concentration	Source
Baz pS151	Rabbit	1/500	A. Wodarz
Baz pS980	Rabbit	1/500	D. St Johnston
Baz pS1085	Rabbit	1/500	A. Wodarz
FLAG (M2)	Mouse	1/5000	Sigma Aldrich
GFP (3E1)	Mouse	1/1000	Cancer Research UK
HA (3F10)	Rat	1/2000	Roche
Myc (sc-40)	Mouse	1/5000	Santa Cruz
RASSF8	Rabbit	1/1000	N. Tapon/Eurogentec
RASSF8 pS209	Rabbit	1/1000	N. Tapon/Eurogentec
Myosin LC pS19 (#3671)	Rabbit	1/1000	Cell Signaling

List of antibodies for Western blotting (continued)

Tubulin (E7)	Mouse	1/5000	DSHB
V5 (R960-25)	Mouse	1/5000	Life Technologies
Wts	Guniea Pig	1/1000	N. Tapon/Eurogentec
Yki pS168	Rabbit	1/5000	N. Tapon/Eurogentec
Yki (69)	Rabbit	1/5000	N. Tapon/Eurogentec

Secondary Antibody	Species	Concentration	Source
HRP anti-rabbit	Donkey	1/5000	GE Healthcare
HRP anti-mouse	Sheep	1/5000	GE Healthcare
HRP anti-rat	Goat	1/5000	GE Healthcare
HRP anti-guinea pig	Rabbit	1/5000	Sigma

2.2.11. Mobility shift assays

In order to achieve better separation for mobility shift assays, 8 % hand-cast gels were used. The separation gel contained 8 % Acrylamide/Bis-acrylamide (Sigma-Aldrich) in a 29:1 ratio, 390 mM Tris (pH 8.8), 0.1 % (w/v) SDS, 0.1 % (w/v) ammonium persulfate and 0.04 % TEMED (v/v). The stacking gel contained 5 % Acrylamide/Bis-acrylamide (Sigma-Aldrich) and 125 mM Tris (pH 6.8). Other ingredients were the same as in the separation gel. The gel was run for 100 minutes at 190 V in a Mini-PROTEAN Tetra Cell with Tris-glycine electrophoresis buffer. Blotting was performed as with pre-cast gels.

2.2.12. Phosphatase assay

Expression and purification of the phosphatase complex

ASPP and PP1α96A were expressed in S2 cells in one well of a 6-well plate, while RASSF8 and Ccdc85 were expressed in a separate well. The cells were lysed with HEPES lysis buffer supplemented with protease inhibitor cocktail (Roche). The

cleared lysates were mixed and bound to 15 µL of GFP-Trap agarose (ChromoTek) or ANTI-FLAG M2 Affinity Gel (Sigma-Aldrich) for 1 h at 4 °C. Unbound proteins were washed away for four times with PBST.

Expression and purification of the substrate

The substrate (FLAG-tagged Baz) was expressed in S2 cells in two wells of a 6-well plate. Before lysis, 50 mM Calyculin A (Sigma-Aldrich) was added to the S2 cell medium to block PP1 and PP2A family phosphatases for 25 minutes, which lead to the hyperphosphorylation of Baz. Then, cells were lysed with RIPA lysis buffer supplemented with Phosphatase Inhibitor Cocktail 2 and 3 (Sigma-Aldrich) and 20 mM NaF. The cleared lysate was bound to 25 µL of ANTI-FLAG M2 Affinity Gel (Sigma-Aldrich) for 1 h at 4 °C. Unbound proteins were washed away for four times with PBST. After washing, FLAG-tagged Baz was eluted from the beads using 50 µL Elution buffer for 20 minutes at 4 °C.

Dephosphorylation reaction

The eluted substrate was added to the ASPP/PP1 complex bound to GFP- or FLAG-beads. The suspension was incubated for the indicated duration at 30 °C. The reaction was stopped by adding Sample Loading buffer.

2.2.13. Buffers and Solutions

TAE

40 mM	Tris
20 mM	Acetic acid
1 mM	EDTA

PBS

137 mM	NaCl
2.7 mM	KCl
10 mM	Na_2HPO_4
1.8 mM	KH_2PO_4

PBST
PBS + 0.1 % (v/v) Tween 20

HEPES lysis buffer

150 mM	NaCl
50 mM	HEPES NaOH pH 7.5 NaCl
0.5 % (v/v)	Triton X-100

RIPA buffer

10 mM	Tris HCl pH 7.4
150 mM	NaCl
1 % (v/v)	Triton X-100
0.1 % (w/v)	SDS
1 % (w/v)	Sodium Deoxycholate

Elution buffer

50 mM	Tris HCl pH 7.4
30 mM	NaCl
150 ng/µL	5x FLAG-peptide

Sample Loading buffer
NuPAGE LDS Sample Buffer (Invitrogen)
NuPAGE Sample Reducing Agent (Invitrogen)

Tris-Glycine electrophoresis buffer

25 mM	Tris
250 mM	Glycine
0.1 %	(w/v) SDS

Tris-Glycine blotting buffer

25 mM	Tris
192 mM	Glycine
20 % (v/v)	Methanol

PBT
PBS + 0.1 % (v/v) Triton X-100

LB (1 L)

10 g	Tryptone
5 g	Yeast extract
5 g	NaCl
1 mM	NaOH

2.3. Fly genetics

2.3.1. Balancer and stock maintenance

Flies were kept at 25 °C. All mutant and transgenic stocks were kept with balancer chromosomes. The balancer chromosomes that were used all contain multiple inversions or translocations that minimise the frequency of crossing-over. The balancers also carried recessive lethal mutations and visible markers. The recessive lethal mutations allow mutants or transgenics to be kept stably together with the balancer chromosome, as all surviving progeny will either have one balancer chromosome and one chromosome carrying the mutation or transgene, or will be homozygous for the mutation/transgene (if not recessive lethal).

The balancer chromosomes that were used are: FM7c for the X chromosome (carrying B^1 as visible marker), CyO for the 2nd chromosome (carrying Cy^1 as visible marker), TM3 Sb for the 3rd chromosome (carrying Sb^1 as visible marker), TM3 Ser for the 3rd chromosome (carrying Ser^1 as visible marker) and TM6b Tb for the 3rd chromosome (carrying Tb^1 and $Antp^{Hu}$ as visible marker).

2.3.2. Recombination of genomic loci

Mutations or transgenes that were located on the same chromosome were combined using female meiotic recombination. Females carrying the two genetic loci of interest were crossed to males with double balancer chromosomes. Single male progeny of this cross were then genotyped (see 2.1.1), selected on G418 (Gibco) antibiotic containing food, characterised by visible markers or by phenotype.

For recombining FRT chromosomes, single males were kept in vials with 300 µL of 25 µg/mL G418 (Gibco) aqueous solution added to the food one day before. As FRT chromosomes that were used in this thesis contained a neomycin resistance gene, flies could be selected based on their viability in vials with G418 containing food.

In the case of recombining UAS-transgenes with GAL4 drivers, male progeny could be selected based on their visible phenotype. Similarly, ubi-transgenes that carried a visible eye marker (w^+) could be selected based on their eye colour.

2.3.3. PhiC31 integrase-mediated generation of transgenic flies

To generate flies with targeted insertion of transgenes, the PhiC31 integrase system was used. In contrast to random insertion, the targeted insertion of transgenes leads to comparable expression levels, as the genomic context of two different insertions is the same. When PhiC31 integrase is present, recombination between a plasmid carrying the attB sequence and genomic DNA that harbours an attP sequence occur, leading to the integration of the plasmid into the genome. Embryos of flies carrying an attP site at a defined position within their genome were injected with a plasmid carrying the transgene and the attB sequence as well as a plasmid coding for PhiC31 integrase (pKC40). The injections were done by the LRI Fly Facility and BestGene.

For this thesis, the following transgenic flies were generated:

Table 2.5.: List of transgenic flies

Plasmid	Fly Line	Bloomington ID	Locus
Ubi-GFP-ASPP	PBacy[+]-attP-9AVK00018	9736	2R (53B2)
Ubi-GFP-ASPP FA	PBacy[+]-attP-9AVK00018	9736	2R (53B2)
Ubi-GFP-PP1α87B	Vie217	N/A	3
Ubi-GFP-PP1α96A	Vie217	N/A	3
Ubi-RASSF8-GFP	Vie217	N/A	3
Ubi-RASSF8-SA-GFP	Vie217	N/A	3
UAS-ASPP-FA-HA	PBacy[+]-attP-9AVK00018	9736	2R (53B2)
UAS-ASPP-HA	PBacy[+]-attP-9AVK00019	9736	2R (53B2)
UAS-Ccdc85	PBacy[+]-attP-3BVK00002	9723	2L (28E7)

2.3.4. P-element excision

To generate the *ccdc85*$^{C1.1}$ mutant, a transposon or more specifically the *P{XP}d06579* P-element was imprecisely excised. This was done by crossing *P{XP}d06579* containing flies to flies expressing the transposase (Δ2-3) that mediates the mobilisation of P-elements. The progeny of the first cross, where the P-element

was mobilised, were then crossed to double balancer flies. This second generation of flies contained male progeny that lost the visible eye colour marker of the P-element (w^+) indicating a successful mobilisation of the P-element. These selected flies were then genotyped for deletions within the *ccdc85* gene using PCR.

2.3.5. GAL4/UAS system

The GAL4/UAS system was used for tissue or pattern specific expression of transgenes. The transgenes were either protein coding or RNAi coding, allowing overexpression or silencing. The expression of the transgene was achieved by crossing flies that express the GAL4 transcription factor under the control of tissue or pattern specific promoters to other flies that carry transgenes fused to UAS promoter regions. In the progeny, GAL4 transcription factor bound to UAS promoter regions to drive the expression of the transgene.

2.3.6. Flp/FRT system

The Flp/FRT system was used to generate mosaic mutant tissue. In a first step, flies with a mutation in the gene of interest were recombined with an FRT site at the base of the chromosome arm. These flies were then crossed with flies that expressed flippase (Flp) and carried an FRT site at the base of the same chromosome arm as the gene of interest additional to a ubiquitously expressed GFP transgene. In all tissues of the progeny where Flp was expressed, the FRT sites could recombine during mitosis.

As a result, a mosaic tissue was generated with different genotypes marked by different intensities of GFP. GFP-negative tissue was homozygous mutant for the gene of interest, weakly GFP-positive tissue was heterozygous mutant, and strongly GFP-positive tissue was of wild type.

2.3.7. MARCM system

The MARCM (Mosaic analysis with a repressible cell marker) system was used to express a transgene in mutant tissue in a mosaic fashion. The MARCM system combines the Flp/FRT system and the GAL4/UAS system and adds in GAL80, a GAL4 repressor. Instead of having the GFP expressing transgene on an FRT chromosome as in the regular Flp/FRT system, it has a ubiquitously expressed GAL80 transgene. In a first step flies that have a mutation in the gene of interest were recombined to an FRT chromosome, together with a transgene fused to UAS promoter regions. Then, these flies were crossed to flies that express Flp, carry the *FRT GAL80* chromosome, ubiquitously express GAL4 and have GFP fused to UAS promoter regions. In the progeny of this cross, all tissue that did not express Flp was heterozygous for the mutation and neither the transgene, nor GFP was expressed as GAL4 was repressed by the ubiquitous expression of GAL80. In tissue with Flp expression, FRT sites could recombine during mitosis, as with the Flp/FRT system.

As a result, a mosaic tissue was generated. GFP-positive tissue was lacking GAL80, thus was homozygous for the mutation. All other GFP-negative tissue had either one or two copies of *GAL80*. In contrast to Flp/FRT mosaics, heterozygous mutant tissue could not be distinguished from wild type tissue, as both did not express GFP.

2.3.8. Modifier screen

For the modifier screen, genomic deficiency lines were selected that had defined genomic deletions and were as small as possible. *ASPP RNAi* was first recombined with *GMR-GAL4*. Then, the resulting flies were crossed to the genomic deficiency lines (see Appendix B) and kept at 29 °C. Adult progeny were screened for eye roughness.

2.3.9. Fly tissue preparation

Eye-antennal and wing imaginal disc

Crosses were set-up at 25 °C. For the generation of mosaic clones using the Flp/FRT system, two different promoters for Flp were used. *eyFlp* expresses Flp only in the

eye, while *hsFlp* is ubiquitously expressed under higher temperatures. When *hsFlp* (Flp under the control of Hsp70 promoter) was used, larvae were shifted to 37 °C for 1 h, 48 h after egg laying. For isolating eye-antennal and wing imaginal discs, wandering third instar larvae were collected.

Pupal retina

For 26 h APF (after puparium formation) pupal retina preparations, white pre-pupae were collected and kept at 25 °C for 26 h. For 40 h APF pupal retina preparations, white pre-pupae were collected, and shifted to 18 °C for 16 h over night (which corresponds to 8 h at 25 °C) and back to 25 °C until they have been at 25 °C for a total of 32 h.

Adult wings

As animal density and quality of food can influence animal size and weight, all wing size quantification experiments were done under density-controlled conditions at 25 °C. Crosses with the same number of flies for different genotypes were kept on apple juice plates with yeast paste for 12 h. The plates were incubated for another 12 h. First instar larvae were collected individually and 50 larvae were placed into one vial. Adult flies were put into ethanol before imaging.

2.4. Immunohistochemistry

2.4.1. Preparation of fly tissues

Larval imaginal discs and pupal retinas were dissected in PBS. The tissue was fixed with 4 % formaldehyde in PBS at room temperature for 20 minutes, protected from light. After fixation, the tissue was washed twice with PBT and then permeabilised with PBS containing 0.3 % (v/v) Triton X-100 for 30 minutes at room temperature. After permeabilisation, tissues were blocked with PBT containing 10 % Normal Goat Serum (NGS) for 30 minutes at room temperature. Primary antibody diluted ap-

propriately (see 2.4.3) was added and the tissue was incubated at 4 °C over night. Unbound primary antibody was washed away using PBT for four times before secondary antibody (see 2.4.3) diluted in PBT with 10 % NGS was added for 1 h at room temperature, protected from light. Unbound secondary antibody was washed away with PBT for four times and lastly, the tissue was mounted in Vectashied with DAPI (Vector) on glass microscopy slides.

2.4.2. Preparation of S2 cells

S2 cells were transfected as normal in one well of a 6-well plate. Two days post transfection, cells were seeded 1:3 (70 µL cell suspension + 130 µL fresh S2 cell medium) on 4-well CultureSlides (BD Falcon). The cells were kept for 1 h at room temperature to allow for adherence to the slides. Cells were washed once with PBS before they were fixed with 4 % formaldehyde in PBS for 10 minutes at room temperature, protected from light. After fixation, cells were washed three times with PBT and blocked with 10 % NGS containing PBT for 15 minutes. Primary antibody was added for 1 h at room temperature, before unbound antibodies were washed away for three times with PBT. Secondary antibody in 10 % NGS containing PBT was added for 30 minutes before unbound antibodies were washed away for four times with PBT. Vectashied with DAPI (Vector) was added for mounting.

2.4.3. List of antibodies used

Table 2.6.: List of antibodies for IHC

Primary Antibody	Species	Concentration	Source
Arm (N2 7A1)	Mouse	1/10	DSHB
ASPP	Rat	1/500	N. Tapon/Eurogentec
Baz	Rabbit	1/500	F. Pichaud
Beta-gal	Mouse	1/500	Promega
Ecad (DCAD2)	Rat	1/100	DSHB
Ex	Rabbit	1/500	A. Laughon

List of antibodies for IHC (continued)

RASSF8 (08)	Rabbit	1/500	N. Tapon/Eurogentec

Secondary Antibody	Species	Concentration	Source
Rhodamine Red X anti-rabbit	Donkey	1/500	Jackson ImmunoResearch
Rhodamine Red X anti-rat	Donkey	1/500	Jackson ImmunoResearch
AlexaFluor 647 anti-mouse	Goat	1/500	Life Technologies
AlexaFluor 488 anti-rabbit	Goat	1/500	Life Technologies

2.4.4. Microscopy techniques and settings

Fluorescence images were acquired on a Zeiss LSM 710 confocal laser-scanning microscope. For whole eye-antennal and wing imaginal disc images a 20x dry lens was used. All other images were acquired using a 63x water immersion lens with water as immersion fluid. The pinhole was set at 1.1 µm for the 63x lens and at 2.0 µm for the 20x lens.

2.5. Mass spectrometry

2.5.1. Sample preparation

Samples were loaded as for Western blotting in NuPAGE Novex 4-12 % Bis-Tris Mini gels (Invitrogen). Samples from phosphatase assays were run for 1 h at 195 V, while samples for proteins identification were only run for 2 cm. The gels were stained with SimplyBlue SafeStain (Invitrogen). For phosphatase assays the whole gel was send to the LRI Protein Analysis and Proteomics facility for trypsinisation and further downstream processing. For protein identification, each lane was cut into eight horizontal slices with a scalpel. The slices were further cut into small pieces and stored in one well of a 96-well plate with 100 µL water per slice. The 96-well plate

was send to the LRI Protein Analysis and Proteomics facility for trypsinisation and further downstream processing.

2.5.2. Quantification and identification of changes in phosphorylation (IP: ASPP)

This part of the method refers to 4.2.4. Three dephosphorylation reactions were carried out for FLAG-Baz: (1) with GFP alone, (2) with ASPP and PP1 and (3) with ASPP, PP1 and RASSF8. For each reaction, one sample at 15 minutes and one sample at 30 minutes reaction time were taken. The six samples were injected three times each (technical replicates) by the LRI Protein Analysis and Proteomics facility. MaxQuant software was used for label-free quantitation.

Changes in the amount of detected phospho-peptides were analysed in Perseus. Six pairwise comparisons were carried out for each of the six samples. For each time point (15 and 30 minutes) comparisons between the control (GFP only) and the two conditions (PP1+ASPP and PP1+ASPP+RASSF8) were carried out. Additionally, the conditions with and without RASSF8 were compared to each other. All Baz phospo-peptides with statistically significant reduced intensities in the conditions where PP1 was present were selected. Phospho-peptides with a posterior error probability (PEP) of larger than $1x10^{-5}$ were filtered out. The PEP indicates how likely it is that the peptide is wrongly identified as being present in the experiment.

To calculate the fold change of peptide intensities, raw intensities were first normalised for each technical replicate to the average of all peptide intensities. The fold change was defined as the ratio between two average normalised intensities. Lastly, the average of all fold change values of significant comparisons was reported.

2.5.3. Quantification and identification of changes in phosphorylation (IP: PP1)

This part of the method refers to 4.2.6. Similar to the experiment described above, three dephosphorylation reactions were carried out for FLAG-Baz: (1) with GFP alone, (2) with PP1 alone or (3) with PP1, ASPP, RASSF8 and Ccdc85. Only one

sample for each condition after 10 minutes of dephosphorylation was taken. The three samples were each split into two aliquots. One half was used for label free quantitation (LFQ) as before (three technical replicates for each sample). The second half was dimethyl-labelled on primary amines using formaldehyde. The GFP treated sample was labelled with deuterated formaldehyde, while the PP1 only and PP1, ASPP, RASSF8 and Ccdc85 treated samples were labelled with normal formaldehyde. Two mixtures were created from the labelled samples: (1) heavy labelled GFP treated sample with PP1 only treated regular labelled sample and (2) heavy labelled GFP treated sample with the PP1, ASPP, RASSF8 and Ccdc85 treated regular labelled sample. Each mixture was injected three times (technical replicates). MaxQuant and Mascot software were used for quantitation.

Changes in the amount of detected phospho-peptides were analysed in Skyline. For label free quantitation (LFQ) two comparisons were made: (1) between GFP treated and PP1 only treated and (2) between PP1 only treated and PP1, ASPP, RASSF8 and Ccdc85 treated. The fold-change was calculated as a ratio of average intensities. The localisation of the phosphorylation was determined using MaxQuant. For each dimethyl-labelled mixture, a direct comparison for each identified peptide could be made between the two different treatments, as they were labelled with either deuterated or normal formaldehyde. Thus, similar to the LFQ, two comparisons could be made. The fold-change was calculated analogously.

2.6. SEM

Adult male flies were collected and transferred to fresh vials for one day allowing the flies to clean themselves. Samples were pre-dried with subsequent washes in 25 %, 50 %, 75 % and twice in 100 % ethanol for 30 minutes each. The last drying step was carried out over night. After pre-drying, samples were fixed, dried using critical point drying and coated with platinum by Nic Tapon. Images were recorded on a Jeol JSM 7700F scanning electron microscope.

2.7. Quantification

2.7.1. Wing size and roundness measurements

Adults fly wings were imaged with a LeicaDFC420C camera mounted on a Zeiss Axioplan2 microscope. ImageJ was used to trace the outline of wing blades. The wing roundness was defined as the ratio of the length divided by the width of the wing blade. The length was measured as a straight line along the whole length of the L4 vein. The width was measured as a straight line across the cross-vein from the anterior to the posterior margin of the wing.

2.7.2. Interommatidial cell counting

The cell outlines of 40 h APF retinas were visualised using anti-E-cadherin antibodies and imaged. Interommatidial cells (IOCs) were counted within a hexagonal region of interest using ImageJ. Each vertex of the hexagon was placed in the centre of the six ommatidia surrounding one central ommatidium. Cells that were bisected by the lines of the hexagon were only counted as half a cell.

Bristle clusters were not counted as IOCs. Bristle misplacement was defined as any hexagon containing either two bristle clusters directly next to each other or when two bristle clusters were not separated by tertiary pigment cells. Missing bristle clusters were not counted as bristle misplacement.

2.7.3. Cell-cell junction signal intensity (Baz)

A single confocal plane was imaged. ImageJ was used to draw a line along the cell-cell contacts of two neighbouring primary pigment cells with their surrounding IOCs. The average signal intensity of five such lines was measured for *ASPP* mutant tissue and wild type tissue.

Chapter 3.

The PP1/ASPP complex

The Affinity Purification and Mass-Spectrometry (AP-MS) results from Matthias Gstaiger's lab (Hauri et al. 2013) suggested that ASPP and N-terminal RASSF family proteins were associated to PP1s. Before I started investigating *Drosophila* ASPP and PP1, only one publication described the association of a fragment of human ASPP2 (called p53BP2) with PP1 (Helps et al. 1995). ASPP family proteins were primarily known for their regulation of p53-mediated transcription (Trigiante and Lu 2006). The link between ASPP family proteins and PP1 was revisited more recently (Liu et al. 2011, Llanos et al. 2011, Skene-Arnold et al. 2013).

In this chapter I show that *Drosophila* ASPP also can also bind to PP1. Furthermore, I provide in vivo evidence for the functional importance of the ASPP/PP1 complex. Lastly, I describe two additional subunits (RASSF8 and Ccdc85) that can associate with the core ASPP/PP1 complex.

3.1. The core ASPP/PP1 complex

3.1.1. ASPP interacts with PP1 via its RVXF motif

In *Drosophila* ASPP, the RVXF motif that precedes four ankyrin repeats and an SH3 domain is conserved (Fig. 3.1A, and see 1.3.1). Furthermore, the characteristic basic and acidic residues that flank both sides of the RVXF motif (Hendrickx et al. 2009)

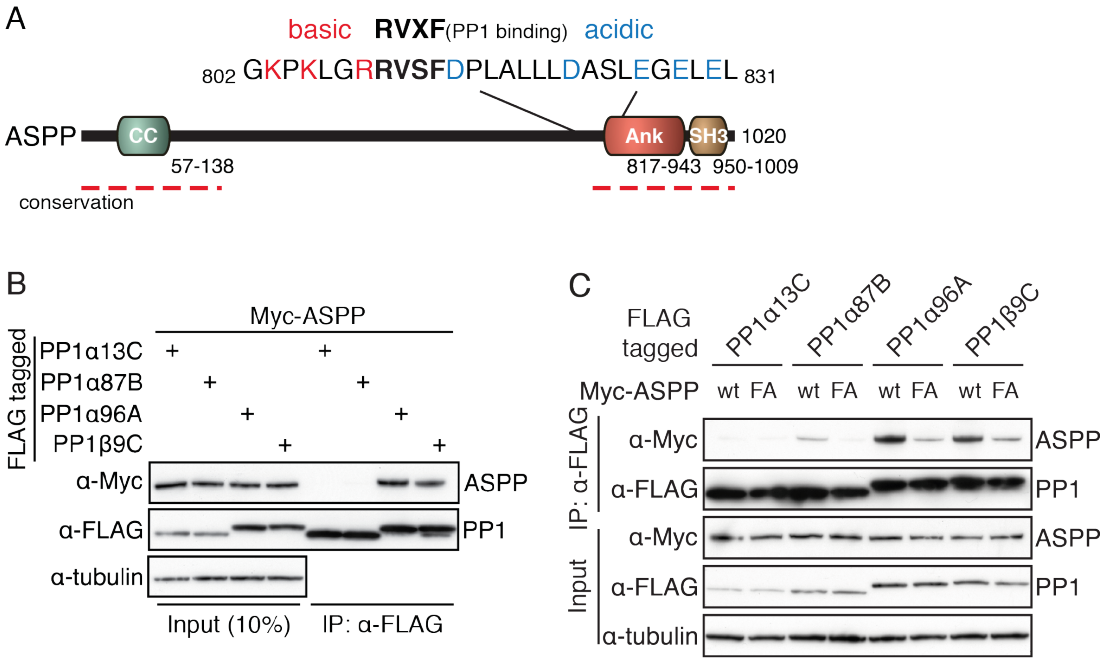

Figure 3.1.: ASPP binds to PP1α96A and PP1β9C via its RVXF motif

(A) Domain structure of ASPP. ASPP is conserved at the both termini, where all identifiable domains are located. Coiled coil region was predicted by jpred3 (Cole et al. 2008). Four ankyrin repeats and SH3 domain annotation based on ASPP2 structure (Gorina and Pavletich 1996). Conserved regions between *Drosophila* ASPP, and human ASPP1/2 are indicated by red dashed lines.

(B, C) Western blots of co-IP experiments using anti-FLAG antibody coupled beads with S2 cell lysates. Cells were transfected with the indicated constructs. Western blots were probed with indicated antibodies. (B) ASPP preferentially binds to PP1α96A and PP1β9C. (C) Mutation of V812 and F814 to alanine within the RVXF motif of ASPP (ASPP-FA) decreases the binding between PP1s and ASPP. A weak binding of ASPP to PP1α87B is visible in this condition in contrast to (B).

are present in *Drosophila* ASPP as well (Fig. 3.1A). The conservation suggests that *Drosophila* ASPP, similar to human ASPP1 and ASPP2, might bind to PP1

Initially, I tested if *Drosophila* ASPP can bind to PP1 in co-immunoprecipitation (co-IP) experiments. The four PP1 catalytic subunits bound to ASPP to different degrees (Fig. 3.1B). ASPP bound to PP1α96A most strongly, followed by PP1β9C. PP1α87B and PP1α13C could bind to ASPP only weakly (Fig. 3.1C, 3.2C). The RVXF motif is required for binding, since mutating V812 and F814 of the motif (ASPP-FA) reduced the binding between ASPP and the PP1 catalytic subunits (Fig. 3.1C). Residual binding remains between ASPP-FA and PP1 under the conditions of the co-IP experiment (Fig. 3.1C). This suggests that residues other than the RVXF motif might participate in the ASPP/PP1 interaction.

3.1.2. The SH3 domain of ASPP contributes to PP1 binding

The strong preference of *Drosophila* ASPP for a subset of PP1 isoforms is not reflected in human ASPP1 or ASPP2 (Skene-Arnold et al. 2013). Human ASPPs bind to all three human PP1 isoforms. Only one of the isoforms, PP1α, shows a slightly stronger binding of ASPP1/2 and iASPP (Skene-Arnold et al. 2013).

To understand what residues in PP1α96A and PP1β9C might be responsible for the stronger binding of ASPP, I aligned the sequences of *Drosophila* and human PP1s. From this alignment, it was evident that the two PP1s that bind to ASPP more weakly lack a short C-terminal stretch, which is shared among all other PP1s, including the three human isoforms (Fig. 3.2A). To show that this C-terminal stretch is essential for ASPP binding, I generated C-terminally truncated PP1α96A (PP1α96A-ΔC) and PP1β9C (PP1β9C-ΔC) that lack residues 304–327 and 304–330 respectively. The truncated PP1s had C-terminal ends that resembled PP1α87B and PP1α13C. In co-IP experiments, ASPP binding to the truncated PP1α96A and PP1β9C was reduced compared to the full-length proteins (Fig. 3.2B). This suggests that the C-terminus of PP1α96A and PP1β9C are important for ASPP binding.

Skene-Arnold et al. have pointed out that the C-terminus of human PP1s contain a class II SH3 domain binding motif (Skene-Arnold et al. 2013). This motif is char-

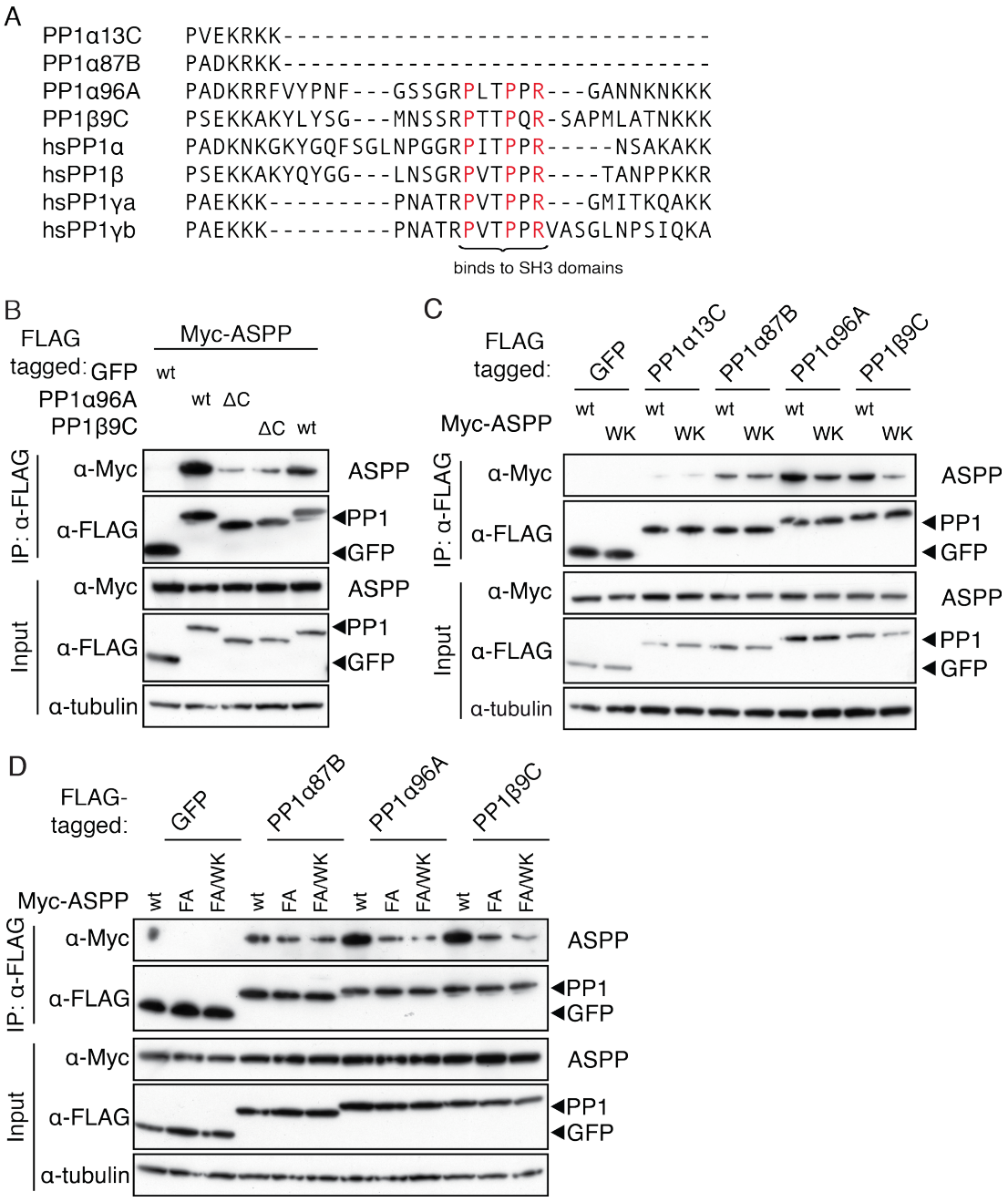

Figure 3.2.: ASPP binds to the C-terminus of PP1α96A and PP1β9C with its SH3 domain

(A) Alignment of the C-terminus of *Drosophila* and human PP1s. PP1α13C and PP1α87B have shorter C-termini that lack the class II SH3 domain binding motif. All human PP1 isoforms possess the binding motif. PxxPxR motif highlighted in red. (B-D) Western blots of co-IP experiments using anti-FLAG antibody coupled beads with S2 cell lysates. Cells were transfected with the indicated constructs. Western blots were probed with indicated antibodies.

(Continues on following page)

acterized by a proline-rich stretch with the consensus sequence of PxxPxR. Human ASPPs can bind to this motif via its SH3 domains (Skene-Arnold et al. 2013). The class II SH3 domain binding motif that is present in all human PP1s is only found in PP1α96A and PP1β9C (Fig. 3.2A), the PP1s that bind to ASPP more strongly.

To test if *Drosophila* ASPP binds to PP1α96A and PP1β9C via its SH3 domain, I generated an ASPP mutant with an SH3 domain that is deficient in binding to PxxPxR motifs (ASPP-WK). The tryptophan to lysine mutation in SH3 domains has been used as binding mutant in unbiased pull-down assays (Bisson et al. 2011) and is thought to maintain the overall structure of the domain (Yang et al. 1995). As predicted, the WK-mutation reduced binding to PP1α96A and PP1β9C in co-IP experiments (Fig. 3.2C). Also as expected, ASPP-WK did not show a decreased binding to PP1α87B and PP1α13C, compared to wild type ASPP (Fig. 3.2C), since these lack the SH3 domain binding motif. These results demonstrate that SH3 domain engagement is important for PP1 binding.

In all above co-IP experiments, ASPP-WK still retained residual PP1 binding. Neither mutating the RVXF motif alone (Fig. 3.1C), nor the SH3 domain alone (Fig. 3.2C) was sufficient to abrogate ASPP/PP1 binding completely. Thus, I generated an RVXF, SH3 double mutant ASPP (ASPP-FA/WK) to test if combining them would further reduce the binding strength to PP1. In co-IP experiments, ASPP-FA/WK did not show further decrease of the binding between ASPP and PP1α96A, or PP1β9C (Fig 3.2D). Together with the observation that PP1α87B was binding to

---

Fig. 3.2: (Continued from previous page)
(B) PP1α96A and PP1β9C need their C-terminus for efficient binding to ASPP. PP1α96A-ΔC lacks residues 304–327 and PP1β9C-ΔC lacks residues 304–330. (C) The SH3 domain of ASPP is required for binding to PP1α96A and PP1β9C. When a key residue of the SH3 domain (W987) is mutated to lysine (ASPP-WK), binding to PP1α96A and PP1β9C is reduced. PP1α13C and PP1α87B, which do not have the class II SH3 domain binding motif, bind to ASPP and ASPP-WK with similar affinities. (D) Mutation of the SH3 domain in addition to the RVXF motif (ASPP-FA/WK) does not further decrease binding to PP1α87B, PP1α96A or PP1β9C, when compared to ASPP-FA. Residual binding between PP1s and ASPP-FA/WK remains.

ASPP-FA, this suggests that other binding surfaces between ASPP and PP1 might exist, or the residual binding correspond to non-specific interaction between overexpressed proteins.

3.1.3. The PxxPxR motif of PP1 and the SH3 domain of ASPP positioned favourably for binding to each other

The proposed binding between the PxxPxR motif of PP1 and the SH3 domain of ASPP involves the C-terminal part of PP1. Despite being present in many of the PP1s used for crystallization, the C-terminus (last 30 residues) is almost always missing in the final structures (e.g., Egloff 1997, Goldberg et al. 1995, Hurley et al. 2007, Ragusa et al. 2010). This suggests that it is flexible in those complexes (Terrak et al. 2004). In contrast, in an ASPP/PP1 complex, the C-terminus of PP1 is likely to be stabilised by binding to the SH3 domain of ASPP. I wished to use an in silico modelling approach to test if the proposed SH3/PxxPxR-interaction is topologically possible.

To date, the only protein structure that resolves a part of the C-terminus of PP1 is a human MYPT1/PP1β complex structure (Terrak et al. 2004). In this structure, residues 299–308 of PP1β associate with the ankyrin repeats that follow the RVXF motif of MYPT1. However, the last residues of PP1β (309–327) that contain the PxxPxR motif are also unresolved in this structure. Intriguingly, MYPT1 and ASPP are very similar. The sequences of the RVXF motif and the following four ankyrin repeats on these proteins perfectly align with each other. Thus, it would be feasible to use the MYPT1/PP1β complex structure to construct a model for an ASPP/PP1 complex.

Skerne-Arnold et al. reasoned similarly and proposed a structural model for ASPP2/PP1β using the MYPT1/PP1β complex structure (Skene-Arnold et al. 2013). Their analysis did not include the SH3 domain of ASPP2. I wanted to go one step further and include the SH3 domain of ASPP2 in order to model the SH3/PxxPxR-interaction. This was achieved by including the structure of an SH3 domain contain-

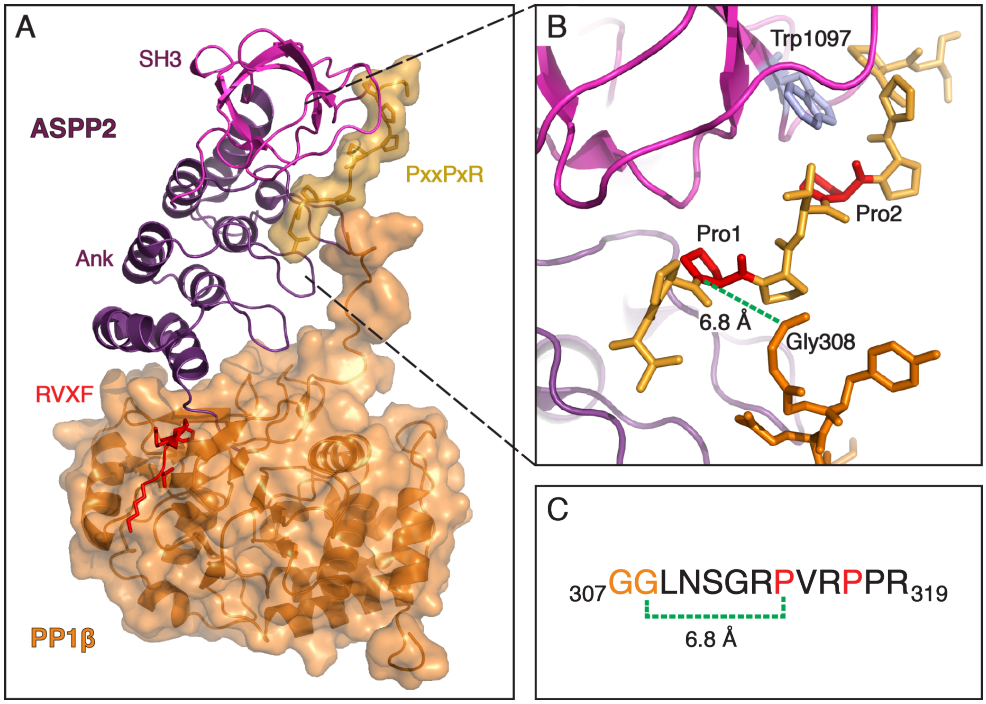

Figure 3.3.: The PxxPxR motif of PP1 could bind to the SH3 domain of ASPP, based on in silico modeling

(A) Model of ASPP2/PP1β complex based on MYPT1/PP1β (PDB: 1S70), ASPP2/p73 (PDB: 4A63) and Ponsin/Paxilin (PDB: 2O9V). ASPP2 was aligned to MYPT1 using their ankyrin repeats and Ponsin was subsequently aligned to ASPP2 using their SH3 domains. ASPP2 is depicted in red (RVXF motif), purple (ankyrin repeats) and pink (SH3 domain). PP1β is shown in orange, while the Paxilin peptide that is analogous to the PP1β C-terminus is shown in light orange.

(B) Detailed view of the PxxPxR motif-containing peptide. The two prolines that characterize the PxxPxR motif are shown in red. W1097 of ASPP2 that corresponds to W987 in *Drosophila* ASPP (mutated in ASPP-WK) is depicted in light blue.

(C) Sequence of C-terminus of PP1β. The two glycines that are visible in the model are highlighted in orange. The two prolines that characterize the PxxPxR motif are highlighted in red. The distance that had to be bridged between G308 and P314 is indicated in green.

ing protein bound to a class II SH3 doman binding peptide. The modeling was done in collaboration with Dr Stephane Mouilleron (LRI Protein Structure core facility).

Our model of ASPP2/PP1β (Fig. 3.3A) used the structure of MYPT1/PP1β (1S70, Terrak et al. 2004), ASPP2/p73 (4A63, Canning et al. 2012) and Pon-sin/paxilin (2O9V, Gehmlich et al. 2007). Based on the model, it is reasonable to assume that the PxxPxR motif of PP1β can bind to the SH3 domain of ASPP2 in the typical orientation of class II binding motifs. The distance between the carbon atom of the carboxyl-group of G308 of PP1β and the nitrogen atom of the amino-group of the first proline that is essential within the PxxPxR motif is only 6.8 Å (Fig. 3.3B). This distance could easily be bridged by the five residues that separate G308 from P314 of PP1β (Fig. 3.3C). Thus, this model supports the hypothesis that in an ASPP/PP1 complex, the SH3 domain could bind to the PxxPxR motif of PP1.

3.2. The ASPP/PP1 complex in vivo

3.2.1. GFP-tagged ASPP localises to cell-cell junctions

In vitro, and in cell culture it has been shown that ASPP family proteins can bind to PP1 (Llanos et al. 2011, Skene-Arnold et al. 2013) and at least ASPP2/PP1 can dephosphorylate the transcriptional co-activator and YAP paralogue TAZ (Liu et al. 2011). In the previous subchapter, I have shown that *Drosophila* ASPP and PP1 can also bind to each other. In this subchapter I will explore the in vivo function of the ASPP/PP1 complex at an organismal level and investigate which of the known *ASPP* null mutant phenotypes (Langton et al. 2009) are PP1-dependent.

To test if the binding between ASPP and PP1 is required in vivo, I generated N-terminally GFP-tagged wild type ASPP and ASPP-FA plasmids for constitutive expression in *Drosophila*. The RVXF mutant instead of the RVXF, SH3 double mutant was chosen, since additional mutation of the SH3 domain did not further decrease PP1 binding (Fig 3.2C). Furthermore, an additional mutation could affect ASPP binding to proteins other than PP1 that relied on the SH3 domain. Using the PhiC31 integrase system, the DNA constructs were inserted into the genome on

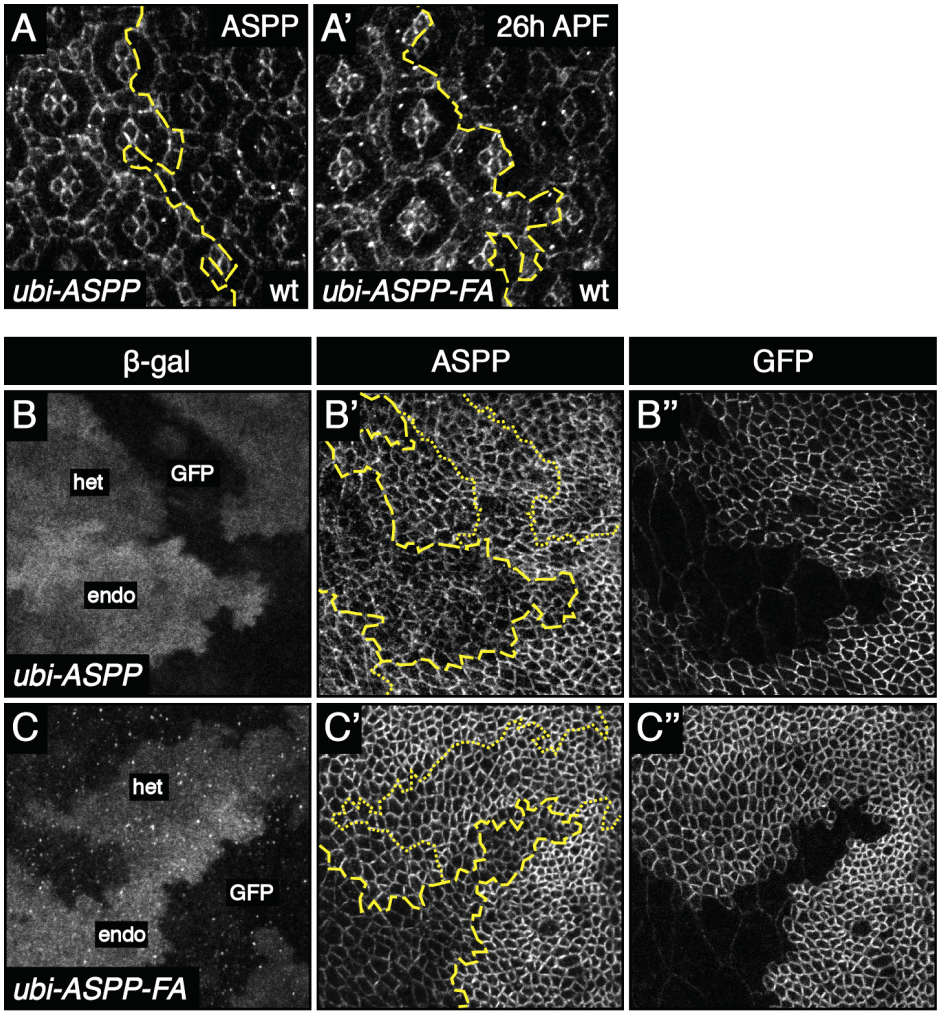

Figure 3.4.: GFP-tagged ASPP and ASPP-FA localise to cell-cell junctions

Confocal X-Y sections of pupal retinas at 26 h APF (A, A') or third instar larval wing discs (B–C") stained with the indicated antibodies. Flp/FRT clones were generated with *eyFlp* (A, A') or *hsFlp* (B–C").

(A), (A') GFP-tagged ASPP and ASPP-FA behaves like endogenous ASPP in the retina. In Flp/FRT clones that express ASPP (A) or ASPP-FA (A') under the *ubiquitin* promoter, ASPP localises to cell-cell junctions. The levels of exogenous protein in the clones (left) are slightly higher than in wild type tissue (right). Clone boundaries are marked with dashed yellow line. (B–C") GFP-tagged ASPP and ASPP-FA behaves like endogenous ASPP in larval wing imaginal discs. In Flp/FRT clones that express ASPP (B–B") or ASPP-FA (C–C") under the *ubiquitin* promoter, ASPP localises to cell-cell junctions. As in the retina, levels of endogenous ASPP are slightly lower (B', C'). Clone boundaries are marked with dashed yellow lines. Using β-galactosidase staining intensity, tissues that only express endogenous ASPP (endo), a mixture (het) or only exogenous, GFP-tagged ASPP (GFP) can be distinguished.

chromosome 2R at 53B2 (*ubi-ASPP* and *ubi-ASPP-FA*). The two insertions were recombined with the $ASPP^{d}$ null-allele.

Initially, I wanted to verify that the transgenes were expressing at close to endogenous levels and that the GFP tag did not interfere with ASPP localisation. To directly compare exogenous with endogenous ASPP, I generated mitotic clones with the Flp/FRT system. Mitotic clones in pupal retinas (Fig. 3.4A, A') and larval wing imaginal discs (Fig. 3.4B', C') that only expressed exogenous ASPP showed that ASPP-GFP localised to cell-cell junctions similarly to endogenous ASPP. In addition, the levels of exogenous ASPP were comparable to, only slightly higher than endogenous ASPP. There was no discernible difference regarding localization and levels between expression of ASPP compared to ASPP-FA. These results suggest that *ubi-ASPP* should be able to rescue loss of endogenous ASPP. Also any difference between *ubi-ASPP* and *ubi-ASPP-FA* should be due to PP1 binding, rather than to differences in localization or expression level.

3.2.2. Eye patterning and wing size determination are dependent on the ASPP/PP1 interaction

ASPP null mutant flies have four described phenotypes: (i) rough eyes and bristle misplacements, (ii) increased wing size, (iii) wing notching when combined with heterozygous *Csk* loss-of-function (Langton et al. 2007) and (iv) anterior scutellar bristle duplication (Langton 2008). In this section, as well the following two sections, I used $ASPP^{d}/ASPP^{8}$ trans-heterozygous flies when I refer to *ASPP* null mutant flies in the text. This was done to minimize the risk of artifacts due to the genetic background in homozygous flies.

First, I investigated the eye development (see 1.1.2 for details on eye development). In a perfectly patterned eye, 12 secondary and tertiary pigment cells that are also referred to as interommatidial cells (IOCs) surround one ommatidium (see Materials and methods for details on quantification). *ASPP* null mutant flies have an increased number of IOCs (15.3±1.6, Fig. 3.5B, E). This is rescued by the expression of ASPP (12.2±0.5, Fig. 3.5C, E), but not ASPP-FA (13.8±1.1, Fig. 3.5D, E). Additionally,

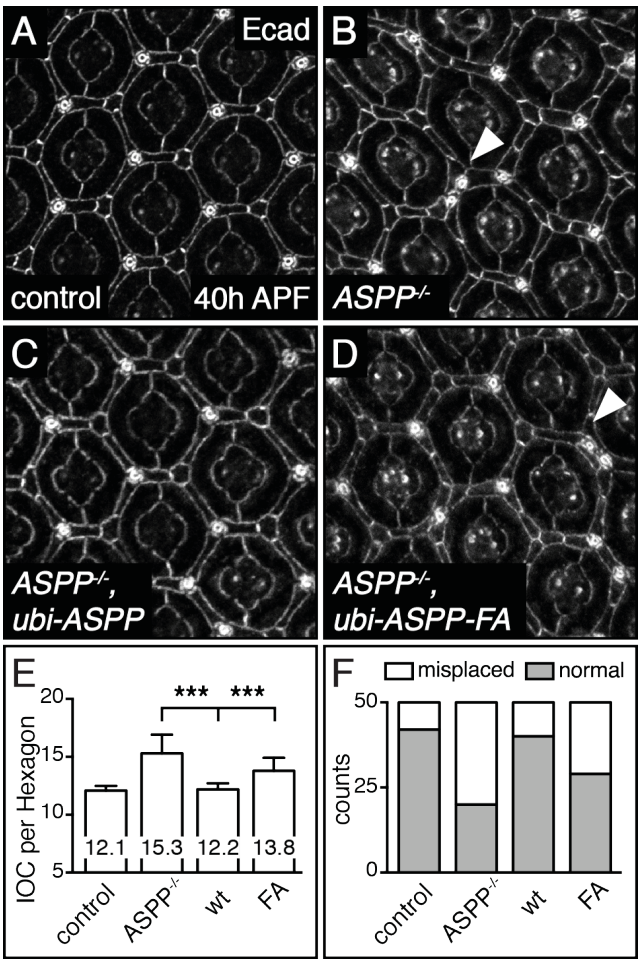

Figure 3.5.: The ASPP-FA mutant fails to rescue eye mispatterning

(A–D) Confocal X-Y sections of pupal retinas at 40 h APF stained with anti-E-cadherin antibody to mark cell outlines. The regular pattern of developing eyes (A) is disrupted in *ASPP* null mutant flies (B). The pattern is restored when exogenous ASPP is expressed (C), but not when ASPP-FA is expressed (D). Bristle misplacements can also be observed (arrowheads in B, D).

(E) ASPP but not ASPP-FA expression restores the number of IOCs in ASPP mutants. Error bars represent the standard deviation of the observed distributions. A one-way ANOVA test indicated that the differences among means were significant ($p<0.001$). Three pairwise comparisons were carried out ($ASPP^{-/-}$ vs. wt, wt vs. *FA* and control vs. wt) and p-values were adjusted using Bonferroni's correction. Significant differences are indicated. *** represents $p<0.001$. IOCs in 50 hexagons from at least 6 retinas were counted per condition.

(F) ASPP but not ASPP-FA reduces the frequency of bristle misplacements in ASPP mutants. Bristle clustering or placement of a bristle in a neighbouring position that should be occupied by a tertiary pigment cell was counted as misplacement. Bristle misplacements were counted in 50 hexagons from at least 6 retinas.

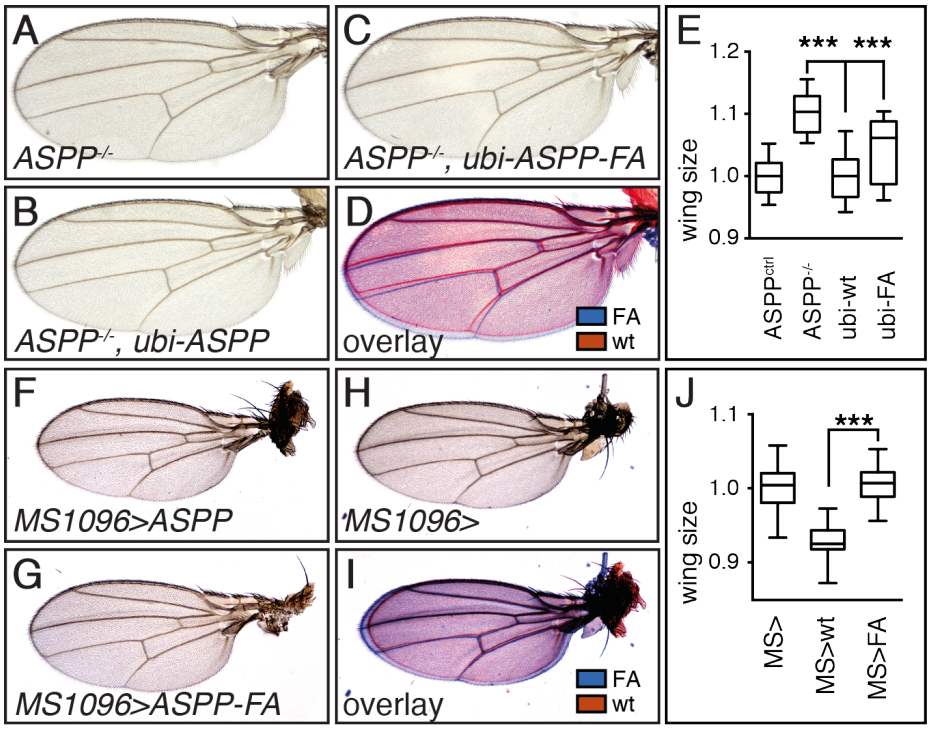

Figure 3.6.: The ASPP-FA mutant partially rescues wing size

(A–C) *ASPP* null mutant flies have enlarged wings (A). The increase in wing size is rescued by the expression of ASPP (B), but not ASPP-FA (C). Wings from female flies shown.

(D) Overlay for direct comparison of rescue with ASPP and ASPP-FA.

(E) Quantification of wing sizes normalised to control wing size. The whiskers of the box-plot indicate minimum and maximum values. A one-way ANOVA test indicated that the differences among means were significant ($p<0.001$). Two pairwise comparisons were carried out (*ASPP-/-* vs. *ubi-ASPP* and *ubi-ASPP* vs. *ubi-ASPP-FA*) and p-values were adjusted using Bonferroni's correction. Significant differences are indicated. *** represents $p<0.001$. At least 20 wings were counted per genotype.

(F–H) Expressing HA-tagged ASPP in the wing of male flies leads to small but significant undergrowth. Compared to expressing ASPP-FA with the *MS1096-GAL4* driver (G), ASPP expressing wings (F) are smaller. Control wings without a UAS-transgene (H) are of similar size to ASPP-FA wings.

(I) Overlay for direct comparison of expression of ASPP and ASPP-FA.

(J) Quantification of wing sizes normalised to control wing size. The whiskers of the box-plot indicate minimum and maximum values. An unpaired t-test showed that mean wing size in *MS1096>ASPP* and *MS1096>ASPP-FA* differ significantly from each other. *** indicates $p<0.001$. At least 20 wings were counted per genotype.

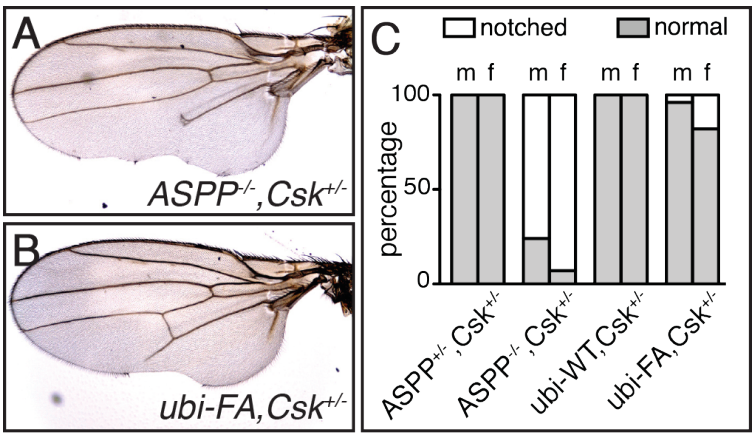

Figure 3.7.: The ASPP-FA mutant partially rescues wing notching

(A) Losing one copy of *Csk* in an *ASPP* null background leads to wing notching.

(B) Expressing exogenous ASPP-FA does not fully rescue the notching phenotype. Notches are smaller than with *ASPP* null.

(C) Quantification of wing notching phenotype. Only the genotypes shown in (A) and (B) showed any notching. 100 wings were analyzed per genotype and sex.

bristle clustering that is prevalent in *ASPP* null mutant flies (Fig. 3.5B) can be rescued with exogenous ASPP, but not ASPP-FA (Fig. 3.5F). These results show that ASPP/PP1 binding is required for eye patterning.

Next, I examined wing sizes. As described previously (Langton et al. 2007), *ASPP* null mutant wings were about 10 % larger than wild type wings (Fig. 3.6A, E). Expression of ASPP in the *ASPP* null background rescued the increase in wing size (Fig. 3.6B, E). However, expression of ASPP-FA only partially rescued the increase in wing size (Fig. 3.6C, E). When directly comparing the rescue with ASPP and ASPP-FA, the median wing size of ASPP-FA-expressing flies was about 6 % larger (Fig. 3.6D, E). Furthermore, expression of UAS-ASPP with the *MS1096-GAL4* driver in the wing of male flies leads to slight undergrowth that is not observed with UAS-ASPP-FA (Fig 3.6F-J). In female flies, there was no significant difference (data not shown), possible because the *MS1096-GAL4* driver is on the X chromosome and therefore more highly expressed in males due to dosage compensation. Together, the loss-of-function and overexpression results show that ASPP/PP1 binding is also required for wing size determination.

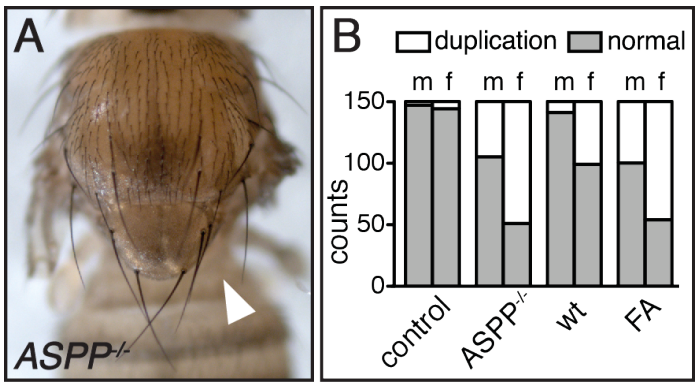

Figure 3.8.: The ASPP-FA mutant does not rescue anterior scutellar bristle duplication

(A) Anterior scutellar bristle duplication in *ASPP* null mutant female on the right side (arrowhead).

(B) ASPP expression in *ASPP* null mutant flies partially rescues the bristle duplication phenotype. ASPP-FA expression does not alter the *ASPP* null phenotype. 150 flies per genotype and sex were analyzed. Anterior scutellar bristle duplication either on the left side, right side or both sides was counted as duplication event.

3.2.3. Activation of *Csk* partially depends on the ASPP/PP1 interaction

ASPP positively regulates the Src-family kinase inhibitor Csk (Langton et al. 2007). Strikingly, wings become notched when one copy of the hypomorphic allele Csk^{1jd8} was introduced in an *ASPP* null mutant background (Fig. 3.7A and Langton et al. 2007). The wing notching could be fully rescued when exogenous ASPP was expressed in this background (Fig. 3.7C). With exogenous ASPP-FA, most wings were rescued (Fig. 3.7C). In the small percentage of flies that had notches, the notches were not as prominent as in the *ASPP* null mutant flies (Fig. 3.7B). Thus, although PP1 binding seems to contribute to the regulation of Csk by ASPP, other ASPP functions are likely to be required for Csk regulation.

3.2.4. Specifying anterior scutellar sensory organs depends on the ASPP/PP1 interaction

Another phenotype observed in *ASPP* null mutant flies is the duplication of anterior scutellar bristles (aSCs, Langton 2008). Whole sensory organs, rather than just the bristles, were duplicated in these instances (Fig. 3.8A). Two bristles emerged from two separate sockets. The duplication occurred on both sides and no bias towards any side was observed. The duplication events (either on the left, right, or on both sides) were more common in females in *ASPP* null mutants (66 %), than in males (30 %). The bristle duplication could be partially rescued by exogenous ASPP but not by ASPP-FA (Fig. 3.8B). The partial rescue of exogenous wild type ASPP suggests that either the slightly higher expression levels (see section 3.2.1) or the GFP tag might interfere with endogenous function. However, PP1 binding to ASPP is clearly required for correct aSC specification.

Taken together, these results demonstrate that the RVXF motif of ASPP is required in vivo for its function. The degree to which a PP1-binding deficient ASPP is able to rescue differs for the different phenotypes. While for eye patterning, wing size determination and aSC specification PP1 binding is strictly required, activation of Csk seems to be at least partially PP1-independent.

3.2.5. PP1α96A and PP1β9C localise to cell-cell junctions in the developing retina

The importance of the RVXF motif of ASPP in vivo implies that the phenotypes seen in *ubi-ASPP-FA* rescue flies are due to reduced PP1 function. If the binding between ASPP and PP1 is essential, PP1 mutants should recapitulate some phenotypes of *ubi-ASPP-FA* rescue flies. The focus of the following analyses was on PP1α87B, PP1α96A and PP1β9C, since they bound to ASPP more strongly (see section 3.1.1) and PP1α13C expression seems to be mostly restricted to testis (Celniker et al. 2009).

In order to be regulated by ASPP, PP1 would be expected to co-localise with ASPP in vivo. To study the localization of PP1s, I generated two transgenic lines for PP1α87B and PP1α96A (*ubi-GFP-PP1α87B* and *ubi-GFP-PP1α96A*) that expressed

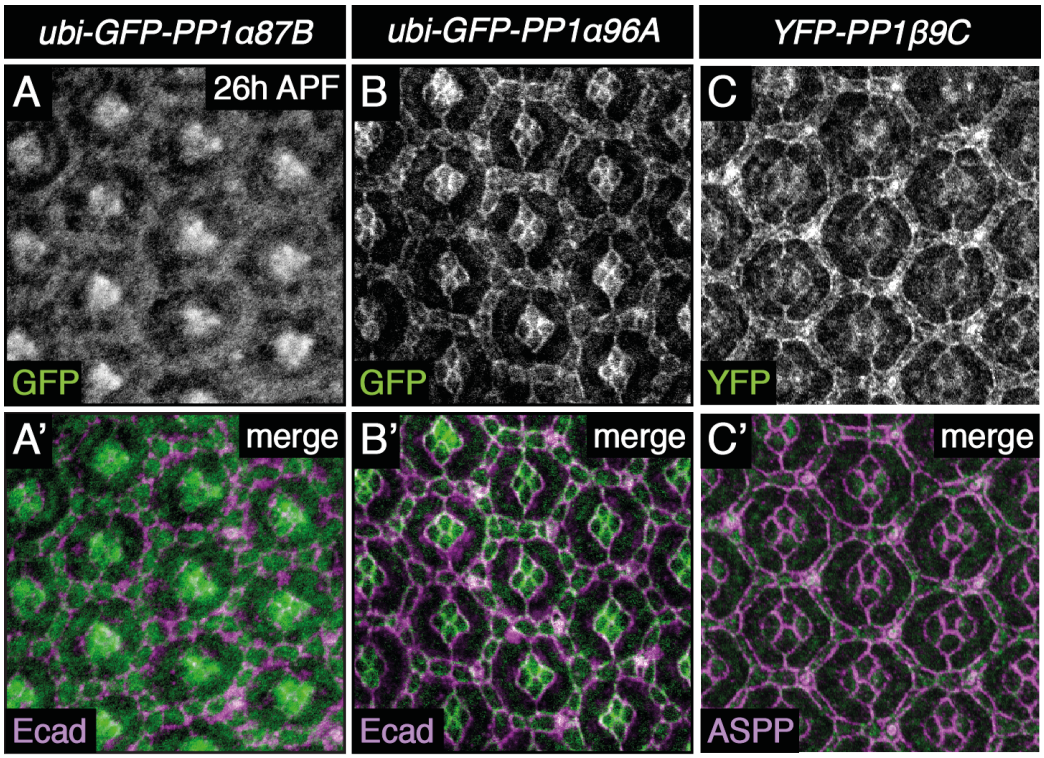

Figure 3.9.: PP1α96A and PP1β9C but not PP1α87B localise to cell-cell junctions in the developing retina

Confocal X-Y sections of pupal retinas at 26 h APF stained with anti-E-cadherin antibody and GFP/YFP-fluorescence.

(A), (A') GFP-PP1α87B localises to the cytoplasm of IOCs at 26 h APF.

(B), (B') GFP-PP1α96A partially co-localises with E-cadherin at cell-cell junctions under the same conditions as in (A).

(C), (C') YFP-PP1β9C partially co-localises with ASPP at cell-cell junctions under the same conditions as in (A).

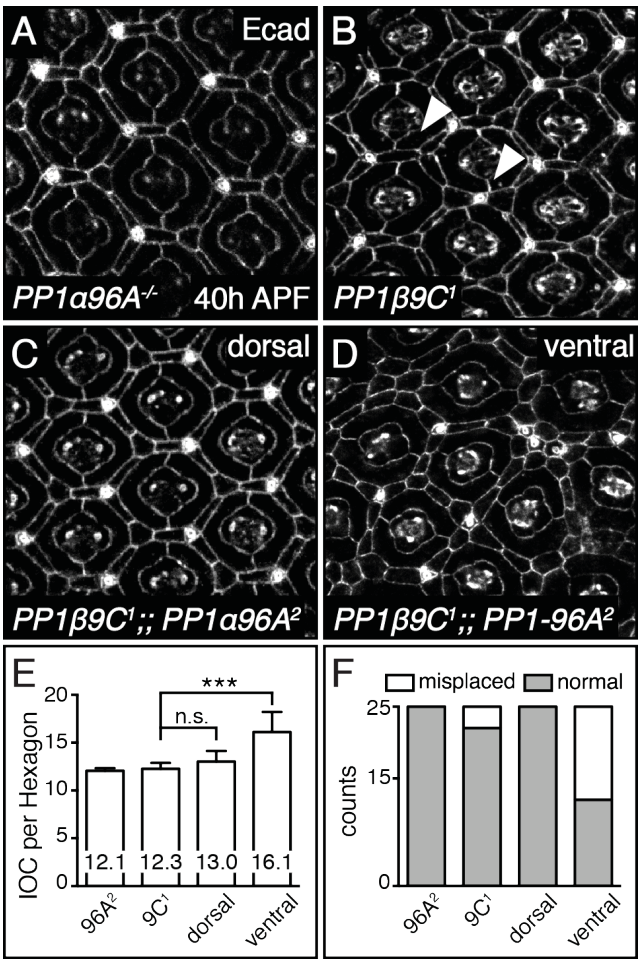

Figure 3.10.: *PP1β9C;PP1α96A* double mutants have an increased number of IOCs in the ventral part of the developing eye

(A–D) Confocal X-Y sections of pupal retinas at 40 h APF stained with anti-E-cadherin antibody to mark cell outlines. Losing *PP1α96A* does not influence eye development (A), while *PP1β9C* hypomorphs (B) show occasional IOC and bristle mispatterning (arrowheads). In $PP1\beta9C^{1}$;;$PP1\alpha96A^{2}$ double mutants, the dorsal part of the eye develops normally (C), while a small ventral patch shows severe mispatterning (D).

(E) Only the ventral part of the retina in $PP1\beta9C^{1}$;;$PP1\alpha96A^{2}$ double mutants has a significant increase in the number of IOCs. Error bars represent the standard deviation of the observed distributions. A one-way ANOVA test indicated that the differences among means were significant ($p<0.001$). Two pairwise comparisons were carried out ($PP1\beta9C^{1}$ vs. dorsal part of $PP1\beta9C^{1}$;;$PP1\alpha96A^{2}$ and $PP1\beta9C^{1}$ vs. ventral part of $PP1\beta9C^{1}$;;$PP1\alpha96A^{2}$) and P-values were adjusted using Bonferroni's correction. Significant and non-significant (n.s.) differences are indicated. *** represents $P<0.001$. IOCs in 25 hexagons from at least 3 retinas were counted per condition. Dorsal and ventral parts in $PP1\beta9C^{1}$;;$PP1\alpha96A^{2}$ flies from the same retinas were analyzed.

(Continues on following page)

N-terminally GFP-tagged proteins under the control of the *ubiquitin* promoter. The constructs were injected into VIE217 flies and targeted to the landing site on 3L using the PhiC31 integrase system. For PP1β9C, I used an existing YFP-trap line (*YFP-PP1β9C*) where a YFP reporter encoded by a P-element transposon vector is spliced in between the first and second exon (Morin et al. 2001). While PP1α87B was cytoplasmic in IOCs at 26 h APF (Fig. 3.9A, A'), a fraction of PP1α96A and PP1β9C localised to cell-cell junctions with E-cadherin or ASPP (Fig. 3.9B-C'). These results do not exclude the possibility that PP1α87B might form a complex with ASPP at the junctions. However, overall, PP1α96A and PP1β9C seem to be better candidates in vivo due to their more specific junctional localization.

3.2.6. Eye patterning is defective in *PP1α96A;PP1β9C* double mutants

Next, I wanted to test if any PP1 mutants would phenocopy *ASPP* null mutants. Out of all described PP1 mutants, only a viable *PP1β9C* hypomorph ($PP1\beta9C^{2}$) was annotated to have any phenotypes that resemble *ASPP* null mutants. $PP1\beta9C^{2}$ flies are described to have a roughened eye and missing aSCs (Deak 1977). Although $PP1\beta9C^{2}$ was not available, another hypomorphic *PP1β9C* allele, $PP1\beta9C^{1}$, that has a missense mutation (V284A) (Raghavan et al. 2000) showed a roughened eye that is caused by bristle misplacements and IOC patterning defects (Fig. 3.10B, F). Furthermore, this allele caused anterior scutellar bristle duplications (Fig. 3.12).

These two phenotypes of $PP1\beta9C^{1}$ flies were reminiscent of *ASPP* null mutants, albeit much weaker. Thus, I tested if the weaker phenotype was due to the fact that PP1α96A could act redundantly with PP1β9C by generating a *PP1β9C;;PP1α96A* double mutant. By itself, $PP1\alpha96A^{2}$ flies are viable null mutants that have no

Fig. 3.10: (Continued from previous page)
(F) $PP1\beta9C^{1};;PP1\alpha96A^{2}$ double mutants show bristle misplacements. Bristle clustering or placement of a bristle in a neighbouring position that should be occupied by a tertiary pigment cell was counted as misplacement. Bristle misplacements were counted in 25 hexagons from at least 3 retinas.

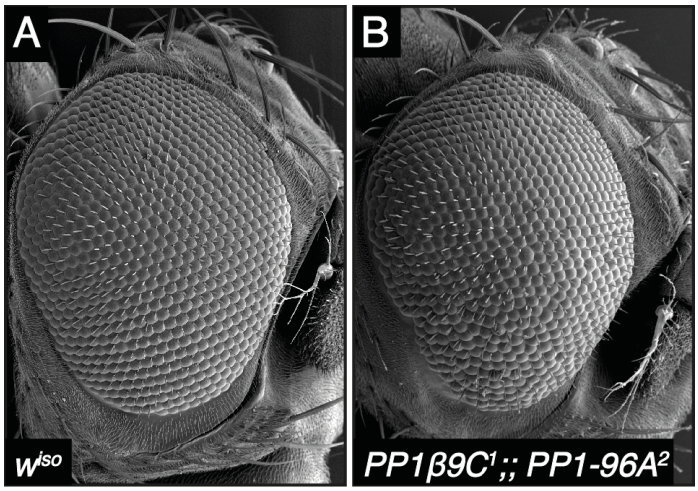

Figure 3.11.: *PP1β9C;PP1α96A* double mutants have patterning defects in the ventral part of eye

Scanning electron micrograph of adult fly eyes. The regular patterning in wild type flies (A) is disrupted in *PP1β9C;PP1α96A* double mutant flies (B). The mispatterning is increased on the ventral side of the eye, while the dorsal side is less severely affected. The ventral side is at the top of the images, while the dorsal side is at the bottom.

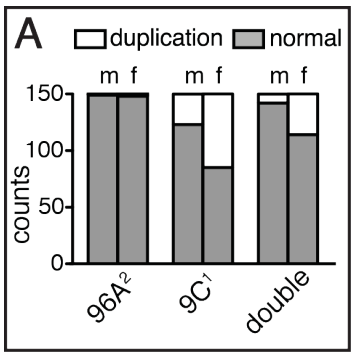

Figure 3.12.: *PP1β9C* mutant flies have duplicated aSCs

While *PP1β9C¹* mutants have a bristle duplication phenotype, *PP1α96A²* does not. 150 flies per genotype and sex were analyzed. *PP1β9C¹;;PP1α96A²* double mutants showed fewer instances of duplicated bristles. aSC duplication either on the left side, right side or both sides was counted as duplication event.

discernible phenotype (Kirchner et al. 2007). In particular, the eye patterning of *PP1α96A* null mutant flies had no visible defects (Fig. 3.10A).

Surprisingly, the eye defect of *PP1β9C¹;;PP1α96A²* flies was more pronounced in the ventral part of the eye (Fig. 3.11B). This difference is reflected in the arrangement of the IOCs and bristles (Fig. 3.10C, D). The number of IOCs in the ventral part of the eye in *PP1β9C¹;;PP1α96A²* flies was significantly higher (16.1±2.1) than in the dorsal part (13.0±1.1) or when compared with *PP1β9C¹* single mutant flies (12.3±0.6). The reason for this difference between the dorsal and ventral part of the eye in *PP1β9C¹;;PP1α96A²* flies is unclear. Nonetheless, the strong genetic interaction between *PP1α96A* and *PP1β9C* but not *PP1α87B* suggests that they act redundantly in eye patterning.

In contrast to eye patterning, removing *PP1α96A* did not enhance the scutellar bristle phenotype of *PP1β9C¹* flies. On the contrary, *PP1β9C¹;;PP1α96A²* flies showed fewer instances of aSC duplications (Fig. 3.12A). This suggests that PP1α96A does not play a role in aSC specification. Taken together, the above results are consistent with a model in which ASPP forms a complex with PP1α96A or PP1β9C to modulate cell-cell rearrangements in the developing fly eye.

3.3. RASSF8 and Ccdc85—two additional subunits of the ASPP/PP1 complex

3.3.1. *Drosophila* Ccdc85 binds to ASPP

In the previous subchapter, I have described that ASPP family proteins are at the core of an ASPP/PP1 complex. They posses a conserved RVXF motif, directly bind to PP1 and are found in PP1β pull-downs (Fig. 1.10 and Hauri et al. 2013). In the network uncovered by the AP-MS experiments, two other proteins families seem to be tightly connected to ASPP and PP1: Ccdc85 (coiled coil domain containing) family proteins and N-terminal RASSF family proteins. In this subchapter, I will investigate extensions to the core ASPP/PP1 complex by *Drosophila* RASSF8 and Ccdc85 and characterize the *ccdc85* gene.

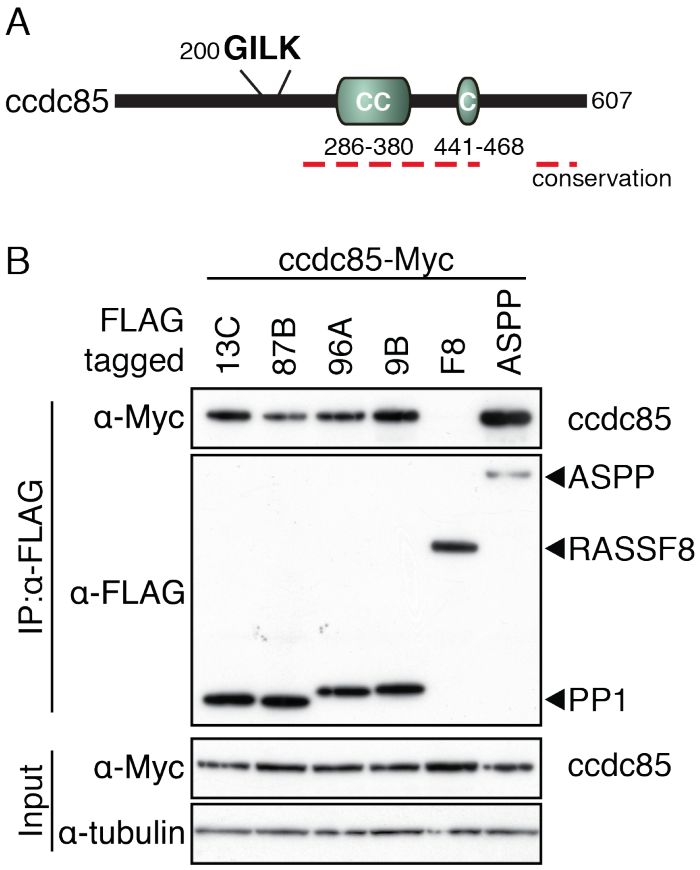

Figure 3.13.: Ccdc85 binds to ASPP and all four PP1 isoforms

(A) Domain structure of Ccdc85. The coiled coil region and the most C-terminal part of Ccdc85 are conserved. Ccdc85 has a non-conserved GILK motif that could serve as PP1 binding site. Coiled coil region predicted by jpred3 (Cole et al. 2008). Conserved regions between *Drosophila* Ccdc85, and human CCDC85A/B/C indicated by dashed red lines.

(B) Western blots of co-IP experiments using anti-FLAG antibody coupled beads with S2 cell lysates. Cells were transfected with the indicated constructs. Western blots were probed with indicated antibodies. Ccdc85 binds to ASPP and all four PP1 isoforms in co-IP experiments.

There are three Ccdc85 homologues in human (CCDC85A/B/C), while there is only one Ccdc85 orthologue in *Drosophila*. Not much is known about this protein family. For human CCDC85A, no information is available beyond annotation as a protein. CCDC85B has been discovered as a nuclear hepatitis delta antigen interacting protein (Brazas and Ganem 1996). More recently, several studies confirmed that CCDC85B is nuclear and suggested that it can regulate transcription via transcription factor TCF4 (Iwai et al. 2008), C/EBPβ (Bezy et al. 2005) or transcription modulator MCRS1 (Du et al. 2006). Functionally, CCDC85C remains uncharacterized, but it localises to tight junctions of radial glia (Mori et al. 2012). Additionally, in AP-MS experiments, CCDC85C was found in pull-downs of YAP (Couzens et al. 2013, Wang et al. 2014).

Drosophila Ccdc85 consists of coiled coil regions but has no other detectable domains or features. The coiled coil regions are conserved between *Drosophila* Ccdc85 and all human CCDC85s (Fig. 3.13A). *Drosophila* Ccdc85 is encoded by *CG17265* and has not been studied previously. I will refer to *CG17265* as *ccdc85* hereafter, following the mammalian nomenclature.

First, I wanted to confirm the AP-MS result for *Drosophila* Ccdc85 and test the binding of Ccdc85 to PP1, ASPP and RASSF8. In co-IP experiments, Ccdc85 was associated to ASPP and all four PP1 isoforms (Fig. 3.13B). Neither *Drosophila* Ccdc85, nor any of the human CCDC85s have an RVXF motif that could facilitate binding to PP1s. However, *Drosophila* Ccdc85 could bind to PP1 via its SILK motif (Fig. 3.13A), a motif of four amino acids that also contributes to PP1 binding (Hendrickx et al. 2009). These observations, together with the AP-MS data suggest that Ccdc85 could be part of an ASPP/PP1 complex.

3.3.2. RASSF8/ASPP/PP1 and Ccdc85/ASPP/PP1 complexes can form

If RASSF8 and Ccdc85 were additional subunits of an ASPP/PP1 complex, they would have to be able to form trimeric RASSF8/ASPP/PP1 and Ccdc85/ASPP/PP1 complexes. In co-IP experiments performed by Jennifer Banerjee in our laboratory,

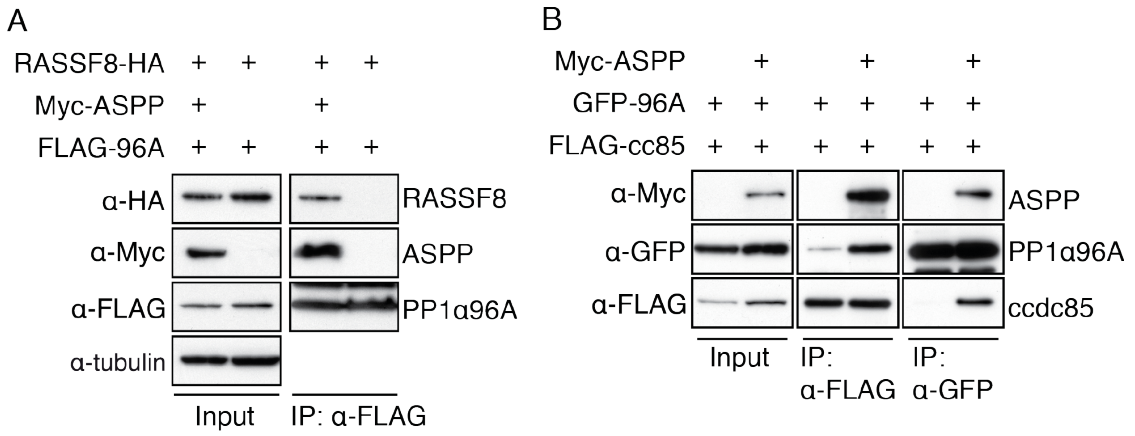

Figure 3.14.: RASSF8 and Ccdc85 each form a trimeric complex with ASPP and PP1

Western blots of co-IP experiments using anti-FLAG antibody coupled beads or GFP-Trap beads with S2 cell lysates. Cells were transfected with the indicated constructs. Western blots were probed with indicated antibodies.

(A) RASSF8 binds to PP1α96A only via ASPP. The experiment for this panel was done by Jennifer Banerjee.

(B) Ccdc85 binds to PP1α96A more strongly when ASPP is present. In the FLAG-Ccdc85 pulldown, PP1α96A can be detected. Levels of pulled-down PP1α96A increase when ASPP is present. In the GFP-PP1α96A pulldowns, Ccdc85 can only be detected when ASPP is present.

RASSF8 could form a trimeric complex with PP1α96A and ASPP (Fig. 3.14A). Furthermore, the binding between RASSF8 and PP1α96A was only observed when ASPP was present (Fig. 3.14A). This result suggests that in the trimeric complex of RASSF8/ASPP/PP1, ASPP serves as the bridging component.

For Ccdc85, the situation is slightly more complex, since it could bind to all four PP1 isoforms without co-expression of ASPP (Fig. 3.13B). Nonetheless, the binding between Ccdc85 and PP1α96A was strongly enhanced when ASPP was present (Fig. 3.14B). This suggests that, analogous to the RASSF8/ASPP/PP1 complex, ASPP can serve as a bridging component for Ccdc85 and PP1. However, additional secondary interactions between Ccdc85 and PP1 might exist.

3.3.3. RASSF8 and Ccdc85 bind to the coiled coil region of ASPP and can form a trimeric complex

To better understand the topology of the trimeric complexes, I mapped the interactions between RASSF8, Ccdc85 and ASPP. Firstly, I used three different ASPP fragments to pull-down RASSF8 in co-IP experiments. The ASPP fragments were covering the conserved N-terminal coiled coil region (1–234), the unconserved middle region (231–795) and the C-terminus containing the RVXF motif, the ankyrin repeats and SH3 domain (796–1020). Consistent with Y2H-data generated in the lab (Eunice Chan—unpublished observations), the coiled coil region of ASPP alone was sufficient for binding to RASSF8 (Fig. 3.15A). Similar to RASSF8, Ccdc85 was able to specifically bind to the coiled coil region of ASPP (Fig 3.15B). These results show that RASSF8 and Ccdc85 bind to the same region of ASPP that is distinct from the PP1 binding site.

To confirm that RASSF8 and Ccdc85 could bind to ASPP independently from PP1, I tested the binding of both proteins to ASPP-FA. Neither RASSF8 binding to ASPP (Fig. 3.15C), nor Ccdc85 binding to ASPP (Fig. 3.15D) was impaired by mutating the RVXF motif. This also implies that the failure of ASPP-FA to rescue *ASPP* null mutant defects (e.g., Fig. 3.5D–F) was not due to changed binding strength of ASPP-FA to RASSF8 or Ccdc85.

As RASSF8 and Ccdc85 bind to the same region of ASPP, they could preclude each other from binding simultaneously. To test this, I conducted co-IP experiments between Ccdc85, RASSF8 and ASPP. Either pulling down RASSF8 or Ccdc85 could only co-IP the other protein when ASPP was present (Fig. 3.16A). This demonstrates that RASSF8, Ccdc85 and ASPP could form a trimeric complex and ASPP bridged this interaction as well. This result also implies that a RASSF8/Ccdc85/ASPP/PP1 tetrameric complex could be possible (Fig. 3.16C). Although co-IP experiments from cell lysates alone cannot conclusively demonstrate the formation of a tetrameric complex, when all four proteins were co-expressed, they could be pulled-down by ASPP (Fig. 3.16B).

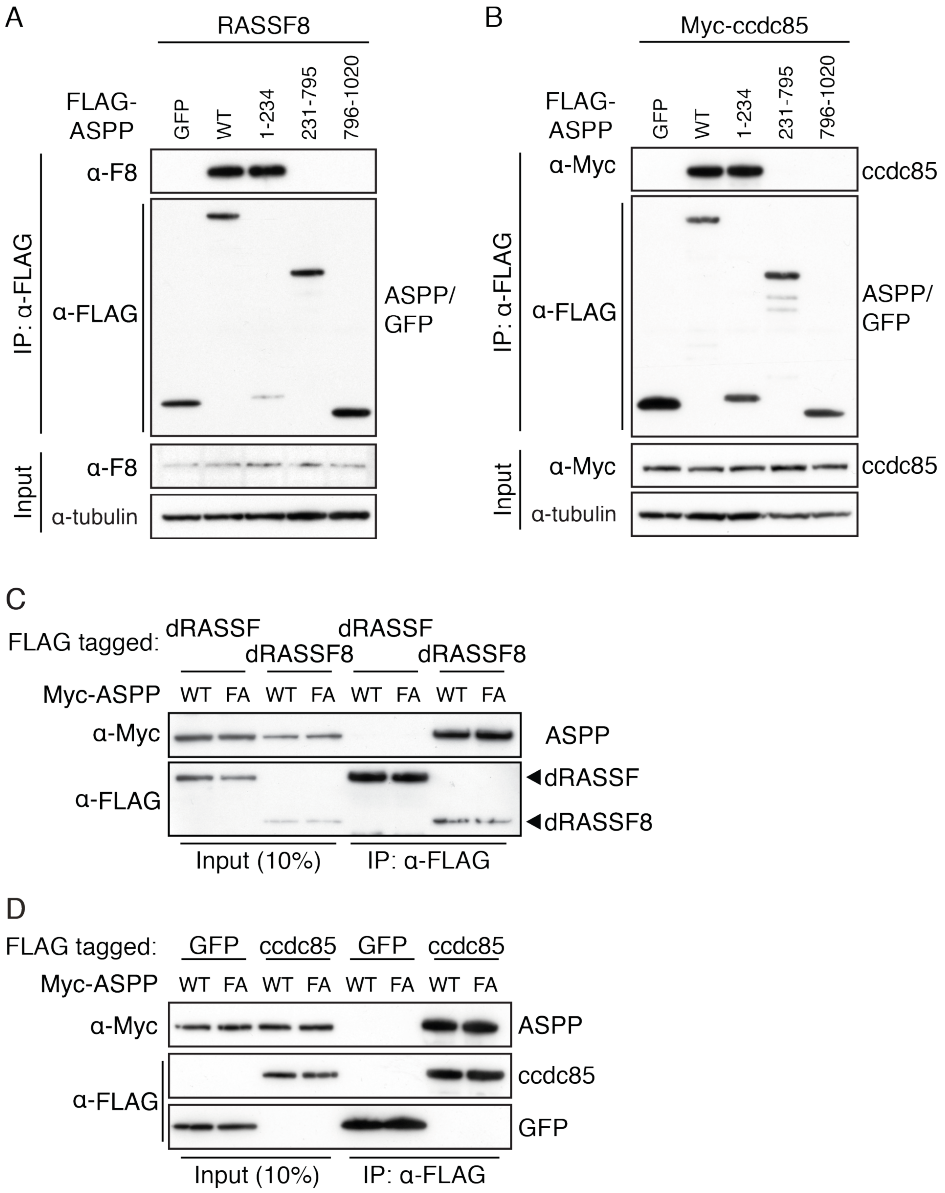

Figure 3.15.: RASSF8 and Ccdc85 bind to the coiled coil region of ASPP

Western blots of co-IP experiments using anti-FLAG antibody coupled beads with S2 cell lysates. Cells were transfected with the indicated constructs. Western blots were probed with indicated antibodies.

(A) The N-terminus of ASPP that contains its coiled coil region is sufficient for RASSF8 binding. The conserved N-terminus (1–234), but neither the unconserved middle part (231–795) nor the ankyrin repeat and SH3 domain containing region bind to RASSF8. (B) The N-terminus of ASPP (1–234) that contains its coiled coil region is sufficient for Ccdc85 binding. (C) RASSF8 binds to ASPP and ASPP-FA with equal strength. RASSF, the classical RA-family protein, was used as negative control. (D) Ccdc85 binds to ASPP and ASPP-FA with equal strength.

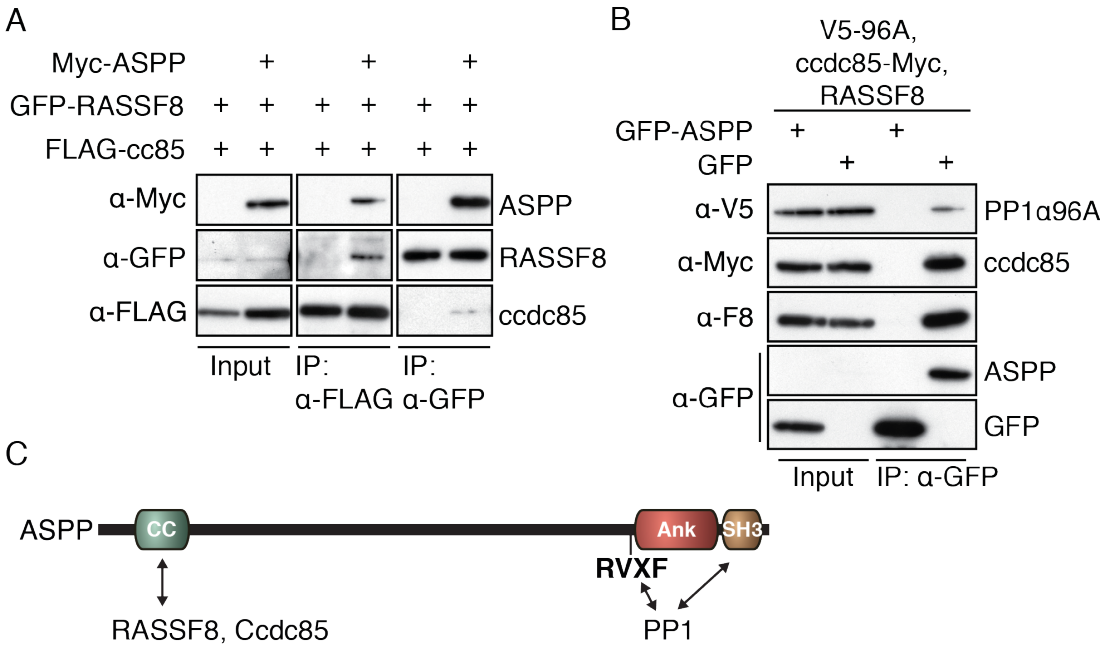

Figure 3.16.: RASSF8 and Ccdc85 form a trimeric complex with ASPP

Western blots of co-IP experiments using anti-FLAG antibody coupled beads or GFP-trap beads with S2 cell lysates. Cells were transfected with the indicated constructs. Western blots were probed with indicated antibodies.

(A) Ccdc85 binds to RASSF8 via ASPP. RASSF8 and Ccdc85 co-purify with each other only when ASPP is present.

(B) PP1α96A, RASSF8 and Ccdc85 co-IP with GFP-ASPP. Note that ASPP levels in the input were very low, but upon concentration by IP, ASPP could be detected.

(C) ASPP could act as a bridging subunit for the tetrameric complex. With its N-terminal coiled coil region it can bind to RASSF8 and Ccdc85, while with its RVXF motif and SH3 domain it can bind to PP1.

3.3.4. *ccdc85* transposon insertions have a rough eye phenotype

The above in vitro co-IP experiments suggest that RASSF8 and Ccdc85 could be part of an ASPP/PP1 complex. In vivo, RASSF8 shares common functionality (e.g., eye patterning) and localization with ASPP (Langton et al. 2009). However, Ccdc85 has not been studied at all in vivo.

For *ccdc85* (Fig. 3.17A), a plethora of fly lines with transposon insertions are available. Transposons will often disrupt the gene where it is inserted. I selected three lines with transposon insertions for further investigation, hoping to obtain a line that

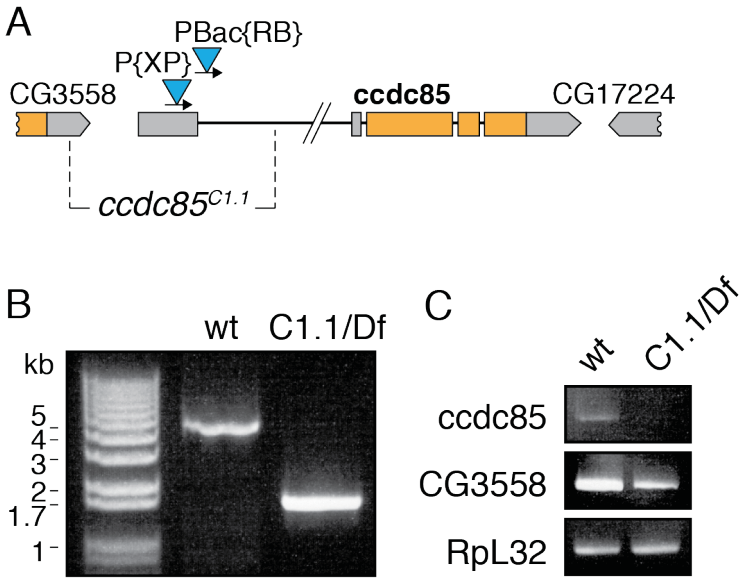

Figure 3.17.: *ccdc85* mutant deletes the 5'-UTR of the gene

(A) Gene structure of *ccdc85*. In the viable $ccdc85^{C1.1}$ mutant, 2.4 kb are removed. The deletion affects the 5'-UTR of *ccdc85* and the 3'-UTR of *CG3558*. The two transposons are inserted in or near the 5'UTR-region of *ccdc85*. Coding exons are marked in orange, non-coding exons in grey.

(B) Agarose gel containing ethidium bromide to visualise the large deletion in $ccdc85^{C1.1}$ mutant. A PCR across the 5'-UTR of *ccdc85* in $ccdc85^{C1.1}/Df(2L)Exel7014$ flies yields a product that is 2.4 kb smaller than in wild type flies.

(C) Agarose gel containing ethidium bromide to visualise mRNA levels of *ccdc85*, its neighbouring gene *CG3558* and *RpL32* as control. RT-PCR of $ccdc85^{C1.1}/Df(2L)Exel7014$ adult flies reveals that *ccdc85* mRNA levels were undetectable, while *CG3558* levels were slightly affected.

has a complete or partial loss-of-function of *ccdc85*. I decided to examine two lines with P-elements within the first non-coding exon (*P{GawB}NP4651*, *P{XP}d06579*) and one containing a piggyBac transposon directly after the first non-coding exon (*PBac{RB}e02956*). All three lines were homozygous viable. Two out of the three lines, *P{XP}d06579* and *PBac{RB}e02956* (Fig. 3.17A), had rough eye phenotypes. Furthermore, the eye phenotype was also observable when either of the two lines were crossed to a *ccdc85* deficiency line (*Df(2L)Exel7014*). This suggests that loss-of-function of Ccdc85 can cause eye roughness.

3.3.5. *ccdc85* null mutants have eye development defects, similar to *ASPP* null mutants

As transposon insertions often only partially disrupt gene function, Nic Tapon mobilised the P-element of *P{XP}d06579* in order to create a null mutant by imprecise excision. He screened 218 mobilizations of the P-element by putting those chromosomes in trans to the *ccdc85* deficiency (*Df(2L)Exel7014*). None were lethal over the deficiency and 12 showed a rough eye phenotype. Only two lines had a rough eye phenotype that was detectably stronger than the original P-element line over the deficiency.

I genotyped all lines that gave a rough eye phenotype by PCR. Only one line ($ccdc85^{C1.1}$) had a sizeable deletion, which removed the first non-coding exon completely (Fig. 3.17A, B). Subsequent sequencing showed that the lesion was from chr2L:2,998,544 to chr2L:3,000,949 and an extra adenine was inserted. In $ccdc85^{C1.1}$, the region that codes for the 3'-UTR of the neighbouring *CG3558* gene is also partially affected. Unfortunately, this includes the polyadenylation signal for the *CG3558* transcript. To test if $ccdc85^{C1.1}$ is a null mutant for *ccdc85*, I performed RT-PCR experiments. *ccdc85* mRNA levels were undetectable for the $ccdc85^{C1.1}$ mutants, while *CG3558* mRNA levels were slightly reduced (Fig. 3.17C). Thus $ccdc85^{C1.1}$ seems to be a null mutant for *ccdc85*, however, it is also likely to be a hypomorph for *CG3558*.

To compare the eye roughness seen in the *ccdc85* loss-of-function flies to *ASPP* loss-of-function, I examined developing retinas at 40 h APF. At this stage, *ccdc85*

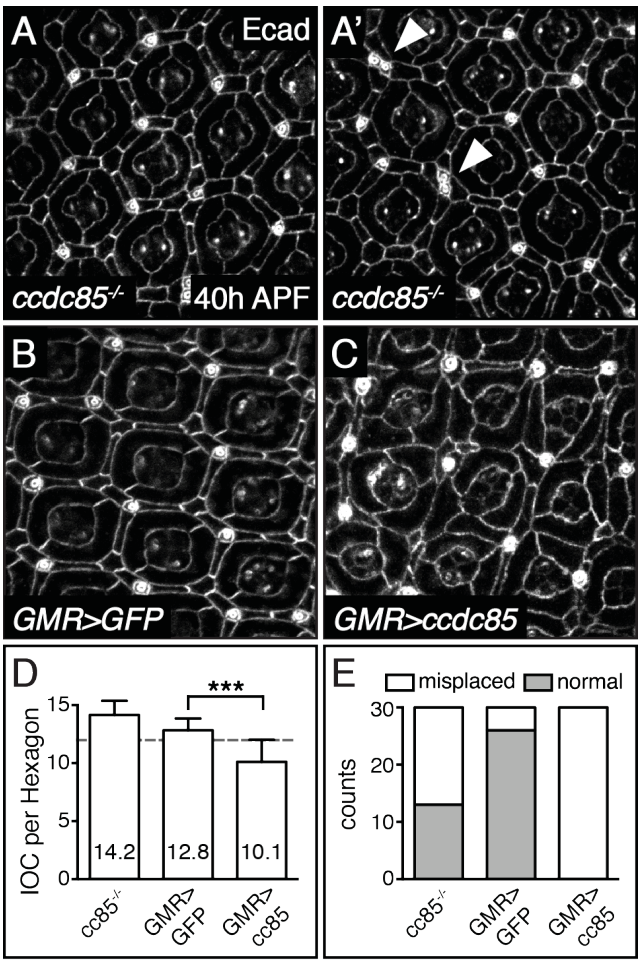

Figure 3.18.: *ccdc85* mutants phenocopy *ASPP* mutant eye phenotypes

(A–D) Confocal X-Y sections of pupal retinas at 40 h APF stained with anti-E-cadherin antibody to mark cell outlines. (A, A') *ccdc85* null mutant flies have defects in eye development. Two examples are shown. The bristle duplication phenotype (arrowheads) resembles the phenotype observed in *ASPP* null mutants (Fig. 3.5B and D). (B,C) Expression of Ccdc85 with a weak *GMR-GAL4* driver (B) causes loss of IOCs and cone cells are surrounded with more than two primary pigment cells.

(D) *ccdc85* null mutants have an increased number of IOCs (14.2±1.2), comparable to *ASPP* null mutants (15.3±1.6, see Fig. 3.5E). Expression of Ccdc85 leads to a significant decrease in the number of IOCs, compared to GFP expression. An unpaired t-test was carried out to determine if the means between GFP and Ccdc85 expression were significantly different from one another. *** indicates $p<0.001$. Grey dashed line indicates the theoretical number of IOCs in a perfectly organised tissue (12.0). IOCs in 30 hexagons from at least 4 retinas were counted per condition.

(E) Loss of *ccdc85*, as well as higher levels of Ccdc85 cause bristle misplacements. Bristle clustering or placement of a bristle in a neighbouring position that should be occupied by a tertiary pigment cell was counted as misplacement. Bristle misplacements were counted in 30 hexagons from at least 4 retinas.

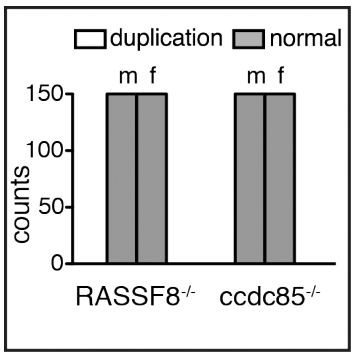

Figure 3.19.: *RASSF8* and *ccdc85* null mutant flies have no defect in anterior scutellar bristles

Neither *RASSF8* nor *ccdc85* null mutant flies have any defects in their aSCs. aSC duplication either on the left side, right side or both sides was counted as duplication event.

null mutant flies show mispatterned IOCs in the eye (Fig. 18A, A'). Similar to *ASPP* null mutants, bristles often cluster together (Fig. 3.18A', F). The number of IOCs (14.2±1.2) is higher than in controls (Fig. 3.18D). It is interesting to note that this number is closer to *ASPP* null mutant eyes (15.3±1.6, see Fig. 3.5E) than to *RASSF8* null mutant eyes (17.6±2.7, see Fig. 4.1F). Furthermore, despite the increase in IOC numbers, only a single layer of IOCs separate primary pigment cells in *ccdc85* and *ASPP* mutants. In contrast, *RASSF8* mutants frequently have multi-layered IOCs (see Fig. 3.18A, A' and Fig. 3.5B in comparison to Fig. 4.1A). These results suggest that Ccdc85 could function together with ASPP in eye development.

In contrast to eye development, neither *RASSF8* nor *ccdc85* null mutant flies (both trans-heterozygous over a genomic deficiency) had any defects in aSCs (Fig. 3.19). This is surprising for *ccdc85* null mutants, as aSC duplication was occasionally observed in $ccdc85^{C1.1}$ homozygous flies (data not shown). These results suggest that although RASSF8 and Ccdc85 might function together in eye development, this might not be true for bristle specification.

Despite the rough eye phenotypes seen in *ASPP* and *RASSF8* mutant flies, ASPP and RASSF8 overexpression does not lead to a rough eye (Paul Langton and Julien Colombani—unpublished observations). However, when I expressed Ccdc85 using a weak eye-specific *GMR-GAL4* driver (see List of Genotypes for details), a very severe

loss of IOCs (10.1±1.9) could be observed (Fig. 3.18C). Expressing GFP (12.8±1.0) as a control did not reduce the number of IOCs (Fig. 3.18B). Together with the loss-of-function phenotype, this suggests that Ccdc85 protein levels need to be tightly controlled to ensure proper eye development.

3.4. Concluding remarks and future directions

In this chapter I have shown that the ASPP/PP1 complex is conserved in *Drosophila*. Two additional proteins, RASSF8 and Ccdc85, can associate with the ASPP/PP1 core complex. Moreover, I have provided in vivo evidence that PP1 binding is essential for the function of ASPP. Mutants of *PP1*, *RASSF8* and *ccdc85* share some phenotypic similarity with *ASPP* mutants. A possible mechanism that could explain the similarity of phenotypes is that the ASPP/PP1 holoenzyme acts as an active phosphatase complex that uses ASPP, RASSF8 and Ccdc85 to restrict the enzymatic activity towards certain substrates. In the next chapter I will explore this possibility and investigate two potential substrates for the ASPP/PP1 complex.

3.4.1. Is the SH3 domain a general PP1-binding domain?

The PxxPxR motif of PP1s is conserved in other animals and even some fungi such as *Aspergillus* (data not shown). Thus, it is possible that many more regulatory subunits use SH3 domains to bind to PP1. Additionally, SH3 domains can be important binding to PP1s, independent of the PxxPxR motif. This has been shown for Dis2 in *Schizosaccharomyces pombe* and Glc7p in *Saccharomyces cerevisiae*, two orthologues of the PP1 family (Hachet et al. 2011, Knaus et al. 2005). Dis2 binds to the regulatory subunit Tea4 (Hachet et al. 2011) and Glc7p binds to Bud14p (Knaus et al. 2005). In both cases, deleting the SH3 domain of the regulatory subunit abrogates the binding to the PP1 catalytic subunit. Thus, the interaction between SH3 domains and PP1s could characterise a distinct category of PP1 regulatory subunits.

Adding the SH3 domain as an additional parameter for PP1 regulatory protein database searches can increase the specificity of the search, as the RVXF motif alone

Figure 3.20.: Dlg has an RVXF motif C-terminally to its SH3-domain
Alignment of the RVXF motif of *Drosophila* and human Dlg. The sequences shown start right after the predicted SH3 domains. Conserved residues are indicated by asterisks. Basic residues are found N-terminally of the motif, while acidic residues can be found C-terminally (not shown). While the basic residues are highly conserved, the primary sequence surrounding the acidic residues is not.

is relatively unspecific due the shortness of the consensus sequence. Searching the human and *Drosophila* proteome using Prosite for any protein that has an SH3 domain and fits to the [KR]-x(0,1)-[VI]-{FIMYDP}-[FW] definition of the RVXF motif, revealed only five proteins with orthologues in both organisms. Excluding proteins with RVXF motifs within known domains reduced the list to one protein, Dlg. *Drosophila* Dlg and three of the four human DLG isoforms (DLG1, DLG2 and DLG3) have the conserved RVXF motif C-terminally of their SH3 domain (Fig. 3.20). Furthermore, DLG3 had already been shown to interact with PP1 and both DLG2 and DLG3 inhibit phosphorylase phosphatase activity of PP1 (Hendrickx et al. 2009), typical of regulatory subunits. Dlg is a baso-laterally localised polarity determinant in epithelial cells that acts together with Scrib and Lgl (see 1.5.6). It is therefore possible that Dlg can specify PP1 activity at the baso-lateral membrane towards specific substrates. Thus, while ASPP would regulate PP1 activity at adherens junctions, Dlg could fulfil a similar function basally. Overall, this preliminary search supports the idea that PP1/SH3 domain binding could be a general interaction mechanism between a subclass of PP1 regulatory subunits and the catalytic subunit.

3.4.2. Is PP1α96A the catalytic subunit of the ASPP/PP1 complex

PP1α96A probably acts as the primary PP1 isoform that binds to ASPP in vivo. It was binding most strongly to ASPP in co-IP experiments (Fig. 3.1C) and was the only PP1 isoform identified by mass spectrometry in a pull-down experiment using GFP-tagged ASPP as a bait (see 5.4.1). Lastly, PP1α96A localises to cell-cell junctions in the retina (Fig. 3.9 B, B'), where ASPP is also found (Langton et al. 2009).

However, it is likely that other PP1 isoforms can act redundantly with PP1α96A. The lack of any detectable phenotype of *PP1α96A* mutants supports the idea of redundancy. The likeliest alternative to PP1α96A is PP1β9C, due to its strong binding to ASPP (Fig. 3.1C) and its junctional localisation (Fig. 3.9 C, C'). However, PP1α13C and PP1α87B could also replace PP1α96A, as ASPP can bind to PP1s independent of its RVXF motif and its SH3 domain (Fig. 3.2D). Another reason why PP1β9C is unlikely to be the only possible replacement for PP1α96A is that even when *PP1β9C* and *PP1α96A* are mutated, the phenotype of the double mutant is different to *ASPP* null mutant or *ASPP-FA* rescue flies (Fig. 3.10 and Fig. 3.12). Thus, despite possibly being the main PP1 isoform that interacts with ASPP, PP1α96A can be replaced by other PP1 isoforms.

3.4.3. Which subunits constitute the ASPP/PP1 holoenzyme?

ASPP and PP1 form the core of the ASPP/PP1 holoenzyme, as ASPP has the RVXF motif and SH3 domain that can directly interact with PP1. RASSF8 and Ccdc85 can attach to this core. It remains unclear if a hetero-tetrameric complex could form. Analytical gel filtration could be used on purified proteins to determine the composition of potential holoenzymes. Furthermore, sucrose gradient centrifugation could be employed for cell or tissue lysates. It is possible that distinct types of holoenzymes may form in vivo. Each type of holoenzyme might be differentially regulated and the substrates may differ.

The non-overlapping phenotypic spectrum of the null mutants suggests that different holoenzymes may form in vivo. While *ASPP* and *ccdc85* mutants have a very similar rough eye phenotype (Fig. 3.5B and 3.18A, A'), *ccdc85* mutants do not share the aSC duplication phenotype seen in *ASPP* mutants (Fig. 5.8B and 5.19). Thus, it is possible that Ccdc85 forms a complex with ASPP and PP1 in the developing retina, but not in sensory organ precursors that give rise to the scutellar bristles. Additionally, expression patterns of ASPP and its interactors could be analysed in different tissues. If Ccdc85 were only important in the retina, it would not have to be co-expressed with ASPP in sensory organ precursors. Together these experiments could indicate which types of ASPP/PP1 holoenzymes are required in which tissue.

3.4.4. What is the function of Ccdc85?

The *ccdc85* mutant that was generated might be hypomorphic for *CG3558*. To verify that the rough eye phenotype was due to the lack of Ccdc85 instead of CG3558, expressing Ccdc85 in $ccdc85^{C1.1}$ flies should restore normal eye patterning, while expressing CG3558 should not.

As Ccdc85 can bind to all four isoforms of PP1 (Fig. 3.13B) it is possible that Ccdc85 and PP1 directly bind to each other, independent of ASPP. Furthermore, overexpression of Ccdc85 in the eye reduces the number of IOCs (Fig. 3.18C) in contrast to ASPP or RASSF8 overexpression (Paul Langton and Julien Colombani—unpublished observations), suggesting an ASPP or RASSF8 independent function. A careful analysis of further *ccdc85* mutant phenotypes could reveal tissues or a developmental context, where ASPP is not required. Ccdc85 could help to recruit other proteins to PP1. With AP-MS experiments (similar to Fig. 5.10) using Ccdc85 as bait, further scaffolds, regulators and substrates that might not directly bind to ASPP or PP1 could be identified.

Chapter 4.

Substrates of the ASPP/PP1 complex

PP1 regulatory subunits can be substrate specifying subunits or inhibitors. ASPP family proteins are likely to be substrate specifying PP1 subunits, since they inhibit PP1 activity towards some substrates, but not others (Helps et al. 1995). Similar to many other substrate specifying subunits (Hendrickx et al. 2009), a fragment of human ASPP2 can inhibit PP1 activity towards phosphorylase, the standard substrate for in vitro PP1 assays (Helps et al. 1995). However, ASPP2 does not inhibit PP1 activity towards myosin light chain (Helps et al. 1995).

In this chapter I describe two potential substrates for the ASPP/PP1 complex: The transcriptional co-activator Yki and the polarity determinant Baz. For Yki, I have not found evidence that it is dephosphorylated by the ASPP/PP1 complex. In the case of Baz, I show in vivo evidence that its localisation is affected by loss of *ASPP* and present a list of residues that are dephosphorylated in vitro.

4.1. Yki is a potential substrate for ASPP/PP1

The transcriptional co-activator Yki was the first candidate substrate I have tested for the ASPP/PP1 complex. Three pieces of evidence suggested that Yki might be associated with the ASPP and N-terminal RASSF protein families: (1) Several reports in mammalian cells have shown that ASPP1/2 regulate core Hippo pathway components. ASPP2/PP1 dephosphorylates TAZ in cell culture on S311, the LATS1/2

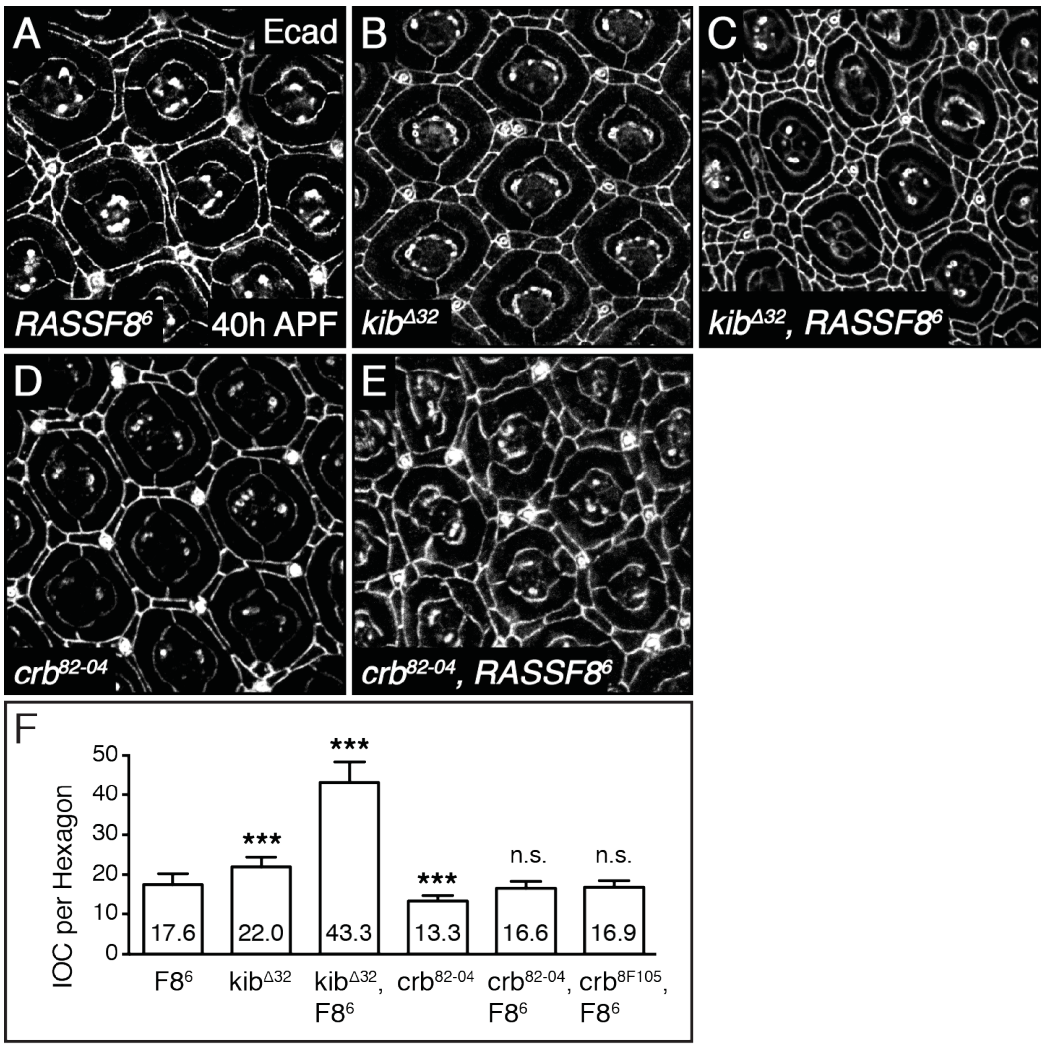

Figure 4.1.: *RASSF8* genetically interacts with *kib*, but not *crb* to regulate IOC number

(A-E) Confocal X-Y sections of pupal retinas carrying *eyFlp* mitotic clones of the indicated mutants at 40 h APF stained with anti-E-cadherin antibody to mark cell outlines.

(A) $RASSF8^{6}$ mutant retinas have extra IOCs. Multi-layering of IOCs is often observed, where IOCs laterally contact other IOCs instead of primary pigment cells.

(B) $kib^{\Delta 32}$ mutant retinas have extra IOCs. IOCs form a single layer of cells in contrast to $RASSF8^{6}$ mutants.

(C) $kib^{\Delta 32}$, RASSF8 double mutant retinas have a substantially increased number of IOCs. Primary pigment cells are mostly unaffected.

(D) $crb^{82\text{-}04}$ mutant retinas resemble wild type retinas.

(E) $crb^{82\text{-}04}$, $RASSF8^{6}$ double mutant retinas are disordered, but have the same number of extra IOCs compared to $RASSF8^{6}$ single mutant retinas.

(Continues on following page)

inhibitory phosphorylation site on TAZ (Liu et al. 2011). Additionally, nuclear ASPP1 can drive the expression of pro-apoptotic genes together with LATS2 (Aylon et al. 2010), while cytoplasmic ASPP1 inhibits LATS1/2 activity towards YAP and TAZ (Vigneron et al. 2010). (2) *Drosophila ASPP* and *RASSF8* mutants have overgrowth phenotypes, such as enlarged wings and rough eyes (including extra IOCs) that are reminiscent of upstream members of Hippo signalling (Langton et al. 2007 2009). (3) In multiple AP-MS experiments, ASPP2 and RASSF8 have been found to bind to YAP and TAZ (Couzens et al. 2013, Hauri et al. 2013, Wang et al. 2014).

4.1.1. RASSF8 does not regulate Ex, a Hippo pathway target

Based on current evidence, it is not entirely clear if ASPP and N-terminal RASSF family proteins would be predicted to activate or inhibit Hippo signalling (if they are involved in Hippo signalling at all). In Drosophila, ASPP and RASSF8 have growth inhibitory functions, suggesting that they should inhibit Yki function. This is consistent with the idea that human ASPP1/2 (Samuels-Lev et al. 2001) and RASSF8 (Lock et al. 2010) might be tumour suppressors. However, this neither fits with cytoplasmic ASPP1 activating YAP/TAZ by inhibiting LATS1/2 (Vigneron et al. 2010), nor with ASPP2/PP1 dephosphorylating and activating TAZ (Liu et al. 2011).

Given the more ample evidence of ASPP and RASSF8 being tumour suppressors, I first tested the hypothesis that they are positive regulators of Hippo signalling. I focused on RASSF8, since it has been reported to bind Wts in a yeast two-hybrid

Figure 4.1: (Continued from previous page)
(F) $kib^{\Delta 32}$,$RASSF8^{6}$ but not $crb^{82\text{-}04}$,$RASSF8^{6}$ double mutant retinas have a significant increase in the number of IOCs compared to $RASSF8^{6}$ mutant retinas. Error bars represent the standard deviation of the observed distributions. A one-way ANOVA test indicated that the differences among means were significant ($p<0.001$). All pairwise comparisons with $RASSF8^{6}$ single mutants were carried out and p-values were adjusted using Bonferroni's correction. Significant differences are indicated. *** represents $p<0.001$, n.s. means not significant. IOCs in 25 hexagons from at least 3 retinas were counted per condition.

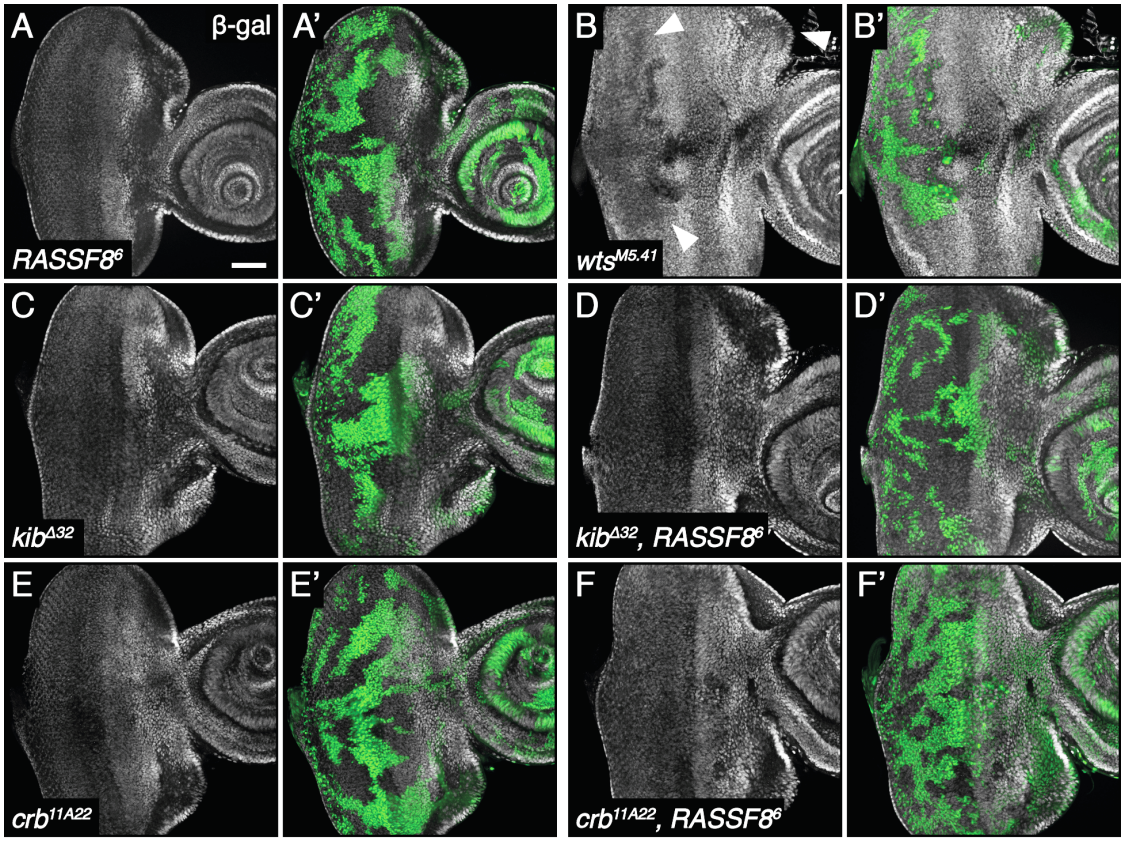

Figure 4.2.: The Hippo pathway reporter *ex-lacZ* is unchanged in *RASSF8* mutants

Confocal X-Y sections of larval eye imaginal discs stained with anti-β-galactosidase antibody to measure transcriptional activity of the Hippo pathway. *ex-lacZ* reporter levels remain unchanged in *RASSF8* single (A, A') and double mutants (D, D', F, F'). In contrast, a mutation in *wts* (B) strongly increases *ex-lacZ* reporter transcription. Wild type areas are marked positively with GFP, mutant areas are GFP-negative. Clones were induced using *eyFlp*. Arrowheads indicate wild type tissue with decreased β-galactosidase staining compared to surrounding mutant tissue. Scale bar represents 50 µm.

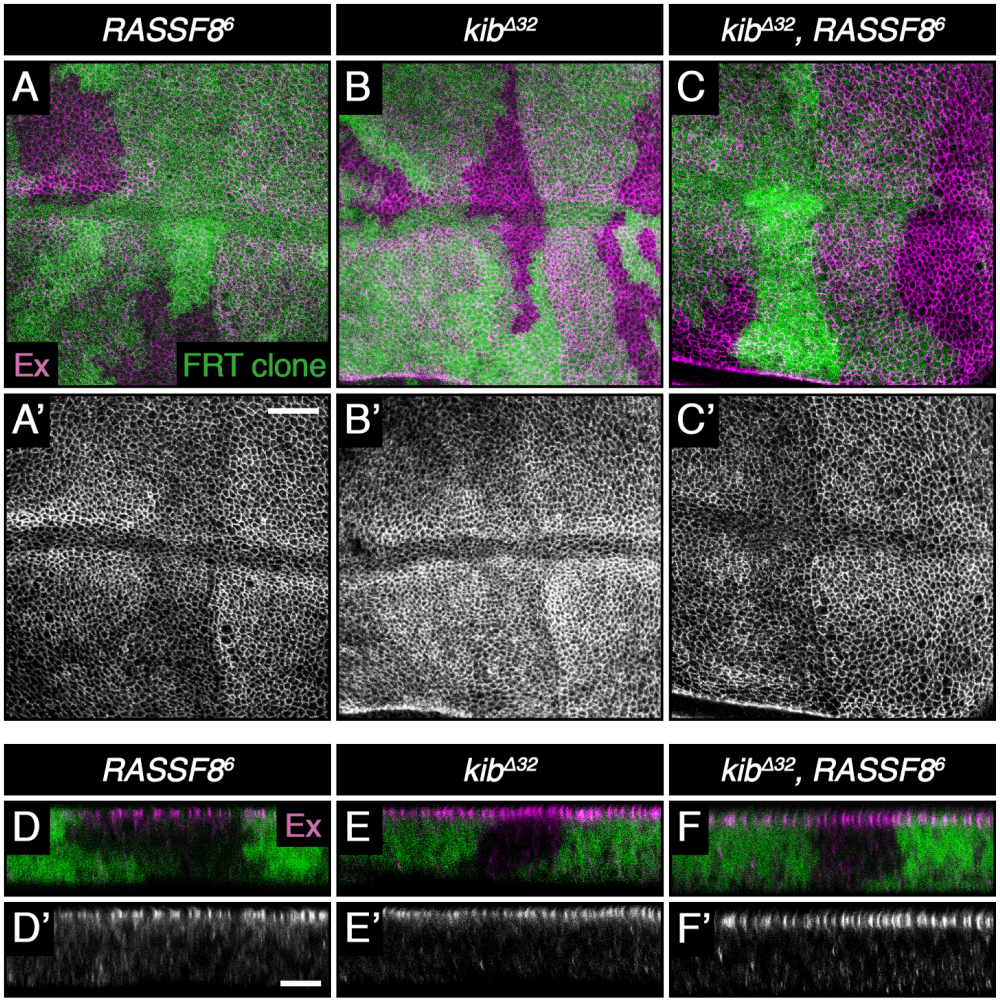

Figure 4.3.: Ex levels are unchanged in *kib* and *RASSF8* clones

(A–C') Confocal X-Y sections of larval imaginal eye discs stained with an anti-Ex antibody. Apical Ex localisation in larval wing imaginal discs is not influenced by loss of *RASSF8* (A, A'), *kib* (B, B') or both (C, C'). Scale bar represents 20 µm.

(D–F) Confocal transverse sections through larval imaginal wing discs stained with an anti-Ex antibody. Wild type areas are marked positively with GFP, mutant areas are GFP-negative. Mitotic clones were induced using *hsFlp*. Scale bar represents 10 µm.

assay (Giot et al. 2003). As previously described, *RASSF8*^{6} single mutant flies had a mild eye roughness phenotype with some extra IOCs (17.6±2.7, Fig. 4.1A—as compared with 12 IOCs in wild type). This is reminiscent of the apically localised upstream activators of Hippo signalling, Kib, Mer, Ex and Crb that act redundantly to regulate growth through Hippo signalling (Genevet and Tapon 2011). Consistent with the literature, *kib*$^{\Delta 32}$ (Genevet et al. 2010) and *crb*$^{82\text{-}04}$ (Ling et al. 2010) single mutants had 22.0±2.4 and 13.3±1.4 IOCs respectively (Fig. 4.1B, D).

If RASSF8 was similar to these upstream activators, a synergistic increase in the number of extra IOCs in double mutant combinations would be expected, such as that observed for the *mer;kib* and *kib;crb* double mutant combinations (Ling et al. 2010, Yu et al. 2010). Indeed, clones in *kib*$^{\Delta 32}$*,RASSF8*^{6} double mutant flies had 43.3±5.1 IOCs per hexagon (Fig. 4.1C), which is more than an additive effect of the single mutants. Despite the massive increase in the number of IOCs, primary pigment cells and cone cells were largely unaffected. However, clones in *crb*$^{82\text{-}04}$*,RASSF8*^{6} double mutant flies did not have significantly more IOCs (16.6±1.7) than in clones of *RASSF8*^{6} single mutants (Fig. 4.1E). This was also observed with another *crb* allele, *crb*^{8F105} (16.9±1.7, Fig. 4.1F). Together, these results show that *kib*, but not *crb* synergises with *RASSF8* to control the number of IOCs.

The multi-layering and increase of IOCs in *kib*$^{\Delta 32}$*,RASSF8*^{6} double mutants are comparable to *hpo* and *wts* null mutant eyes (Hamaratoglu et al. 2006). This suggests that *kib* and *RASSF8* might act redundantly to promote Hippo signalling. It has been reported that double mutants of upstream members of Hippo signalling, but not single mutants show a detectable upregulation of Yki target genes (Ling et al. 2010, Yu et al. 2010). Thus, I tested if *ex*, a widely used transcriptional target of Hippo signalling is affected in double mutants of *RASSF8*^{6} with *kib*$^{\Delta 32}$ and *crb*^{11A22}. However, neither *kib*$^{\Delta 32}$*,RASSF8*^{6} double mutants, nor *crb*^{11A22}*,RASSF8*^{6} double mutants showed elevated *ex* transcription in imaginal eye discs using the *ex-lacZ* enhancer trap line, which carries a transposon-encoded *lacZ* reporter at the endogenous *ex* locus (Fig. 4.2D, F). β-galactosidase staining in these combinations was comparable to single mutants of *RASSF8*^{6}, *kib*$^{\Delta 32}$ and *crb*^{11A22} (Fig. 4.2A, C, E). As expected,

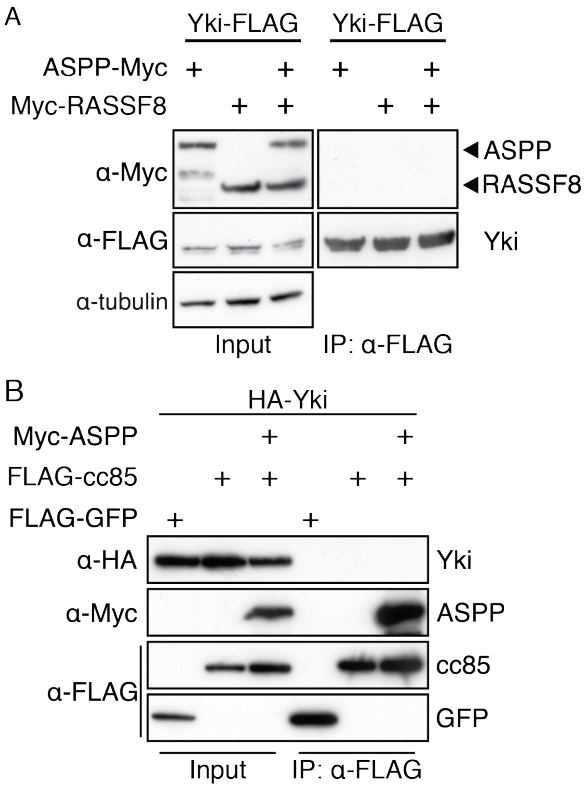

Figure 4.4.: No binding between Yki and ASPP, RASSF8 or Ccdc85

Western blots of co-IP experiments using anti-FLAG antibody-coupled beads and S2 cell lysates. Cells were transfected with the indicated constructs. Western blots were probed with indicated antibodies.

(A) In a pull-down of Yki, neither ASPP, nor RASSF8 are detected when the two protein are expressed separately or together.

(B) In a pull-down of Ccdc85, Yki does not co-IP. Co-expressed ASPP in contrast is co-IPed by Ccdc85.

$wts^{M5.41}$ mutants showed strongly elevated β-galactosidase levels (Fig. 4.2B). Similar to the transcriptional *ex-lacZ* reporter, Ex protein levels remained unchanged in either $RASSF8^{6}$ and $kib^{\Delta 32}$ single mutant or $kib^{\Delta 32}$,$RASSF8^{6}$ double mutant wing imaginal discs (Fig. 4.3). Thus, although *RASSF8* and *kib* synergistically regulate the number of IOCs, this does not seem to be via Hippo signalling.

4.1.2. ASPP, RASSF8 and Ccdc85 do not bind to Yki in co-IP experiments

Although the in vivo data suggested that RASSF8 might not function as a Hippo signalling upstream element such as Kib, I still wanted to test whether RASSF8, together with ASPP could dephosphorylate Yki. Analogous to ASPP2 in mammalian cells (Liu et al. 2011), the dephosphorylation could remove the inhibitory phosphate of Yki. Alternatively, more consistent with the idea that ASPP and RASSF8 are tumour suppressors, the dephosphorylation could remove an activating rather than an inhibitory phosphate. Either way, binding of Yki to an ASPP/PP1 complex would be required for effective dephosphorylation. Indeed, both RASSF8 and ASPP2 have been recovered in several AP-MS experiments, using YAP and TAZ as baits (Couzens et al. 2013, Hauri et al. 2013, Kohli et al. 2014, Wang et al. 2014).

In co-IP experiments, Yki did not bind to ASPP or RASSF8, alone or in combination (Fig. 4.4A). Similarly, Ccdc85 alone or a Ccdc85/ASPP complex did not bind to Yki (Fig. 4.5B). These results do not rule out that Yki might bind to PP1 directly. However, the data does not provide evidence that an ASPP/PP1 complex may dephosphorylate Yki.

4.1.3. ASPP, RASSF8 and PP1 do not regulate Yki S168 phosphorylation in S2 cells

The negative results from the co-IP experiments do not exclude the possibility that weak binding between the ASPP/PP1 complex and Yki occurs. This might be sufficient in vivo for efficient dephosphorylation. Thus, I decided to test in S2 cells, if overexpressing or knocking down components of the ASPP/PP1 complex has an influence on Yki S168 phosphorylation. Expressing either RASSF8, ASPP, ASPP-FA or the negative regulator of Hippo signalling RASSF in S2 cells slightly decreased Yki S168 phosphorylation (Fig. 4.5A). However, the reduction was very subtle and variable between experiments, especially when compared to the substantial and reproducible increase of Yki S168 phosphorylation elicited by Hpo expression.

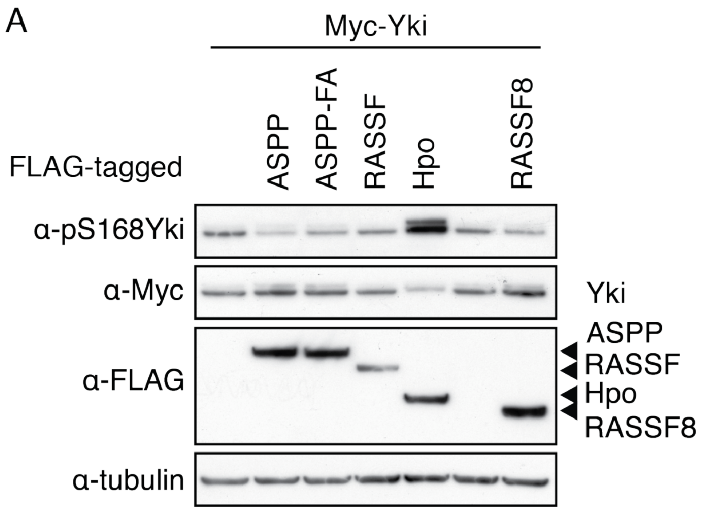

Figure 4.5.: Expression of ASPP or RASSF8 does not significantly influence Yki S168 phosphorylation

Western blots of S2 cell lysates. Cells were transfected with the indicated constructs. Western blots were probed with indicated antibodies. Yki S168 phosphorylation is slightly reduced when ASPP is co-expressed. Reduction is variable between experiments. In contrast, the Yki S168 phosphorylation is always increased when Hpo is expressed.

When ASPP or individual PP1 catalytic subunits were knocked-down, no significant change in S168 phosphorylation of endogenous Yki was observed (Fig. 4.6C, D). Efficient knockdown was confirmed using tagged proteins (Fig. 4.6A, B), since no antibodies were available to detect endogenous ASPP or PP1s in S2 cells. These results suggest that in S2 cells, Yki is not dephosphorylated by an ASPP/PP1 complex. However, there are several caveats with the cell-based experiments as discussed below (see 4.2.3).

In conclusion, I could not uncover any evidence that ASPP/PP1 dephosphorylates Yki in *Drosophila*. This does not rule out that Yki is dephosphorylated by ASPP/PP1 in different cellular contexts. Weak binding between Yki and the ASPP/PP1 complex might occur in vivo and could regulate transcriptional targets of Yki in other tissues than the larval eye or wing imaginal discs.

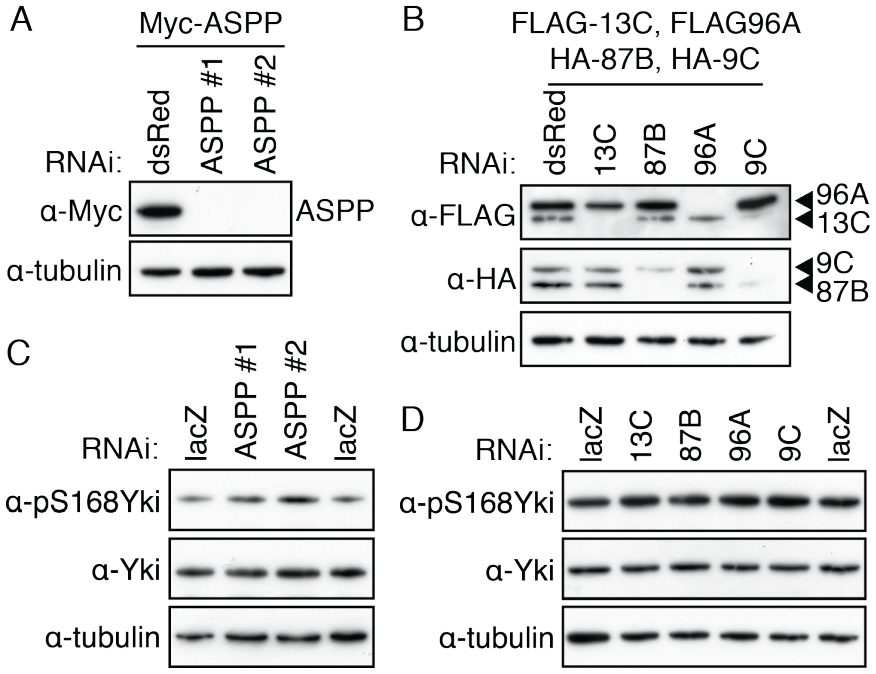

Figure 4.6.: Knock-down of ASPP, RASSF8 or PP1 have no effect on Yki S168 phosphorylation

Western blots of S2 cell lysates. Cells were transfected with the indicated constructs/treated with the indicated dsRNAs. Western blots were probed with indicated antibodies.

(A) Exogenous ASPP is efficiently knocked-down with two different dsRNAs. (B) Exogenous PP1s are efficiently knocked-down with dsRNAs designed to be specific for each PP1 subunit.

(C) Knock-down of ASPP has no effect on endogenous Yki S168 phosphorylation.

(D) Knock-down of PP1s has no effect on endogenous Yki S168 phosphorylation.

4.2. Baz is a potential substrate for ASPP/PP1

In parallel to Yki, I considered the polarity protein Baz as a second candidate substrate for the ASPP/PP1 complex. Three pieces of evidence suggest that Baz might be associated with the ASPP/PP1 complex: (1) PAR3, the mammalian orthologue of Baz, has been found to bind to ASPP2 and regulate tight junction formation together with ASPP2 (Cong et al. 2010, Sottocornola et al. 2010). Especially during the de novo formation of tight junctions, ASPP2 is required to localise PAR3 (Cong et al. 2010). (2) PP1 alone can directly dephosphorylate PAR3 on several serine residues (Traweger et al. 2008). (3) Baz has been found to physically interact with ASPP and RASSF8. In yeast two-hybrid data generated in our lab, Baz could bind to *Drosophila* RASSF8 (Eunice Chan—unpublished observations), human RASSF8 has been found to co-purify with PAR3 (Brajenovic et al. 2004) and PAR3 could pull-down RASSF7, 9 and 10 in the AP-MS experiments carried out by our collaborators (Fig. 1.10).

4.2.1. ASPP regulates the junctional localisation of Baz in the developing retina

As Baz localisation in many systems is regulated by phosphorylation (see 1.5.3), dephosphorylation by the ASPP/PP1 complex could affect it. I decided to investigate Baz localisation in the developing retina, since PP1 (Fig. 3.9B, C), ASPP and RASSF8 (Langton et al. 2009) are all junctionally localised and their inactivation leads to phenotypic consequences in this tissue (Langton et al. 2007 2009 and Chapter 3).

In $ASPP^{d}$ mitotic mutant clones, the intensity of Baz at cell-cell junctions in IOCs was reduced, in comparison to adjacent wild type tissue (Fig. 4.7 A, B). This result shows that ASPP is required for proper Baz localisation in developing retinas. The reduction of Baz localisation in *ASPP* mutant clones is incomplete, suggesting that other localisation cues might stabilise Baz at cell-cell junctions. An example of redundant localisation cues for polarity proteins is found in follicle cells. There, aPKC

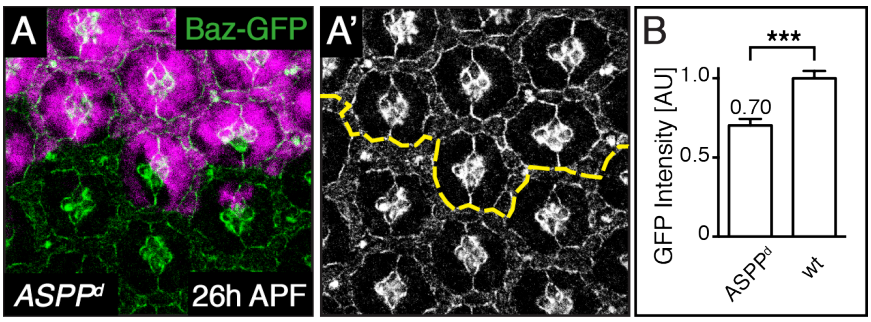

Figure 4.7.: Baz is mislocalised in *ASPP* mutant clones

(A, A') Confocal X-Y sections of pupal retinas at 26 h APF. Baz-GFP fluorescence is detected. Flp/FRT clones were generated with *eyFlp* and marked by absence of mCherry (purple). In *ASPP* mutant retinas, Baz levels at cell-cell junctions are reduced. Clone boundary marked with dashed yellow line.

(B) Quantification of GFP intensity of cell-cell contacts between IOCs and primary pigment cells in mutant and wild type tissue of retina shown in A. An unpaired t-test showed that the mean intensities differ significantly from each other. *** indicates $p<0.001$. Five traces of the contacts between the IOCs surrounding two primary pigment cells were analyzed for each condition. GFP intensity was normalised to the mean of fluorescent signal intensity in the wild type tissue.

localises correctly in *baz* and *crb* single mutant mitotic clones, but not in double mutant clones (Fletcher et al. 2012). Similarly, Baz was localised correctly in *crb* mutant retinas (Fig. 4.8A), but when ASPP was additionally knocked-down, Baz was barely detectable at cell-cell junctions (Fig. 4.8C). This suggests that, additionally to known polarity proteins, ASPP is also necessary for stabilising Baz at cell-cell junctions.

4.2.2. ASPP can bind to Baz via RASSF8

Baz needs to bind to PP1, in order to be dephosphorylated by an ASPP/PP1 complex. It has been suggested that mouse PAR3 could directly bind to PP1 (Traweger et al. 2008). To test the binding between PP1 and Baz in *Drosophila*, I performed co-IP experiments. Baz showed weak interaction with PP1s, but associated with RASSF8 more strongly (Fig. 4.9A). In contrast to human PAR3 and ASPP2 (Cong et al. 2010, Sottocornola et al. 2010), no binding between Baz and ASPP was detectable.

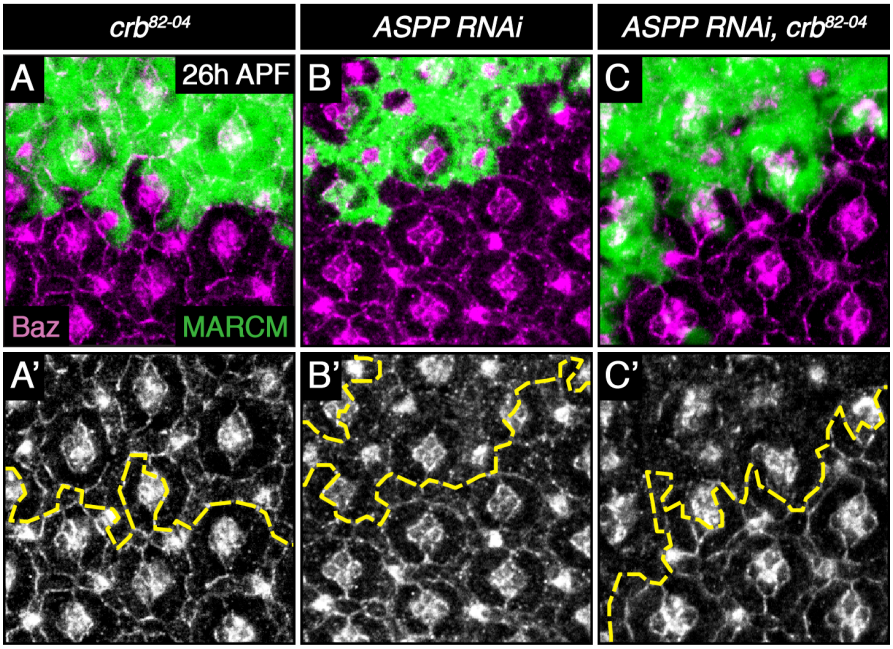

Figure 4.8.: ASPP and Crb are required to localise Baz to cell-cell junctions

Confocal X-Y sections of pupal retinas at 26 h APF stained with an anti-Baz antibody. MARCM clones were generated with *eyFlp* and marked by GFP.

(A, A') In $crb^{82\text{-}04}$ mutant retinas, Baz localisation is largely unaffected. Clone boundaries marked with dashed yellow line.

(B, B') In retinas where ASPP is knocked down, Baz localisation at cell-cell junctions is reduced.

(C, C') Depleting ASPP in a $crb^{82\text{-}04}$ mutant retina completely removes Baz from cell-cell junctions.

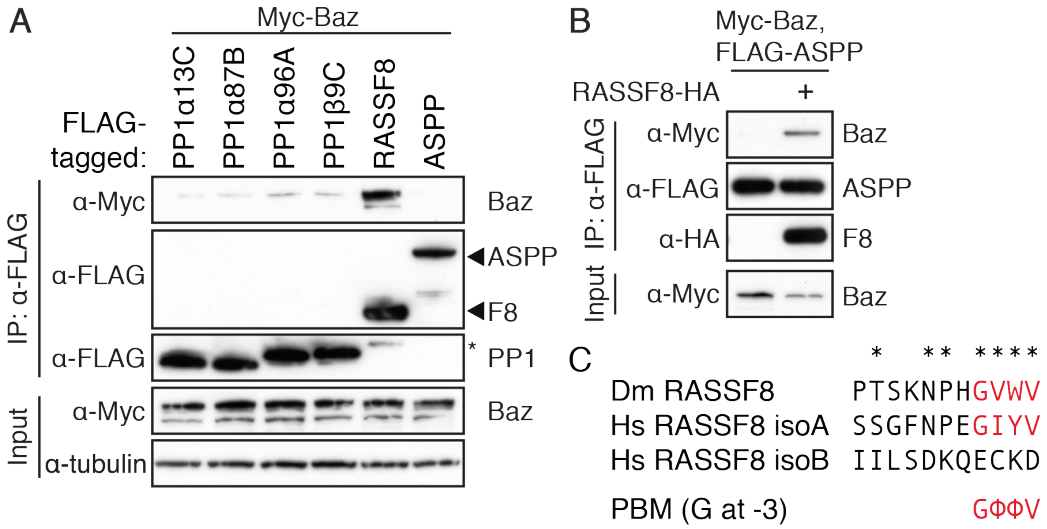

D

Protein	Unique peptides (iso A)	Unique peptides (iso B)	Ratio (B/A)
RASSF8	301	246	0.8
ASPP2	271	281	1.0
ASPP1	113	110	1.0
PP1α	88	88	1.0
PP1β	60	55	0.9
PP1γ	66	61	0.9
PAR3	245	9	0.0
PAR3β	16	0	0.0
PAR6β	7	0	0.0
PAR6γ	17	0	0.0
PKCι	19	0	0.0
PATJ	10	0	0.0
MPDZ	13	0	0.0
CCDC85C	9	0	0.0
14-3-3η	63	7	0.1
14-3-3θ	30	4	0.1
14-3-3γ	23	5	0.2
14-3-3β	28	7	0.3
14-3-3ε	55	14	0.3
14-3-3ζ	28	13	0.5

Figure 4.9.: Baz binds to ASPP via RASSF8

(A, B) Western blots of co-IP experiments using anti-FLAG antibody-coupled beads and S2 cell lysates. Cells were transfected with the indicated constructs. Western blots were probed with indicated antibodies.

(A) Baz co-IPs with RASSF8, but not with ASPP. All four PP1 isoforms weakly bind to Baz.

(Continues on following page)

As only RASSF8 and Baz strongly interacted with each other, we hypothesized that RASSF8 helps to bridge the interaction between Baz and ASPP/PP1. Indeed, ASPP could interact with Baz only in the presence of RASSF8 in co-IP experiments (Fig. 4.9B). *Drosophila* RASSF8 and isoform A of human RASSF8 have a putative PDZ-domain binding motif (PBM) that is not present in the alternatively spliced human RASSF8 isoform B (Fig. 4.9C). The last four residues fit to a group of PBMs that have a glycine as their fourth to last residue (Tonikian et al. 2008). This group does not belong to any of the four classes of PBMs. Baz and PAR3 have three PDZ-domains that could bind to the PBM of RASSF8. The interaction networks that were constructed by Matthias Gstaiger's lab (Hauri et al. 2013) were based on isoform B of RASSF8, the isoform without the PBM. Thus, to test if the PBM was important for PAR3 binding, I cloned isoform A of human RASSF8 into a Flp-In vector for insertion into HEK293 cells, followed by AP-MS experiments. Matthias Gstaiger confirmed that the PBM of human RASSF8 is required for PAR3 binding (Fig. 4.9D). In contrast to isoform B, isoform A of RASSF8 could pull-down substantial amounts of PAR3. Known polarity determinants were detected as well. Members of the PAR complex (see 1.5.2) such as PAR6β/γ (Par6 in Drosophila), PKCι (aPKC in Drosophila), a member of the CRB complex (see 1.5.2) PATJ/MPDZ (both orthologous to Patj) and different 14-3-3 isoforms were pulled-down (Fig. 4.9D). Additionally, CCDC85C was also a specific binding partner of isoform A of RASSF8. Together these results

---

Figure 4.9: (Continued from previous page)

(B) Baz co-IPs with ASPP only when RASSF8 is present.

(C) Alignment between the C-terminus of human and *Drosophila* RASSF8. *Drosophila* RASSF8 and isoform A of human RASSF8 have a putative PDZ-binding motif. Asterisks indicate conserved residues in human (isoform A) and *Drosophila* RASSF8.

(D) Table with number of identified peptides in AP-MS experiments, where human RASSF8 were pulled-down. Isoform A of human RASSF8, but not isoform B is able to pull-down PAR3. Number of peptides for isoform A is average of 2 experiments. Ratios close to 1 indicates no difference between isoforms A and B, ratios close to 0 indicates preferential binding to isoform A. This experiment was performed by Matthias Gstaiger.

suggest that RASSF8 bridges the interaction between Baz/PAR3 and the ASPP/PP1 core complex in *Drosophila* and mammalian systems.

4.2.3. ASPP, RASSF8 and PP1 do not influence Baz phosphorylation in intact S2 cells

Next, I tested if the ASPP/PP1 complex could dephosphorylate Baz. Phospho-specific antibodies for pS151, pS1085 (Krahn et al. 2009) and pS980 (Morais-de Sá et al. 2010) are available. A complication for interpreting phosphorylation results in S2 cells is that Baz is degraded into smaller fragments, during purification (Fig. 4.9A, 4.10B and Krahn et al. 2009). Each phospho-specific antibody seems to bind to fragments of different molecular weight (Krahn et al. 2009). To prevent Baz degradation, in all subsequent lysates of Baz expressing S2 cells that are not used for co-IP experiments, I lysed with RIPA buffer (see 2.2.13) instead of the normal HEPES lysis buffer unless otherwise stated. These more stringent lysis conditions were sufficient to prevent all degradation and Baz appears as a single band on Western blots (e.g., Fig. 4.10A).

I successfully tested the anti-pS151 and anti-pS1085 antibodies using Baz S151A and S1085A mutants, which showed a reduced signal (Fig. 4.10A). To test the anti-pS980 antibody, I co-expressed aPKC with Baz and detected an increased signal (Fig. 4.10B, lysis was not performed in RIPA buffer). Using these antibodies, I could not detect a decrease of phosphorylation of Baz when overexpressing ASPP or RASSF8 (Fig. 4.10C). Only the expression of PP1α96A and PP1β9C decreased S1085 phosphorylation (Fig. 4.10C). However, this was not always reproducible. Moreover, when ASPP or RASSF8 were knocked-down, no changes in Baz phosphorylation were observed (Fig. 4.10D). Only the knock-down of Microtubule star (Mts), the PP2A catalytic subunit, resulted in an increase in S151 and S980 phosphorylation (Fig. 4.10D). This is different to the observation of Krahn et al., who reported an increase in S1085, but not in S151 and S980 phosphorylation upon Mts depletion (Krahn et al. 2009). The reason for this discrepancy is not clear.

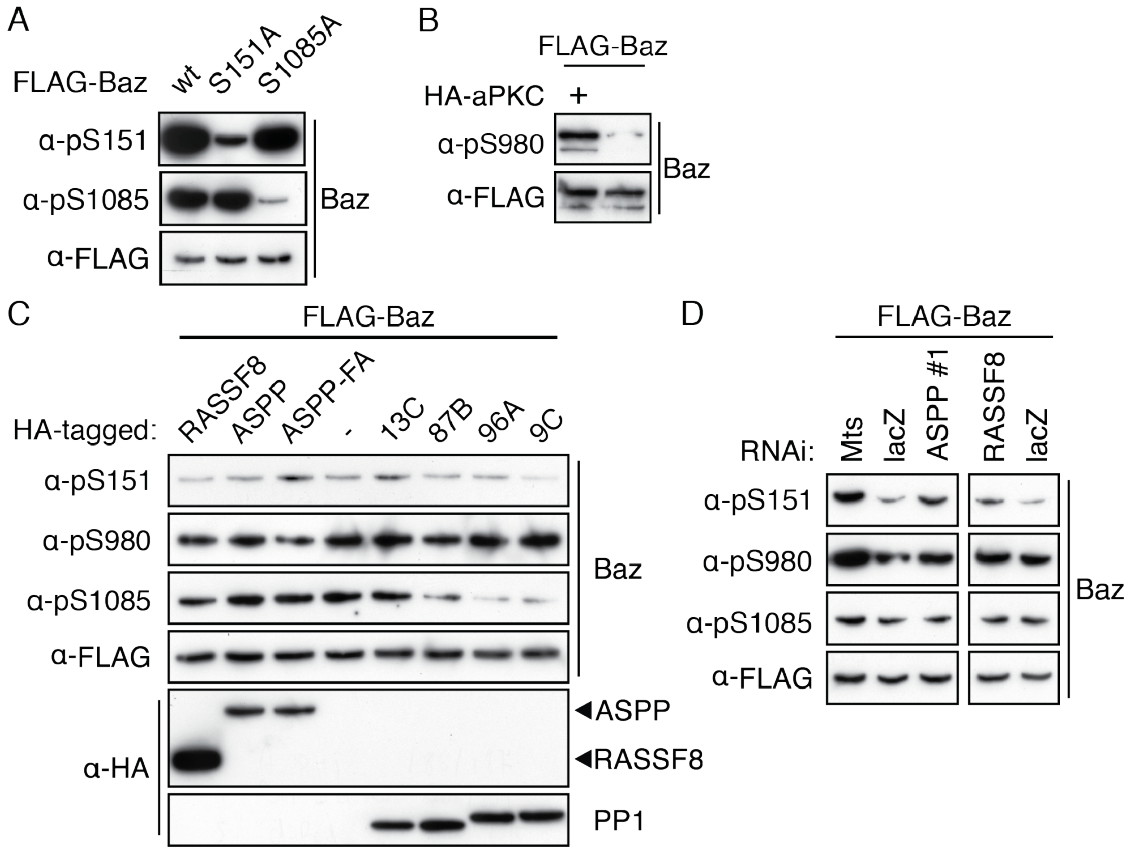

Figure 4.10.: Baz phosphorylation is largely unaffected by expression or knock-down of PP1, ASPP or RASSF8

Western blots of S2 cell lysates. Cells were transfected with the indicated constructs/or treated with the indicated dsRNAs. Western blots were probed with indicated antibodies.

(A) The anti-pS151 and anti-pS1085 antibodies primarily recognise wild type Baz that have intact S151 and S1085 residues.

(B) The anti-pS980 antibody recognises phosphorylation of S980 induced by ectopic expression of aPKC. Lysis with normal lysis buffer instead of RIPA buffer.

(C) PP1α96A or PP1β9C expression weakly decreases S1085 phosphorylation of Baz. This effect was not robustly seen across multiple repeats.

(D) Knock-down of ASPP and RASSF8 does not influence Baz phosphorylation. In contrast Mts knock-down increases S151 and S980 phosphorylation of Baz.

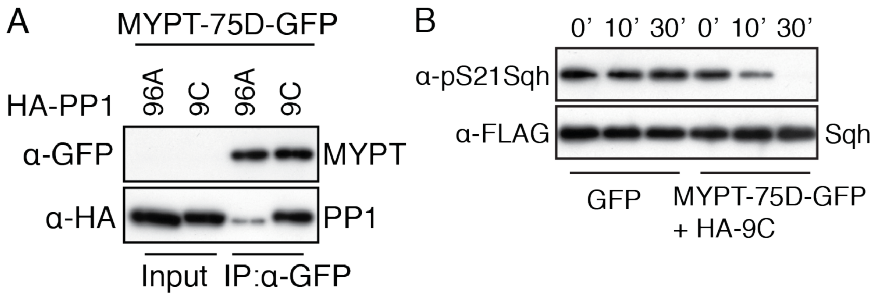

Figure 4.11.: Sqh is dephosphorylated in vitro by the MYPT-75D/PP1β9C complex

(A) Western blots of co-IP experiments using GFP-trap beads with S2 cell lysates. Cells were transfected with the indicated constructs. Western blots were probed with indicated antibodies. MYPT-75D/PP1β9C complex forms in S2 cells, when both proteins are co-expressed. MYPT-75D binds more strongly to PP1β9C than to PP1α96A. (B) Western blots of in vitro phosphatase assay. Sqh was purified from Calyculin A-treated S2 cells and eluted from anti-FLAG antibody coupled beads. MYPT-75D and PP1β9C were purified from S2 cells using GFP-trap beads. Sqh is dephosphorylated by the MYPT-75D/PP1β9C complex. Under these conditions, Sqh remains stable over 30 minutes and dephosphorylation does not occur when no PP1β9C is present.

Overall, as for the experiments with Yki, cell-based assays have several caveats. Importantly, overexpressing only one subunit of the ASPP/PP1 complex might not be sufficient to increase PP1 activity. Furthermore, it is likely that S2 cells do not express any ASPP (Cherbas et al. 2011). Thus, there might be no endogenous ASPP/PP1 complex that could be affected by RNAi. Due to these limitations, I decided to carry out dephosphorylation assays in vitro, where I can control the components of the phosphatase complex used in the assay.

4.2.4. In vitro dephosphorylation of Baz reveals ten putative dephosphorylation sites

Most published in vitro dephosphorylation assays use phosphorylase as a generic substrate to measure phosphatase activity of the PP1 catalytic subunit. Commercial kits are available for this purpose. However, in my case, I wished to detect the dephosphorylation of a specific substrate by PP1 that is associated with its regulatory subunits. A similar experiment with a non-generic substrate and a PP1

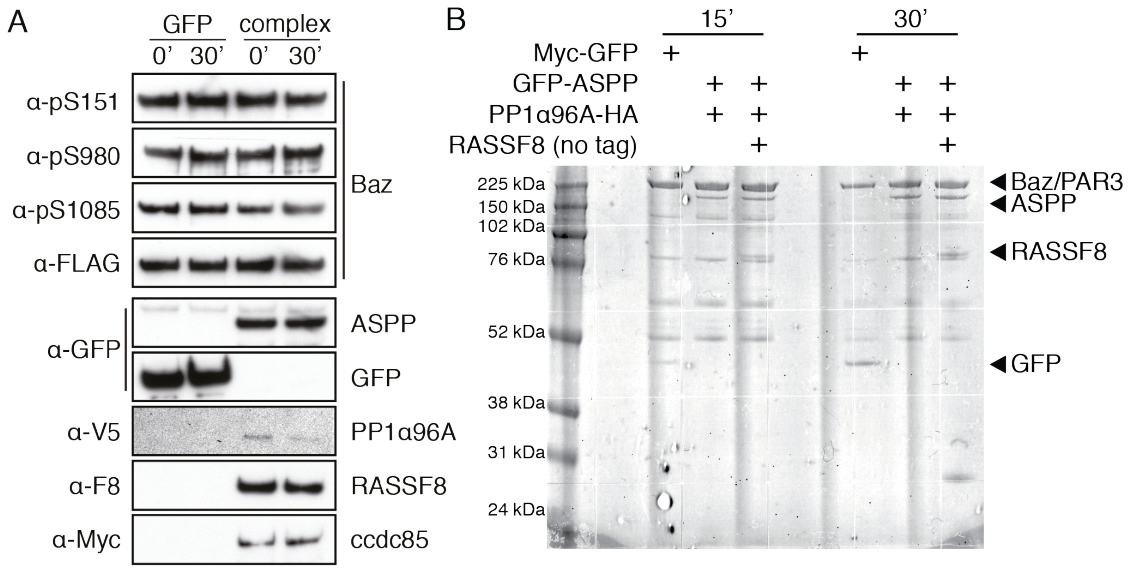

C

Residue	Significant comparisons	Dependent on RASSF8	Change [fold±SD]	Conserved
169/180	2	yes	1.7±0.6	no
235/239	2	yes	2.8±0.4	no
712	2	no	2.5±0.9	yes
806/815	4	yes	3.7±0.6	no
1126/1131	4	yes	1.9±0.4	no
1410	4	no	3.3±1.6	no

Figure 4.12.: Ten serine/threonine residues of Baz were weakly dephosphorylated in vitro

(A) Western blots of in vitro phosphatase assay. Baz was purified from Calyculin A-treated S2 cells and eluted from anti-FLAG antibody coupled beads. The ASPP/PP1 complex was purified from S2 cells using GFP-trap beads. Phospho-specific antibodies did not detect any dephosphorylation of Baz on S151, S980 and S1085 after in vitro dephosphorylation by the ASPP/PP1 complex.

(B) Coomassie stained gel for label-free mass spectrometric analysis by the LRI Protein Analysis and Proteomics facility. Sample preparation as in (A). Two dephosphorylation time points (15 minutes and 30 minutes) with three conditions each (GFP only, ASPP/PP1 without RASSF8 and ASPP/PP1 with RASSF8) were analysed. ASPP, RASSF8 and Baz are detectable by Coomassie staining, while PP1α96A is not.

(C) Summary of serine/threonine residues that were statistically significantly dephosphorylated in vitro. 6 phospho-peptides containing a total of 10 serine/threonine residues were weakly dephosphorylated when RASSF8 was present, or when ASPP/PP1 without RASSF8 was compared to GFP only. Only T712 of Baz is conserved in human PAR3. For more details on data analysis, see Materials and Methods.

complex had been done before (Vereshchagina et al. 2004). In this work, bacterially expressed Sqh (Spaghetti squash), the *Drosophila* orthologue of Myosin regulatory light chain—MRLC, was dephosphorylated by a PP1β9C/MYPT-75D complex and dephosphorylation was detected using a phospho-specific antibody.

Instead of using bacterially expressed proteins, I decided to express all proteins in *Drosophila* S2 cells. The reason is twofold. Firstly, PP1 purified from *E. coli* has a different substrate specificity spectrum and can even dephosphorylate phospho-tyrosine residues (MacKintosh et al. 1996). This is reportedly caused by the incorporation of different metal ions (Mn^{2+} rather than Zn^{2+} or Fe^{2+} for the native enzyme) in the catalytic centre. Secondly, in S2 cells, the substrate can be hyperphosphorylated at multiple residues by phosphatase inhibitor treatment. This allows hyperphosphorylation of substrates at most sites, even those for which the kinase is unknown, allowing for an unbiased screen of all potential dephosphorylation sites. Subsequently, dephosphorylated residues can be identified by quantitative mass spectrometry.

As a proof of principle that proteins expressed in S2 cells can work in an in vitro dephosphorylation assay, I first established the assay using the well-characterized MYPT-75D/PP1β9C complex together with Sqh as a substrate. S21 of Sqh is known to be dephosphorylated by MYPT-75D/PP1β9C (Vereshchagina et al. 2004). The phosphorylation status of S21 can be monitored with a phospho-specific human anti-MRLC antibody that cross-reacts with *Drosophila* Sqh (Lee and Treisman 2004). I could confirm in co-IP experiments that a MYPT-75D/PP1β9C complex formed and, as expected, MYPT-75D preferentially bound to PP1β9C in comparison to PP1α96A (Fig. 4.11A). Furthermore, I could observe dephosphorylation of S21 of Sqh in vitro within 10 minutes of adding MYPT-75D/PP1β9C, but not by adding GFP (Fig. 4.11B). Thus purifying the components for the phosphatase assay from S2 cells was a valid approach. The substrate remained stable over 30 minutes under the conditions of the assay, and no unspecific dephosphorylation took place when PP1β9C was absent.

Using the same set-up, I tested dephosphorylation of Baz by ASPP/PP1. Exogenous Baz was hyperphosphorylated by Calyculin A treatment of the expressing S2

cells, purified and added to ASPP/PP1 complexes that also contained RASSF8. The ASPP/PP1 complexes were isolated by pull-down of GFP-tagged ASPP. Within 30 minutes, no dephosphorylation of S151, S980 or S1085 was observed (Fig. 4.12A). Nonetheless, it was still possible that other serine or threonine residues had been dephosphorylated. To detect dephosphorylation of other residues, I repeated the dephosphorylation assay for two time points (15 and 30 minutes) with GFP alone, with ASPP/PP1 or ASPP/PP1/RASSF8 and sent gel purified Baz (Fig. 4.12B) for mass spectrometric analysis at the LRI Protein Analysis and Proteomics facility. The reason to differentiate between ASPP/PP1 with and without RASSF8 was that it seemed plausible that RASSF8 would be required for ASPP/PP1 to bind to Baz for effective dephosphorylation. MaxQuant software was used for label-free quantitation in collaboration with Dr Karin Barnouin (LRI Protein Analysis and Proteomics facility). Out of all Baz phospho-peptides, six were significantly and consistently reduced (Fig. 4.12C). The identification of the phosphorylated residue in an individual peptide was sometimes ambiguous. In these cases all serine or threonine residues within the peptide were considered as candidates. Some dephosphorylation events were seemingly dependent on RASSF8, while others were not (i.e., ASPP and PP1 alone were sufficient).

4.2.5. Only one of the putative dephosphorylation sites affects Baz localisation in S2 cells

Baz was mislocalised in *ASPP* mutant mitotic clones (Fig. 4.7), which could have been caused by hyperphosphorylation of Baz due to the lack of the ASPP/PP1 complex. In order to test this hypothesis, I expressed GFP-tagged Baz in S2 cells. Wild type Baz is membrane-associated in S2 cells (Matos Simões et al. 2010 and Fig. 4.13A). Furthermore, Baz can become cytoplasmic (GFP-Baz-N, residues 1–1096, Fig. 4.13B), when its C-terminal region, which contains the phosphoinositide binding domain, is removed (Matos Simões et al. 2010). The cytoplasmic localisation suggests that this S2 cell-based assay might be suitable to detect the dissociation of Baz from the membrane upon phosphorylation.

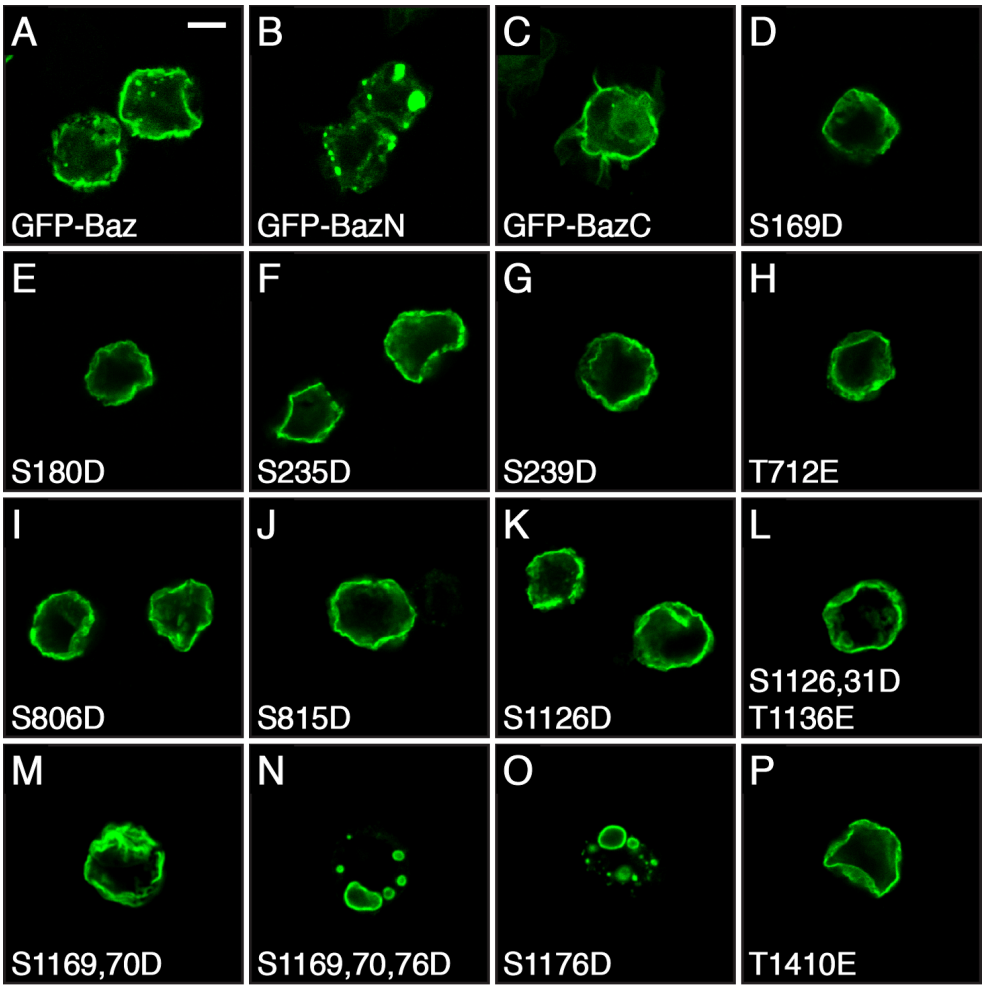

Figure 4.13.: Mutating S1176 of Baz leads to vesicular localisation in S2 cells

Confocal X-Y section of S2 cells transfected with GFP-Baz constructs. Scale bar represents 20 µm.

(A) Baz localises to the plasma membrane of S2 cells.

(B) The N-terminus of Baz (residues 1–1096) localises in aggregates in the cytoplasm.

(C) The C-terminus of Baz (residues 1097–1464) is sufficient for membrane localisation in S2 cells. GFP-BazC harbours its phosphatidylinositol-phosphate binding site.

(D–P) Most phospho-mimicking Baz mutations at putative dephosphorylation sites do not influence the binding of Baz to the plasma membrane. Mutating S1176 to aspartate is sufficient to mislocalise Baz to vesicular structures (O).

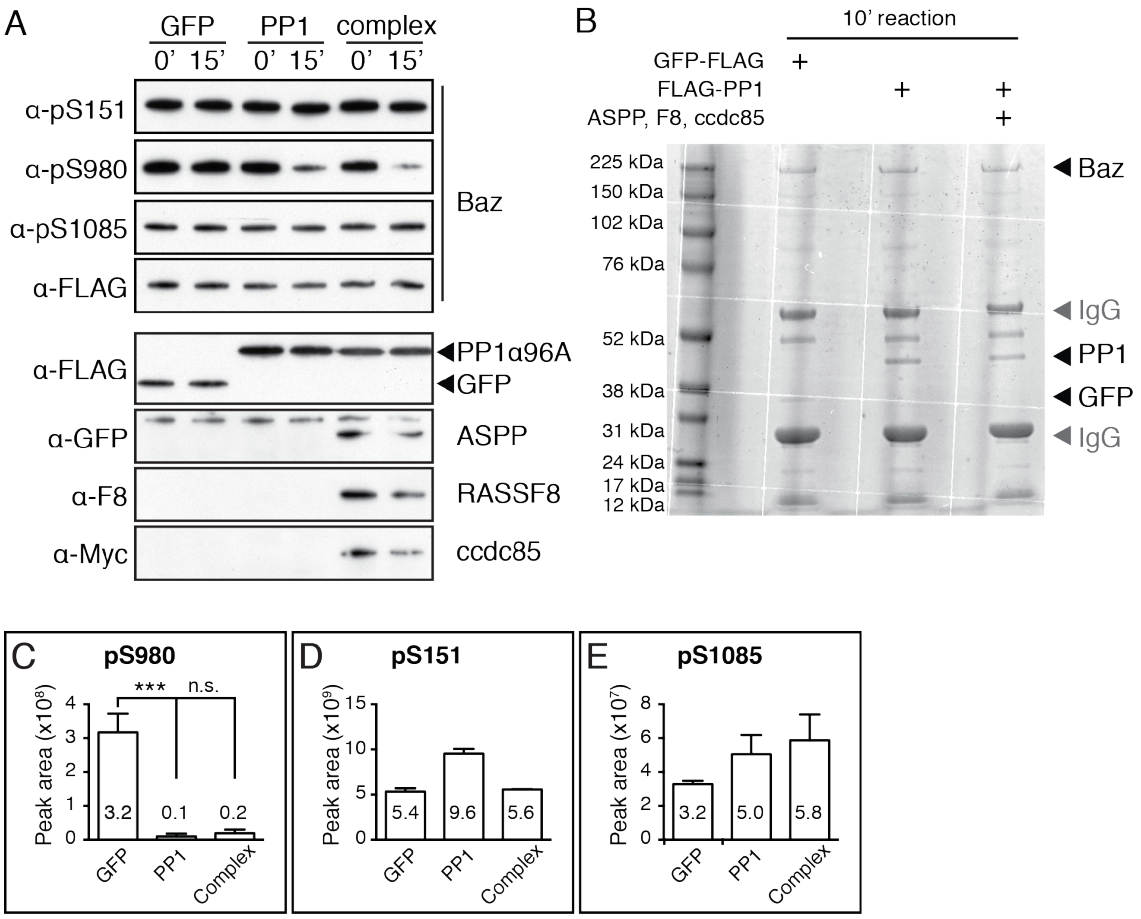

Figure 4.14.: Improved in vitro dephosphorylation assay reveals six weakly and six strongly dephosphorylated serine/threonine residues of Baz, including S980

(A) Western blots of in vitro phosphatase assay. Baz was purified from Calyculin A-treated S2 cells and eluted from anti-FLAG antibody coupled beads. ASPP/PP1 complex was purified from S2 cells using anti-FLAG antibody coupled beads. S980 is dephosphorylated within 15 minutes, while S151 and S1085 are not. Slightly increased dephosphorylation was observed when ASPP, RASSF8 and Ccdc85 were present.

(B) Coomassie stained gel for label free and dimethyl-labelled mass spectrometric analysis by the LRI Protein Analysis and Proteomics facility. Sample preparation as in (A). One time point (10 minutes) with three conditions (GFP, PP1α96A, PP1α96A with ASPP, RASSF8 and Ccdc85). GFP, PP1α96A and Baz show identifiable bands, while ASPP, RASSF8 and Ccdc85 do not.

(C–E) Quantification results of peptides containing pS151, pS980 and pS1085 using label-free quantification. While S980 phosphorylation is 31-fold and 16-fold lower when PP1, or the ASPP/PP1 complex is present, S151 and S1085 phosphorylation are not reduced. For a list of all phospho-peptides that were changed after dephosphorylation and details of statistical analysis see Appendix A.

Thus, I generated phospho-mimicking mutants for all 10 putative dephosphorylation sites and included three additional sites S1169, S1170 and S1176, since these were closest to the PIP binding region (1173–1197) of Baz (Krahn et al. 2010). Each mutant was expressed in S2 cells. However, no Baz mutant showed a cytoplasmic localisation that was comparable to the N-terminal region of Baz (Fig. 4.13D–P). Surprisingly, mutating S1176 to aspartate was sufficient to localise Baz to intracellular vesicular structures (Fig. 4.13N, O). These results suggests that hyperphosphorylation of none of tested residues was sufficient for removing Baz from the membrane in S2 cells.

4.2.6. Second in vitro dephosphorylation of Baz reveals seven novel putative dephosphorylation sites

The first dephosphorylation assay was not optimal for two reasons. Firstly, there was no positive control to verify that any dephosphorylation was taking place, proving that the isolated complexes were active. Secondly, also possibly connected to the first issue, PP1 concentration in the ASPP pull-downs was very low (Fig. 4.12A) and could not be detected by Coomassie staining (Fig. 4.12B). Thus, I decided to repeat the dephosphorylation assay but instead of pulling down ASPP, I pulled down PP1 directly to ensure that enough PP1 was present in the assay. With this approach, I could observe a dephosphorylation of S980, but not of S151 or S1085 (Fig. 4.14A). This showed that the isolated complexes were active, but that dephosphorylation was nevertheless not promiscuous. The presence of ASPP, RASSF8 and Ccdc85 in addition to PP1 alone slightly enhanced the dephosphorylation of S980.

I repeated this pull-down for mass spectrometric analysis by the LRI Protein Analysis and Proteomics facility. In contrast to the ASPP-pulldowns, PP1 was Coomassie stainable (Fig. 4.14B). However, ASPP, RASSF8 and Ccdc85 were less abundant (Fig. 4.14A) and not Coomassie stainable (Fig. 4.14B). The samples were split into two aliquots. One half was used for label-free quantification (LFQ), while the other half was dimethyl-labelled on primary amines using formaldehyde and quantified as two mixtures (GFP mixed with PP1 and PP1 mixed with PP1 complex, for details see Materials and Methods). Mascot was used for quantification. It was reassuring to

see that the dephosphorylation of S151, S980 and S1085 detected by mass spectrometry (Fig. 4.14C–E) corresponded well with the result obtained with phospho-specific antibodies (Fig. 4.14A). From these quantifications I identified 10 dephosphorylated peptides with LFQ and 6 dephosphorylated peptides with dimethyl-labelling on visual inspection (see Appendix A). The top candidate from this experiment was T720, as it is conserved in human PAR3 and its phosphorylation was consistently reduced in both approaches. In summary, the second run of the assay yielded seven novel potential serine/threonine residues that might be dephosphorylated by ASPP/PP1 not found in the first run of the assay.

4.3. Concluding remarks and future directions

In this chapter I have addressed a core challenge within the PP1 field: Identifying specific serine/threonine residues that are dephosphorylated by a PP1 holoenzyme. For this purpose, I established a protocol for effective hyperphosphorylation of putative substrates and their subsequent dephosphorylation by the PP1 holoenzyme. In collaboration with Dr Bram Snijders and Dr Karin Barnouin of the LRI Protein Analysis and Proteomics facility we established label-free and post-labelling methods for identification and quantification of putative dephosphorylation sites. Although I could not find evidence that Yki is dephosphorylated by the ASPP/PP1 complex, the identified serine/threonine residues that were dephosphorylated in Baz provide a foundation for further cell-based and in vivo validation. In the next chapter I will explore the regulation of ASPP and RASSF8 as well as a more unbiased approach to identify novel substrates and regulators of the ASPP/PP1 complex.

4.3.1. Is YAP/TAZ dephosphorylation by ASPP/PP1 conserved in Drosophila?

I could not uncover any evidence that Yki is dephosphorylated by an ASPP/PP1 complex. In mammals, at least TAZ is directly dephosphorylated by ASPP2/PP1 (Liu et al. 2011) and the inhibition of LATS1/2 by ASPP1 (Vigneron et al. 2010) would

be coherent with ASPP1/PP1 dephosphorylating YAP. In line with this, ASPP2 or PP1 expression strongly enhanced YAP transcriptional activity in a cell-based assay (Hauri et al. 2013). Given this data in mammalian systems, it is possible that the regulation of YAP/TAZ by ASPP1/2 is not conserved in *Drosophila*. This would not be the only regulatory mode of YAP/TAZ that is not present for Yki. For instance, the phosphodegron that is responsible for YAP/TAZ ubiquitylation and proteasomal degradation upon phosphorylation by LATS1/2 (Zhao et al. 2010 and see 1.4.2) is not conserved in Drosophila, nor does loss of the fly orthologue of the mammalian ubiquitin ligase complex ($SCF^{\beta TRcP}$ in mammals, SCF^{slimb} in flies) affect Yki stability (Paulo Ribeiro—unpublished observations). In addition, YAP and TAZ possess C-terminal PDZ-binding motifs, which are not conserved in dipteran Yki proteins (Bossuyt et al. 2014, Hilman and Gat 2011).

It was suggested that the whole junctional regulatory machinery of YAP/TAZ may have been rewired during the evolution of Neodiptera, which includes *Drosophila* (Bossuyt et al. 2014). Some elements of the regulatory machinery have been lost such as AMOT and the Yki PDZ-binding motif while others were gained such as the myosin Dachs (Bossuyt et al. 2014, Genevet and Tapon 2011). This shift in Hippo pathway regulation is mirrored by a change of apico-basal polarity in insects, exemplified by the emergence of the basal septate junction as a functional equivalent to the apical tight junction (St Johnston and Ahringer 2010 and see 1.5.8). However, the cause-effect relationship between these two events is unclear. Thus, it is tempting to speculate that ASPP/PP1 regulation of YAP phosphorylation may have been lost in *Drosophila* as part of this evolutionary shift.

However, with the successful dephosphorylation of Baz in vitro, it would be possible to carry out an in vitro dephosphorylation assay of Yki. This might reveal that Yki S168 could be dephosphorylated by ASPP/PP1 after all. Alternatively, other serine/threonine residues might be dephosphorylated. For instance, it is possible that, as yet uncharacterised activating rather than inhibitory phosphorylation sites on Yki might be targets of the ASPP/PP1 complex. This would resolve the puzzling observation that genetic evidence suggests that ASPP proteins function as growth

suppressors both in flies and mice (Kampa et al. 2009, Langton et al. 2007, Vives et al. 2006), while dephosphorylation of the inhibitory site on YAP/TAZ/Yki would be expected to promote growth.

4.3.2. How can the phosphatase assay be improved?

The IP of the ASPP/PP1 holoenzyme for the phosphatase assays was not very efficient. In the GFP-ASPP pull-down, there was no Coomassie detectable PP1α96A (Fig. 4.12B). In contrast, the FLAG-PP1α96A pull-down might have yielded many PP1α96A catalytic subunits unbound to any regulatory subunits, or bound to other endogenously expressed regulatory subunits, rather than bound to ASPP, RASSF8 and Ccdc85 (Fig. 4.14B). In the first case there was possibly no or only little dephosphorylation, in the second case there might have been ASPP, RASSF8 and Ccdc85-independent dephosphorylation. A potential solution to this would be a step-wise purification protocol with larger amounts of starting material. In the first step, FLAG-PP1α96A would be purified as before. Instead of directly using this for the dephosphorylation assay, FLAG-PP1α96A and its associated proteins could be eluted and a second GFP-ASPP purification carried out. With sufficient starting material, this would yield a much higher fraction of ASPP/PP1 complexes. As a complementary approach, we are investigating the possibility of carrying out human ASPP/PP1 complex purification from HEK293 cells. Preliminary data suggest that a better stoichiometry of catalytic to regulatory subunits may be achievable using ASPP2 pulldowns (Teresa Bertran—unpublished observations). In addition, a comparison of Baz and PAR3 in vitro dephosphorylation assay results should be helpful in identifying functionally important sites.

An alternative to in vitro dephosphorylation assays to identify ASPP/PP1 target sites would be an unbiased phospho-proteome analysis. In collaboration with Dr Bram Snijders, Dr Helen Flynn and Dr Steven Howell, I have prepared whole fly lysates of *ASPP*^{d} mutant and wild type flies for post-labelling and subsequent phospho-proteome analysis. This approach has not proceeded further than a technical proof-of-principle phase. Although there are limitations, such as the difficulty of phospho-

site identification on low-abundance proteins in a complex mixture, this might prove to be a fruitful avenue for the discovery of novel substrates for any PP1 holoenzyme subunit.

4.3.3. Is Baz dephosphorylated by ASPP/PP1 in vivo?

The second in vitro dephosphorylation assays revealed seven additional serine/threonine residues that might be dephosphorylated in Baz. To test if these play a role in localising Baz to the membrane in vivo, the S2 cell based assay would be one possible option. An alternative would be to generate transgenic flies expressing phospho-mimicking Baz and test their junctional localisation and whether their expression in the eye phenocopies ASPP mutants. It might be necessary to perform these experiments in a *baz* null background, as Baz can oligomerise (Benton and St Johnston 2003) and wild type Baz might rescue any functional defect of the phospho-mimicking Baz. It is also probable that multiple phosphorylation sites might need to be targeted to observe a robust effect.

To test whether the Baz mislocalisation in *ASPP* mutant mitotic clones is truly due to loss of the ASPP/PP1 complex, rather than a PP1-independent function of ASPP (Fig. 4.7), an alternative experiment could also be carried out. In the case of PP1 dependence, Baz should be mislocalised in *ASPP-FA* rescue tissue as it is in *ASPP* mutant tissue. However, the anti-Baz antibody was not sensitive enough to detect any difference in localisation (data not shown). Thus, the Baz-GFP line (Fig. 4.7) could be used instead. The GFP fluorescence signal of Baz-GFP reports small differences in Baz intensity better than the antibody due to superior signal-to-noise ratio (compare Fig. 4.7 to Fig. 4.8.).

Additionally, phospho-specific antibodies could be generated to show that hyperphosphorylated Baz accumulates in *ASPP* null mutant tissue. Anti-pS980 antibody can detect endogenous Baz in vivo (Morais-de Sá et al. 2010, Walther and Pichaud 2010). Thus, it would be possible to test if S980, or other hyperphosphorylation (e.g., S1176) is observed in ASPP-FA mutant mitotic clones. I will discuss the potential functional implications of Baz dephosphorylation by ASPP/PP1 in the main discussion (see 6.3).

Chapter 5.

Regulators and substrates of the ASPP/PP1 complex

In Chapter 4, I applied a targeted approach and tested two potential substrates of the ASPP/PP1 complex based on protein-protein interaction data from mammalian systems. The discovery of Ccdc85 as a subunit of the PP1 holoenzyme showed that unbiased approaches are valuable for identifying novel interactors of the ASPP/PP1 complex.

In this chapter, I explore potential leads from publicly available unbiased interaction screens. I describe two potential regulators of RASSF8/ASPP (Wts and Seven in Absentia—Sina) and an additional scaffold (Magi) that may anchor RASSF8 at cell-cell junctions. Furthermore, in GFP-ASPP pull-downs from *Drosophila* heads, I identified several potential novel ASPP interactors, which are specific to the central nervous system. Lastly, I use a genetic modifier screen based on available protein-protein interaction data to identify further potential targets and regulators of the ASPP complex.

5.1. Wts phosphorylates RASSF8

In a genome-wide yeast two-hybrid screen, RASSF8 was shown to bind to Wts (Giot et al. 2003). Based on this result, Julien Colombani, who worked on ASPP and RASSF8 in our lab, tried to confirm this interaction in co-IP experiments, but never succeeded (Julien Colombani—unpublished observations). More recently, a collab-

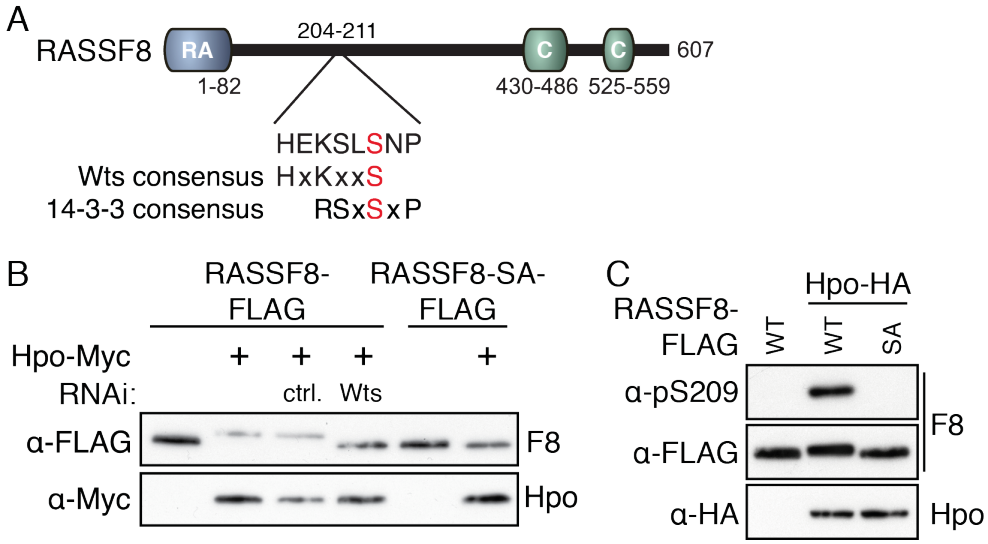

Figure 5.1.: RASSF8 is phosphorylated by Wts on S209

(A) Domain structure of RASSF8. The RA domain was identified by SMART (Letunic et al. 2012). The coiled coil regions were predicted by jpred3 (Cole et al. 2008). The RASSF8 sequence surrounding S209 fit to the Wts consensus phosphorylation motif and to a mode I 14-3-3 binding motif. (B, C) Western blots of S2 cell lysates. Cells were transfected with the indicated constructs/dsRNAs. Western blots were probed with the indicated antibodies. (B) RASSF8 shows mobility shift, when co-expressed with Hpo. Mobility shift is abolished, when Wts is knocked-down. The RASSF8 S209A mutant does not shift when co-expressed with Hpo. (C) The anti-pS209 antibody can detect phosphorylation of RASSF8.

orator, Dr Cathie Pfleger (Mount Sinai Hospital, New York) found RASSF8 in a biochemical screen for Wts kinase substrates. As a substrate, RASSF8 would not have to associate with Wts at high affinity to be efficiently phosphorylated (Pinna and Ruzzene 1996), potentially explaining the negative co-IP result. With this information in hand, I decided to re-examine the relationship between Wts and RASSF8.

5.2. Wts phosphorylates RASSF8 at S209

To confirm the result from the Wts kinase substrate screen, I conducted gel mobility shift assays using hand-cast SDS-PAGE gels. In these assays, phosphorylated proteins can migrate differentially compared to the non-phosphorylated form. Co-transfection

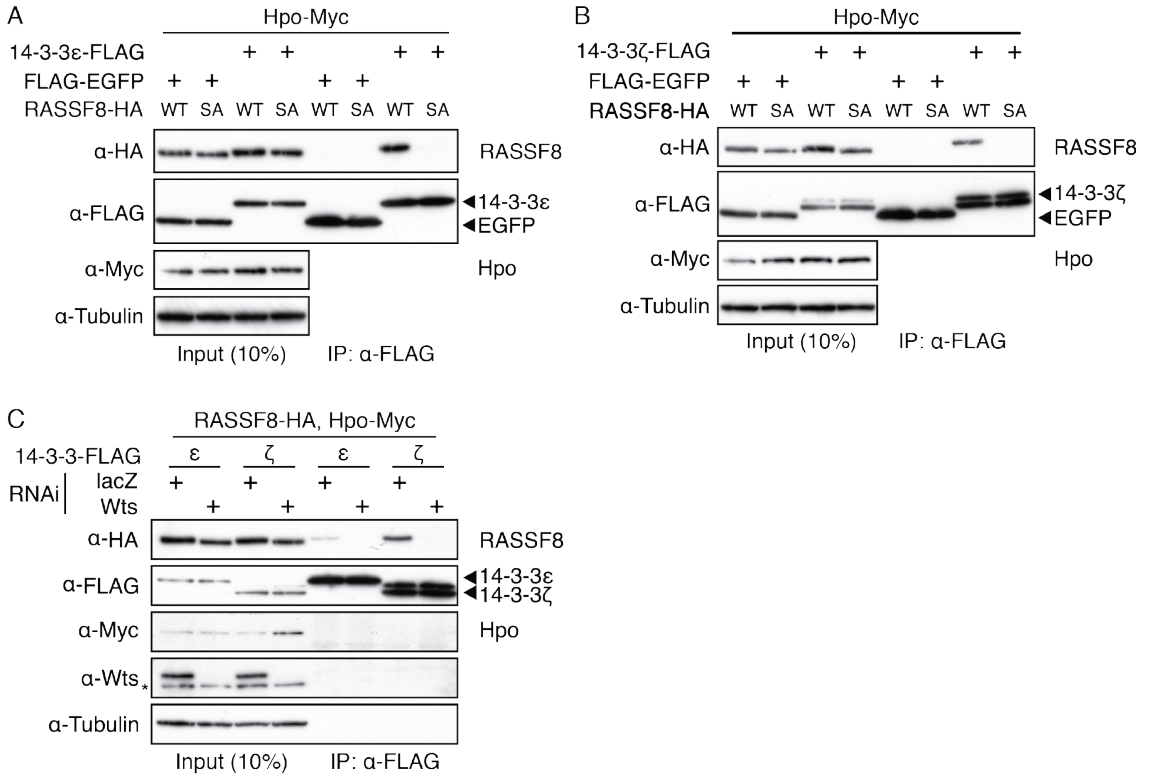

Figure 5.2.: RASSF8 S209 phosphorylation generates a 14-3-3 binding site

Western blots of co-IP experiments using anti-FLAG antibody-coupled beads from S2 cell lysates. Cells were transfected with the indicated constructs/dsRNAs. Western blots were probed with the indicated antibodies. 14-3-3ε (A) and 14-3-3ζ (B) bind to RASSF8 but not RASSF8 S209A, when co-transfected with Hpo. For 14-3-3ε and 14-3-3ζ binding to RASSF8, phosphorylation by Wts is required.

of RASSF8 with Hpo in S2 cells resulted in reduced mobility (upward shift) compared with RASSF8 alone, suggesting that RASSF8 is phosphorylated upon Hpo expression (Fig. 5.1B). The rationale for co-expressing Hpo instead of Wts is that exogenous Wts is not highly active in S2 cells, while Hpo and MST kinases can homodimerize and potently self-activate upon overexpression (Avruch et al. 2012). Expression of Hpo then activates endogenous Wts (Wu et al. 2003). To test whether Wts is required for the Hpo-induced RASSF8 mobility shift, I used RNAi to deplete Wts in cells overexpressing Hpo. Upon Wts depletion, Hpo was no longer able to induce a RASSF8 mobility shift (Fig. 5.1B). This is consistent with the idea that Wts rather than Hpo can phosphorylate RASSF8.

Drosophila RASSF8 has only one serine, S209, that fits the Wts consensus motif (H-x-x-[HKR]-x-[ST], Hao et al. 2008). I mutated this serine and tested the resultant mutant (RASSF8 S209A) for the Hpo-induced mobility shift. Interestingly, the S209A mutant was no longer able to shift upon Hpo co-expression (Fig. 5.1B). Lastly, I raised a phospho-specific antibody using a pS209 peptide (see Materials and Methods). This antibody only recognized RASSF8 when it was co-transfected with Hpo, but not the RASSF8 S209A mutant, even when co-expressed with Hpo (Fig. 5.1C). Together, these results suggest that Wts can phosphorylate RASSF8 at S209.

5.3. Wts phosphorylation generates a 14-3-3 binding site

Wts phosphorylation of Yki at S168 creates a 14-3-3 binding site (Dong et al. 2007, Oh and Irvine 2008 and 1.4.2). RASSF8 phosphorylation by Wts might also promote 14-3-3 binding, analogously to Yki. This hypothesis is supported by the observation that the S209 phosphorylation site (Fig. 5.1A) fits to a mode I 14-3-3 binding site (Johnson et al. 2010).

Indeed, RASSF8 could bind to both *Drosophila* 14-3-3 isoforms (ε and ζ) when co-expressed with Hpo (Fig. 5.2A, B). Under the same conditions, RASSF8 S209A did not bind to 14-3-3 (Fig. 5.2A, B). Binding between RASSF8 and 14-3-3 ε and ζ is dependent on S209 phosphorylation, as co-transfection with Hpo while knocking-down Wts abrogates binding (Fig. 5.3C). In summary, these experiments suggest that phosphorylation of RASSF8 S209 by Wts creates a 14-3-3 binding site.

5.4. Wts phosphorylation does not change binding to known interaction partners

14-3-3 protein binding is thought to have three potential consequences for the target protein (Bridges and Moorhead 2005): (1) Binding to 14-3-3 can cause conformational changes, (2) 14-3-3 can displace other binding partners by occupying the

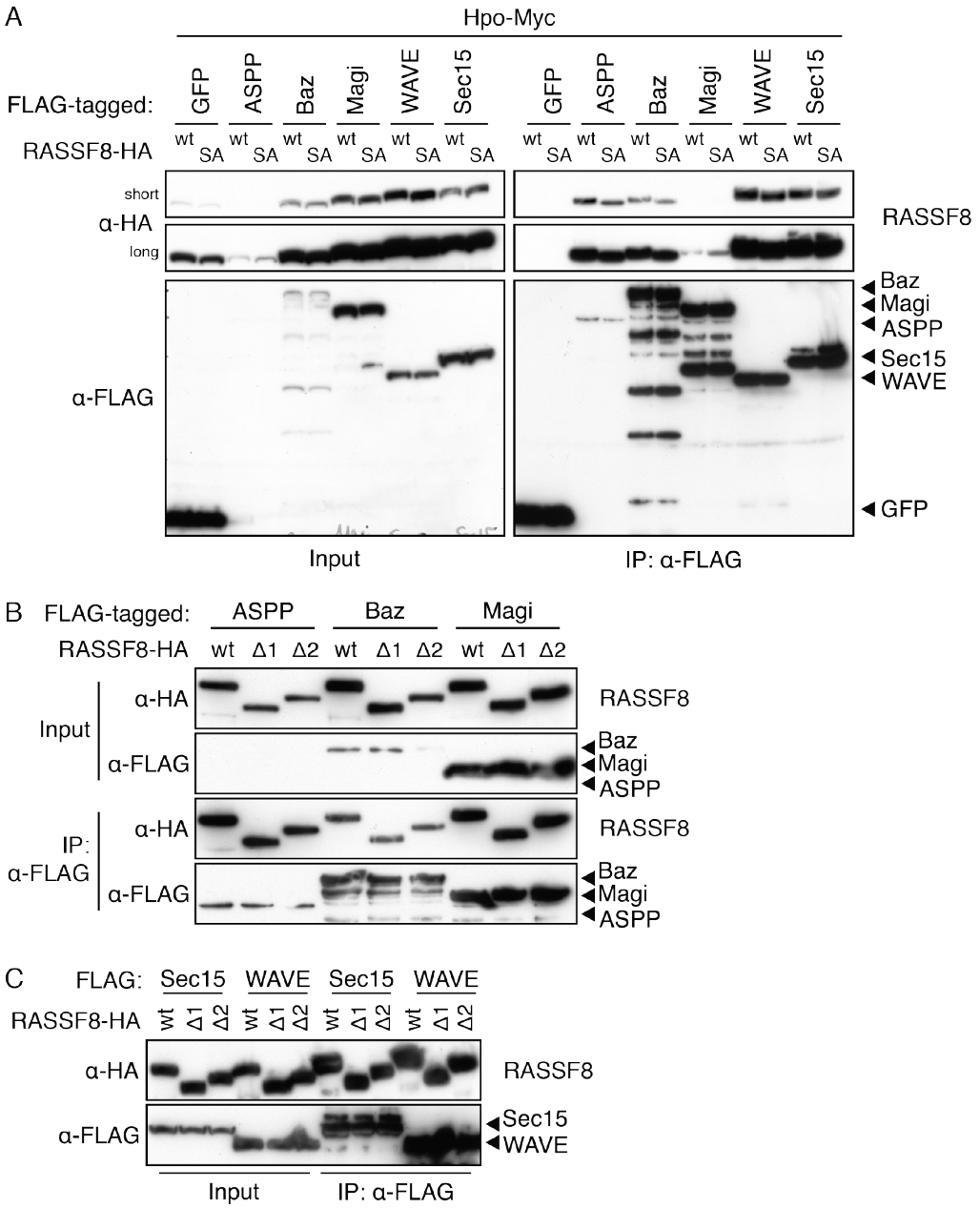

Figure 5.3.: RASSF8 phosphorylation by Wts does not inhibit binding to ASPP, Baz, Magi, WAVE or Sec15

Western blots of co-IP experiments using anti-FLAG antibody coupled beads from S2 cell lysates. Cells were transfected with the indicated constructs. Western blots were probed with indicated antibodies.

(A) All known interactors co-IP with RASSF8 and RASSF8 S209A equally well. Co-transfection with Hpo ensures that S209 of RASSF8 is phosphorylated.

(B, C) Deletions of RASSF8 where residues 135–213 (RASSF8-Δ1) and 180–220 (RASSF8-Δ2) were replaced with the two residues GS show no difference in binding to known RASSF8 interactors.

same binding surface or (3) the 14-3-3 dimer brings together two interaction partners with each 14-3-3 monomer binding to one partner. Given the numerous verified interactors of RASSF8, I decided the test if 14-3-3 binding would affect their association with RASSF8. Additional to ASPP and Baz (as mentioned in previous chapters), RASSF8 binds to the junctional scaffold Magi (see 5.3), the exocyst component Sec15 (Eunice Chan—unpublished observations) and the Arp2/3 (Actin-related protein)-activating protein WAVE (WASP family Verprolin-homologous protein) (Eunice Chan—unpublished observations). When Hpo was co-expressed with RASSF8 to phosphorylate S209, none of the interactors were displaced (Fig. 5.3A). All bound to RASSF8 to a similar extend as to RASSF8 S209A. This result shows that phosphorylation of S209 is insufficient to affect binding between RASSF8 and its known interactors.

Using an overexpression approach as in Fig. 5.3A, it is difficult to obtain a stoichiometric RASSF8/14-3-3 complex where all RASSF8 proteins are phosphorylated and bound to 14-3-3. Indeed, a relatively small proportion of overexpressed RASSF8 is associated with 14-3-3 in Fig. 5.2A, B. This is a confounding factor that may mask an effect of 14-3-3 binding of RASSF8 to its partners. Clearly, phosphorylation of RASSF8 alone was not sufficient to affect binding to its interactors, as most of RASSF8 is phosphorylated, indicated by the complete shift of RASSF8 upon Hpo expression (Fig. 4.1B). Thus, to test the importance of the 14-3-3 binding surface of RASSF8 in interacting with its known partners, I generated two RASSF8 deletion mutants that lacked the 14-3-3 binding site. In the two mutants, residues 135–213 (RASSF8-Δ1) and 180–220 (RASSF8-Δ2) were replaced with two residues, GS. However, both mutants could bind to ASPP, Baz, Magi (Fig. 5.3B), Sec15 and WAVE (Fig. 5.3C) to a similar degree as wild type RASSF8. These results shows that the know interactors do not rely on the region surrounding the 14-3-3 binding site to bind to RASSF8. Thus, it suggests that 14-3-3 binding to RASSF8 may not affect their ability to interact with RASSF8.

5.5. The in vivo function of RASSF8 phosphorylation remains unclear

Since RASSF8 phosphorylation and 14-3-3 binding did not seem to have an effect on association with its known interaction partners, I decided to test in vivo whether RASSF8 function is dependent on phosphorylation. Thus, I generated C-terminally GFP-tagged RASSF8 and RASSF8-SA for targeted insertion using the PhiC31 integrase system. The constructs were inserted into the genome on chromosome 3L. The two insertion lines (*ubi-RASSF8* and *ubi-RASSF8-SA*) were recombined with the $RASSF8^{6}$ null-allele.

Initially, I verified that both GFP-tagged forms of RASSF8 were expressed and localised to adherens junctions. In larval wing imaginal discs, RASSF8 and RASSF8-SA co-localised with E-cadherin at adherens junctions (Fig. 4A, B). The S209A mutation did not interfere with correct localisation. To test if S209 phosphorylation could mislocalise RASSF8, I expressed Wts in the posterior compartment of the wing using the *en-GAL4* driver. Wts expression caused a notable reduction in the size of the posterior compartment (Fig. 5.5A, A'), but had no influence on RASSF8 localisation (Fig. 5.5A, B).

Furthermore, both transgenes were able to rescue the rough eye phenotype (data not shown) of $RASSF8^{6}$ adult flies and restored wing roundness (Fig. 5.6A-E). Wing size was not significantly different between $RASSF8^{6}$ flies and the rescued flies (Fig. 5.6F). There was a small difference in wing roundness between *ubi-RASSF8* and *ubi-RASSF8-SA*, though given the modest size of this effect, its biological relevance is questionable (Fig. 5.6E). In summary, these results suggest that RASSF8 phosphorylation by Wts does not influence its junctional localisation and that S209 phosphorylation is dispensable for wing and eye morphogenesis. Although 14-3-3 can bind to RASSF8 upon phosphorylation in S2 cells, the biological significance of this interaction remains unclear.

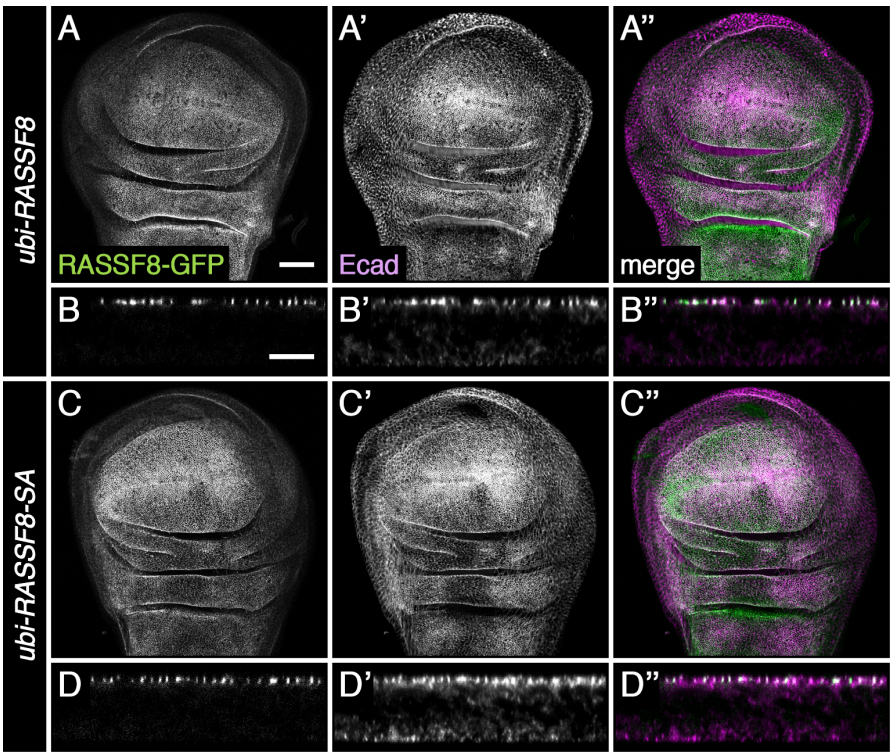

Figure 5.4.: GFP-tagged RASSF8 and RASSF8-SA are localised at adherens junctions

Confocal X-Y sections (A–A", C–C") and transverse sections (B–B", D–D") of third instar imaginal wing discs stained with anti-E-cadherin antibody. Scale bar represents 50 µm (A–A", C–C") and 10 µm (B–B", D–D"). GFP-tagged RASSF8 and RASSF8-SA co-localise with E-cadherin at adherens junctions.

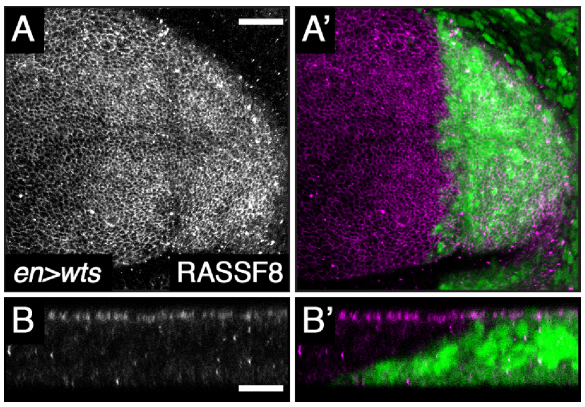

Figure 5.5.: RASSF8 localisation is unaffected by Wts expression

Confocal X-Y section (A, A') and transverse section (B, B') of a third instar wing imaginal disc stained with anti-RASSF8 antibody. Scale bar represents 20 µm (A, A') and 10 µm (B, B'). Expression of Wts with *en-GAL4* does not influence the localisation of RASSF8.

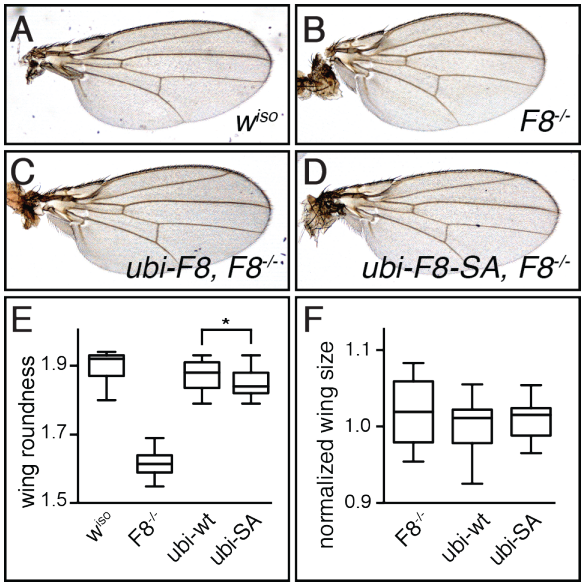

Figure 5.6.: RASSF8 and RASSF8-SA expression rescue the wing shape defect of *RASSF8* mutant

(A–D) Adult wings of the indicated genotypes. *RASSF8* null mutant wings (B) are rounder than wild type wings (A). RASSF8 (C) and RASSF8-SA (D) expression in *RASSF8* null backgrounds rescues the wing shape defect.

(E) Quantification of wing roundness (ratio of proximal-distal axis and anterior/posterior). An unpaired t-test showed that mean wing size in *ubi-RASSF8* and *ubi-RASSF8-SA* differ significantly from each other. * indicates $p<0.05$. At least 20 wings were counted per genotype.

(F) Quantification of wing sizes normalised to RASSF8 rescue wings. A one-way ANOVA test indicated that the differences among means were not significant ($p>0.05$).

5.5.1. Degradation of ASPP by the proteasome

With the identification of RASSF8 and Ccdc85 as bona fide components of the ASPP/PP1 complex, it is possible to search for common interactors identified in public datasets with all proteins of the holoenzyme. Genome-wide interactor screens are often plagued with high false positive rates. However, proteins that interact with more than one subunit of the ASPP/PP1 holoenzyme are more likely to be true positives. One such interactor is the RING domain containing E3 ubiquitin ligase Sina (Li et al. 1997). Three interactions discovered in yeast two-hybrid screens pointed at Sina as a regulator of ASPP/PP1: (1) The human Sina orthologue SIAH1 binds to ASPP2 (Wang et al. 2011a), (2) *Drosophila* Sina binds to RASSF8 (Giot et al. 2003) and the closely related *Drosophila* Sina homologue (SinaH) binds to Ccdc85 (Giot et al. 2003).

Human ASPP2 is ubiquitylated and degraded by the proteasome (Zhu et al. 2005). However the responsible E3 ligase was not known when I started examining ASPP/PP1 regulation. Thus, I decided to test if Sina can ubiquitylate and degrade the ASPP/PP1 complex. Jennifer Banerjee from our lab performed the in vivo Sina experiments shown below. During our work, another group confirmed that human ASPP2 could be ubiquitylated by SIAH2 and degraded by the proteasome (Kim et al. 2014).

5.5.2. Sina binds to ASPP and mediates its degradation

First, I tested if Sina could bind to ASPP. Co-transfecting ASPP with Sina in S2 cells lead to the degradation of ASPP (Fig. 5.7A). However, there was a detectable amount of ASPP binding to a Sina C87A (Fig. 5.7A), a mutant that is catalytically inactive (Hu and Fearon 1999) due to its impaired binding to one of the catalytic Zn^{2+}-cations. Furthermore, ASPP levels were comparable between co-expressing ASPP with GFP or Sina C87A, suggesting that Sina C87A was indeed inactive.

Additionally, when the proteasomal inhibitors MG132 and LLnL were added to S2 cells, ASPP degradation upon Sina co-expression was reduced (Fig. 5.7B). A

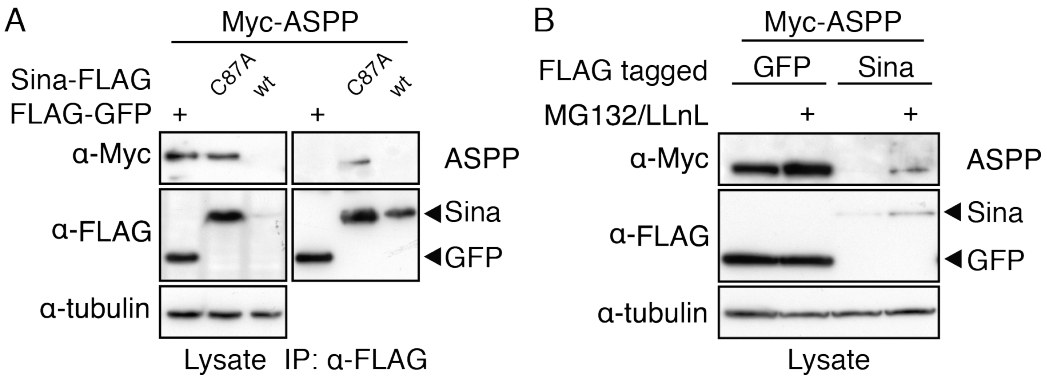

Figure 5.7.: Sina binds to ASPP and induces ASPP degradation

Western blots of co-IP experiments using anti-FLAG antibody coupled beads from S2 cell lysates (A), or just S2 cell lysates (B). Cells were transfected with the indicated constructs. Western blots were probed with indicated antibodies. (A) ASPP binds to the catalytically inactive Sina C87A mutant. Co-transfection of Sina and ASPP lead to the degradation of ASPP.

(B) Treatment of S2 cells with the proteasome inhibitors MG132 and LLnL stabilises ASPP and Sina. A smear indicates possible ubiquitylation of ASPP.

smear was observed above the ASPP band on Western blots, potentially indicating ubiquitylation. MG132/LLnL also stabilised ASPP but not GFP, without Sina co-transfection, suggesting that endogenous Sina (or another E3 ligase) may control ASPP levels in S2 cells. Together, the above results provide in vitro evidence that Sina can bind to ASPP to ubiquitylate and degrade ASPP via the proteasome.

5.5.3. Sina reduces ASPP and RASSF8 levels in vivo

To show that Sina can regulate ASPP levels in vivo, Jennifer Banerjee expressed Sina using the *ptc-GAL4* driver in larval wing imaginal discs. Using antibodies to detect endogenous ASPP and RASSF8, she could observe a reduction of ASPP (Fig. 5.8A–A') and RASSF8 levels (Fig. 5.8C–C'). The adherens junctions were not obviously affected. Levels of Arm, the *Drosophila* orthologue of the transcription factor β-catenin that is a core component of adherens junctions, were unchanged (Fig. 5.8A", C"). The reduction of ASPP and RASSF8 levels was dependent on the enzymatic function of Sina, since a Sina mutant that lacked the catalytic RING domain (Sina-ΔRING) had

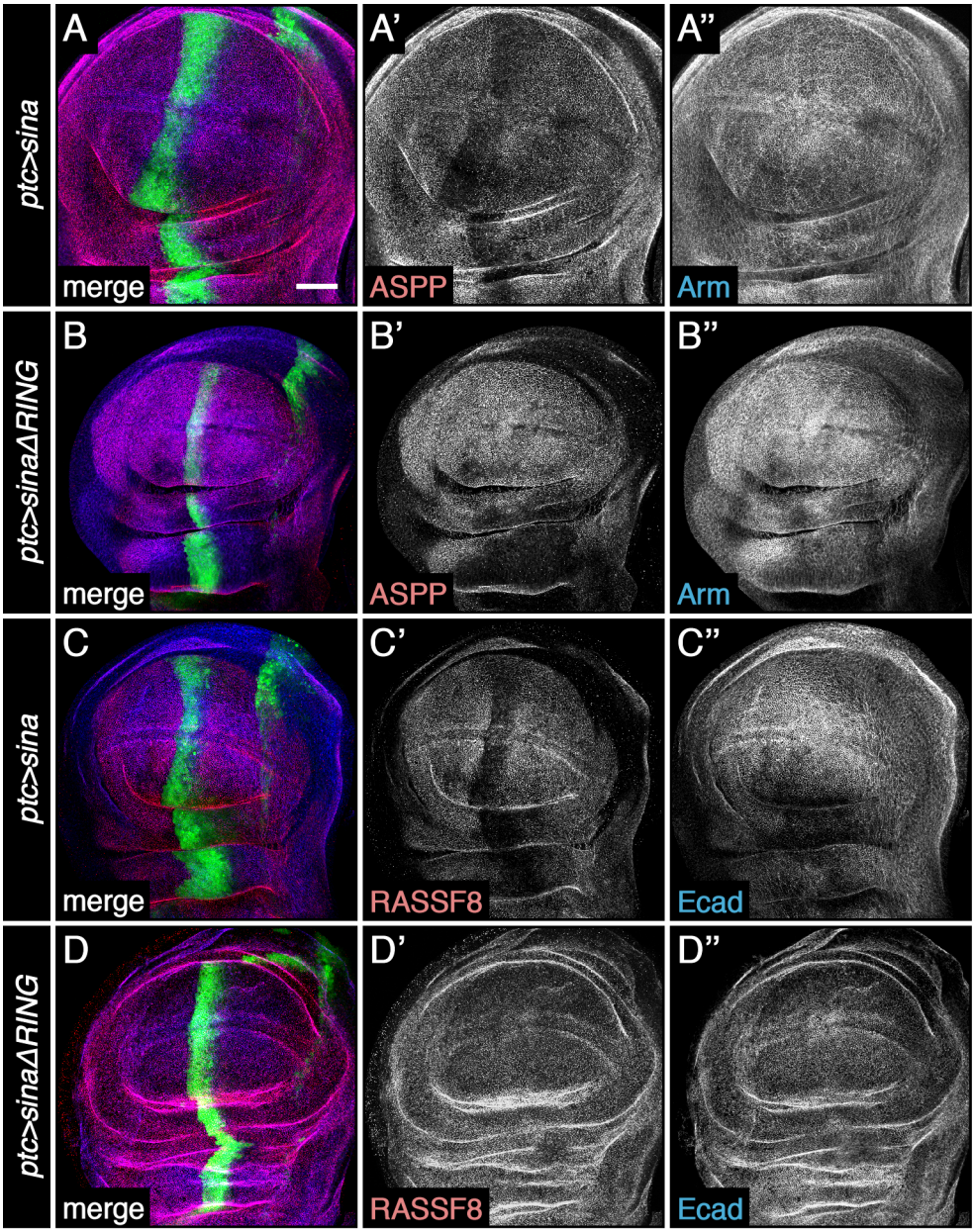

Figure 5.8.: Sina expression in vivo leads to the degradation of ASPP and RASSF8

Confocal X-Y sections of larval wing imaginal discs stained with indicated antibodies. Scale bar represents 50 µm.

Expression of Sina using *ptc-GAL4* driver causes the degradation of ASPP (A') but not arm (A"). Similarly, RASSF8 is degraded when Sina is expressed (D'), but E-cadherin is not (D"). Sina that lacks its catalytic RING domain can neither degrade ASPP (B') nor RASSF8 (D').

These experiments were performed by Jennifer Banerjee.

no effect (Fig. 5.8B, D). These results show that in vivo, Sina can regulate ASPP and RASSF8 levels.

5.6. Magi, a junctional scaffold protein binds to RASSF8

Another potential interactor of the ASPP/PP1 complex is Magi, a PDZ and WW domain containing junctional protein: (1) In a yeast two-hybrid screen for *Drosophila* RASSF8 interactors performed in the lab (Eunice Chan—unpublished observations), RASSF8 specifically bound to the two WW domains of Magi and (2) a human ASPP2 peptide containing its PPXY motif, a common WW domain binding motif, could bind to MAGI1 (Pirozzi et al. 1997). Although *Drosophila* Magi is largely uncharacterised (Beller et al. 2002), the human orthologues of Magi are known to associate with multiple junctional proteins through their PDZ and WW domains and are thought to be a junctional scaffolds (Shin et al. 2006). Through Magi, the ASPP/PP1 complex could be connected to other junctional proteins.

5.6.1. RASSF8 binds to Magi via its PPXY motif

First, I tested in co-IP experiments if *Drosophila* Magi could bind to RASSF8 or ASPP. Under these conditions only RASSF8, but not ASPP could co-IP with Magi (Fig. 5.9B). However, ASPP was able to bind to Magi via RASSF8, thereby forming a trimeric complex.

The yeast two-hybrid data suggested that RASSF8 could directly bind to the WW domain of Magi (Fig. 5.9A). Indeed, RASSF8 has a PPXY motif (Fig. 5.9A) that is conserved in orthologues of RASSF8 in other insects, but not in human RASSF7 or RASSF8. Using co-IP experiments, I showed that RASSF8 does indeed associate with Magi in S2 cells (Fig. 5.9B). When Y297 of the PPXY motif of RASSF8 was mutated to alanine, Magi could no longer bind to RASSF8 (Fig. 5.9C). Conversely, when both WW domains were deleted in Magi, RASSF8 could no longer bind to Magi (Fig. 5.9D). Mutating either of the conserved prolines of the WW domains of Magi

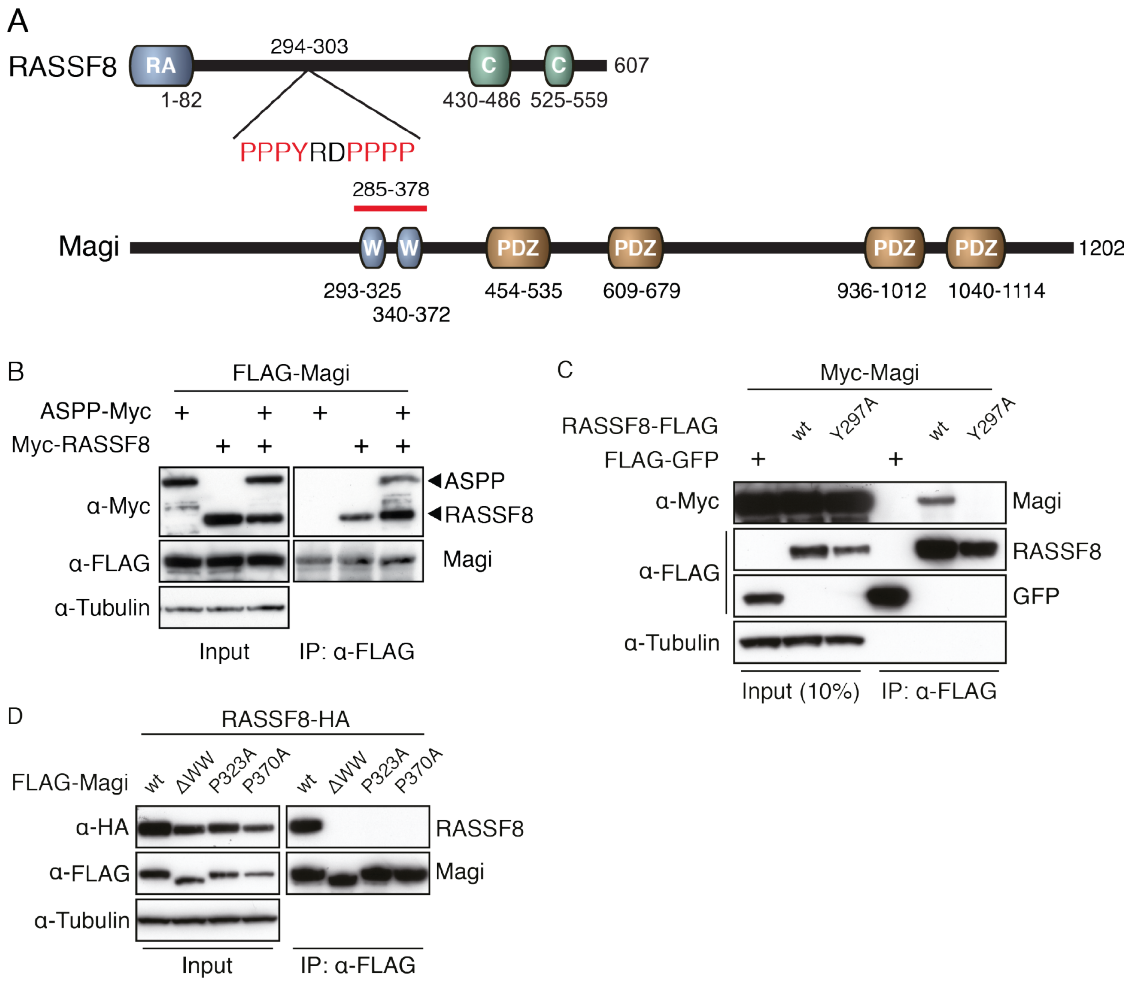

Figure 5.9.: Magi binds to the PPXY motif of RASSF8 via its WW domains

(A) Domain structure of RASSF8 showing its PPXY motif and domain structure of Magi. Magi has two WW domains and four PDZ domains. Domain annotation taken from Uniprot. Red line indicates minimal fragment that was able to bind to RASSF8 in a yeast two-hybrid assay.

(B–D) Western blots of co-IP experiments using anti-FLAG antibody coupled beads from S2 cell lysates. Cells were transfected with the indicated constructs. Western blots were probed with indicated antibodies.

(B) RASSF8 co-IPs with Magi and can bridge the interaction between ASPP and Magi.

(C) Magi co-IPs with RASSF8 but not with RASSF8 Y297A, mutant for the PPXY motif.

(D) Both WW domains of Magi are required for binding to RASSF8. When both WW domains are deleted (ΔWW) or a key proline of either WW domain is mutated, RASSF8 can no longer bind to Magi.

was also sufficient to abolish binding to RASSF8, suggesting that RASSF8 could bind to either WW domain. Together, these results show that Magi and RASSF8 can bind to each other via a PPXY motif/WW domain interaction.

Dr Alexandre Djiane, a collaborator, is investigating the in vivo relevance of the Magi-RASSF8 interaction. The result of this study will be presented elsewhere. It does appear that *Magi* mutants present many phenotypic similarities with *RASSF8* and *ASPP* mutants.

5.7. Identification of novel binding partners of ASPP

ASPP is at the centre of the ASPP/PP1 complex. Through its RVXF motif, it can directly bind to PP1. At the same time it might serve as a platform to extend the reach of PP1, or for the complex to be tethered to scaffolds and regulators (such as RASSF8 and Ccdc85). Unbiased AP-MS approaches in human HEK293 cells have proven successful in identifying novel interactors of the ASPP/PP1 complex. Ccdc85, a protein that had not been associated to ASPP or PP1 function before, was found to be associated (see Chapter 3). To identify novel and tissue-specific binding partners of ASPP in Drosophila, I pulled down HA-tagged ASPP from *Drosophila* adult heads and embryos and sent all bound protein to the LRI Protein Analysis and Proteomics facility for identification of the binding partners.

5.7.1. Several CNS specific potential interactors of ASPP were identified

The obtained data was analysed using ProHits. For the identified proteins from adult heads (Fig. 5.10A), proteins that were found in previous experiments using the same tissue but unrelated baits were excluded. For embryos, no similar experiments had been performed in the lab, thus all results are shown (Fig. 5.10B). Overall, data quality of the adult fly head experiment was higher. More peptides were identified for ASPP (the bait) and two known interactors, PP1α96A and RASSF8, were found. Furthermore, PP1α96A only co-purified with ASPP but not ASPP-FA. In the pull-

A

		Peptides identified			
Drosophila	Human ortholog	WT	FA	ctrl.	other
ASPP	ASPP1, ASPP2	129	215	0	0
CG43367	NBEAL1, NBEAL2	15	28	2	0
PIP82	-	8	5	0	0
PP1α96A	**PPP1CA, PPP1CC**	**8**	**0**	**0**	**0**
Liprin-α	PPFIA1	7	20	0	0
CG10362	PDZD8	6	4	1	0
CG2145	ENDOU	5	4	0	3
tgo	ARNT	4	3	0	0
moe	MSN	4	7	0	1
boss	GPRC5B	0	3	0	1
RASSF8*	**RASSF8**	**0**	**0**	**0**	**0**

B

		Peptides identified		
Drosophila	Human ortholog	WT	FA	ctrl.
ASPP	ASPP1, ASPP2	37	44	0
fne	ELAVL2, ELAVL4	9	12	0
ssx	ELAVL2, ELAVL4	5	7	0
yps	YBX1	4	3	0
pUf68	PUF60	4	0	0
Jabba	-	3	2	1
CG13900	SF3B3	0	4	0

Figure 5.10.: AP-MS experiment with ASPP as bait recovers PP1α96A and RASSF8

Table of potential ASPP interactors recovered in AP-MS experiments from *tub-GAL4>UAS-ASPP-HA*, *tub-GAL4>UAS-ASPP-FA-HA* or *tub-GAL4>* (ctrl.) adult head tissue (A) and embryos (B). HA-antibody-coupled beads were used for pull-down of ASPP. Identified proteins were filtered to exclude metabolic enzymes, heat-shock proteins, mitochondrial proteins, and extracellular proteins. All proteins with more than 3 identified peptides in ASPP or ASPP-FA pulldowns are shown.

(A) ProHits was used to filter out any proteins that were identified in previous experiments done in the lab with other, unrelated baits (other). Known interactors marked with bold letters. RASSF8 was not identified using ProHits but only using a different search engine (Scaffold). * RASSF8 was found with ASPP and ASPP-FA as bait. All other proteins were identified by ProHits and Scaffold.

down from embryos, only RNA binding proteins (Fne, Ssx, Yps, PUf68 and CG13900) and a lipid droplet associated protein, Jabba, were identified. All these proteins are likely to be very abundant in embryos, suggesting they might constitute artefacts. Analysis of further pull-downs from embryos using unrelated baits would reveal if they were specifically binding to ASPP.

In contrast, for adult heads, I could filter out all proteins that are highly abundant in eye and brain tissue by comparing the ASPP pull-downs with pull-downs of unrelated proteins, performed in the lab. While some of the remaining interactors are head or CNS-specific such as CG43367, PIP82, Liprin-α, CG10362 and Boss, other interactors are ubiquitously expressed (Celniker et al. 2009). In summary, I used AP-MS experiments in specific *Drosophila* tissues to identify potential novel interactors of ASPP. Identifying known binding partners such as PP1α96A and RASSF8 among novel interactors gave confidence in the quality of the data. Together, this suggests that it is possible to use the AP-MS approach to identify tissue specific scaffolds, regulators and substrates of the ASPP/PP1 complex.

5.8. A genetic modifier screen identified modulators of the ASPP rough eye phenotype

Additionally to the publicly available interactor databases, we have carried out interactome screens for ASPP and N-terminal RASSF family proteins ourselves (see above) and together with collaborators (Hauri et al. 2013). To test if any of these potential interactors could be regulators or substrates of the ASPP/PP1 complex, I decided to screen for modifiers of the ASPP/PP1-dependent rough eye phenotype using genomic deficiency lines (see Appendix B for full list of interactors screened). For non-*Drosophila* interactors, the closest orthologues were determined by BLAST searches. The fly crosses and subsequent screening were done by Nic Tapon.

All genomic deficiency lines were crossed to flies expressing *GMR-GAL4*-driven *ASPP RNAi* (Fig. 5.11B). The screened flies were heterozygous for the deficiency. Thus, any observed modification of the *ASPP RNAi* phenotype was caused by reduc-

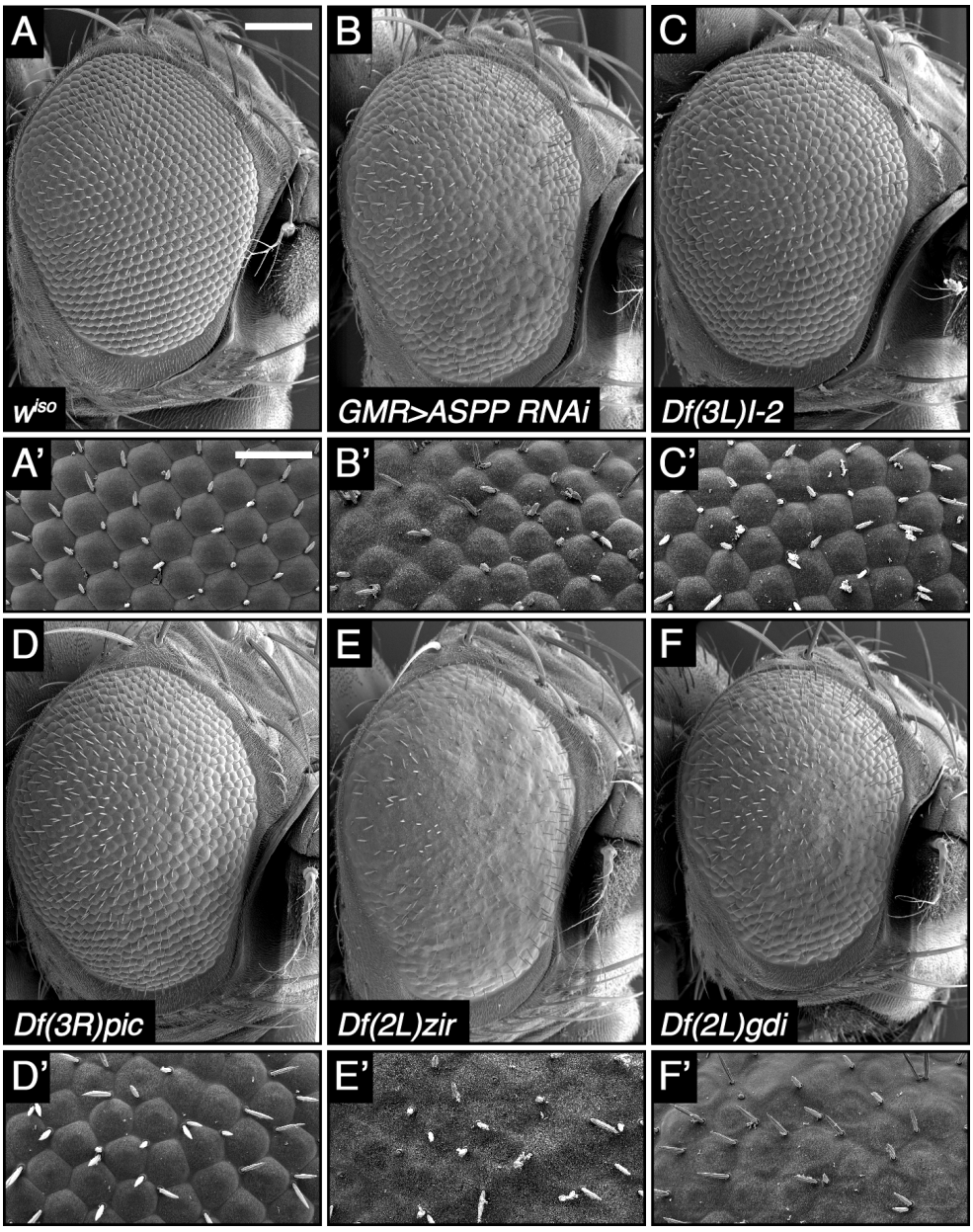

Figure 5.11.: A modifier screen identified potential regulators and targets of ASPP/PP1 in the eye

Scanning electron micrograph of adult fly eyes and close-up view of ommatidia. The regular patterning in wild type flies (A, A') is disrupted when ASPP is knocked down (B, B'). Heterozygous genomic deficiencies were screened for modification of the *ASPP RNAi* phenotype. Examples of suppressors (C–D') and enhancers (E–E') shown. All flies were kept at 29 °C for stronger expression of ASPP RNAi. Scale bar for (A–F) represents 100 µm, for (A'-F') 30 µm.

ing gene dosage by half. Out of 58 deficiency lines we recovered 16 enhancers and 2 suppressors (examples in Fig. 5.11C-F). The strongest suppressor was I-2, an inhibitor of PP1 (Fig. 5C, C'). This validated the rationale of the screen, as it suggested that the lack of ASPP/PP1 activity in *ASPP RNAi* flies could be rescued when general PP1 activity was increased. This result confirms that ASPP is a regulatory subunit of a PP1 complex and activates the catalytic function of PP1. In summary, the modifier screen was able to identify a subset of genes that might be regulators or effectors of the ASPP/PP1 complex, additional to being physical interactors.

As most deficiencies deleted more than one gene, it is possible that the observed effects were caused by the heterozygosity of neighbouring genes. Thus, further experiments with single gene mutants are required to confirm that the potential interactors were modifying the *ASPP RNAi* phenotype and not neighbouring genes. If any of these genetic interactions are confirmed, the corresponding candidates could be tested as potential modulators or targets of the ASPP/PP1 complex in further work.

5.9. Concluding remarks and future directions

In this chapter I have explored three interactors and potential regulators of RASSF8 and ASPP. The in vivo function of these interactors remains unclear and it is possible that they could only affect RASSF8 and ASPP independently from their PP1-function. Additionally, I complemented the AP-MS experiments from Matthias Gstaiger's lab in human HEK 293 cells with comparable experiments using *Drosophila* tissues. This allowed me to identify several potential novel ASPP interactors. Lastly, we tested if missing one genomic copy of all identified interactors could modify the ASPP dependent rough eye phenotype. Further experiments will be required to validate if the hits from the screen could modify ASPP/PP1 function or serve as substrates. In the next chapter I will summarise the findings of this thesis and discuss the function of the ASPP/PP1 in the context of previous work.

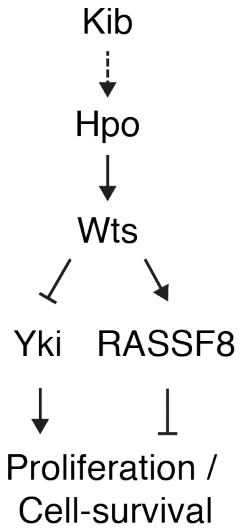

Figure 5.12.: Model of RASSF8 as an effector of Hippo signalling
Wts might activate the inhibitory function of RASSF8 in proliferation and cell survival by phosphorylation.

5.9.1. What is the role of RASSF8 S209 phosphorylation?

Although known RASSF8 interactors were not affected by RASSF8 S209 phosphorylation and the deletion of the region surrounding the 14-3-3 binding site (Fig. 5.3), it is possible that other as yet unidentified interactors might associate with RASSF8 differentially when 14-3-3 is bound. Since RASSF8 is a scaffold protein, two scenarios can be considered. 14-3-3 might increase or decrease the binding affinity of RASSF8 to its partners. Pull-down experiments with either RASSF8 or a RASSF8/14-3-3 complex as baits coupled to mass spectrometry for the identification of differential binding partners could be carried out. The main technical difficulty of such an approach is to generate a sufficient amount of a stoichiometric complex of RASSF8 with 14-3-3 to serve as bait. Alternatively, RASSF8 or a RASSF8 deletion mutant, lacking the 14-3-3 binding region could be used as baits. One potential confounding factor of this approach is that 14-3-3 might not act by directly competing with a RASSF8 partner for the same binding surface, but might instead induce a conformational change in RASSF8 that could alter its interaction profile. The former experiment has the benefit of being able to identify interactors that increase or decrease binding affinity

when 14-3-3 is bound to RASSF8, while the latter can only detect interactors that have a decreased affinity to the RASSF8/14-3-3 complex.

It is also possible that 14-3-3 might be bridging RASSF8 and Baz (Benton and St Johnston 2003), which is known to bind to 14-3-3, although this was not apparent using overexpressed proteins (Fig. 5.3A). Lastly, it is possible that phosphorylation can cause RASSF8 to localise to other regions within the cell. However, this might be context dependent and for example only happen when oncogenic Ras is present (for more detailed discussion, see 6.7).

Additional in vivo experiments could be carried out to determine the function of RASSF8/14-3-3 complexes. It is possible that Hippo signalling relies on RASSF8/14-3-3 as downstream effectors (Fig. 5.12). Based on *RASSF8* null mutant phenotypes, *RASSF8* seems to inhibit proliferation or promote apoptosis (Langton et al. 2009). Additionally, the strong genetic interaction between *RASSF8* and *kib* in regulating IOC numbers (Fig. 4.1) suggests that Wts might act on Yki and RASSF8/14-3-3 in parallel to inhibit proliferation and promote apoptosis. This model predicts that RASSF8, but not RASSF8-SA can rescue the synergistic increase of IOCs of *kib* and *RASSF8* null mutants. In this or similar sensitised backgrounds for activated or inhibited hippo signalling, the role of RASSF8 phosphorylation could be uncovered. Lastly, the rescue observed with *ubi-RASSF8-SA* (Fig. 5.6) might be due to the use of the *ubiquitin* promoter rather than the endogenous *RASSF8* promoter. Therefore, generating a knock-in allele of *RASSF8-SA* using genome editing techniques might reveal a phenotype for this mutation.

5.9.2. Where is the ASPP/PP1 complex regulated by Sina?

Expressing Sina in larval wing imaginal discs reduced the levels of ASPP and RASSF8 (Fig. 5.8). However, it is not known in which physiological contexts Sina could be required for ASPP and RASSF8 regulation. Sina has a well established role in specifying the neuronal cell fate in photoreceptors (Carthew and Rubin 1990) and sensory organ precursors (Pi et al. 2001) through the degradation of the transcriptional repressor Ttk (Li et al. 1997, Tang et al. 1997). However, Sina might have a much

broader role, as it seems to be ubiquitously expressed in most tissues and developmental stages (Celniker et al. 2009).

To address the question of tissue specificity, double mutants of *sina* and *ASPP* could be analysed and compared to *sina* mutants. In *sina* mutants, some phenotypes might be caused by an excess of ASPP. This would be rescued by removing *ASPP*. Furthermore, the regulation of ASPP levels by Sina might explain why ASPP overexpression does not give any strong phenotypes (Paul Langton and Julien Colombani—unpublished observations). To show that this is the case, ASPP could be expressed in a *sina* mutant, or mutant ASPP that cannot bind to Sina could be expressed. Together these experiments would shed light on the regulation of ASPP by proteasomal degradation in physiological contexts.

Chapter 6.

Discussion

In my thesis I have investigated constituents, substrates and regulators of the ASPP/PP1 complex. In the concluding discussion I will briefly summarise my main findings. To put my results into a broader perspective I will discuss the importance of junctional localisation of ASPP/PP1, its role in modulating junction formation, particularly through the dephosphorylation of Baz, and a potential evolutionary link between ASPP family proteins and RASSF8.

6.1. Summary of results

Although the interaction between ASPP2 (then known as p53BP2) and PP1 was discovered almost twenty years ago, (Helps et al. 1995), this connection has only received more attention relatively recently (Liu et al. 2011, Llanos et al. 2011, Skene-Arnold et al. 2013). Published research (see 1.3.5 and 1.4.3) established ASPP family proteins as PP1 interactors (Egloff 1997, Helps et al. 1995, Llanos et al. 2011, Skene-Arnold et al. 2013) and defined TAZ as a potential substrate of the ASPP/PP1 complex (Liu et al. 2011). However, many questions remained unanswered. In my thesis I addressed some of these questions, which can be grouped into three broad categories corresponding to my three result chapters: (1) Constituents of the ASPP/PP1 holoenzyme, (2) substrates and (3) regulation of ASPP/PP1.

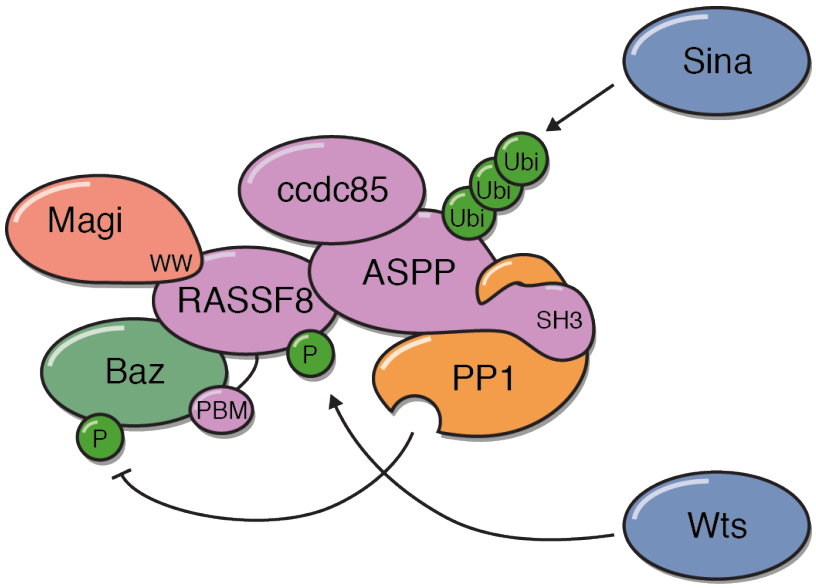

Figure 6.1.: Summary of findings

Drosophila ASPP interacts with PP1 via its RVXF motif and its SH3 domain. Additionally, the adaptor proteins RASSF8 and Ccdc85 can bind to the ASPP/PP1 core complex. RASSF8 is associated to two junctional components, Baz and Magi, via its PBM and PPXY motif respectively. Wts and Sina are potential regulatory inputs for the ASPP/PP1 complex that could phosphorylate RASSF8 and ubiquitylate ASPP.

In summary (Fig. 6.1), I have shown that, similar to human ASPP family proteins, *Drosophila* ASPP interacts with PP1 via its RVXF motif (see 3.1.1) and its SH3 domain (see 3.1.2). This interaction is important in vivo for ASPP function (see 3.2). I also showed that the adaptor proteins RASSF8 and Ccdc85 could bind to the ASPP/PP1 core complex (see 3.3). Out of two tested substrates for the ASPP/PP1 complex, I found evidence that Baz might be dephosphorylated by ASPP/PP1. Binding is not direct, but mediated by the PBM of RASSF8 (see 4.2). Another junctional protein, Magi, can also bind to RASSF8 (see 5.3.1). Lastly, I have identified Wts and Sina as potential regulatory inputs into the ASPP/PP1 complex that could phosphorylate RASSF8 (5.1) and ubiquitylate ASPP (see 5.2) respectively. The function of RASSF8 phosphorylation remains unknown, but ubiquitylation of ASPP leads to its degradation (see 5.2).

6.2. How is the ASPP/PP1 complex localised to junctions?

As discussed in 1.2, a key role for PP1 regulatory subunits is to localise the catalytic subunit to the correct subcellular localisation, in proximity to the substrate. The localisation of ASPP and RASSF8 at adherens junctions in *Drosophila* (Langton et al. 2009) and of ASPP2 at tight junctions in mice and various mammalian cells (Cong et al. 2010, Sottocornola et al. 2010) has been described before. However, it was unclear how these proteins are localised to junctions. In this thesis, I described the interactions of RASSF8 with two known junctional proteins, Baz (see 4.2) and Magi (see 5.3) that might explain the anchoring of the ASPP/PP1 complex at the apical junctions (adherens junctions in *Drosophila* and tight junctions in mammals).

The binding of human RASSF8 to PAR3 was mediated by its conserved PBM, since only isoform A, which contains the PBM could pull-down PAR3 (see 4.2.2). It is likely that this binding is conserved in Drosophila, as *Drosophila* RASSF8 has a PBM as well (see 4.2.2). As Baz/PAR3 directly associates with the plasma membrane by binding to phosphoinositide lipids (Horikoshi et al. 2011, Krahn et al. 2010, Wu et al. 2007a), RASSF8 could be anchored via Baz/PAR3. It is possible that RASSF8 becomes restricted to the apical junction together with Baz/PAR3, which is specifically localised by multiple phosphorylation reactions (see 1.5.3). ASPP, PP1 and Ccdc85 could be subsequently localised to the apical junction via RASSF8. This would predict that not only ASPP (Langton et al. 2009), but also PP1 (or at least a pool of PP1 that is part of the ASPP/PP1 complex) and Ccdc85 should be mislocalised when RASSF8 is lost. An attractive model is that Baz/PAR3 not only recruits the ASPP/PP1 complex to the apical junction, but ASPP/PP1 in turn could stabilise Baz.

Whether the binding of RASSF8 to Magi could provide a membrane anchor for RASSF8 and the ASPP/PP1 complex in *Drosophila* is less clear. Although the mammalian MAGI1 isoform is associated with the plasma membrane at tight junctions via the adhesion molecule JAM4 (Hirabayashi et al. 2003), this is unlikely to be the

case in Drosophila, as JAM family adhesion molecules are not conserved. Conversely, RASSF8 is unlikely to be the only membrane anchor for Magi (via Baz) in Drosophila, as loss of RASSF8 has no effect on Magi localisation (Alexandre Djiane—unpublished observations). Further work on *Drosophila* Magi might reveal interactors that can directly bind to the plasma membrane. The situation in mammals is probably different from Drosophila, as the PPXY motif of RASSF8, which is necessary for the interaction with Magi, is not conserved. It is possible that the ASPP/PP1 complex associates with mammalian MAGI isoforms via ASPP1 or ASPP2 instead of RASSF8 (see below).

By binding to other junctional scaffolds via their WW and PDZ domains, Baz and Magi could incorporate RASSF8 and possibly the ASPP/PP1 complex in a bigger junctional scaffold protein network. The resulting spatial proximity of PP1 with other junctional proteins is equivalent to an increased junctional concentration. The proximity could be sufficient to promote the dephosphorylation of the junctional proteins nearby. This hypothesis could be tested. For instance, *ASPP-FA* rescue mutants would then be expected to have hyperphosphorylated junctional proteins, which could be revealed in whole fly phospho-proteome analyses (as mentioned in 4.3.2). In the next section I will discuss the potential influence of ASPP/PP1 on one particular junctional protein, Baz.

6.3. What is the role of Baz dephosphorylation?

It is not yet clear, if the Baz mislocalisation in *ASPP* null mutant mitotic clones is entirely due to reduced Baz dephosphorylation by PP1 function. This could be tested in several ways (see 4.3.3). However, even if the mislocalisation in this specific experiment was independent of dephosphorylation, it is still very likely that the ASPP/PP1 complex can dephosphorylate and regulate Baz/PAR3 in vivo, given that the ASPP can bind to Baz via RASSF8 (see 4.2.2) and PP1 can dephosphorylate Baz/PAR3 in vitro (see 4.2.6 and Traweger et al. 2008).

Which sites could be dephosphorylated and what function would the dephosphorylation have? I will discuss four sets of possible dephosphorylation sites: (1) the aPKC S980 site, (2) the Par1 S151 and S1085 sites, (3) potential Rho-kinase phosphorylation sites and (4) T720, which was uncovered in the second in vitro kinase assay. These sites are all conserved between Baz and PAR3. The focus on conserved phosphorylation sites is sensible since the Baz mislocalisation in *ASPP* mutant mitotic clones (see 4.2.1) is reminiscent of the reduction of PAR3 levels at tight junctions, when ASPP2 is lost (Cong et al. 2010, Sottocornola et al. 2010). If Baz/PAR3 mislocalisation was dependent on PP1 function in both cases, the dephosphorylation sites involved are likely to be conserved.

Dephospohrylation of S980

The most obvious residue that could be dephosphorylated by ASPP/PP1 is S980, as S980 phosphorylation was strongly reduced by PP1 in vitro (see 4.2.6). However, dephosphorylation of S980 by ASPP/PP1 does not fit with the observation that Baz is mislocalised in *ASPP* mutant tissue. Instead of being mislocalised, S980 hyperphosphorylated Baz should rather be even more concentrated at adherens junctions, as S980 phosphorylation promotes the dissociation of Baz from aPKC, thus removing Baz from the sub-apical region (see 1.5.3). In follicle cells (Morais-de Sá et al. 2010) and in photoreceptor cells (Walther and Pichaud 2010), S980E phospho-mimicking mutant Baz localisation is indistinguishable from that of wild type Baz. Furthermore, the only tissue, where expressing the phospho-mimicking mutant causes a phenotype is in the oocyte, where Gurken protein, that is normally found in the anterior dorsal corner, is mislocalised (Morais-de Sá et al. 2010). This subsequently leads to embryos where the dorsal appendages are defective. If loss of *ASPP* caused Baz S980 hyperphosphorylation, this should lead to similar defects of the dorsal appendages of *ASPP* null mutant embryos. However, during the collection of embryos for ASPP AP-MS experiments (see 5.4), I did not detect any such defects (data not shown). Thus, although ASPP/PP1 might dephosphorylate S980 in some situations, other

residues would have to be dephosphorylated as well to explain the Baz mislocalisation phenotype.

Dephosphorylation of S151 and S1085

The second category of candidate residues for dephosphorylation by ASPP/PP1 are the Par1 phosphorylation sites, S151 and S1085. In vitro PP1 was unable to dephosphorylate either S151 and S1085 (see 4.2.6) in contrast to similar experiments using mammalian PP1 and PAR3 (Traweger et al. 2008). However, if ASPP/PP1 dephosphorylated S151 or S1085, this could explain the Baz mislocalisation, as phosphorylation of as S151 and S1085 phosphorylation leads to the removal of Baz from membrane (see 1.5.3). Thus, the ASPP/PP1 complex could stabilise Baz at the adherens junctions by dephosphorylating S151 or S1085. Since PP1 could not dephosphorylate S151 and S1085 in vitro, this hypothesis could be tested in vivo. Baz junctional localisation could for instance be analysed in *ASPP,par1* double mutants, to test if loss of *par1* compensates for *ASPP* loss-of-function.

Dephosphorylation of Rho-kinase phosphorylation sites

The third set of potential phosphorylation sites that could be targeted by ASPP/PP1 is the set of Rho-kinase phosphorylation sites at the C-terminus of Baz (Matos Simões et al. 2010). Although the exact site or sites were not identified, truncation analyses revealed that Rho-kinase is likely to phosphorylate residues close to the basic residues that are required to bind to negatively charged phosphatidylinositides. The accumulation of negative charges upon phosphorylation could counterbalance the basic residues in the phosphoinositide binding patch, thereby causing loss of membrane association. Since membrane attachment of Baz is observed in S2 cells (see 4.2.5) and can be influenced by Rho-kinase expression (Matos Simões et al. 2010), it should be possible to identify potential ASPP/PP1 dephosphorylation sites that are Rho-kinase target sites by expressing phospho-mimicking Baz mutants in S2 cells. The key residues that are important for the association of PAR3 with phosphatidylinositides are K1013 and K1014 (Horikoshi et al. 2011), which are conserved in *Drosophila* (K1173 and

K1174). The closest phosphorylatable serine/threonine residues of Baz are S1169, S1170 and S1176. Interestingly, Baz S1176D was not localised to the plasma membrane, but rather in intracellular vesicular structures in S2 cells (see 4.2.5). Whether this mislocalisation has anything to do with phosphatidylinositol binding remains to be determined. A complication is that none of these three residues is conserved in PAR3. However, this may not be completely surprising, as Rho-kinase phosphorylation of T833 of PAR3, which is not close to its phosphatidylinositol binding site, disrupts aPKC binding instead (Nakayama et al. 2008). Thus, if S1176 dephosphorylation were important for the attachment of Baz to the plasma membrane, this would not explain why ASPP2 is important for the localisation of PAR3 at tight junctions.

Dephosphorylation of other phosphorylation sites

Lastly, of the sites that were uncovered in the dephosphorylation assays (see 4.2.6), the best candidate residue is T720. The dephosphorylation of T720 was consistent between the label-free quantification and the dimethyl-labelled MS experiments. T720 seemed to be more efficiently dephosphorylated when ASPP, RASSF8 and Ccdc85 were present. T720 is conserved in PAR3 (T668). To test if this site is hyperphosphorylated when ASPP is lost, a phospho-specific antibody could be generated and tested in *ASPP* mutant mitotic clones. In addition, T720E phospho-mimicking Baz would be expected to be mislocalised in S2 cells and in vivo. Equivalent experiments could be performed in mammalian cells using a T668E mutant form of PAR3. If none of the above-mentioned sites turned out to be dephosphorylated by ASPP/PP1 in vivo, the other sites that were dephosphorylated in vitro could be tested.

6.4. How does the activation of Csk by ASPP fit with its role as PP1 regulatory subunit?

Our lab has reported that ASPP and RASSF8 can stabilise adherens junctions through activating Csk, which restricts Src activity at the adherens junctions (Langton et al. 2007 2009). Supernumerary IOCs in *ASPP* and *RASSF8* mutants, as well

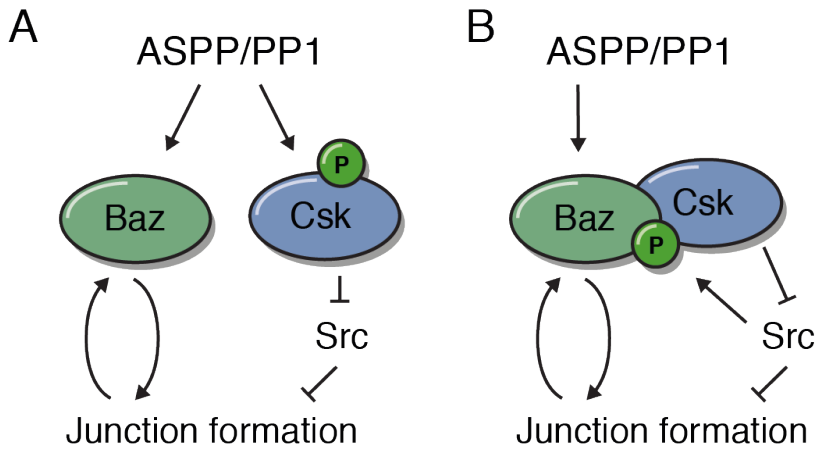

Figure 6.2.: Baz could recruit Csk to adherens junctions

(A) ASPP/PP1 could act independently on Baz and Csk. This could explain the genetic interaction between *ASPP* and *Csk* (Langton et al. 2007), as well as the mislocalisation of Baz in *ASPP* mutant tissue. Downstream, Baz and Csk are both involved in the formation and maintenance of adherens junctions.

(B) Alternatively, ASPP/PP1 could only act on Baz, which in turn could recruit Csk, similar to PAR3 (Wang et al. 2006). The binding site of Csk requires a phosphorylation by Src in the case of PAR3 (Wang et al. 2006). This model is simpler as the first one, as it involves Baz as a single ASPP/PP1 substrate for junctional remodelling.

as the defects in inter-IOC contacts during retinal morphogenesis had been attributed to the ability of ASPP to activate Csk (Langton et al. 2007 2009). Indeed, in mammalian cells, Src has been reported to induce cadherin internalisation, both by direct phosphorylatio, as in the case of VE-Cadherin (Gong et al. 2014), and via ubiquitylation by the Src-activated ligase Hakai in the case of E-cadherin (Fujita et al. 2002). However, in my thesis I suggested that ASPP and RASSF8 were required for retinal morphogenesis as part of an ASPP/PP1 complex that might dephosphorylate Baz. Are these two models compatible with each other?

The simplest way to encompass both models is to hypothesise that ASPP/PP1 can act on Csk and Baz in parallel (Fig. 6.2A). ASPP/PP1 could activate Csk and stabilise Baz by phosphorylation. Csk and Baz both then contribute to proper junction formation. In this model, ASPP/PP1 could activate Csk by dephosphorylation, as loss of PP1 binding in ASPP leads to Csk dependent wing notching (see 3.2.3). ASPP/PP1 is unlikely to dephosphorylate the only known serine/threonine phospho-

rylation site (S364 in human CSK), as its phosphorylation activates CSK (Vang et al. 2001). Thus other phosphorylation sites may be involved that could be identified by in vitro dephosphorylation assays with Csk as substrate.

Alternatively, Csk activation could be dependent on Baz stabilisation (Fig. 6.2B). For PAR3 it had been shown that EGF stimulation leads to the phosphorylation of Y1127 of PAR3 via Src and another Src family kinase, Yes (Wang et al. 2006). The phosphorylation creates a binding site for the SH2 domain of CSK (Songyang et al. 1994). Thus, PAR3 might recruit CSK to tight junctions, where it inhibits Src activity (Wang et al. 2006). A similar mechanism could act in *Drosophila*. ASPP would stabilise Baz at adherens junctions by dephosphorylation and Src would phosphorylate Baz to create a Csk binding site. Csk would then bind to Baz and in turn inhibit Src, thus stabilising adherens junctions. In this model, the Csk-dependent wing notching in PP1 binding deficient ASPP rescue flies (see 3.2.3) could be due to impaired Baz localisation, rather than Csk hyperphosphorylation, elegantly reducing the number of dephosphorylation events required to explain the experimental observations. However, Y1127 of PAR3 is not directly conserved in Baz, although Y1284 of Baz fits an SH2 domain-binding consensus sequence (Songyang et al. 1994) reasonably well. A few key experiments could be carried out to provide evidence for this model. Most importantly, a Src phosphorylation site that promotes the binding of Csk would need to be identified in Baz. Furthermore, Csk should co-localise with ASPP and Baz and this localisation should be lost in the absence of Baz.

6.5. Does *Drosophila* ASPP have a nuclear function?

Although our lab has never observed *Drosophila* ASPP or RASSF8 localised anywhere else than at adherens junctions, it is possible that they could have a nuclear role similar to human ASPP family proteins (see 1.3.2) and RASSF7 (see 1.3.8). Junctional tethering may be conditional on cell type or proliferation status. The Ran-GDP dependent nuclear localisation signal of ASPP1/2 (Lu et al. 2014) is conserved in *Drosophila* ASPP. Thus, ASPP should be able to translocate into the nucleus. Whether

Drosophila ASPP is able to promote p53 dependent transcription is doubtful, as key residues that mediate binding of human ASPP1/2 to p53 are not conserved in *Drosophila* ASPP (Langton et al. 2007). However, ASPP could have p53-independent nuclear functions. It remains unclear, if ASPP, once in the nucleus, could bind to PP1. It is possible that the nuclear function of ASPP is completely distinct from its junctional role as PP1 regulatory subunit and it might for example serve as a transcriptional co-factor (Aylon et al. 2010, Samuels-Lev et al. 2001). To check if ASPP or RASSF8 can translocate to the nuclear in vivo, the transgenic *ubi-ASPP* and *ubi-RASSF8* flies that I generated could be used to screen for nuclear localisation in different tissues.

6.6. How is ASPP/PP1 function regulated?

Two modes of regulation could prevent ASPP from binding to PP1. Firstly, the C-terminal PxxPxR motif of PP1 can be phosphorylated by Cdk2 in a cell-cycle dependent manner during early and mid-mitosis (Dohadwala et al. 1994, Kwon et al. 1997). Although this phosphorylation has been described to auto-inhibit PP1 (Dohadwala et al. 1994), it could also prevent ASPP from binding to PP1, as a phosphomimicking mutation of the PxxPxR motif inhibits PP1 from binding to ASPP family proteins (Skene-Arnold et al. 2013). Thus, during mitosis, the phosphorylation could prevent ASPP from binding to PP1. Secondly, *Drosophila* ASPP has a serine residue within its RVXF motif that could be phosphorylated (see Fig. 3.1). Introduction of a negative charge within the RVXF motif can disrupt binding to PP1 (Egloff 1997).

6.7. What are the overlapping and non-overlapping roles of ASPP, RASSF8 and Ccdc85?

Even though *ASPP*, *RASSF8*, *ccdc85* and *kib* mutants all cause rough eye phenotypes (see 3.2.2, 3.3.5 and 4.1.1), there are subtle differences. The number of IOCs is highest in *kib* mutant retinal mitotic clones with 22.0±2.4 (Fig. 4.1D). However, despite this

large number of IOCs, all extra IOCs are neatly arranged in single layers (Fig. 4.1B and Genevet et al. 2010, Yu et al. 2010). This suggests that during remodelling (see 1.1.3), only apoptosis is impaired, while cell-cell adhesion is not affected. This is in stark contrast to *RASSF8* mutant retinas, where the total number of IOCs (17.6±2.7) is lower than in *kib* mutant mitotic clones. Despite fewer extra IOCs, multi-layering can often be observed (Fig. 4.1A and Langton et al. 2009). The multi-layering is consistent with the idea that loss of *RASSF8* influences inter-IOC contacts. Thus, despite the strong genetic interaction between *RASSF8* and *kib* (see 4.1.1), they might act on distinct processes.

Qualitatively and quantitatively, the *ASPP* and *ccdc85* mutant retinas also differ from *RASSF8* mutant retinas (also see 3.3.5 for additional discussion). The number of extra IOCs in *ASPP* and *ccdc85* mutant retinas is lower than in RASSF8 mutant retinas (15.3±1.6 and 14.2±1.2 respectively). Together with the observation that *RASSF8* null mutant flies have a round wing phenotype (Langton et al. 2009) that is not observed in *ASPP* (Langton et al. 2007) or *ccdc85* null mutant flies (data not shown), this suggests that Ccdc85 might closely functions together with ASPP, while RASSF8 might have additional, ASPP-independent functions. Analysing expression patterns of ASPP, RASSF8 and Ccdc85 in different tissues and developmental stages might be helpful in determining in which contexts they are all required and where they carry out independent functions.

6.8. Have ASPP family proteins and RASSF8 undergone convergent evolution?

The phosphorylation of *Drosophila* RASSF8 by Wts (see 5.1.1) and the binding to Magi (see 5.3.1) are probably not conserved in human RASSF8 (or any other human N-terminal RASSF family proteins), as the required sequence motifs are absent. However, human ASPP1 can be phosphorylated by LATS1/2 (Aylon et al. 2010) and an ASPP2 peptide that contains its PPXY motif can bind to human MAGI1 (Pirozzi et al. 1997), suggesting that in humans, ASPP1/2 might carry out

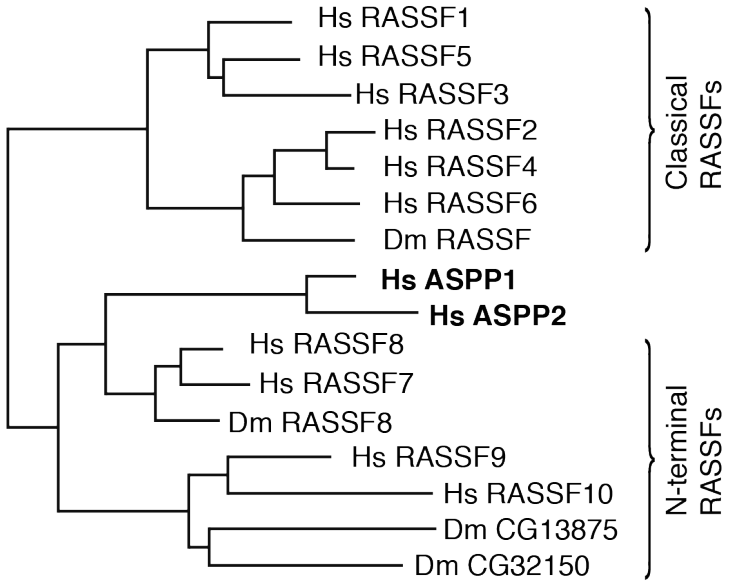

Figure 6.3.: The RA-like domain of ASPP1/2 is more closely related to the RASSF8 RA domain than to other RA domains

A distance tree based on a multiple alignment between the RA and RA-like domains of human ASPP1/2 and classical as well as N-terminal RASSF family proteins suggests that the RA-like domain of ASPP1/2 are closely related to the RASSF7/8 group of proteins.

some of the functions of *Drosophila* RASSF8. Given the conserved binding between ASPP and RASSF8, it is possible that Magi association and phosphorylation by an activated Hippo pathway kinase cascade evolved separately in *Drosophila* RASSF8 and human ASPP1/2. A direct evolutionary link between the motifs in *Drosophila* RASSF8 and human ASPP1/2 is not obvious, as the sequences surrounding the motifs do not bear any resemblance to each other.

A third feature that human ASPP1/2 shares with N-terminal RASSF8 family proteins is its RA-like domain. Distance-based methods suggest that the RA-like domains of human ASPP1/2 (see 1.3.1) are very closely related to the RA domains of N-terminal RASSF family (Fig. 6.3). Furthermore, using the RA-like domain of ASPP1/2 in a BLAST search for all *Drosophila* proteins returns the RA domain of RASSF8 as the closest match (data not shown). Similarly, searching for human proteins with the RA-like domain of ASPP1/2 returns the RA domain of human RASSF8

as the closest match following ASPP1/2 (data not shown). The similarly between the RA-like domain of ASPP1/2 and RASSF8 suggests that their function might be conserved. Thus, similar to ASPP1/2 /(Wang et al. 2013a, Wang et al. 2013b), *Drosophila* RASSF8 could also bind to oncogenic Ras and phosphorylation of *Drosophila* RASSF8 could be required for its nuclear translocation when oncogenic Ras is present—comparable to ASPP1 (Aylon et al. 2010). Taken together, since ASPP family proteins and RASSF8 share these three motifs/domains with each other, it is possible that convergent evolution equipped them with a similar set of functionality. Analysing ASPP and N-terminal RASSF family proteins in other organisms could test the hypothesis of convergent evolution.

Appendix A.

Baz dephosphorylation sites

Peptide abundances were quantified with Skyline. The localisation of the phosphorylation was determined in Perseus. All phospho-peptides with reduced abundance when dephosphorylated either with PP1 alone, or when ASPP, RASSF8 and Ccdc85 were also present (see 4.2.6) were filtered using a PEP-Score criterion (see Material and Methods for details).

The ratio of the abundance of phospho-peptide between GFP treatment and dephosphorylation with PP1 only, as well as the ratio between PP1 dephosphorylation only and the dephosphorylation with the whole complex were calculated. A value above 1 suggests that the indicated residue was dephosphorylated by PP1 alone or that addition of ASPP, RASSF8 and Ccdc85 further increased dephosphorylation. All measurements were done in three technical replicates. Unpaired t-tests were carried out for all ratios. The given p-values have no correction for multiple testing.

The top hit, T720 is highlighted in bold. It was consistently dephosphorylated by PP1 alone and more strongly when ASPP, RASSF8 and Ccdc85 were present. Furthermore, T720 is conserved in PAR3.

S151 and S1085 were also listed in the tables below in italics as examples for phosphorylated residues that were unchanged when detected by antibody staining on Western blots (Fig. 3.14A).

Residue	Change GFP/PP1 [fold]	P-value	Change PP1/Complex [fold]	P-value	Conserved
180	0.3	0.0009	2.5	0.0020	no
429	9.9	0.0009	5.3	0.1239	no
436	357.4	0.0009	3.4	0.2428	yes
720	**1.4**	**0.0009**	**5.6**	**0.0038**	**yes**
980	31.1	0.0007	0.5	0.2958	yes
1040	1.7	0.0009	1.9	0.0036	no
1126	1.5	0.0057	2.0	0.0033	no
1136	17.1	0.0065	6.2	0.0268	no
1401	8.7	0.0004	22.0	0.0005	no
1410	331.3	< 0.0001	1.3	0.4267	no
151	*0.6*	*0.0004*	*1.7*	*0.0002*	*yes*
1085	*0.6*	*0.0589*	*0.9*	*0.4930*	*yes*

Figure A.1.: Identified residues that were dephosphorylated in vitro—LFQ

Residue	Change GFP/PP1 [fold]	P-value	Change PP1/Complex [fold]	P-value	Conserved
169/180	0.5	0.0008	1.6	0.2315	no
720	**7.6**	**0.0147**	**1.6**	**0.1038**	**yes**
980	23.1	0.0007	4.5	0.0004	yes
1049	5.4	0.0060	3.7	< 0.0001	yes
1126	3.1	0.0001	2.0	0.0007	no
1410	9.6	< 0.0001	N/A	N/A	no
151	*0.9*	*0.7620*	*5.8*	*0.0003*	*yes*

Figure A.2.: Identified residues that were dephosphorylated in vitro—dimethyl-labelled quantification

Appendix B.

Modifier screen

All genomic deficiency lines that were screened (see 5.5 for details) are listed below. The gene names of human orthologues are given if orthologues are existent. The source of the protein-protein interaction data is indicated, as well as the binding partner. Enhancers of the *ASPP RNAi* phenotype (Fig. 5.11B, B') have a positive number in the result column, while suppressors have a negative number. The value of this number represents the strength of enhancement/suppression observed. E.g., removing one copy of *zir* (3) strongly enhanced the phenotype (see Fig. 5.11E, E'), while removing one copy of *gdi* (2) moderately enhanced the phenotype (see Fig. 5.11F, F').

Gene Name	Human Ortholog	Screened deficiency	Source	Interaction	Result
Zir	DOCK7	Df(2L)Exel6001	Gstaiger	F10	3
Cora	EPB41	Df(2R)Exel6069			3
Gdi	GDIB	Df(2L)Exel6022	Gstaiger	F10	2
blow	-	Df(2R)Exel6053	Public	dCcdc85	2
blos1	BLOC1S1	Df(2R)Exel6284	Public	dCcdc85	2
CG34383	PLEKHA5	Df(3R)Exel6170	LRI Y2H	dF8	2
sec15	EXOC6/6B	Df(3R)BSC508	LRI Y2H	dF8	2
Csk	CSK	Df(3R)Exel6276		activated by dASPP	2
Magi	MAGI1-4	Df(2R)Exel6072	Thesis	dF8	2
AnxB10	ANXA1	Df(1)BSC648	Gstaiger	ASPP2/F9	1
Syt1	SYT17	Df(2L)Exel6277	Public	CCDC85	1

Figure B.1.: Results of modifier screen

(Continues on following page)

Gene Name	Human Ortholog	Screened deficiency	Source	Interaction	Result
esn	PRICKLE1/2	Df(2R)Exel6283	Public	dCcdc85	1
yki	YAP1	Df(2R)BSC356	Public	CCDC85	1
CG4572	IPP2	Df(3R)BSC636	Gstaiger	ASPP2/F7/YAP	1
Btk	BTK	Df(2L)BSC200		SRC target	1
Puc	MKP5	Df(3R)Exel6263		inhibiting JNK	1
l-2	GGCT	Df(3L)BSC394	Gstaiger	ASPP2/PP1	-2
pic	DDB1	Df(3R)Exel6167	Gstaiger	F9/F10	-2
wts	LATS2	Df(3R)Exel8194	Public	CCDC85	0
faf	USP9X	Df(3R)ED6361	Gstaiger	F9/F10	0
cpb	CAPZB	Df(2L)BSC521	LRI	dASPP	0
Liprin-alpha	PPFIA1-4	Df(2L)Exel7027	LRI	dASPP	0
SCAR	WAVE1/2	Df(2L)BSC145	LRI Y2H	dF8	0
Lrch	LRCH2	Df(2L)BSC294	Gstaiger	F10	0
pk	PRIC1	Df(2R)BSC263	Gstaiger	F9/F10	0
Vang	VANG1	Df(2R)BSC271	Gstaiger	F9/F10	0
CG4679	PTCD3	Df(2R)BSC272	LRI	dASPP	0
inaD	MPDZ	Df(2R)BSC864	Public	dF8	0
CG30415	-	Df(2R)BSC778	LRI	ASPP	0
usnp	SNP29	Df(2R)BSC600	Gstaiger	F7	0
Letm1	LETM1	Df(2R)BSC602	LRI	dASPP	0
Ptp61F	PTN13	Df(3L)BSC289	Gstaiger	F10	0
kst	SPTBN1-4	Df(3L)Exel6093	LRI Y2H	dF8	0
exo70	EXOC7	Df(3L)BSC815	Public	CCDC85	0
Mcm7	MCM7	Df(3L)ED4413	Gstaiger	F10	0
CG14168	PDLIM7	Df(3L)BSC393	Public	dF8	0
pallidin	BLOC1S6	Df(3L)BSC675	Public	dF8	0
yps	CPVL	Df(3L)BSC396	LRI	dASPP	0
sina	SIAH1	Df(3L)Exel9003	Public	ASPP2	0
CG32196	GGCT	Df(3L)ED225	Gstaiger	F7/F9/F10	0
dysb	DTNBP1	Df(3L)BSC776	Public	dCcdc85	0
kug	FAT2	Df(3L)BSC731	LRI	dF8	0
mub	PCBP1	Df(3L)BSC284	Gstaiger	F9/F10	0
Hem	NCKAP1	Df(3L)Exel6138	LRI Y2H	dF8	0
CG11984	KCMF1	Df(3R)BSC506	Gstaiger	F9/F10	0
rin	G3BP1	Df(3R)Exel6169	Gstaiger	F9/F10	0
CG3259	TRAF3IP1	Df(3R)BSC487	Public	ASPP1	0
btsz	SYTL4	Df(3R)BSC842	Public	CCDC85	0
Caf1	RBBP4	Df(3R)BSC471	Gstaiger	F9/F10	0
FK506-bp1	FKBP4	Df(3R)BSC741	LRI	dF8	0
mats	MOB1A	Df(3R)BSC685	Public	CCDC85	0
CG34355	-	Df(3R)Exel9014	LRI	dASPP	0
exo84	EXOC8	Df(3R)BSC751	Public	CCDC85	0
CG5521	RALGAPA2	Df(3R)ED6235	LRI	dASPP	0
Apc	APC	Df(3R)BSC789	Public	ASPP1	0
Yurt	EPB41L1-5	Df(3R)Exel7320			0
esn	PRICKLE1/2	Df(2R)BSC262	Public	dCcdc85	0
ziz	DOCK10/11	Df(2L)Exel7031		Similar to dZir	0

(Continued from previous page)

Bibliography

(1965). *From Nobel Lectures Physiology or Medicine 1922-1941.* Elsevier Publishing Company, Amsterdam.

Adams, M.D., Celniker, S.E., Holt, R.A., Evans, C.A., Gocayne, J.D. et al. (2000). The genome sequence of Drosophila melanogaster. *Science* 287(5461), 2185–2195.

Afonso, C. and Henrique, D. (2006). PAR3 acts as a molecular organizer to define the apical domain of chick neuroepithelial cells. *J. Cell Sci.* 119(20), 4293–4304.

Alonso, A., Sasin, J., Bottini, N., Friedberg, I., Friedberg, I. et al. (2004). Protein tyrosine phosphatases in the human genome. *Cell* 117(6), 699–711.

Aragona, M., Panciera, T., Manfrin, A., Giulitti, S., Michielin, F. et al. (2013). A mechanical checkpoint controls multicellular growth through YAP/TAZ regulation by actin-processing factors. *Cell* 154(5), 1047–1059.

Armstrong, J.F., Kaufman, M.H., Harrison, D.J. and Clarke, A.R. (1995). High-frequency developmental abnormalities in p53-deficient mice. *Curr. Biol.* 5(8), 931–936.

Atwood, S.X., Chabu, C., Penkert, R.R., Doe, C.Q. and Prehoda, K.E. (2007). Cdc42 acts downstream of Bazooka to regulate neuroblast polarity through Par-6 aPKC. *J. Cell Sci.* 120(18), 3200–3206.

Atwood, S.X. and Prehoda, K.E. (2009). aPKC phosphorylates Miranda to polarize fate determinants during neuroblast asymmetric cell division. *Curr. Biol.* 19(9), 723–729.

Avruch, J., Zhou, D., Fitamant, J., Bardeesy, N., Mou, F. et al. (2012). Protein kinases of the Hippo pathway: regulation and substrates. *Seminars in cell & developmental biology* 23(7), 770–784.

Aylon, Y., Ofir-Rosenfeld, Y., Yabuta, N., Lapi, E., Nojima, H. et al. (2010). The Lats2 tumor suppressor augments p53-mediated apoptosis by promoting the nuclear proapoptotic function of ASPP1. *Genes Dev.* 24(21), 2420–2429.

Bachmann, A., Schneider, M., Theilenberg, E., Grawe, F. and Knust, E. (2001). Drosophila Stardust is a partner of Crumbs in the control of epithelial cell polarity. *Nature* 414(6864), 638–643.

Bachmann, A., Timmer, M., Sierralta, J., Pietrini, G., Gundelfinger, E.D. et al. (2004). Cell type-specific recruitment of Drosophila Lin-7 to distinct MAGUK-based protein complexes defines novel roles for Sdt and Dlg-S97. *J. Cell Sci.* 117(10), 1899–1909.

Badouel, C., Gardano, L., Amin, N., Garg, A., Rosenfeld, R. et al. (2009). The FERM-domain protein Expanded regulates Hippo pathway activity via direct interactions with the transcriptional activator Yorkie. *Dev. Cell* 16(3), 411–420.

Bao, S. (2014). Notch controls cell adhesion in the Drosophila eye. *PLoS Genet.* 10(1), e1004087.

Bao, S. and Cagan, R. (2005). Preferential adhesion mediated by Hibris and Roughest regulates morphogenesis and patterning in the Drosophila eye. *Dev. Cell* 8(6), 925–935.

Bao, S., Fischbach, K.F., Corbin, V. and Cagan, R.L. (2010). Preferential adhesion maintains separation of ommatidia in the Drosophila eye. *Dev. Biol.* 344(2), 948–956.

Baumgartner, R., Poernbacher, I., Buser, N., Hafen, E. and Stocker, H. (2010). The WW Domain Protein Kibra Acts Upstream of Hippo in Drosophila. *Dev. Cell* 18(2), 309–316.

Baumgartner, S., Littleton, J.T., Broadie, K., Bhat, M.A., Harbecke, R. et al. (1996). A Drosophila neurexin is required for septate junction and blood-nerve barrier formation and function. *Cell* 87(6), 1059–1068.

Behr, M., Riedel, D. and Schuh, R. (2003). The claudin-like megatrachea is essential in septate junctions for the epithelial barrier function in Drosophila. *Dev. Cell* 5(4), 611–620.

Beller, M., Blanke, S., Brentrup, D. and Jäckle, H. (2002). Identification and expression of Ima, a novel Ral-interacting Drosophila protein. *Mech. Dev.* 119 Suppl 1, S253–60.

Bennett, D., Lyulcheva, E. and Alphey, L. (2006). Towards a Comprehensive Analysis of the Protein Phosphatase 1 Interactome in Drosophila. *J. Mol. Biol.* 364(2), 196–212.

Benton, R. and St Johnston, D. (2003). Drosophila PAR-1 and 14-3-3 inhibit Bazooka/PAR-3 to establish complementary cortical domains in polarized cells. *Cell* 115(6), 691–704.

Bergamaschi, D., Samuels, Y., O'Neil, N.J., Trigiante, G., Crook, T. et al. (2003). iASPP oncoprotein is a key inhibitor of p53 conserved from worm to human. *Nat. Genet.* 33(2), 162–167.

Betschinger, J., Mechtler, K. and Knoblich, J.A. (2003). The Par complex directs asymmetric cell division by phosphorylating the cytoskeletal protein Lgl. *Nature* 422(6929), 326–330.

Bezy, O., Elabd, C., Cochet, O., Petersen, R.K., Kristiansen, K. et al. (2005). Delta-interacting protein A, a new inhibitory partner of CCAAT/enhancer-binding protein beta, implicated in adipocyte differentiation. *J. Biol. Chem.* 280(12), 11432–11438.

Bilder, D., Li, M. and Perrimon, N. (2000). Cooperative regulation of cell polarity and growth by Drosophila tumor suppressors. *Science* 289(5476), 113–116.

Bilder, D. and Perrimon, N. (2000). Localization of apical epithelial determinants by the basolateral PDZ protein Scribble. *Nature* 403(6770), 676–680.

Bilder, D., Schober, M. and Perrimon, N. (2003). Integrated activity of PDZ protein complexes regulates epithelial polarity. *Nat. Cell Biol.* 5(1), 53–58.

Bisson, N., James, D.A., Ivosev, G., Tate, S.A., Bonner, R. et al. (2011). Selected reaction monitoring mass spectrometry reveals the dynamics of signaling through the GRB2 adaptor. *Nat. Biotechnol.* 29(7), 653–658.

Blanchetot, C., Chagnon, M., Dubé, N., Hallé, M. and Tremblay, M.L. (2005). Substrate-trapping techniques in the identification of cellular PTP targets. *Methods* 35(1), 44–53.

Boedigheimer, M. and Laughon, A. (1993). Expanded: a gene involved in the control of cell proliferation in imaginal discs. *Development* 118(4), 1291–1301.

Bollen, M., Peti, W., Ragusa, M.J. and Beullens, M. (2010). The extended PP1 toolkit: designed to create specificity. *Trends Biochem. Sci.* 35(8), 450–458.

Bossuyt, W., Chen, C.L., Chen, Q., Sudol, M., McNeill, H. et al. (2014). An evolutionary shift in the regulation of the Hippo pathway between mice and flies. *Oncogene* 33(10), 1218–1228.

Boyce, M., Bryant, K.F., Jousse, C., Long, K., Harding, H.P. et al. (2005). A selective inhibitor of eIF2alpha dephosphorylation protects cells from ER stress. *Science* 307(5711), 935–939.

Brajenovic, M., Joberty, G., Küster, B., Bouwmeester, T. and Drewes, G. (2004). Comprehensive proteomic analysis of human Par protein complexes reveals an interconnected protein network. *J. Biol. Chem.* 279(13), 12804–12811.

Brautigan, D.L. (2013). Protein Ser/Thr phosphatases–the ugly ducklings of cell signalling. *FEBS J.* 280(2), 324–345.

Brazas, R. and Ganem, D. (1996). A cellular homolog of hepatitis delta antigen: implications for viral replication and evolution. *Science* 274(5284), 90–94.

Bridges, D. and Moorhead, G.B.G. (2005). 14-3-3 proteins: a number of functions for a numbered protein. *Science's STKE : signal transduction knowledge environment* 2005(296), re10.

Brittle, A., Thomas, C. and Strutt, D. (2012). Planar polarity specification through asymmetric subcellular localization of Fat and Dachsous. *Curr. Biol.* 22(10), 907–914.

Brittle, A.L., Repiso, A., Casal, J., Lawrence, P.A. and Strutt, D. (2010). Four-jointed modulates growth and planar polarity by reducing the affinity of dachsous for fat. *Curr. Biol.* 20(9), 803–810.

Brumby, A.M. and Richardson, H.E. (2003). scribble mutants cooperate with oncogenic Ras or Notch to cause neoplastic overgrowth in Drosophila. *EMBO J.* 22(21), 5769–5779.

Bulgakova, N.A. and Knust, E. (2009). The Crumbs complex: from epithelial-cell polarity to retinal degeneration. *J. Cell Sci.* 122(Pt 15), 2587–2596.

Byun, M.R., Hwang, J.H., Kim, A.R., Kim, K.M., Hwang, E.S. et al. (2014). Canonical Wnt signalling activates TAZ through PP1A during osteogenic differentiation. *Cell Death Differ.* 21(6), 854–863.

Cagan, R.L. and Ready, D.F. (1989). The emergence of order in the Drosophila pupal retina. *Dev. Biol.* 136(2), 346–362.

Campisi, J. and d'Adda di Fagagna, F. (2007). Cellular senescence: when bad things happen to good cells. *Nat. Rev. Mol. Cell Biol.* 8(9), 729–740.

Canning, P., von Delft, F. and Bullock, A.N. (2012). Structural basis for ASPP2 recognition by the tumor suppressor p73. *J. Mol. Biol.* 423(4), 515–527.

Carthew, R.W. (2007). Pattern formation in the Drosophila eye. *Curr. Opin. Genet. Dev.* 17(4), 309–313.

Carthew, R.W. and Rubin, G.M. (1990). seven in absentia, a gene required for specification of R7 cell fate in the Drosophila eye. *Cell* 63(3), 561–577.

Celniker, S.E., Dillon, L.A.L., Gerstein, M.B., Gunsalus, K.C., Henikoff, S. et al. (2009). Unlocking the secrets of the genome. *Nature* 459(7249), 927–930.

Chalmers, A.D., Pambos, M., Mason, J., Lang, S., Wylie, C. et al. (2005). aPKC, Crumbs3 and Lgl2 control apicobasal polarity in early vertebrate development. *Development* 132(5), 977–986.

Chan, E.H.Y., Nousiainen, M., Chalamalasetty, R.B., Schäfer, A., Nigg, E.A. et al. (2005). The Ste20-like kinase Mst2 activates the human large tumor suppressor kinase Lats1. *Oncogene* 24(12), 2076–2086.

Chan, J.J., Flatters, D., Rodrigues-Lima, F., Yan, J., Thalassinos, K. et al. (2013). Comparative analysis of interactions of RASSF1-10. *Adv. Biol. Regu.* .

Chan, S.W., Lim, C.J., Chong, Y.F., Pobbati, A.V., Huang, C. et al. (2011). Hippo pathway-independent restriction of TAZ and YAP by angiomotin. *J. Biol. Chem.* 286(9), 7018–7026.

Chen, C.L., Gajewski, K.M., Hamaratoglu, F., Bossuyt, W., Sansores-Garcia, L. et al. (2010). The apical-basal cell polarity determinant Crumbs regulates Hippo signaling in Drosophila. *Proc. Natl. Acad. Sci. U. S. A.* 107(36), 15810–15815.

Chen, L., Johnson, R.C. and Milgram, S.L. (1998). P-CIP1, a novel protein that interacts with the cytosolic domain of peptidylglycine alpha-amidating monooxygenase, is associated with endosomes. *J. Biol. Chem.* 273(50), 33524–33532.

Cherbas, L., Willingham, A., Zhang, D., Yang, L., Zou, Y. et al. (2011). The transcriptional diversity of 25 Drosophila cell lines. *Genome Res.* 21(2), 301–314.

Chien, S., Reiter, L.T., Bier, E. and Gribskov, M. (2002). Homophila: human disease gene cognates in Drosophila. *Nucleic Acids Res.* 30(1), 149–151.

Chikh, A., Matin, R.N.H., Senatore, V., Hufbauer, M., Lavery, D. et al. (2011). iASPP/p63 autoregulatory feedback loop is required for the homeostasis of stratified epithelia. *EMBO J.* 30(20), 4261–4273.

Cho, E., Feng, Y., Rauskolb, C., Maitra, S., Fehon, R. et al. (2006). Delineation of a Fat tumor suppressor pathway. *Nat. Genet.* 38(10), 1142–1150.

Choy, M.S., Hieke, M., Kumar, G.S., Lewis, G.R., Gonzalez-DeWhitt, K.R. et al. (2014). Understanding the antagonism of retinoblastoma protein dephosphorylation by PNUTS provides insights into the PP1 regulatory code. *Proc. Natl. Acad. Sci. U. S. A.* 111(11), 4097–4102.

Clark, H.F., Brentrup, D., Schneitz, K., Bieber, A., Goodman, C. et al. (1995). Dachsous encodes a member of the cadherin superfamily that controls imaginal disc morphogenesis in Drosophila. *Genes Dev.* 9(12), 1530–1542.

Cole, C., Barber, J.D. and Barton, G.J. (2008). The Jpred 3 secondary structure prediction server. *Nucleic Acids Res.* 36(Web Server issue), W197–201.

Cong, W., Hirose, T., Harita, Y., Yamashita, A., Mizuno, K. et al. (2010). ASPP2 regulates epithelial cell polarity through the PAR complex. *Curr. Biol.* 20(15), 1408–1414.

Connor, J.H., Weiser, D.C., Li, S., Hallenbeck, J.M. and Shenolikar, S. (2001). Growth arrest and DNA damage-inducible protein GADD34 assembles a novel signaling complex containing protein phosphatase 1 and inhibitor 1. *Mol. Cell. Biol.* 21(20), 6841–6850.

Cordenonsi, M., Zanconato, F., Azzolin, L., Forcato, M., Rosato, A. et al. (2011). The Hippo transducer TAZ confers cancer stem cell-related traits on breast cancer cells. *Cell* 147(4), 759–772.

Cori, G.T. and Cori, C.F. (1945). The enzymatic conversion of phosphorylase a to b. *J. Mol. Biol.* .

Couzens, A.L., Knight, J.D.R., Kean, M.J., Teo, G., Weiss, A. et al. (2013). Protein interaction network of the mammalian Hippo pathway reveals mechanisms of kinase-phosphatase interactions. *Science signaling* 6(302), rs15.

Dancheck, B., Ragusa, M.J., Allaire, M., Nairn, A.C., Page, R. et al. (2011). Molecular investigations of the structure and function of the protein phosphatase 1-spinophilin-inhibitor 2 heterotrimeric complex. *Biochemistry (Mosc.)* 50(7), 1238–1246.

Dar, A.C., Das, T.K., Shokat, K.M. and Cagan, R.L. (2012). Chemical genetic discovery of targets and anti-targets for cancer polypharmacology. *Nature* 486(7401), 80–84.

Deak, I.I. (1977). Mutations of Drosophila melanogaster that affect muscles. *J. Embryol. Exp. Morphol.* 40, 35–63.

Dehal, P. and Boore, J.L. (2005). Two rounds of whole genome duplication in the ancestral vertebrate. *PLoS Biol.* 3(10), e314.

Desai, R., Sarpal, R., Ishiyama, N., Pellikka, M., Ikura, M. et al. (2013). Monomeric α-catenin links cadherin to the actin cytoskeleton. *Nat. Cell Biol.* 15(3), 261–273.

Dobzhansky, T. (1931). The Decrease of Crossing-Over Observed in Translocations, and Its Probable Explanation. *Am. Nat.* 65(698), 214–232.

Dohadwala, M., da Cruz e Silva, E.F., Hall, F.L., Williams, R.T., Carbonaro-Hall, D.A. et al. (1994). Phosphorylation and inactivation of protein phosphatase 1 by cyclin-dependent kinases. *Proc. Natl. Acad. Sci. U. S. A.* 91(14), 6408–6412.

Dombrádi, V., Axton, J.M., Brewis, N.D., da Cruz e Silva, E.F., Alphey, L. et al. (1990). Drosophila contains three genes that encode distinct isoforms of protein phosphatase 1. *European journal of biochemistry / FEBS* 194(3), 739–745.

Dombrádi, V., Mann, D.J., Saunders, R.D. and Cohen, P.T. (1993). Cloning of the fourth functional gene for protein phosphatase 1 in Drosophila melanogaster from its chromosomal location. *European journal of biochemistry / FEBS* 212(1), 177–183.

Donehower, L.A., Harvey, M., Slagle, B.L., McArthur, M.J., Montgomery, C.A. et al. (1992). Mice deficient for p53 are developmentally normal but susceptible to spontaneous tumours. *Nature* 356(6366), 215–221.

Dong, J., Feldmann, G., Huang, J., Wu, S., Zhang, N. et al. (2007). Elucidation of a Universal Size-Control Mechanism in Drosophila and Mammals. *Cell* 130(6), 1120–1133.

Drees, F., Pokutta, S., Yamada, S., Nelson, W.J. and Weis, W.I. (2005). Alpha-catenin is a molecular switch that binds E-cadherin-beta-catenin and regulates actin-filament assembly. *Cell* 123(5), 903–915.

Du, X., Wang, Q., Hirohashi, Y. and Greene, M.I. (2006). DIPA, which can localize to the centrosome, associates with p78/MCRS1/MSP58 and acts as a repressor of gene transcription. *Exp. Mol. Pathol.* 81(3), 184–190.

Dupont, S., Morsut, L., Aragona, M., Enzo, E., Giulitti, S. et al. (2011). Role of YAP/TAZ in mechanotransduction. *Nature* 474(7350), 179–183.

Egloff, M.P. (1997). Structural basis for the recognition of regulatory subunits by the catalytic subunit of protein phosphatase 1. *EMBO J.* 16(8), 1876–1887.

Espanel, X. and Sudol, M. (2001). Yes-associated protein and p53-binding protein-2 interact through their WW and SH3 domains. *J. Biol. Chem.* 276(17), 14514–14523.

Eto, M., Kitazawa, T., Matsuzawa, F., Aikawa, S.I., Kirkbride, J.A. et al. (2007). Phosphorylation-induced conformational switching of CPI-17 produces a potent myosin phosphatase inhibitor. *Structure* 15(12), 1591–1602.

Faivre-Sarrailh, C., Banerjee, S., Li, J., Hortsch, M., Laval, M. et al. (2004). Drosophila contactin, a homolog of vertebrate contactin, is required for septate junction organization and paracellular barrier function. *Development* 131(20), 4931–4942.

Falvella, F.S., Manenti, G., Spinola, M., Pignatiello, C., Conti, B. et al. (2006). Identification of RASSF8 as a candidate lung tumor suppressor gene. *Oncogene* 25(28), 3934–3938.

Feng, Y. and Irvine, K.D. (2007). Fat and expanded act in parallel to regulate growth through warts. *Proc. Natl. Acad. Sci. U. S. A.* 104(51), 20362–20367.

Fernández, B.G., Gaspar, P., Brás-Pereira, C., Jezowska, B., Rebelo, S.R. et al. (2011). Actin-Capping Protein and the Hippo pathway regulate F-actin and tissue growth in Drosophila. *Development* 138(11), 2337–2346.

Fischer, E.H. and Krebs, E.G. (1955). Conversion of phosphorylase b to phosphorylase a in muscle extracts. *J. Biol. Chem.* 216(1), 121–132.

Fletcher, G.C., Lucas, E.P., Brain, R., Tournier, A. and Thompson, B.J. (2012). Positive feedback and mutual antagonism combine to polarize crumbs in the Drosophila follicle cell epithelium. *Curr. Biol.* 22(12), 1116–1122.

Fujita, Y., Krause, G., Scheffner, M., Zechner, D., Leddy, H.E.M. et al. (2002). Hakai, a c-Cbl-like protein, ubiquitinates and induces endocytosis of the E-cadherin complex. *Nat. Cell Biol.* 4(3), 222–231.

Furuse, M. and Tsukita, S. (2006). Claudins in occluding junctions of humans and flies. *Trends Cell Biol.* 16(4), 181–188.

Gascuel, O. (1997). BIONJ: an improved version of the NJ algorithm based on a simple model of sequence data. *Mol. Biol. Evol.* 14(7), 685–695.

Gasque, G., Conway, S., Huang, J., Rao, Y. and Vosshall, L.B. (2013). Small molecule drug screening in Drosophila identifies the 5HT2A receptor as a feeding modulation target. *Scientific reports* 3, srep02120.

Gehmlich, K., Pinotsis, N., Hayess, K., van der Ven, P.F.M., Milting, H. et al. (2007). Paxillin and ponsin interact in nascent costameres of muscle cells. *J. Mol. Biol.* 369(3), 665–682.

Genevet, A. and Tapon, N. (2011). The Hippo pathway and apico-basal cell polarity. *Biochem. J.* 436(2), 213–224.

Genevet, A., Wehr, M.C., Brain, R., Thompson, B.J. and Tapon, N. (2010). Kibra is a regulator of the Salvador/Warts/Hippo signaling network. *Dev. Cell* 18(2), 300–308.

Genova, J.L. and Fehon, R.G. (2003). Neuroglian, Gliotactin, and the Na+/K+ ATPase are essential for septate junction function in Drosophila. *J. Cell Biol.* 161(5), 979–989.

Gewirtz, D.A. (2013). Autophagy and senescence: a partnership in search of definition. *Autophagy* 9(5), 808–812.

Gibbons, J.A., Kozubowski, L., Tatchell, K. and Shenolikar, S. (2007). Expression of human protein phosphatase-1 in Saccharomyces cerevisiae highlights the role of phosphatase isoforms in regulating eukaryotic functions. *J. Biol. Chem.* 282(30), 21838–21847.

Giot, L., Bader, J.S., Brouwer, C., Chaudhuri, A., Kuang, B. et al. (2003). A protein interaction map of Drosophila melanogaster. *Science* 302(5651), 1727–1736.

Godin-Heymann, N., Wang, Y., Slee, E. and Lu, X. (2013). Phosphorylation of ASPP2 by RAS/MAPK pathway is critical for its full pro-apoptotic function. *PloS one* 8(12), e82022.

Goldberg, J., Huang, H.B., Kwon, Y.G., Greengard, P., Nairn, A.C. et al. (1995). Three-dimensional structure of the catalytic subunit of protein serine/threonine phosphatase-1. *Nature* 376(6543), 745–753.

Gong, H., Gao, X., Feng, S., Siddiqui, M.R., Garcia, A. et al. (2014). Evidence of a common mechanism of disassembly of adherens junctions through Gα13 targeting of VE-cadherin. *J. Exp. Med.* 211(3), 579–591.

Gorina, S. and Pavletich, N.P. (1996). Structure of the p53 tumor suppressor bound to the ankyrin and SH3 domains of 53BP2. *Science* 274(5289), 1001–1005.

Goulev, Y., Fauny, J.D., Gonzalez-Marti, B., Flagiello, D., Silber, J. et al. (2008). SCALLOPED interacts with YORKIE, the nuclear effector of the hippo tumor-suppressor pathway in Drosophila. *Curr. Biol.* 18(6), 435–441.

Grzeschik, N.A. and Knust, E. (2005). IrreC/rst-mediated cell sorting during Drosophila pupal eye development depends on proper localisation of DE-cadherin. *Development* 132(9), 2035–2045.

Grzeschik, N.A., Parsons, L.M., Allott, M.L., Harvey, K.F. and Richardson, H.E. (2010). Lgl, aPKC, and Crumbs regulate the Salvador/Warts/Hippo pathway through two distinct mechanisms. *Curr. Biol.* 20(7), 573–581.

Hachet, O., Berthelot-Grosjean, M., Kokkoris, K., Vincenzetti, V., Moosbrugger, J. et al. (2011). A phosphorylation cycle shapes gradients of the DYRK family kinase Pom1 at the plasma membrane. *Cell* 145(7), 1116–1128.

Halder, G., Dupont, S. and Piccolo, S. (2012). Transduction of mechanical and cytoskeletal cues by YAP and TAZ. *Nat. Rev. Mol. Cell Biol.* 13(9), 591–600.

Hamaratoglu, F., Willecke, M., Kango-Singh, M., Nolo, R., Hyun, E. et al. (2006). The tumour-suppressor genes NF2/Merlin and Expanded act through Hippo signalling to regulate cell proliferation and apoptosis.l. *Nat. Cell Biol.* 8(1), 27–36.

Hao, Y., Chun, A., Cheung, K., Rashidi, B. and Yang, X. (2008). Tumor suppressor LATS1 is a negative regulator of oncogene YAP. *J. Biol. Chem.* 283(9), 5496–5509.

Harris, T.J.C. and Peifer, M. (2005). The positioning and segregation of apical cues during epithelial polarity establishment in Drosophila. *J. Cell Biol.* 170(5), 813–823.

Harris, T.J.C. and Tepass, U. (2010). Adherens junctions: from molecules to morphogenesis. *Nat. Rev. Mol. Cell Biol.* 11(7), 502–514.

Harvey, K.F., Pfleger, C.M. and Hariharan, I.K. (2003). The Drosophila Mst ortholog, hippo, restricts growth and cell proliferation and promotes apoptosis. *Cell* 114(4), 457–467.

Hauri, S., Wepf, A., van Drogen, A., Varjosalo, M., Tapon, N. et al. (2013). Interaction proteome of human Hippo signaling: modular control of the co-activator YAP1. *Mol. Syst. Biol.* 9, 713.

Helps, N.R., Barker, H.M., Elledge, S.J. and Cohen, P.T. (1995). Protein phosphatase 1 interacts with p53BP2, a protein which binds to the tumour suppressor p53. *FEBS Lett.* 377(3), 295–300.

Hemmings, B.A., Resink, T.J. and Cohen, P. (1982). Reconstitution of a Mg-ATP-dependent protein phosphatase and its activation through a phosphorylation mechanism. *FEBS Lett.* 150(2), 319–324.

Hendrickx, A., Beullens, M., Ceulemans, H., Den Abt, T., Van Eynde, A. et al. (2009). Docking motif-guided mapping of the interactome of protein phosphatase-1. *Chemistry & biology* 16(4), 365–371.

Heroes, E., Lesage, B., Görnemann, J., Beullens, M., Van Meervelt, L. et al. (2013). The PP1 binding code: a molecular-lego strategy that governs specificity. *FEBS J.* 280(2), 584–595.

Herron, B.J., Rao, C., Liu, S., Laprade, L., Richardson, J.A. et al. (2005). A mutation in NFkB interacting protein 1 results in cardiomyopathy and abnormal skin development in wa3 mice. *Hum. Mol. Genet.* 14(5), 667–677.

Hill, V.K., Underhill-Day, N., Krex, D., Robel, K., Sangan, C.B. et al. (2011). Epigenetic inactivation of the RASSF10 candidate tumor suppressor gene is a frequent and an early event in gliomagenesis. *Oncogene* 30(8), 978–989.

Hilman, D. and Gat, U. (2011). The evolutionary history of YAP and the hippo/YAP pathway. *Mol. Biol. Evol.* 28(8), 2403–2417.

Hirabayashi, S., Tajima, M., Yao, I., Nishimura, W., Mori, H. et al. (2003). JAM4, a junctional cell adhesion molecule interacting with a tight junction protein, MAGI-1. *Mol. Cell. Biol.* 23(12), 4267–4282.

Hirashima, M., Sano, K., Morisada, T., Murakami, K., Rossant, J. et al. (2008). Lymphatic vessel assembly is impaired in Aspp1-deficient mouse embryos. *Dev. Biol.* 316(1), 149–159.

Ho, L.L., Wei, X., Shimizu, T. and Lai, Z.C. (2010). Mob as tumor suppressor is activated at the cell membrane to control tissue growth and organ size in Drosophila. *Dev. Biol.* 337(2), 274–283.

Hoege, C. and Hyman, A.A. (2013). Principles of PAR polarity in Caenorhabditis elegans embryos. *Nat. Rev. Mol. Cell Biol.* 14(5), 315–322.

Hong, Y., Stronach, B., Perrimon, N., Jan, L.Y. and Jan, Y.N. (2001). Drosophila Stardust interacts with Crumbs to control polarity of epithelia but not neuroblasts. *Nature* 414(6864), 634–638.

Horikoshi, Y., Hamada, S., Ohno, S. and Suetsugu, S. (2011). Phosphoinositide binding by par-3 involved in par-3 localization. *Cell Struct. Funct.* 36(1), 97–102.

Hossain, Z., Ali, S.M., Ko, H.L., Xu, J., Ng, C.P. et al. (2007). Glomerulocystic kidney disease in mice with a targeted inactivation of Wwtr1. *Proc. Natl. Acad. Sci. U. S. A.* 104(5), 1631–1636.

Hu, G. and Fearon, E.R. (1999). Siah-1 N-terminal RING domain is required for proteolysis function, and C-terminal sequences regulate oligomerization and binding to target proteins. *Mol. Cell. Biol.* 19(1), 724–732.

Huang, H.B., Horiuchi, A., Watanabe, T., Shih, S.R., Tsay, H.J. et al. (1999). Characterization of the inhibition of protein phosphatase-1 by DARPP-32 and inhibitor-2. *J. Biol. Chem.* 274(12), 7870–7878.

Huang, J., Wu, S., Barrera, J., Matthews, K. and Pan, D. (2005). The Hippo signaling pathway coordinately regulates cell proliferation and apoptosis by inactivating Yorkie, the Drosophila Homolog of YAP. *Cell* 122(3), 421–434.

Huang, W., Lv, X., Liu, C., Zha, Z., Zhang, H. et al. (2012). The N-terminal phosphodegron targets TAZ/WWTR1 protein for SCFβ-TrCP-dependent degradation in response to phosphatidylinositol 3-kinase inhibition. *J. Biol. Chem.* 287(31), 26245–26253.

Hurd, T.W., Fan, S., Liu, C.J., Kweon, H.K., Hakansson, K. et al. (2003). Phosphorylation-dependent binding of 14-3-3 to the polarity protein Par3 regulates cell polarity in mammalian epithelia. *Curr. Biol.* 13(23), 2082–2090.

Hurley, T.D., Yang, J., Zhang, L., Goodwin, K.D., Zou, Q. et al. (2007). Structural basis for regulation of protein phosphatase 1 by inhibitor-2. *J. Biol. Chem.* 282(39), 28874–28883.

Hutterer, A., Betschinger, J., Petronczki, M. and Knoblich, J.A. (2004). Sequential roles of Cdc42, Par-6, aPKC, and Lgl in the establishment of epithelial polarity during Drosophila embryogenesis. *Dev. Cell* 6(6), 845–854.

Ikeda, M., Kawata, A., Nishikawa, M., Tateishi, Y., Yamaguchi, M. et al. (2009). Hippo pathway-dependent and -independent roles of RASSF6. *Science signaling* 2(90), ra59.

Ishikawa, H.O., Takeuchi, H., Haltiwanger, R.S. and Irvine, K.D. (2008). Four-jointed is a Golgi kinase that phosphorylates a subset of cadherin domains. *Science* 321(5887), 401–404.

Islam, R., Wei, S.Y., Chiu, W.H., Hortsch, M. and Hsu, J.C. (2003). Neuroglian activates Echinoid to antagonize the Drosophila EGF receptor signaling pathway. *Development* 130(10), 2051–2059.

Iwabuchi, K., Bartel, P.L., Li, B., Marraccino, R. and Fields, S. (1994). Two cellular proteins that bind to wild-type but not mutant p53. *Proc. Natl. Acad. Sci. U. S. A.* 91(13), 6098–6102.

Iwai, A., Hijikata, M., Hishiki, T., Isono, O., Chiba, T. et al. (2008). Coiled-coil domain containing 85B suppresses the beta-catenin activity in a p53-dependent manner. *Oncogene* 27(11), 1520–1526.

Izaki, T., Kamakura, S., Kohjima, M. and Sumimoto, H. (2005). Phosphorylation-dependent binding of 14-3-3 to Par3beta, a human Par3-related cell polarity protein. *Biochem. Biophys. Res. Commun.* 329(1), 211–218.

Jia, J., Zhang, W., Wang, B., Trinko, R. and Jiang, J. (2003). The Drosophila Ste20 family kinase dMST functions as a tumor suppressor by restricting cell proliferation and promoting apoptosis. *Genes Dev.* 17(20), 2514–2519.

Johnson, C., Crowther, S., Stafford, M.J., Campbell, D.G., Toth, R. et al. (2010). Bioinformatic and experimental survey of 14-3-3-binding sites. *Biochem. J.* 427(1), 69–78.

Johnson, D.F., Moorhead, G., Caudwell, F.B., Cohen, P., Chen, Y.H. et al. (1996). Identification of protein-phosphatase-1-binding domains on the glycogen and myofibrillar targetting subunits. *European journal of biochemistry / FEBS* 239(2), 317–325.

Justice, R.W., Zilian, O., Woods, D.F., Noll, M. and Bryant, P.J. (1995). The Drosophila tumor suppressor gene warts encodes a homolog of human myotonic dystrophy kinase and is required for the control of cell shape and proliferation. *Genes Dev.* 9(5), 534–546.

Kampa, K.M., Acoba, J.D., Chen, D., Gay, J., Lee, H. et al. (2009). Apoptosis-stimulating protein of p53 (ASPP2) heterozygous mice are tumor-prone and have attenuated cellular damage-response thresholds. *Proc. Natl. Acad. Sci. U. S. A.* 106(11), 4390–4395.

Kango-Singh, M., Nolo, R., Tao, C., Verstreken, P., Hiesinger, P.R. et al. (2002). Shar-pei mediates cell proliferation arrest during imaginal disc growth in Drosophila. *Development* 129(24), 5719–5730.

Kelker, M.S., Page, R. and Peti, W. (2009). Crystal structures of protein phosphatase-1 bound to nodularin-R and tautomycin: a novel scaffold for structure-based drug design of serine/threonine phosphatase inhibitors. *J. Mol. Biol.* 385(1), 11–21.

Kempkens, O., Médina, E., Fernandez-Ballester, G., Ozüyaman, S., Le Bivic, A. et al. (2006). Computer modelling in combination with in vitro studies reveals similar binding affinities of Drosophila Crumbs for the PDZ domains of Stardust and DmPar-6. *Eur. J. Cell Biol.* 85(8), 753–767.

Kiel, C., Foglierini, M., Kuemmerer, N., Beltrao, P. and Serrano, L. (2007). A genome-wide Ras-effector interaction network. *J. Mol. Biol.* 370(5), 1020–1032.

Kim, H., Claps, G., Möller, A., Bowtell, D., Lu, X. et al. (2014). Siah2 regulates tight junction integrity and cell polarity through control of ASPP2 stability. *Oncogene* 33(15), 2004–2010.

Kirchner, J., Gross, S., Bennett, D. and Alphey, L. (2007). Essential, overlapping and redundant roles of the Drosophila protein phosphatase 1 alpha and 1 beta genes. *Genetics* 176(1), 273–281.

Kirchner, J., Vissi, E., Gross, S., Szöor, B., Rudenko, A. et al. (2008). Drosophila Uri, a PP1alpha binding protein, is essential for viability, maintenance of DNA integrity and normal transcriptional activity. *BMC molecular biology* 9, 36.

Kita, A., Matsunaga, S., Takai, A., Kataiwa, H., Wakimoto, T. et al. (2002). Crystal structure of the complex between calyculin A and the catalytic subunit of protein phosphatase 1. *Structure* 10(5), 715–724.

Knaus, M., Cameroni, E., Pedruzzi, I., Tatchell, K., De Virgilio, C. et al. (2005). The Bud14p-Glc7p complex functions as a cortical regulator of dynein in budding yeast. *EMBO J.* 24(17), 3000–3011.

Kohli, P., Bartram, M.P., Habbig, S., Pahmeyer, C., Lamkemeyer, T. et al. (2014). Label-free quantitative proteomic analysis of the YAP/TAZ interactome. *Am. J. Physiol.-Cell Ph.* 306(9), C805–18.

Krahn, M.P., Egger-Adam, D. and Wodarz, A. (2009). PP2A antagonizes phosphorylation of Bazooka by PAR-1 to control apical-basal polarity in dividing embryonic neuroblasts. *Dev. Cell* 16(6), 901–908.

Krahn, M.P., Klopfenstein, D.R., Fischer, N. and Wodarz, A. (2010). Membrane targeting of Bazooka/PAR-3 is mediated by direct binding to phosphoinositide lipids. *Curr. Biol.* 20(7), 636–642.

Kumar, J.P. (2010). Retinal determination the beginning of eye development. *Curr. Top. Dev. Biol.* 93, 1–28.

Kwon, Y.G., Lee, S.Y., Choi, Y., Greengard, P. and Nairn, A.C. (1997). Cell cycle-dependent phosphorylation of mammalian protein phosphatase 1 by cdc2 kinase. *Proc. Natl. Acad. Sci. U. S. A.* 94(6), 2168–2173.

Lai, Z.C., Wei, X., Shimizu, T., Ramos, E., Rohrbaugh, M. et al. (2005). Control of cell proliferation and apoptosis by mob as tumor suppressor, mats. *Cell* 120(5), 675–685.

LaJeunesse, D.R., McCartney, B.M. and Fehon, R.G. (1998). Structural analysis of Drosophila merlin reveals functional domains important for growth control and subcellular localization. *J. Cell Biol.* 141(7), 1589–1599.

Langton, P. (2008). *dASPP and Boa regulate C-terminal Src kinase activity to control epithelial proliferation and integrity.* Ph.D. thesis, University College London.

Langton, P., Colombani, J., Aerne, B. and Tapon, N. (2007). Drosophila ASPP Regulates C-Terminal Src Kinase Activity. *Dev. Cell* 13(6), 773–782.

Langton, P.F., Colombani, J., Chan, E.H.Y., Wepf, A., Gstaiger, M. et al. (2009). The dASPP-dRASSF8 complex regulates cell-cell adhesion during Drosophila retinal morphogenesis. *Curr. Biol.* 19(23), 1969–1978.

Laprise, P., Beronja, S., Silva-Gagliardi, N.F., Pellikka, M., Jensen, A.M. et al. (2006). The FERM protein Yurt is a negative regulatory component of the Crumbs complex that controls epithelial polarity and apical membrane size. *Dev. Cell* 11(3), 363–374.

Laprise, P., Lau, K.M., Harris, K.P., Silva-Gagliardi, N.F., Paul, S.M. et al. (2009). Yurt, Coracle, Neurexin IV and the Na(+),K(+)-ATPase form a novel group of epithelial polarity proteins. *Nature* 459(7250), 1141–1145.

Larkin, M.A., Blackshields, G., Brown, N.P., Chenna, R., McGettigan, P.A. et al. (2007). Clustal W and Clustal X version 2.0. *Bioinformatics (Oxford, England)* 23(21), 2947–2948.

Larson, D.E., Liberman, Z. and Cagan, R.L. (2008). Cellular behavior in the developing Drosophila pupal retina. *Mech. Dev.* 125(3-4), 223–232.

Lee, A. and Treisman, J.E. (2004). Excessive Myosin activity in mbs mutants causes photoreceptor movement out of the Drosophila eye disc epithelium. *Mol. Biol. Cell* 15(7), 3285–3295.

Lee, C.M., Yang, P., Chen, L.C., Chen, C.C., Wu, S.C. et al. (2011). A novel role of RASSF9 in maintaining epidermal homeostasis. *PloS one* 6(3), e17867.

Lei, Q.Y., Zhang, H., Zhao, B., Zha, Z.Y., Bai, F. et al. (2008). TAZ promotes cell proliferation and epithelial-mesenchymal transition and is inhibited by the hippo pathway. *Mol. Cell. Biol.* 28(7), 2426–2436.

Lesage, B., Beullens, M., Pedelini, L., Garcia-Gimeno, M.A., Waelkens, E. et al. (2007). A complex of catalytically inactive protein phosphatase-1 sandwiched between Sds22 and inhibitor-3. *Biochemistry (Mosc.)* 46(31), 8909–8919.

Letunic, I., Doerks, T. and Bork, P. (2012). SMART 7: recent updates to the protein domain annotation resource. *Nucleic Acids Res.* 40(Database issue), D302–5.

Li, S., Li, Y., Carthew, R.W. and Lai, Z.C. (1997). Photoreceptor cell differentiation requires regulated proteolysis of the transcriptional repressor Tramtrack. *Cell* 90(3), 469–478.

Ling, C., Zheng, Y., Yin, F., Yu, J., Huang, J. et al. (2010). The apical transmembrane protein Crumbs functions as a tumor suppressor that regulates Hippo signaling by binding to Expanded. *Proc. Natl. Acad. Sci. U. S. A.* 107(23), 10532–10537.

Liu, C.Y., Lv, X., Li, T., Xu, Y., Zhou, X. et al. (2011). PP1 cooperates with ASPP2 to dephosphorylate and activate TAZ. *J. Biol. Chem.* 286(7), 5558–5566.

Liu, C.Y., Zha, Z.Y., Zhou, X., Zhang, H., Huang, W. et al. (2010). The hippo tumor pathway promotes TAZ degradation by phosphorylating a phosphodegron and recruiting the SCFbeta-TrCP E3 ligase. *J. Biol. Chem.* 285(48), 37159–37169.

Llanos, S., Royer, C., Lu, M., Bergamaschi, D., Lee, W.H. et al. (2011). The Inhibitory Member of the Apoptosis Stimulating Proteins of p53 Family (iASPP) Interacts with Protein Phosphatase 1 (PP1) via a Non-Canonical Binding Motif. *J. Biol. Chem.* 286(50), 43039–44.

Llimargas, M., Strigini, M., Katidou, M., Karagogeos, D. and Casanova, J. (2004). Lachesin is a component of a septate junction-based mechanism that controls tube size and epithelial integrity in the Drosophila tracheal system. *Development* 131(1), 181–190.

Lock, F.E., Underhill-Day, N., Dunwell, T., Matallanas, D., Cooper, W. et al. (2010). The RASSF8 candidate tumor suppressor inhibits cell growth and regulates the Wnt and NF-κB signaling pathways. *Oncogene* 29(30), 4307–4316.

Lu, M., Breyssens, H., Salter, V., Zhong, S., Hu, Y. et al. (2013). Restoring p53 function in human melanoma cells by inhibiting MDM2 and cyclin B1/CDK1-phosphorylated nuclear iASPP. *Cancer Cell* 23(5), 618–633.

Lu, M., Zak, J., Chen, S., Sanchez-Pulido, L., Severson, D.T. et al. (2014). A code for RanGDP binding in ankyrin repeats defines a nuclear import pathway. *Cell* 157(5), 1130–1145.

MacKintosh, C., Garton, A.J., McDonnell, A., Barford, D., Cohen, P.T. et al. (1996). Further evidence that inhibitor-2 acts like a chaperone to fold PP1 into its native conformation. *FEBS Lett.* 397(2-3), 235–238.

Manning, G., Whyte, D.B., Martinez, R., Hunter, T. and Sudarsanam, S. (2002). The protein kinase complement of the human genome. *Science* 298(5600), 1912–1934.

Martin-Belmonte, F., Gassama, A., Datta, A., Yu, W., Rescher, U. et al. (2007). PTEN-mediated apical segregation of phosphoinositides controls epithelial morphogenesis through Cdc42. *Cell* 128(2), 383–397.

Mathew, D., Gramates, L.S., Packard, M., Thomas, U., Bilder, D. et al. (2002). Recruitment of scribble to the synaptic scaffolding complex requires GUK-holder, a novel DLG binding protein. *Curr. Biol.* 12(7), 531–539.

Matos Simões, S.d., Blankenship, J.T., Weitz, O., Farrell, D.L., Tamada, M. et al. (2010). Rho-kinase directs Bazooka/Par-3 planar polarity during Drosophila axis elongation. *Dev. Cell* 19(3), 377–388.

Maynes, J.T., Bateman, K.S., Cherney, M.M., Das, A.K., Luu, H.A. et al. (2001). Crystal structure of the tumor-promoter okadaic acid bound to protein phosphatase-1. *J. Biol. Chem.* 276(47), 44078–44082.

Maynes, J.T., Luu, H.A., Cherney, M.M., Andersen, R.J., Williams, D. et al. (2006). Crystal structures of protein phosphatase-1 bound to motuporin and dihydromicrocystin-LA: elucidation of the mechanism of enzyme inhibition by cyanobacterial toxins. *J. Mol. Biol.* 356(1), 111–120.

McCaffrey, L.M. and Macara, I.G. (2011). Epithelial organization, cell polarity and tumorigenesis. *Trends Cell Biol.* 21(12), 727–735.

McCartney, B.M., Kulikauskas, R.M., LaJeunesse, D.R. and Fehon, R.G. (2000). The neurofibromatosis-2 homologue, Merlin, and the tumor suppressor expanded function together in Drosophila to regulate cell proliferation and differentiation. *Development* 127(6), 1315–1324.

McGill, M.A., McKinley, R.F.A. and Harris, T.J.C. (2009). Independent cadherin-catenin and Bazooka clusters interact to assemble adherens junctions. *J. Cell Biol.* 185(5), 787–796.

McKinley, R.F.A., Yu, C.G. and Harris, T.J.C. (2012). Assembly of Bazooka polarity landmarks through a multifaceted membrane-association mechanism. *J. Cell Sci.* 125(Pt 5), 1177–1190.

Médina, E., Williams, J., Klipfell, E., Zarnescu, D., Thomas, G. et al. (2002). Crumbs interacts with moesin and beta(Heavy)-spectrin in the apical membrane skeleton of Drosophila. *J. Cell Biol.* 158(5), 941–951.

Meiselbach, H., Sticht, H. and Enz, R. (2006). Structural analysis of the protein phosphatase 1 docking motif: molecular description of binding specificities identifies interacting proteins. *Chemistry & biology* 13(1), 49–59.

Miller, D.T. and Cagan, R.L. (1998). Local induction of patterning and programmed cell death in the developing Drosophila retina. *Development* 125(12), 2327–2335.

Miller, E., Yang, J., DeRan, M., Wu, C., Su, A.I. et al. (2012). Identification of serum-derived sphingosine-1-phosphate as a small molecule regulator of YAP. *Chemistry & biology* 19(8), 955–962.

Mo, J.S., Yu, F.X., Gong, R., Brown, J.H. and Guan, K.L. (2012). Regulation of the Hippo-YAP pathway by protease-activated receptors (PARs). *Genes Dev.* 26(19), 2138–2143.

Monserrate, J.P. and Brachmann, C.B. (2007). Identification of the death zone: a spatially restricted region for programmed cell death that sculpts the fly eye. *Cell Death Differ.* 14(2), 209–217.

Moorhead, G.B.G., De Wever, V., Templeton, G. and Kerk, D. (2009). Evolution of protein phosphatases in plants and animals. *Biochem. J.* 417(2), 401–409.

Mori, N., Kuwamura, M., Tanaka, N., Hirano, R., Nabe, M. et al. (2012). Ccdc85c encoding a protein at apical junctions of radial glia is disrupted in hemorrhagic hydrocephalus (hhy) mice. *Am. J. Pathol.* 180(1), 314–327.

Morin, X., Daneman, R., Zavortink, M. and Chia, W. (2001). A protein trap strategy to detect GFP-tagged proteins expressed from their endogenous loci in Drosophila. *Proc. Natl. Acad. Sci. U. S. A.* 98(26), 15050–15055.

Morin-Kensicki, E.M., Boone, B.N., Howell, M., Stonebraker, J.R., Teed, J. et al. (2006). Defects in yolk sac vasculogenesis, chorioallantoic fusion, and embryonic axis elongation in mice with targeted disruption of Yap65. *Mol. Cell. Biol.* 26(1), 77–87.

Muslin, A.J., Tanner, J.W., Allen, P.M. and Shaw, A.S. (1996). Interaction of 14-3-3 with signaling proteins is mediated by the recognition of phosphoserine. *Cell* 84(6), 889–897.

Myers, E.W., Sutton, G.G., Delcher, A.L., Dew, I.M., Fasulo, D.P. et al. (2000). A whole-genome assembly of Drosophila. *Science* 287(5461), 2196–2204.

Nagai-Tamai, Y., Mizuno, K., Hirose, T., Suzuki, A. and Ohno, S. (2002). Regulated protein-protein interaction between aPKC and PAR-3 plays an essential role in the polarization of epithelial cells. *Genes Cells* 7(11), 1161–1171.

Nakayama, M., Goto, T.M., Sugimoto, M., Nishimura, T., Shinagawa, T. et al. (2008). Rho-kinase phosphorylates PAR-3 and disrupts PAR complex formation. *Dev. Cell* 14(2), 205–215.

Nam, S.C. and Choi, K.W. (2003). Interaction of Par-6 and Crumbs complexes is essential for photoreceptor morphogenesis in Drosophila. *Development* 130(18), 4363–4372.

Nelson, K.S., Furuse, M. and Beitel, G.J. (2010). The Drosophila Claudin Kune-kune is required for septate junction organization and tracheal tube size control. *Genetics* 185(3), 831–839.

Nishioka, N., Inoue, K.i., Adachi, K., Kiyonari, H., Ota, M. et al. (2009). The Hippo signaling pathway components Lats and Yap pattern Tead4 activity to distinguish mouse trophectoderm from inner cell mass. *Dev. Cell* 16(3), 398–410.

Nolo, R., Morrison, C.M., Tao, C., Zhang, X. and Halder, G. (2006). The bantam microRNA is a target of the hippo tumor-suppressor pathway. *Curr. Biol.* 16(19), 1895–1904.

Notari, M., Hu, Y., Koch, S., Lu, M., Ratnayaka, I. et al. (2011). Inhibitor of apoptosis-stimulating protein of p53 (iASPP) prevents senescence and is required for epithelial stratification. *Proc. Natl. Acad. Sci. U. S. A.* 108(40), 16645–16650.

O'Connell, N., Nichols, S.R., Heroes, E., Beullens, M., Bollen, M. et al. (2012). The molecular basis for substrate specificity of the nuclear NIPP1:PP1 holoenzyme. *Structure* 20(10), 1746–1756.

Oda, H., Uemura, T., Harada, Y., Iwai, Y. and Takeichi, M. (1994). A Drosophila homolog of cadherin associated with armadillo and essential for embryonic cell-cell adhesion. *Dev. Biol.* 165(2), 716–726.

Oh, H. and Irvine, K.D. (2008). In vivo regulation of Yorkie phosphorylation and localization. *Development* 135(6), 1081–1088.

Oh, H. and Irvine, K.D. (2009). In vivo analysis of Yorkie phosphorylation sites. *Oncogene* 28(17), 1916–1927.

Oh, H., Reddy, B.V.V.G. and Irvine, K.D. (2009). Phosphorylation-independent repression of Yorkie in Fat-Hippo signaling. *Dev. Biol.* 335(1), 188–197.

Okada, M., Nada, S., Yamanashi, Y., Yamamoto, T. and Nakagawa, H. (1991). CSK: a protein-tyrosine kinase involved in regulation of src family kinases. *J. Biol. Chem.* 266(36), 24249–24252.

Olsen, J.V., Blagoev, B., Gnad, F., Macek, B., Kumar, C. et al. (2006). Global, in vivo, and site-specific phosphorylation dynamics in signaling networks. *Cell* 127(3), 635–648.

Oshima, K. and Fehon, R.G. (2011). Analysis of protein dynamics within the septate junction reveals a highly stable core protein complex that does not include the basolateral polarity protein Discs large. *J. Cell Sci.* 124(16), 2861–2871.

Pagliarini, R.A. and Xu, T. (2003). A genetic screen in Drosophila for metastatic behavior. *Science* 302(5648), 1227–1231.

Pantalacci, S., Tapon, N. and Léopold, P. (2003). The Salvador partner Hippo promotes apoptosis and cell-cycle exit in Drosophila. *Nat. Cell Biol.* 5(10), 921–927.

Paul, S.M., Ternet, M., Salvaterra, P.M. and Beitel, G.J. (2003). The Na+/K+ ATPase is required for septate junction function and epithelial tube-size control in the Drosophila tracheal system. *Development* 130(20), 4963–4974.

Perry, M.M. (1968). Further studies on the development of the of Drosophila melanogaster. II. The interommatidial bristles. *J. Morphol.* 124(2), 249–262.

Peti, W., Nairn, A.C. and Page, R. (2013). Structural basis for protein phosphatase 1 regulation and specificity. *FEBS J.* 280(2), 596–611.

Petronczki, M. and Knoblich, J.A. (2001). DmPAR-6 directs epithelial polarity and asymmetric cell division of neuroblasts in Drosophila. *Nat. Cell Biol.* 3(1), 43–49.

Pi, H., Wu, H.J. and Chien, C.T. (2001). A dual function of phyllopod in Drosophila external sensory organ development: cell fate specification of sensory organ precursor and its progeny. *Development* 128(14), 2699–2710.

Pinna, L.A. and Ruzzene, M. (1996). How do protein kinases recognize their substrates? *Biochim. Biophys. Acta* 1314(3), 191–225.

Pirozzi, G., McConnell, S.J., Uveges, A.J., Carter, J.M., Sparks, A.B. et al. (1997). Identification of novel human WW domain-containing proteins by cloning of ligand targets. *J. Biol. Chem.* 272(23), 14611–14616.

Plant, P.J., Fawcett, J.P., Lin, D.C.C., Holdorf, A.D., Binns, K. et al. (2003). A polarity complex of mPar-6 and atypical PKC binds, phosphorylates and regulates mammalian Lgl. *Nat. Cell Biol.* 5(4), 301–308.

Polesello, C. and Tapon, N. (2007). Salvador-warts-hippo signaling promotes Drosophila posterior follicle cell maturation downstream of notch. *Curr. Biol.* 17(21), 1864–1870.

Praskova, M., Khoklatchev, A., Ortiz-Vega, S. and Avruch, J. (2004). Regulation of the MST1 kinase by autophosphorylation, by the growth inhibitory proteins, RASSF1 and NORE1, and by Ras. *Biochem. J.* 381(2), 453–462.

Raghavan, S., Williams, I., Aslam, H., Thomas, D., Szöor, B. et al. (2000). Protein phosphatase 1beta is required for the maintenance of muscle attachments. *Curr. Biol.* 10(5), 269–272.

Ragusa, M.J., Dancheck, B., Critton, D.A., Nairn, A.C., Page, R. et al. (2010). Spinophilin directs protein phosphatase 1 specificity by blocking substrate binding sites. *Nat. Struct. Mol. Biol.* 17(4), 459–464.

Rauskolb, C., Pan, G., Reddy, B.V.V.G., Oh, H. and Irvine, K.D. (2011). Zyxin links fat signaling to the hippo pathway. *PLoS Biol.* 9(6), e1000624.

Recino, A., Sherwood, V., Flaxman, A., Cooper, W.N., Latif, F. et al. (2010). Human RASSF7 regulates the microtubule cytoskeleton and is required for spindle formation, Aurora B activation and chromosomal congression during mitosis. *Biochem. J.* 430(2), 207–213.

Reither, G., Chatterjee, J., Beullens, M., Bollen, M., Schultz, C. et al. (2013). Chemical activators of protein phosphatase-1 induce calcium release inside intact cells. *Chemistry & biology* 20(9), 1179–1186.

Ribeiro, P., Holder, M., Frith, D., Snijders, A.P. and Tapon, N. (2014). Crumbs promotes expanded recognition and degradation by the SCF(Slimb/β-TrCP) ubiquitin ligase. *Proc. Natl. Acad. Sci. U. S. A.* 111(19), E1980–9.

Ribeiro, P.S., Josué, F., Wepf, A., Wehr, M.C., Rinner, O. et al. (2010). Combined functional genomic and proteomic approaches identify a PP2A complex as a negative regulator of Hippo signaling. *Mol. Cell* 39(4), 521–534.

Ridley, A.J. (2006). Rho GTPases and actin dynamics in membrane protrusions and vesicle trafficking. *Trends Cell Biol.* 16(10), 522–529.

Rimm, D.L., Koslov, E.R., Kebriaei, P., Cianci, C.D. and Morrow, J.S. (1995). Alpha 1(E)-catenin is an actin-binding and -bundling protein mediating the attachment of F-actin to the membrane adhesion complex. *Proc. Natl. Acad. Sci. U. S. A.* 92(19), 8813–8817.

Robinson, B.S., Huang, J., Hong, Y. and Moberg, K.H. (2010). Crumbs regulates Salvador/Warts/Hippo signaling in Drosophila via the FERM-domain protein Expanded. *Curr. Biol.* 20(7), 582–590.

Rodriguez-Viciana, P., Sabatier, C. and McCormick, F. (2004). Signaling specificity by Ras family GTPases is determined by the full spectrum of effectors they regulate. *Mol. Cell. Biol.* 24(11), 4943–4954.

Rotter, V., Schwartz, D., Almon, E., Goldfinger, N., Kapon, A. et al. (1993). Mice with reduced levels of p53 protein exhibit the testicular giant-cell degenerative syndrome. *Proc. Natl. Acad. Sci. U. S. A.* 90(19), 9075–9079.

Morais-de Sá, E., Mirouse, V. and St Johnston, D. (2010). aPKC phosphorylation of Bazooka defines the apical/lateral border in Drosophila epithelial cells. *Cell* 141(3), 509–523.

Sachdev, S., Hoffmann, A. and Hannink, M. (1998). Nuclear localization of IkappaB alpha is mediated by the second ankyrin repeat: the IkappaB alpha ankyrin repeats define a novel class of cis-acting nuclear import sequences. *Mol. Cell. Biol.* 18(5), 2524–2534.

Sah, V.P., Attardi, L.D., Mulligan, G.J., Williams, B.O., Bronson, R.T. et al. (1995). A subset of p53-deficient embryos exhibit exencephaly. *Nat. Genet.* 10(2), 175–180.

Samuels-Lev, Y., O'Connor, D.J., Bergamaschi, D., Trigiante, G., Hsieh, J.K. et al. (2001). ASPP proteins specifically stimulate the apoptotic function of p53. *Mol. Cell* 8(4), 781–794.

Sansores-Garcia, L., Bossuyt, W., Wada, K.I., Yonemura, S., Tao, C. et al. (2011). Modulating F-actin organization induces organ growth by affecting the Hippo pathway. *EMBO J.* 30(12), 2325–2335.

Satohisa, S., Chiba, H., Osanai, M., Ohno, S., Kojima, T. et al. (2005). Behavior of tight-junction, adherens-junction and cell polarity proteins during HNF-4alpha-induced epithelial polarization. *Exp. Cell Res.* 310(1), 66–78.

Sawyer, J.K., Harris, N.J., Slep, K.C., Gaul, U. and Peifer, M. (2009). The Drosophila afadin homologue Canoe regulates linkage of the actin cytoskeleton to adherens junctions during apical constriction. *J. Cell Biol.* 186(1), 57–73.

Schlegelmilch, K., Mohseni, M., Kirak, O., Pruszak, J., Rodriguez, J.R. et al. (2011). Yap1 acts downstream of α-catenin to control epidermal proliferation. *Cell* 144(5), 782–795.

Schulte, J., Tepass, U. and Auld, V.J. (2003). Gliotactin, a novel marker of tricellular junctions, is necessary for septate junction development in Drosophila. *J. Cell Biol.* 161(5), 991–1000.

Scotto-Lavino, E., Garcia-Diaz, M., Du, G. and Frohman, M.A. (2010). Basis for the isoform-specific interaction of myosin phosphatase subunits protein phosphatase 1c beta and myosin phosphatase targeting subunit 1. *J. Biol. Chem.* 285(9), 6419–6424.

Sherwood, V., Manbodh, R., Sheppard, C. and Chalmers, A.D. (2008). RASSF7 Is a Member of a New Family of RAS Association Domain-containing Proteins and Is Required for Completing Mitosis. *Mol. Biol. Cell* 19(4), 1772–1782.

Sherwood, V., Recino, A., Jeffries, A., Ward, A. and Chalmers, A.D. (2009). The N-terminal RASSF family: a new group of Ras-association-domaincontaining proteins, with emerging links to cancer formation. *Biochem. J.* 425(2), 303–311.

Shi, Y. (2009). Serine/threonine phosphatases: mechanism through structure. *Cell* 139(3), 468–484.

Shin, K., Fogg, V.C. and Margolis, B. (2006). Tight junctions and cell polarity. *Annu. Rev. Cell Dev. Biol.* 22, 207–235.

Silva, E., Tsatskis, Y., Gardano, L., Tapon, N. and McNeill, H. (2006). The tumor-suppressor gene fat controls tissue growth upstream of expanded in the hippo signaling pathway. *Curr. Biol.* 16(21), 2081–2089.

Simon, M.A., Xu, A., Ishikawa, H.O. and Irvine, K.D. (2010). Modulation of fat:dachsous binding by the cadherin domain kinase four-jointed. *Curr. Biol.* 20(9), 811–817.

Simons, M. and Mlodzik, M. (2008). Planar cell polarity signaling: from fly development to human disease. *Annu. Rev. Genet.* 42, 517–540.

Simpson, M.A., Cook, R.W., Solanki, P., Patton, M.A., Dennis, J.A. et al. (2009). A mutation in NFkappaB interacting protein 1 causes cardiomyopathy and woolly haircoat syndrome of Poll Hereford cattle. *Anim. Genet.* 40(1), 42–46.

Skene-Arnold, T.D., Luu, H.A., Uhrig, R.G., De Wever, V., Nimick, M. et al. (2013). Molecular mechanisms underlying the interaction of protein phosphatase-1c with ASPP proteins. *Biochem. J.* 449(3), 649–659.

Slee, E.A., Gillotin, S., Bergamaschi, D., Royer, C., Llanos, S. et al. (2004). The N-terminus of a novel isoform of human iASPP is required for its cytoplasmic localization. *Oncogene* 23(56), 9007–9016.

Snow, P.M., Bieber, A.J. and Goodman, C.S. (1989). Fasciclin III: a novel homophilic adhesion molecule in Drosophila. *Cell* 59(2), 313–323.

Songyang, Z., Shoelson, S.E., McGlade, J., Olivier, P., Pawson, T. et al. (1994). Specific motifs recognized by the SH2 domains of Csk, 3BP2, fps/fes, GRB-2, HCP, SHC, Syk, and Vav. *Mol. Cell. Biol.* 14(4), 2777–2785.

Sotillos, S., Díaz-Meco, M.T., Caminero, E., Moscat, J. and Campuzano, S. (2004). DaPKC-dependent phosphorylation of Crumbs is required for epithelial cell polarity in Drosophila. *J. Cell Biol.* 166(4), 549–557.

Sottocornola, R., Royer, C., Vives, V., Tordella, L., Zhong, S. et al. (2010). ASPP2 binds Par-3 and controls the polarity and proliferation of neural progenitors during CNS development. *Dev. Cell* 19(1), 126–137.

St Johnston, D. and Ahringer, J. (2010). Cell polarity in eggs and epithelia: parallels and diversity. *Cell* 141(5), 757–774.

Stock, A.M., Robinson, V.L. and Goudreau, P.N. (2000). Two-component signal transduction. *Annu. Rev. Biochem.* 69, 183–215.

Sun, G. and Irvine, K.D. (2011). Regulation of Hippo signaling by Jun kinase signaling during compensatory cell proliferation and regeneration, and in neoplastic tumors. *Dev. Biol.* 350(1), 139–151.

Takahashi, S., Ebihara, A., Kajiho, H., Kontani, K., Nishina, H. et al. (2011). RASSF7 negatively regulates pro-apoptotic JNK signaling by inhibiting the activity of phosphorylated-MKK7. *Cell Death Differ.* 18(4), 645–655.

Takekuni, K., Ikeda, W., Fujito, T., Morimoto, K., Takeuchi, M. et al. (2003). Direct binding of cell polarity protein PAR-3 to cell-cell adhesion molecule nectin at neuroepithelial cells of developing mouse. *J. Biol. Chem.* 278(8), 5497–5500.

Tanentzapf, G. and Tepass, U. (2003). Interactions between the crumbs, lethal giant larvae and bazooka pathways in epithelial polarization. *Nat. Cell Biol.* 5(1), 46–52.

Tang, A.H., Neufeld, T.P., Kwan, E. and Rubin, G.M. (1997). PHYL acts to down-regulate TTK88, a transcriptional repressor of neuronal cell fates, by a SINA-dependent mechanism. *Cell* 90(3), 459–467.

Tapon, N., Harvey, K.F., Bell, D.W., Wahrer, D.C.R., Schiripo, T.A. et al. (2002). salvador Promotes both cell cycle exit and apoptosis in Drosophila and is mutated in human cancer cell lines. *Cell* 110(4), 467–478.

Tepass, U. (2012). The apical polarity protein network in Drosophila epithelial cells: regulation of polarity, junctions, morphogenesis, cell growth, and survival. *Annu. Rev. Cell Dev. Biol.* 28, 655–685.

Tepass, U., Gruszynski-DeFeo, E., Haag, T.A., Omatyar, L., Török, T. et al. (1996). shotgun encodes Drosophila E-cadherin and is preferentially required during cell rearrangement in the neurectoderm and other morphogenetically active epithelia. *Genes Dev.* 10(6), 672–685.

Terrak, M., Kerff, F., Langsetmo, K., Tao, T. and Dominguez, R. (2004). Structural basis of protein phosphatase 1 regulation. *Nature* 429(6993), 780–784.

Terry-Lorenzo, R.T., Elliot, E., Weiser, D.C., Prickett, T.D., Brautigan, D.L. et al. (2002). Neurabins recruit protein phosphatase-1 and inhibitor-2 to the actin cytoskeleton. *J. Biol. Chem.* 277(48), 46535–46543.

Thompson, B.J. and Cohen, S.M. (2006). The Hippo pathway regulates the bantam microRNA to control cell proliferation and apoptosis in Drosophila. *Cell* 126(4), 767–774.

Tidow, H., Andreeva, A., Rutherford, T.J. and Fersht, A.R. (2007). Solution structure of ASPP2 N-terminal domain (N-ASPP2) reveals a ubiquitin-like fold. *J. Mol. Biol.* 371(4), 948–958.

Tompa, P. (2005). The interplay between structure and function in intrinsically unstructured proteins. *FEBS Lett.* 579(15), 3346–3354.

Tonikian, R., Zhang, Y., Sazinsky, S.L., Currell, B., Yeh, J.H. et al. (2008). A specificity map for the PDZ domain family. *PLoS Biol.* 6(9), e239.

Toonen, J., Liang, L. and Sidjanin, D.J. (2012). Waved with open eyelids 2 (woe2) is a novel spontaneous mouse mutation in the protein phosphatase 1, regulatory (inhibitor) subunit 13 like (Ppp1r13l) gene. *BMC genetics* 13, 76.

Tordella, L., Koch, S., Salter, V., Pagotto, A., Doondeea, J.B. et al. (2013). ASPP2 suppresses squamous cell carcinoma via RelA/p65-mediated repression of p63. *Proc. Natl. Acad. Sci. U. S. A.* 110(44), 17969–17974.

Traweger, A., Wiggin, G., Taylor, L., Tate, S.A., Metalnikov, P. et al. (2008). Protein phosphatase 1 regulates the phosphorylation state of the polarity scaffold Par-3. *Proc. Natl. Acad. Sci. U. S. A.* 105(30), 10402–10407.

Treisman, J.E. (2012). Retinal differentiation in Drosophila. *Wiley Interdisciplinary Reviews: Developmental Biology* 2(4), 545–557.

Trigiante, G. and Lu, X. (2006). ASPP [corrected] and cancer. *Nat. Rev. Cancer* 6(3), 217–226.

Tsaytler, P., Harding, H.P., Ron, D. and Bertolotti, A. (2011). Selective inhibition of a regulatory subunit of protein phosphatase 1 restores proteostasis. *Science* 332(6025), 91–94.

Tyler, D.M. and Baker, N.E. (2007). Expanded and fat regulate growth and differentiation in the Drosophila eye through multiple signaling pathways. *Dev. Biol.* 305(1), 187–201.

Udan, R.S., Kango-Singh, M., Nolo, R., Tao, C. and Halder, G. (2003). Hippo promotes proliferation arrest and apoptosis in the Salvador/Warts pathway. *Nat. Cell Biol.* 5(10), 914–920.

Underhill-Day, N., Hill, V. and Latif, F. (2011). N-terminal RASSF family: RASSF7-RASSF10. *Epigenetics* 6(3), 284–292.

Vang, T., Torgersen, K.M., Sundvold, V., Saxena, M., Levy, F.O. et al. (2001). Activation of the COOH-terminal Src kinase (Csk) by cAMP-dependent protein kinase inhibits signaling through the T cell receptor. *The Journal of experimental medicine* 193(4), 497–507.

Varelas, X. (2014). The Hippo pathway effectors TAZ and YAP in development, homeostasis and disease. *Development* 141(8), 1614–1626.

Varelas, X., Samavarchi-Tehrani, P., Narimatsu, M., Weiss, A., Cockburn, K. et al. (2010). The Crumbs complex couples cell density sensing to Hippo-dependent control of the TGF-β-SMAD pathway. *Dev. Cell* 19(6), 831–844.

Vereshchagina, N., Bennett, D., Szöor, B., Kirchner, J., Gross, S. et al. (2004). The essential role of PP1beta in Drosophila is to regulate nonmuscle myosin. *Mol. Biol. Cell* 15(10), 4395–4405.

Vigneron, A.M., Ludwig, R.L. and Vousden, K.H. (2010). Cytoplasmic ASPP1 inhibits apoptosis through the control of YAP. *Genes Dev.* 24(21), 2430–2439.

Vives, V., Su, J., Zhong, S., Ratnayaka, I., Slee, E. et al. (2006). ASPP2 is a haploinsufficient tumor suppressor that cooperates with p53 to suppress tumor growth. *Genes Dev.* 20(10), 1262–1267.

Volodko, N., Gordon, M., Salla, M., Ghazaleh, H.A. and Baksh, S. (2014). RASSF tumor suppressor gene family: Biological functions and regulation. *FEBS Lett.* 588(16), 2671–2684.

Wada, K.I., Itoga, K., Okano, T., Yonemura, S. and Sasaki, H. (2011). Hippo pathway regulation by cell morphology and stress fibers. *Development* 138(18), 3907–3914.

Wakula, P., Beullens, M., Ceulemans, H., Stalmans, W. and Bollen, M. (2003). Degeneracy and function of the ubiquitous RVXF motif that mediates binding to protein phosphatase-1. *J. Biol. Chem.* 278(21), 18817–18823.

Walther, R.F. and Pichaud, F. (2010). Crumbs/DaPKC-dependent apical exclusion of Bazooka promotes photoreceptor polarity remodeling. *Curr. Biol.* 20(12), 1065–1074.

Wang, J., Huo, K., Ma, L., Tang, L., Li, D. et al. (2011a). Toward an understanding of the protein interaction network of the human liver. *Mol. Syst. Biol.* 7, 536.

Wang, P., Bai, Y., Song, B., Wang, Y., Liu, D. et al. (2011b). PP1A-Mediated Dephosphorylation Positively Regulates YAP2 Activity. *PloS one* 6(9), e24288.

Wang, Q., Hurd, T.W. and Margolis, B. (2004). Tight junction protein Par6 interacts with an evolutionarily conserved region in the amino terminus of PALS1/stardust. *J. Biol. Chem.* 279(29), 30715–30721.

Wang, W., Huang, J. and Chen, J. (2011c). Angiomotin-like proteins associate with and negatively regulate YAP1. *J. Biol. Chem.* 286(6), 4364–4370.

Wang, W., Li, X., Huang, J., Feng, L., Dolinta, K.G. et al. (2014). Defining the protein-protein interaction network of the human hippo pathway. *Mol. Cell. Proteomics* 13(1), 119–131.

Wang, X.D., Lapi, E., Sullivan, A., Ratnayaka, I., Goldin, R. et al. (2011d). SUMO-modified nuclear cyclin D1 bypasses Ras-induced senescence. *Cell Death Differ.* 18(2), 304–314.

Wang, Y., Du, D., Fang, L., Yang, G., Zhang, C. et al. (2006). Tyrosine phosphorylated Par3 regulates epithelial tight junction assembly promoted by EGFR signaling. *EMBO J.* 25(21), 5058–5070.

Wang, Y., Godin-Heymann, N., Dan Wang, X., Bergamaschi, D., Llanos, S. et al. (2013a). ASPP1 and ASPP2 bind active RAS, potentiate RAS signalling and enhance p53 activity in cancer cells. *Cell Death Differ.* 20(4), 525–534.

Wang, Y., Wang, X.D., Lapi, E., Sullivan, A., Jia, W. et al. (2012). Autophagic activity dictates the cellular response to oncogenic RAS. *Proc. Natl. Acad. Sci. U. S. A.* 109(33), 13325–13330.

Wang, Z., Liu, Y., Takahashi, M., Van Hook, K., Kampa-Schittenhelm, K.M. et al. (2013b). N terminus of ASPP2 binds to Ras and enhances Ras/Raf/MEK/ERK activation to promote oncogene-induced senescence. *Proc. Natl. Acad. Sci. U. S. A.* 110(1), 312–317.

Wei, S.Y., Escudero, L.M., Yu, F., Chang, L.H., Chen, L.Y. et al. (2005). Echinoid is a component of adherens junctions that cooperates with DE-Cadherin to mediate cell adhesion. *Dev. Cell* 8(4), 493–504.

Willecke, M., Hamaratoglu, F., Kango-Singh, M., Udan, R., Chen, C.L. et al. (2006). The fat cadherin acts through the hippo tumor-suppressor pathway to regulate tissue size. *Curr. Biol.* 16(21), 2090–2100.

Wodarz, A., Ramrath, A., Grimm, A. and Knust, E. (2000). Drosophila atypical protein kinase C associates with Bazooka and controls polarity of epithelia and neuroblasts. *J. Cell Biol.* 150(6), 1361–1374.

Wohlgemuth, S., Kiel, C., Krämer, A., Serrano, L., Wittinghofer, F. et al. (2005). Recognizing and Defining True Ras Binding Domains I: Biochemical Analysis. *J. Mol. Biol.* 348(3), 741–758.

Wolff, T. and Ready, D.F. (1993). *Pattern formation in the Drosophila retina. In: The Development of Drosophila melanogaster*, volume 2, chapter 22, pages 1277–1325. Cold Spring Harbor Laboratory Press.

Woods, D.F. and Bryant, P.J. (1991). The discs-large tumor suppressor gene of Drosophila encodes a guanylate kinase homolog localized at septate junctions. *Cell* 66(3), 451–464.

Wu, H., Feng, W., Chen, J., Chan, L.N., Huang, S. et al. (2007a). PDZ domains of Par-3 as potential phosphoinositide signaling integrators. *Mol. Cell* 28(5), 886–898.

Wu, S., Huang, J., Dong, J. and Pan, D. (2003). hippo encodes a Ste-20 family protein kinase that restricts cell proliferation and promotes apoptosis in conjunction with salvador and warts. *Cell* 114(4), 445–456.

Wu, S., Liu, Y., Zheng, Y., Dong, J. and Pan, D. (2008). The TEAD/TEF family protein Scalloped mediates transcriptional output of the Hippo growth-regulatory pathway. *Dev. Cell* 14(3), 388–398.

Wu, V.M., Schulte, J., Hirschi, A., Tepass, U. and Beitel, G.J. (2004). Sinuous is a Drosophila claudin required for septate junction organization and epithelial tube size control. *J. Cell Biol.* 164(2), 313–323.

Wu, V.M., Yu, M.H., Paik, R., Banerjee, S., Liang, Z. et al. (2007b). Drosophila Varicose, a member of a new subgroup of basolateral MAGUKs, is required for septate junctions and tracheal morphogenesis. *Development* 134(5), 999–1009.

Xu, T., Wang, W., Zhang, S., Stewart, R.A. and Yu, W. (1995). Identifying tumor suppressors in genetic mosaics: the Drosophila lats gene encodes a putative protein kinase. *Development* 121(4), 1053–1063.

Yamada, S., Pokutta, S., Drees, F., Weis, W.I. and Nelson, W.J. (2005). Deconstructing the cadherin-catenin-actin complex. *Cell* 123(5), 889–901.

Yamanaka, T., Horikoshi, Y., Sugiyama, Y., Ishiyama, C., Suzuki, A. et al. (2003). Mammalian Lgl forms a protein complex with PAR-6 and aPKC independently of PAR-3 to regulate epithelial cell polarity. *Curr. Biol.* 13(9), 734–743.

Yang, C.h., Axelrod, J.D. and Simon, M.A. (2002). Regulation of Frizzled by fat-like cadherins during planar polarity signaling in the Drosophila compound eye. *Cell* 108(5), 675–688.

Yang, J.P., Hori, M., Sanda, T. and Okamoto, T. (1999). Identification of a novel inhibitor of nuclear factor-kappaB, RelA-associated inhibitor. *J. Biol. Chem.* 274(22), 15662–15670.

Yang, W., Malek, S.N. and Desiderio, S. (1995). An SH3-binding site conserved in Bruton's tyrosine kinase and related tyrosine kinases mediates specific protein interactions in vitro and in vivo. *J. Biol. Chem.* 270(35), 20832–20840.

Yi, C., Troutman, S., Fera, D., Stemmer-Rachamimov, A., Avila, J.L. et al. (2011). A tight junction-associated Merlin-angiomotin complex mediates Merlin's regulation of mitogenic signaling and tumor suppressive functions. *Cancer Cell* 19(4), 527–540.

Yin, F., Yu, J., Zheng, Y., Chen, Q., Zhang, N. et al. (2013). Spatial organization of Hippo signaling at the plasma membrane mediated by the tumor suppressor Merlin/NF2. *Cell* 154(6), 1342–1355.

Yu, F.X., Zhang, Y., Park, H.W., Jewell, J.L., Chen, Q. et al. (2013). Protein kinase A activates the Hippo pathway to modulate cell proliferation and differentiation. *Genes Dev.* 27(11), 1223–1232.

Yu, F.X., Zhao, B., Panupinthu, N., Jewell, J.L., Lian, I. et al. (2012). Regulation of the Hippo-YAP pathway by G-protein-coupled receptor signaling. *Cell* 150(4), 780–791.

Yu, J., Zheng, Y., Dong, J., Klusza, S., Deng, W.M. et al. (2010). Kibra Functions as a Tumor Suppressor Protein that Regulates Hippo Signaling in Conjunction with Merlin and Expanded. *Dev. Cell* 18(2), 288–299.

Zhang, L., Ren, F., Zhang, Q., Chen, Y., Wang, B. et al. (2008). The TEAD/TEF family of transcription factor Scalloped mediates Hippo signaling in organ size control. *Dev. Cell* 14(3), 377–387.

Zhang, N., Bai, H., David, K.K., Dong, J., Zheng, Y. et al. (2010). The Merlin/NF2 tumor suppressor functions through the YAP oncoprotein to regulate tissue homeostasis in mammals. *Dev. Cell* 19(1), 27–38.

Zhao, B., Li, L., Lu, Q., Wang, L.H., Liu, C.Y. et al. (2011). Angiomotin is a novel Hippo pathway component that inhibits YAP oncoprotein. *Genes Dev.* 25(1), 51–63.

Zhao, B., Li, L., Tumaneng, K., Wang, C.Y. and Guan, K.L. (2010). A coordinated phosphorylation by Lats and CK1 regulates YAP stability through SCF(beta-TRCP). *Genes Dev.* 24(1), 72–85.

Zhao, B., Wei, X., Li, W., Udan, R.S., Yang, Q. et al. (2007). Inactivation of YAP oncoprotein by the Hippo pathway is involved in cell contact inhibition and tissue growth control. *Genes Dev.* 21(21), 2747–2761.

Zhao, B., Ye, X., Yu, J., Li, L., Li, W. et al. (2008). TEAD mediates YAP-dependent gene induction and growth control. *Genes Dev.* 22(14), 1962–1971.

Zhu, Z., Ramos, J., Kampa, K., Adimoolam, S., Sirisawad, M. et al. (2005). Control of ASPP2/(53BP2L) protein levels by proteasomal degradation modulates p53 apoptotic function. *J. Biol. Chem.* 280(41), 34473–34480.